UNIVERSITY OF CALIFORNIA SAN DIEGO

Mechanisms and Models of Muscle Loss in Rotator Cuff Disease

A dissertation submitted in partial satisfaction of the
requirements for the degree Doctor of Philosophy
in
Bioengineering
by
Michael C. Gibbons

Committee in Charge:

Samuel R. Ward, Chair
Adam J. Engler, Co-Chair
Ju Chen
Karen Christman
Simon Schenk
Anshu Singh

2018

The Dissertation of Michael C. Gibbons is approved, and it is acceptable in quality and form for publication on microfilm and electronically:

_____

_____

_____

_____

_____

Co-Chair

_____

Chair

University of California San Diego

2018

EPIGRAPH

And this I believe: that the free, exploring mind of the individual human is the most valuable thing in the world. And this I would fight for: the freedom of the mind to take any direction it wishes, undirected. And this I must fight against: any idea, religion, or government which limits or destroys the individual. This is what I am and what I am about.

John Steinbeck, East of Eden

TABLE OF CONTENTS

LIST OF FIGURES

LIST OF TABLES

ACKNOWLEDGEMENTS

I would like to acknowledge the remarkable mentorship I have received throughout my academic career. In particular, I would like to acknowledge the mentorship and support of my committee chairs, Professors Sam Ward and Adam Engler, whose intellectual and professional encouragement over the last five years has been invaluable to my development as a scientist, engineer, and leader. Similarly, Dr. Anshu Singh has been an invaluable resource as far as my understanding of clinical practice and translation of research to patient care is concerned. I would also like to acknowledge the mentorship of Professor Kristen Cardinal of Cal Poly SLO, who first inspired me to pursue a graduate degree and remains an influential mentor to this day.

I would also like to acknowledge my lab mates in both the Engler and Ward labs. In particular, I would like to acknowledge (now Professor) Gretchen Meyer for her mentorship early in my graduate studies, and (now Professor) Bahar Shahidi and Dr. David Berry for their constant support and entertainment for the last several years. I would also be remiss if I did not acknowledge the work of Mary Esparza, who has contributed more hours to the works presented here than anyone would care to count.

Finally, I would like to acknowledge my family and friends for their unwavering support. In particular, I would like to thank my parents, Chris and Cyndy Gibbons, for their unconditional love and for instilling in me the drive and curiosity that have been critical to my achievements to date. I also would like to acknowledge my siblings, Brian and Maggie Gibbons, and my friends David Nicholas, Andrew van Cleve, Gordon Chow, and Bobby Chacon, who have kept me grounded and who together share my fondest and most important memories. And finally, I would like to acknowledge Aimee Raleigh, who has opened a new world of experiences to me and serves as a daily source of love, support, and inspiration.

Chapter 1, in full, is a reprint of the material as it appears in the Journal of Orthopedic Research 2018. Michael C. Gibbons, Anshu Singh, Adam J. Engler, Samuel R. Ward. The dissertation/thesis author was the primary investigator of this material.

Chapter 2, in full, is a reprint of the material as it appears in the Journal of Orthopedic Research 2016. Michael C. Gibbons, Eugene Sato, Damien Bachasson, Timothy Cheng, Hassan Azimi, Simon

Schenk, Adam J. Engler, Anshu Singh, Samuel R. Ward. The dissertation/thesis author was the primary investigator of this material.

Chapter 3, in full, is a reprint of the material as it appears in the Journal of Bone and Joint Surgery 2017. Michael C. Gibbons, Anshu Singh, Oke Anakwenze, Timothy Cheng, Maxwill Dylan Pomerantz, Simon Schenk, Adam J. Engler, Samuel R. Ward. The dissertation/thesis author was the primary investigator of this material.

Chapter 4, in full, is a reprint of the material as it appears in PLOS One 2018. Michael C. Gibbons, Kathleen Fisch, Rajeswari Pichika, Timothy Cheng, Adam J. Engler, Simon Schenk, John G. Lane, Anshu Singh, Samuel R. Ward. The dissertation/thesis author was the primary investigator of this material.

Chapter 5, in part is currently being prepared for submission for publication of the material. Michael C. Gibbons, Morgan Silldorff, Hiroshi Okuno, Mary C. Esparza, Christopher Migdal, Seth Johnson, Matthew MacEwen, Simon Schenk, Samuel R. Ward. The dissertation/thesis author was the primary investigator of this material.

Chapter 6, in part, is currently being prepared for submission for publication of the material. Mario Vargas-Vila, Michael C. Gibbons, Mary C. Esparza, Shingo Miyazaki, Seth Johnson, Koichi Masuda, Anshu Singh, Samuel R. Ward. The dissertation/thesis author was a primary investigator of this material.

Chapter 7, in part is currently being prepared for submission for publication of the material. Michael C. Gibbons, Severin Ruoss, Kathleen M. Fisch, Brigitte von Rechenberg, Martin Flück, Christian Gerber, Samuel R. Ward. The dissertation/thesis author was the primary investigator of this material.

Chapter 8, in part, is currently being prepared for submission for publication of the material. Michael C. Gibbons, Mario Vargas-Vila, Kathleen M. Fisch, Anshu Singh, Samuel R. Ward. The dissertation/thesis author was a primary investigator of this material.

Chapter 9, in part, is currently being prepared for submission for publication of the material. Bahar Shahidi, Michael C. Gibbons, Mary Esparza, Vinko Zlomislic, R Todd Allen, Anshu Singh,

Christian Gerber, Steve R. Garfin, Samuel R. Ward. The dissertation/thesis author was a primary investigator of this material.

VITA

2013 Bachelor of Science, California Polytechnic State University

Major Field: Biomedical Engineering
Professor Kristen Cardinal

2013 Master of Science, California Polytechnic State University

Major Field: Biomedical Engineering: Stem Cell Research Specialization
Professor Thomas Rando, Professor Kristen Cardinal

2018 Doctor of Philosophy, Bioengineering, University of California San Diego

Major Field: Bioengineering
Professor Samuel Ward, Professor Adam Engler

ABSTRACT OF THE DISSERTATION

Mechanisms and Models of Muscle Loss in Rotator Cuff Disease

by

Michael C. Gibbons

Doctor of Philosophy in Bioengineering

University of California, San Diego, 2018

Professor Samuel Ward, Chair

Professor Adam Engler, Co-Chair

One in five people have a rotator cuff tear, increasing with age to 50% of patients in the eighth decade of life. This creates a large burden on the healthcare system, as outcomes of tendon repair are poor and functional recovery even after successful tendon repair is limited. Strongly associated with rotator cuff tendon tears are irreversible muscle loss and muscle fatty infiltration, which serve as key clinical indicators of disease progression and predictors of surgical outcome. The prevailing biological and treatment paradigms have attributed these negative muscle changes to atrophy and subsequent space-filling by adipocytes. However, atrophy is a well-defined, self-limiting, and generally reversible response to unloading, which does not adequately explain the irreversibility of muscle loss in these patients. In human muscle biopsies, we discovered a novel phenotype of muscle fiber degeneration in which segments of muscle fiber membranes and cytoplasm are disrupted, leading to alternately hyper- and hypo-cellular degenerative regions. While muscle regeneration is increased in these biopsies, in some cases degenerative regions appear to resolve by adipocyte deposition within the fascicular architecture in a process of fatty replacement. Together with our finding that sarcomeres remodel normally in full-thickness but not massive tears, these data provide a compelling explanation for irreversibility of muscle

loss in chronic, massive tears; total muscle volume is permanently reduced over time, and the remaining muscle is no longer sensitive to mechanical loading. After exhaustive characterization of small- and large-animal models of RCT in the context of these human findings, we determined that rabbit and sheep each adequately recapitulate the tissue-level degenerative processes found clinically. Using these models, we have begun to define the biological processes involved in chronic muscle degeneration, which include cellular stress and membrane damage responses, inhibition of growth and metabolism (particularly oxidative phosphorylation), prolonged inflammation, and competing processes of cell death and survival, while protein catabolic processes commonly associated with atrophy are notably absent. In conclusion, the findings of muscle degeneration and replacement of muscle fibers with adipose tissue described here provide a new paradigm for understanding and treating muscle loss in chronic rotator cuff disease.

Chapter 1. The Role of Mechanobiology in Progression of Rotator Cuff Muscle Atrophy and Degeneration

Abstract

Rotator cuff (RC) muscles undergo several detrimental changes following mechanical unloading resulting from RC tendon tear. In this review, we highlight the pathological causes and consequences of mechanical alterations at the whole muscle, muscle fiber, and muscle resident cell level as they relate to RC disease progression. In brief, the altered mechanical loads associated with RC tear lead to architectural, structural, and compositional changes at the whole-muscle and muscle fiber level. At the cellular level, these changes equate to direct disruption of mechanobiological signaling, which is exacerbated by mechanically-regulated biophysical and biochemical changes to the cellular and extra-cellular environment (also known as the stem cell 'niche'). Together, these data have important implications for both pre-clinical models and clinical practice. In pre-clinical models, it is important to recapitulate both the atrophic and degenerative muscle loss found in humans using clinically relevant modes of injury. Clinically, understanding the mechanics and underlying biology of the muscle will impact both surgical decision-making and rehabilitation protocols, as interventions that may be good for atrophic muscle will have a detrimental effect on degenerating muscle, and vice versa.

Key Words: Rotator Cuff, Muscle Mechanics, Skeletal Muscle Biology, Muscle Mechanobiology, Muscle Atrophy, Muscle Degeneration

Introduction

Rotator cuff tears affect over 20% of the general population, with prevalence increasing with age[1]. Mechanical failure of the RC tendon, often preceded by pathological changes in the tendon microstucture[2-6], is the primary cause of RC disease. Equally important from a clinical perspective are the resulting detrimental changes in RC muscle structure and composition, which play a prominent role in both the failure of RC tendon repairs as well as the persistent functional deficits observed in many

patients[7]. Indeed, these muscular changes are a primary method by which RC disease is staged clinically[8], based on the relative ease of noninvasive CT and MRI imaging of muscle compared to tendon and the negative relationship between intramuscular fat accumulation and clinical outcomes[7; 9]. Our understanding of the biological processes that govern the replacement of muscle by fat and fibrosis remains limited, but the role of altered mechanics in the progressive decline of RC muscle is central both to the existing data and prevailing hypotheses regarding RC muscle fate after tendon tear and/or repair. A summary of key factors involved in controlling and actuating skeletal muscle remodeling, which is arguably the most sensitive tissue to changes in mechanical loading in the RC, is outlined in Figure 1.

Figure 1.1 Conceptual control system diagram representing 33 key controllers and actuators of muscle gain (green) and loss (red) that may be affected in rotator cuff muscle pathology. Black lines represent processes that may contribute to muscle gain or loss, depending on context. Lines ending in arrowheads indicate a proliferative, intensifying or otherwise increasing effect on the indicated element, while lines ending in perpendicular lines indicate an inhibitory or otherwise diminishing effect. Dashed lines denote downstream processes that feed backward through the system to modulate upstream cell populations or processes. Additionally, system elements are color-coded by predominant functional category and shaded to indicate biological category, though again some elements may contribute to gain or loss in a context dependent manner. It is important to note that this is not a comprehensive map and does not show all known or possible interactions.

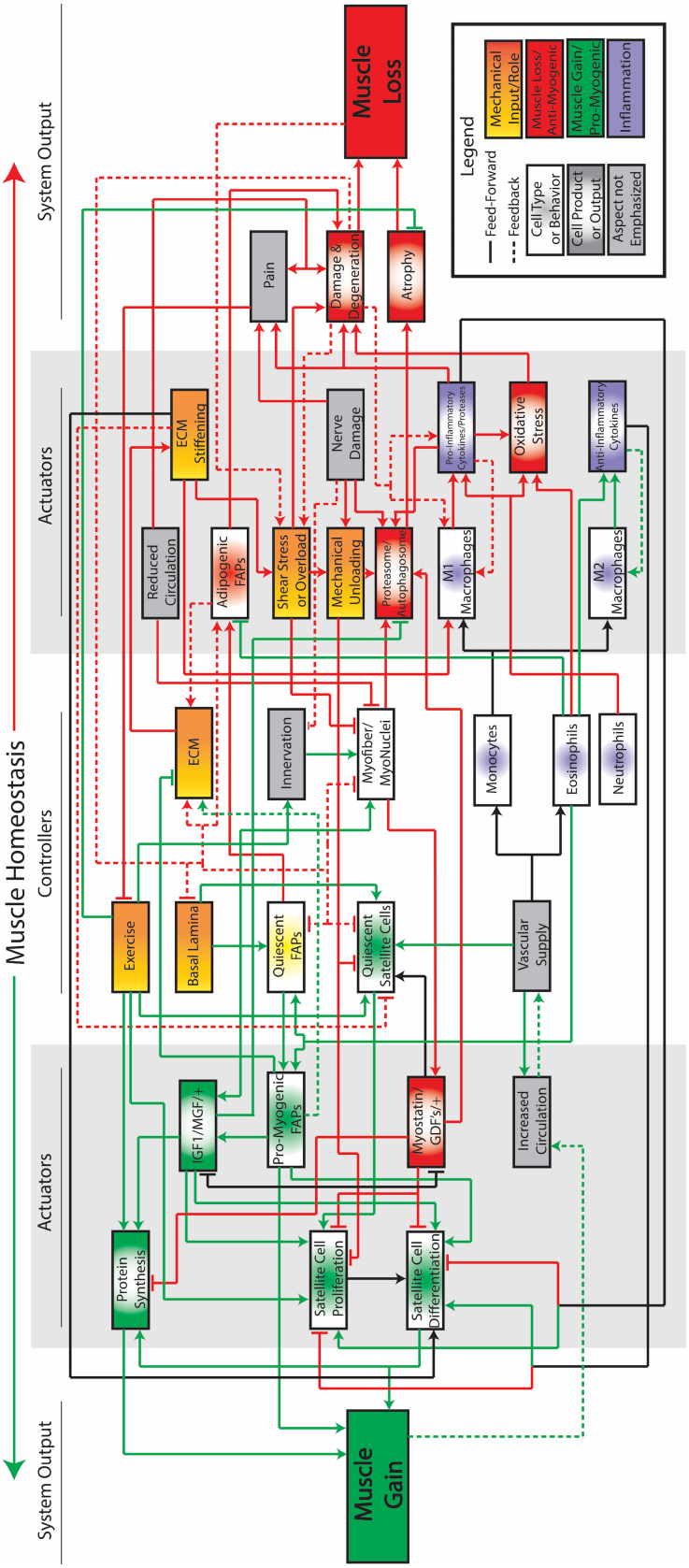
Muscle Homeostasis
System Output
Actuators
Controllers
Actuators
System Output
Muscle Loss
Muscle Gain
Pain
Damage & Degeneration
Atrophy
ECM Stiffening
Nerve Damage
Pro-Inflammatory Cytokines/Proteases
Oxidative Stress
Anti-Inflammatory Cytokines
Reduced Circulation
Adipogenic FAPs
Shear Stress or Overload
Mechanical Unloading
Proteasome/ Autophagosome
M1 Macrophages
M2 Macrophages
ECM
Innervation
Myofiber/ MyoNuclei
Monocytes
Eosinophils
Neutrophils
Exercise
Basal Lamina
Quiescent FAPs
Quiescent Satellite Cells
Vascular Supply
IGF1/MGF/+
Pro-Myogenic FAPs
Myostatin/ GDFs/+
Increased Circulation
Protein Synthesis
Satellite Cell Proliferation
Satellite Cell Differentiation
Legend
Feed-Forward
Feedback
Mechanical Input/Role
Muscle Loss/ Anti-Myogenic
Muscle Gain/ Pro-Myogenic
Inflammation
Cell Type or Behavior
Cell Product or Output
Aspect not Emphasized

The phenotype of muscle disuse atrophy is primarily the result of mechanical unloading, which can occur via tendon failure, bed rest, casting, hindlimb suspension (in rodents), or otherwise decreased voluntary muscle activation[10-14]. Nerve injury or dysfunction may also cause atrophy, though the atrophy phenotype in denervation has a distinct molecular signature compared to disuse[15]. Regardless of the inciting event, atrophy is characterized by increased contractile protein turnover coupled with diminished protein synthesis[15], leading to a reversible[13; 16; 17] reduction in muscle force-producing capacity. In RC disease, disuse muscle atrophy, absent a nerve injury, appears to dominate the early phase of RC disease[18-21] (Figure 2, Atrophic Stage).

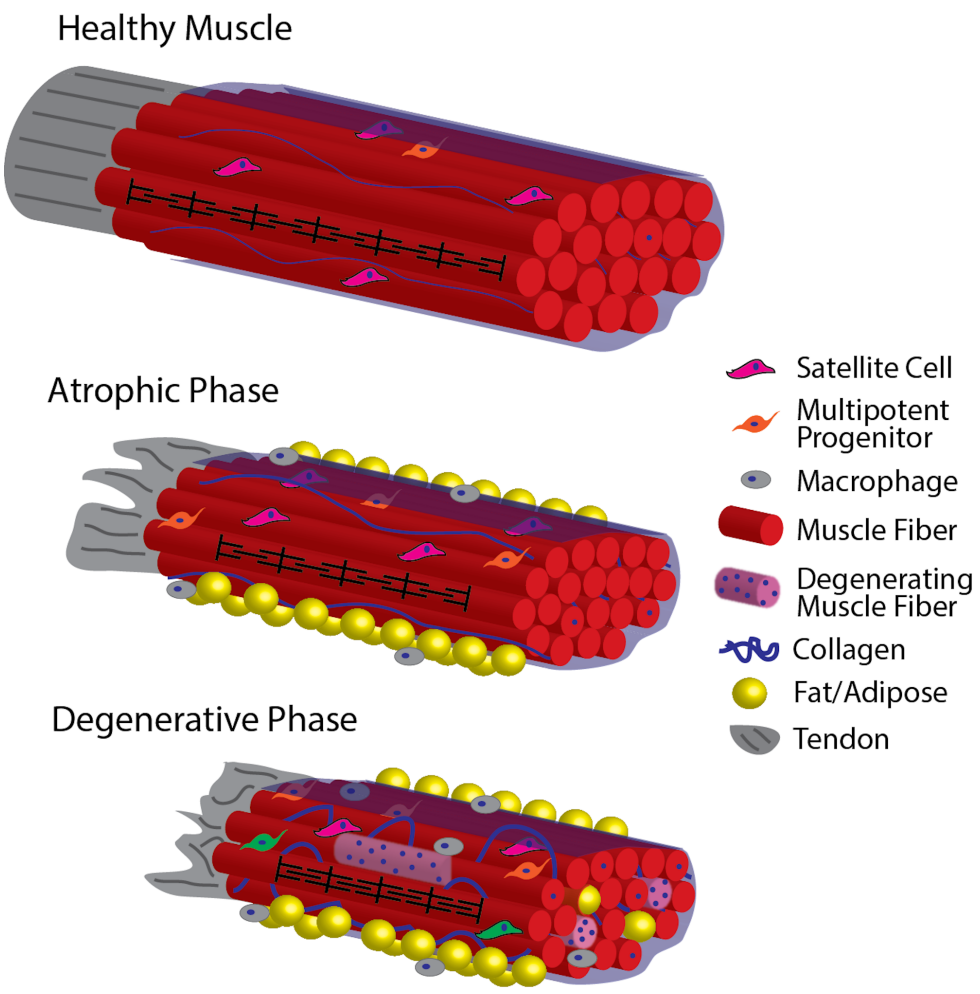

Figure 1.2 Schematic of progression of muscle pathology through different stages of RC disease. In healthy muscle with intact tendon (represented as a single fascicle connected to a tendon for simplicity), densely-packed muscle fibers are organized into fascicles by perimycium (translucent blue sheath), sarcomere length is maintained (black pattern on center-front fiber, not to scale), and muscle resident cells remain quiescent (note that cells are not to scale). With tendon disruption, RC muscle progresses to the atrophic disease stage, where muscle fibers become shorter, fiber cross-sectional area is reduced, and fat, fibrosis, and inflammation appear, while muscle architecture and overall muscle fiber and satellite cell numbers remain relatively constant. In the advanced, degenerative stage of RC disease, muscle fiber architecture is altered as sarcomeres remain chronically short, and damage and degeneration-regeneration becomes apparent (represented by the heterogeneous, hypercellular/myophagocytic light-pink fibers and centrally-nucleated, otherwise healthy fibers, respectively). The accumulation of inflammatory cells, collagen, and fat in both the inter-fascicular space (yellow spheres outside blue perimycium) and intra-fascicular space (yellow spheres between fibers) is more pronounced in the degenerative phase. Resident stem cell function is also disrupted in this stage of disease (represented in green in this schematic).

Contrary to muscle atrophy, which is self-limiting and not thought to alter overall muscle fiber structure, organization, or number[22], muscle fibers can also accumulate structural damage, leading to

altered sarcomere structure, degeneration and ultimately muscle fiber death (Figure 1, Damage/Degeneration). Altered mechanics are also implicated in this mode of muscle loss, though the mechanism is more complex than the unloading-induced muscle atrophy described above. For example, in other muscle pathologies including Duchenne muscular dystrophy[23-25], abnormal shear stress is implicated in sarcolemmal disruption. Muscle overloading, particularly during eccentric contraction, is known to induce muscle damage and regeneration[16; 17; 26-29] (Figure 1, Shear Stress or Overload). However, in these and other examples there are several mediators of muscle degeneration-regeneration that influence the rate and degree of muscle injury and recovery. These include inflammation and resident stem cell function, which are themselves influenced by passive changes in the micromechanical environment[26; 30-33] (Figure 1, ECM Stiffening). In advanced RC disease, muscle degeneration and reduced muscle fiber numbers driven by these mechanobiological changes appear to be the prominent mode of muscle loss[34] (Figure 2, Degenerative Stage).

Since RC disease progression can result in both unloading and overloading, the changing mechanobiological environment of the muscle can significantly impair the body's attempt at regeneration, and this in turn may explain the irreversible loss of muscle and poor surgical outcomes that define RC disease. In this review, we summarize our current understanding of biomechanical environment changes and specific aspects of that environment that contribute to the clinically intractable deficits that result from chronic RC tear at the whole muscle, muscle fiber, and single cell levels. In this context, we will highlight differences between the atrophic and degenerative aspects of disease, focusing on the roles of mechanical unloading and matrix stiffening and their detrimental effects on muscle physiology at each length scale.

Whole Muscle Remodeling After RC Injury

As RC tendon tears progress over time, the RC muscles become mechanically unloaded and begin to retract. Mechanical unloading is potentially compounded by pain-induced diminution of voluntary muscle contraction. Suprascapular nerve dysfunction may also impact muscle remodeling,

though the prevalence of neuropathy in RC tears appears to be limited[35]. As the muscle retracts, muscle fibers shorten via serial sarcomere subtraction[36] and the muscle becomes fibrotic[37] (discussed in further detail below). This causes the working range of the muscle to decrease, and it has been hypothesized to increase RC muscles' susceptibility to injury during repair given the high muscle tension and strain required to repair the retracted tendon to its footprint[38; 39].

A second consequence of chronic muscle retraction is increased muscle fiber-bundle stiffness[37; 40]. Because single fiber passive mechanics are not altered with RC tear, this stiffening is likely attributable to increased fibrosis, i.e. collagen content in the muscle[40] (Figure 1, ECM Stiffening). While fibrosis predicts stiffness to a degree[37; 40], the existing data suggests that muscle stiffness is dictated by additional variables. One possible contributor is reduced sarcomere number following tear, which would lead to higher average sarcomere strains for a given change in muscle length[36; 41]. Another possibility is that ECM modification, and not just content, dictate total ECM stiffness (and cell-ECM interactions). Specifically, increased collagen cross-linking (associated with increased stiffness[42]) has been demonstrated in degenerated RC tendon[43], though it has yet to be measured in RC muscle. Whether or not increased matrix stiffness is protective (via increased load distribution in passive stretch) or detrimental (via increased active shear stress) to muscle fibers remains unknown.

In contrast to tissue level stiffening, changes in whole muscle biomechanics are more complicated. Similar to findings in fiber bundles, a human case series[44] and two separate animal models[21; 45] found increased whole muscle stiffness over time following tendon transection. However, a cadaver study that involved samples with higher fat infiltration found that high fat accumulation correlated with softer muscle overall[46]. A possible explanation for these findings is that whole muscle stiffness tracks with fiber bundle stiffness until muscle tissue loss hits a critical threshold, at which point whole muscle mechanics are dictated by a combination of muscle- and non-muscle tissue mechanics. Indeed, one prevailing hypothesis is that accumulation of adipose tissue serves as a necessary mechanical buffer to counter changes in muscle volume and pennation angle, in order to preserve a maximum possible amount of muscle force producing capacity[47]. As RC disease progresses and stiff muscle[40; 48] is replaced by more

extensible fat[49], overall organ extensibility increases, even though there is no evidence suggesting that remaining muscle tissue becomes more extensible itself. The resulting tissue is a complex and compartmentalized biomechanical system, which can in turn give rise to significant but localized changes in the micromechanical environment that impact both individual muscle fibers and resident stem cells.

Mechanical (Un)Loading Drives Muscle Fiber Pathology

The paradigm of mechanical unloading followed by muscle remodeling, progressive muscle atrophy, and fat accumulation has been central to RC muscle research for over two decades[8]. In the literature, this process is often interchangeably referred to as 'fatty infiltration', 'fatty atrophy', and 'fatty degeneration', with the latter two referencing specific modes of muscle loss. In this section, we discuss the effects of RC tear on individual muscle fibers, highlighting the biological importance of differentiating muscle atrophy from degeneration and focusing on the differential role that mechanical loads play in each of these distinct mechanisms of muscle loss.

In parallel with alterations at the whole muscle level, individual muscle fibers undergo several detrimental changes as a result of chronic unloading, with distinct stages across the disease spectrum. In terms of muscle architecture, muscle fibers in full-thickness tears have decreased sarcomeric order and increased accumulation of small (<1μm) intracellular lipid droplets[50], but normal sarcomere length[41] is maintained via serial sarcomere subtraction[36; 51]. However in large or massive (>5cm retraction) RC tears, normal sarcomere remodeling is not observed, and sarcomeres are significantly shorter than in either intact or full thickness tears[36]. The implications of these findings are two-fold: first, this suggest that muscle with moderate tears are more likely than larger tears to remodel and remain functional after repair, and second, that repair of massive tears may fail due to a combination of over-strained sarcomeres immediately after repair and failure to adapt sarcomere length over time[36].

Beyond architectural changes, RC muscle undergoes continuous muscle loss throughout the course of disease. In the 'early' phase of disease, radial atrophy of the RC muscle occurs as mechanical load is reduced following smaller and/or less chronic RC tendon tear[18; 19] (Figure 1, Mechanical

Unloading, Atrophy; Figure 2, middle panel), possibly heightened by passive stress shielding resulting from the stiffer matrix discussed above, or inflammatory signals known to activate catabolic pathways within muscle discussed below[10; 11; 15; 52]. This atrophic muscle loss encompasses a cell-intrinsic, self-limiting process where protein turnover is tightly controlled by the interplay of anabolic[52] and catabolic[15] pathways; it is not generally considered a putative mechanism of muscle fiber deletion[22]. With decreased load, strain-dependent signaling proteins at the Z-disk[53] and costamere[54] become less active, leading to decreased anabolic signaling[52; 55] and increased signaling and activity of the two principal mechanisms of protein degradation in the cell: the ubiquitin-proteasome[55-57] and the autophagosome/lysosome[15] (Figure 1, Protein Synthesis, Proteasome/ Autophagosome). In muscle atrophy, proteins are freed from the Z-disk via the combined action of calpains[58; 59] and muscle-specific E3 ubiquitin ligases[56]. These freed contractile proteins are subsequently degraded, thus reducing the force-producing capacity of the muscle. Importantly, protein loss in muscle atrophy is highly specific; only ubiquitinated proteins are degraded, while proteins still anchored to the Z-disk are protected from the catabolic machinery and overall muscle architecture is preserved.

As RC disease progresses, the muscle is more likely to experience higher axial loads (due to diminished total cross-sectional area)[60] and higher shear forces when activated (due to increased stiffness of the matrix)[61; 62]. Both axial and shear stress are known cause direct mechanical injury to the sarcolemma[23; 27] (Figure 1, Shear Stress or Overload). This, along with potential increases in permeability caused by local inflammatory cells (discussed below)[61; 63], leads to increased calcium in the muscle fiber because of direct diffusion and sarcoplasmic reticulum disruption[64; 65]. Increased calcium may then increase calcium-sensitive calpain activity, which along with their role in contractile protein turnover in atrophy[65; 66] are also implicated in cellular apoptosis[67; 68] and necrosis[69]. Together with the direct overload/shear injury, these indirect mediators of protein turnover and cell death (as well as the hypothesized increase in oxidative stress and a protease-rich inflammatory environment discussed below) likely explain the recently described muscle damage and degeneration of muscle fibers found in advanced rotator cuff disease[34] (Figure 1, Damage and Degeneration).

Can Satellite Cells Maintain Muscle Homeostasis Post-Injury?

Satellite cells (SCs), the primary myogenic stem cell of adult muscle, play an integral role in adult myogenesis and homeostasis, particularly in the context of muscle's response to exercise/reloading[26; 70] and recovery from damage or injury[31; 71] (Figure 1, Quiescent Satellite Cells, Satellite Cell Proliferation/Differentiation). Notably, while SCs are required for muscle regeneration, they are dispensable in the context of fiber hypertrophy[72; 73]. Given the muscle degeneration present in advanced RC disease[34], understanding the fate of SCs in RC disease is paramount to understanding why muscle loss is generally irreversible after RC tear.

Like many other adult stem cells, the SC is highly dependent on it's physical environment, i.e. niche[74]. This niche consists of the region between the sarcolemma and the basal lamina of the muscle fiber[75], with SC fate determined by dynamic interactions with each structure[76] (Figure 1, Basal Lamina, ECM). The physical and biochemical composition of the niche is important in the maintenance of SC quiescence[77], potency[78], and possibly even myogenic fate[79], with ECM proteins and particularly collagens IV and VI playing a notable role in the regulation of SCs by the basal lamina[80; 81]. The dependency of SC function on niche composition suggests a central role of force transmission in the maintenance of SC stemness. Changes in matrix composition directly alter the way SCs experience load based on local niche stiffness[78], and may also affect SC focal adhesions based on altered integrin-binding substrate availability[82]. Alterations in the matrix also alter SC function indirectly because the matrix serves as a local reservoir and co-modulator of growth factors critical to SC modulation[78; 83; 84] (Figure 1, IGF1/MGF/+, Myostatin/GDF's/+). As mechanical loads change, the matrix undergoes damage and remodeling which determine the rate of release and/or sequestration of these factors[85; 86].

Indeed, SC function is highly dependent on niche stiffness (Figure 1, ECM Stiffening). During in vitro culture, SCs proliferate, self-renew, and differentiate best on substrates with normal muscle stiffness (~11kPa)[48; 87]. On stiff substrates (~10^6 kPa) differentiation into myotubes is favored[87], while the maintenance of quiescence is favored on softer substrates (~2kPa)[77]. In RC disease, increased matrix

stiffness may skew SCs toward differentiation and away from self-renewal, which may deplete the SC pool and diminish the muscle's regenerative capacity in the long run[88]. However, evaluation of this hypothesis is difficult, because although RC muscles have reduced SC populations compared to other muscles[89], once SCs are removed from the pathological environment of the torn RC, their proliferation, differentiation, and fusion characteristics are not different between no-tear and full-thickness tears[89].

Beyond the static stiffness of the niche, mechanical loading is also important in the maintenance and activation of the SC pool (Figure 1, Exercise, Mechanical Unloading, Satellite Cell Proliferation/Differentiation). SCs can be activated by mechanical loading in vitro[32] and exercise in vivo, though the effects of exercise are multifactorial and the relative contribution of mechanical load to overall exercise-induced activation is difficult to determine in vivo[16; 26; 90] (Figure 1, Exercise). The complementary finding is also true; in most models, unloading reduces total SC number and potency of remaining SCs[11]. Therefore, reduced muscle activity levels following RC tear in the atrophic stage of disease may ultimately contribute to diminished regenerative capacity in the degenerative phase of disease.

Further complicating the evaluation of SCs in the context of RC disease are other potential environmental contributors to SC dysfunction known to occur in the torn RC. The torn RC environment demonstrates altered expression of soluble factors[91-94] as well as increased inflammation[34; 95; 96] and oxidative stress[97-99], which are all potent mediators of SC function[30; 100; 101] that may be exacerbated by muscle injury. Pro-inflammatory signaling and oxidative stress stimulate SC proliferation, but blocks differentiation[100; 101] and self-renewal[102] via the TNF/TWEAK/NF-κB and Notch signaling axes, while anti-inflammatory signals aid in differentiation[103] (Figure 1, Monocytes, M1/M2 Macrophages, Eosinophils, Neutrophils, Pro-Inflammatory Cytokines/Proteases, Oxidative Stress, Anti-Inflammatory Cytokines). These effects may also be modulated by interplay of other myogenic regulatory factors that are likely altered in the torn RC, including members of the TGF-β superfamily (GDF and BMP subfamilies in particular)[52; 104] and IGF/GH axis[105-107], all of which influence SC dynamics (Figure 1, IGF1/MGF/+, Myostatin/GDF's/+). While classically 'pro-' and 'anti-' inflammatory or myogenic

signaling suggests a binary effect (i.e. either 'good' or 'bad'), the effects of these factors on muscle homeostasis are dependent on the environment as a whole. For example, in acute inflammatory situations, these factors are coordinated to promote muscle homeostasis, as proliferation of SCs occurs prior to fusion, regeneration, and return to quiescence[30; 76; 108; 109]. However, with chronic inflammation, prolonged pro-inflammatory and anti-myogenic signaling may simultaneously inhibit muscle regeneration and SC pool maintenance, leading to both short- and long-term deficits in muscle regenerative capacity.

Multipotent Progenitors – Potential Sources of Fat and Fibrosis

Progressive fat accumulation and fibrosis in RC tears at the whole-muscle level is indisputable, but the cell population(s) responsible remain unresolved. Further complicating our understanding of fat accumulation mechanisms is the finding that lipid-filled cells accumulate in distinct locations (epimuscular, interfascicular, and intrafascicular) within the muscle structure[34; 110], where lipid in different anatomical locations may be the result of disparate cellular processes or cell populations. SCs are theoretically capable of adopting an adipogenic fate[111; 112], and the lipid content of mature muscle fibers is known to increase with tear[50]. However, there is no current consensus on whether SCs can trans-differentiate into adipocytes in vivo[113; 114], and at a minimum the niche must be significantly manipulated in vitro to alter SC fate[115; 116].

Multipotent adipose stem cells (ASCs) have also been implicated in fat accumulation, particularly at the epimuscular border[110]. In this region, adjacent to existing fat depots, there is evidence that RC tear leads to a whitening of the normally beige epimuscular fat depot, with implications for paracrine signaling that may affect muscle regeneration[110]. Yet fat accumulation does not strictly proceed from the muscle border, particularly in more advanced disease[117]. As such, two additional native muscle stem cell populations, fibro/adipogenic progenitors (FAPs) and perivascular stem cells/pericytes have been the focus of research into the source of fat in torn RC muscle. A comprehensive discussion of the role of these cell types in skeletal muscle is beyond the scope of this review and can be found elsewhere[118; 119].

The bipotent FAP population, first described independently by Uezumi[120] and Joe[121] in 2010, is the most attractive candidate of the muscle resident cells implicated in RC disease progression (Figure 1, Quiescent FAPs). With an indispensible role in normal muscle regeneration (where they synthesize new, regenerative matrix)[122; 123] and ability to differentiate into either adipocytes or fibroblasts[120; 121] (Figure 1, Pro-Myogenic FAPs, Adipogenic FAPs), dysfunction of FAP's could be implicated in all three detrimental changes in torn RC (muscle loss, fibrosis/stiffening, and fat accumulation). Indeed, the conditions under which FAPs take on an adipogenic fate exist in the inflammatory environment of the torn human RC[123], and a small animal model has shown potential for adipogenic differentiation of FAPs in the context of RC tear[124].

Unlike FAPs, pericytes are a heterogeneous population[125], are not muscle specific, and are capable of differentiating into a wider array of mesenchymal cells, including skeletal muscle[126], adipocytes[127], fibroblasts[128; 129], and others[127; 130]. In non-muscle tissues, matrix stiffening causes pericytes to adopt a myofibroblast/fibrotic phenotype[128; 129], which leads to a positive fibrotic feedback loop[131]. In the same small animal RC tear model used to evaluate FAP fate, pericytes were found to contribute to both adipogenic and fibrogenic cell populations[124], though more stringent cell classification and more clinically relevant models (discussed below) are needed to definitively characterize and study the source(s) of adipocytes in RC disease.

A caveat to the findings presented in this section is that, due to a lack of a definitive marker for either FAPs or pericytes, studies of these cell populations are inherently studies of mixed populations that share a small number of specific markers. Of particular note is the overlap between markers for pericytes, FAPs, and many other subpopulations that are generally considered mesenchymal stem cells[132]. One such marker, PW1, is a good example of this conundrum; PW1+ stem cells have been found in many tissue types[133] and share many other markers and characteristics with pericytes, including myogenic potential[134], yet PW1+ cells and classical pericytes are distinct populations[135]. As such, differentiating between these cell populations remains a challenge, and complicates efforts to identify or describe a unique cell population primarily responsible for fat accumulation in RC disease, if such a population exists.

Mechanobiology of Inflammatory Cells – Regulating the Regulators

Infiltration and persistence of inflammatory cells is a key feature of the RC disease process in both tendon[5; 136] and muscle[34; 95]. Understanding inflammatory cell population dynamics is particularly important given the complex role of timing and specific inflammatory milieu in modulating the changes in muscle fibers and resident stem cells described in the preceding sections. Here, we will highlight findings in the broad field of inflammatory cell mechanobiology[137; 138] as they relate to the pathology of RC tears.

Inflammatory cells are known to accumulate in the tendon in the earliest stages of disease, where they are thought to modulate the degeneration of the tendon that eventually leads to muscle unloading[3; 96; 98; 139]. Therefore, it is possible that the original inflammatory response observed in RC muscles is the result of local degeneration-related signaling from the tendon. While it is unclear if RC tendon and muscle share common degenerative mechanisms at the cellular or molecular level, based on the high degree of physical and biochemical cross-talk between the two tissues[140; 141] it is possible that inflammatory or degenerative findings in muscle may inform research in tendon, and vice versa.

Of the inflammatory cell populations, the myeloid class generally and monocyte/macrophage subpopulation in particular is commonly implicated in modulating skeletal muscle responses to injury and disease[142] (Figure 1, Monocytes, Eosinophils, Neutrophils, M1/M2 Macrophages). While the complexity of the inflammatory milieu is beyond the scope of this review and has been reviewed elsewhere[143; 144], in general, when muscle fibers and surrounding matrix are damaged in healthy muscle, myeloid cells are recruited to the injury region by a combination of released cytokines/chemokines and subsequent increased matrix permeability[145]. This acute inflammation is marked by M1 macrophage polarization[146] and release of pro-inflammatory cytokines[142] and proteases[147]. Resolution, characterized by M2 macrophage polarization[146] and expression of anti-inflammatory and often pro-fibrotic and pro-survival cytokine and growth factor release, quickly follows in non-pathological situations[103]. This normal regenerative cascade appears to be altered in RC disease.

Increased matrix stiffening and matrix remodeling in RC disease likely influence both inflammatory cell migration[148] and cytokine release profile, skewing toward reduced migration speed[149] and prolonged, enhanced release of pro-inflammatory cytokines[150] on stiffer matrix (though these findings have not been evaluated specifically in RC muscle). While in some diseases abnormal inflammation alone is enough to drive muscle damage and degeneration[151], it remains to be seen whether pro-inflammatory cells and signals are active participants in RC muscle degeneration, or if persistent inflammation is the result of continual muscle injury.

Clinical Considerations and Concerns of Pre-Clinical Models

These findings have important clinical significance, but many questions still remain. Muscle atrophy and degeneration are fundamentally different mechanisms of muscle loss, and must thus be treated with fundamentally different interventions. From a rehabilitation perspective, selecting the correct intervention is complicated by the existence of both modes of muscle loss along the spectrum of disease. Mechanical reloading (i.e. exercise and/or tendon repair) is generally sufficient to recover from atrophy[13; 16; 17; 152], including limited evidence for this finding in RC[153]. But in a stiff, degenerating muscle, exercise and the damage that may result from mechanical overload may accelerate the pace of muscle loss[23; 25; 34]. In torn RC this is particularly concerning, as the normal inflammatory and regenerative processes that are associated with positive muscle changes following exercise are likely impaired[30; 102; 150].

In terms of surgical intervention and repair, the altered muscle architecture and increased stiffness must be considered, particularly in chronic, massive tears[154-156]. These pathological changes suggest that repair of large tears may be futile from a functional standpoint, as repair may cause more damage[38] and the muscle may not adapt sarcomere number and length normally[36]. Tendon repair alone is also unlikely to ameliorate the pro-degenerative/anti-regenerative environment of the chronically torn cuff, further diminishing the likelihood of successful functional restoration in large and massive tears. Given these findings, two issues still remain: our ability to reliably measure these important biological phenomena

clinically, and a framework in which this type of biomechanical and biological information can be used for clinical and surgical decision-making.

Two final confounding issues in studying the biomechanical and cellular regulators of RC disease are discrepancies between animal models and human patients or patient-derived cells, and inconsistencies in findings between different laboratories. Briefly, while large animal models recapitulate the muscle stiffening and atrophy found in the early phase of RC disease[18; 19; 21; 40; 45], small animal models require a nerve injury (denervation) to achieve a similar phenotype[157-159]. However, nerve injury (denervation in particular) is a relatively rare feature of clinical RC disease, and may confound results from such models as the mechanisms of denervation atrophy and disuse atrophy are not equivalent[15]. To date, no animal model has demonstrated the accumulation of muscle damage and cellular degeneration found in humans, and only the sheep model seems to accumulate fat to a degree that is similar to patients with advanced disease[21]. This is problematic when trying to translate animal research to the clinic, as preclinical models do not share the disease processes that govern the most intractable clinical cases. Complicating this issue are differences in cell markers and behavior between humans and animals, differences in patient demographics between human studies, and inconsistencies in isolation methods that are used to identify SCs, FAPs, and pericytes. This leads to potentially significant and confounding discrepancies between the cell populations evaluated from model to model and study to study, and likely contributes to the conflicting effects of various factors on resident cell dynamics reported in different publications.

Conclusions

Skeletal muscle is in a constant state of dynamic equilibrium between contractile protein gain and loss. In RC disease, the role of the macro- and micro-mechanical environment is paramount. The initial insult to the muscle is fundamentally an unloading event, where tendon tear and pain lead to direct mechanical unloading and indirect disuse, both of which lead to muscle atrophy. The secondary and tertiary effects of the initial unloading insult are also mechanically sensitive. With prolonged retraction of the muscle, the matrix becomes stiff, leading to potentially increased incidence of muscle damage while

simultaneously creating an environment in which regeneration is likely inhibited, which may help explain the progressive, irreversible muscle loss due to degeneration observed in RC disease.

Acknowledgements

We would like to acknowledge funding from the National Institutes of Health (NIAMS T32-AR060712, M.C.G. and NICHD R01-HD073180 S.R.W.) and the Muscular Dystrophy Association (241665 A.J.E.). We have no conflicts of interest to disclose.

This chapter, in full, is a reprint of the material as it appears in the Journal of Orthopedic Research 2018. Michael C. Gibbons, Anshu Singh, Adam J. Engler, Samuel R. Ward. The dissertation/thesis author was the primary investigator of this material.

References

1. Yamamoto A, Takagishi K, Osawa T, Yanagawa T, Nakajima D, Shitara H, Kobayashi T. 2010. Prevalence and risk factors of a rotator cuff tear in the general population. Journal of Shoulder and Elbow Surgery 19:116-120.

2. Brooks C, Revell W, Heatley F. 1992. A quantitative histological study of the vascularity of the rotator cuff tendon. Journal of Bone & Joint Surgery, British Volume 74:151-153.

3. Longo UG, Franceschi F, Ruzzini L, Rabitti C, Morini S, Maffulli N, Denaro V. 2008. Histopathology of the supraspinatus tendon in rotator cuff tears. The American journal of sports medicine 36:533-538.

4. Lundgreen K, Lian Ø, Scott A, Engebretsen L. 2013. Increased levels of apoptosis and p53 in partial-thickness supraspinatus tendon tears. Knee Surgery, Sports Traumatology, Arthroscopy 21:1636-1641.

5. Matthews T, Hand G, Rees J, Athanasou N, Carr A. 2006. Pathology of the torn rotator cuff tendon. Bone & Joint Journal 88:489-495.

6. Riley G, Goddard M, Hazleman B. 2001. Histopathological assessment and pathological significance of matrix degeneration in supraspinatus tendons. Rheumatology 40:229-230.

7. Gladstone JN, Bishop JY, Lo IK, Flatow EL. 2007. Fatty infiltration and atrophy of the rotator cuff do not improve after rotator cuff repair and correlate with poor functional outcome. The American journal of sports medicine 35:719-728.

8. Goutallier D, Postel J-M, Bernageau J, Lavau L, Voisin M-C. 1994. Fatty muscle degeneration in cuff ruptures: pre-and postoperative evaluation by CT scan. Clinical orthopaedics and related research 304:78-83.

9. Hebert-Davies J, Teefey SA, Steger-May K, Chamberlain AM, Middleton W, Robinson K, Yamaguchi K, Keener JD. 2017. Progression of Fatty Muscle Degeneration in Atraumatic Rotator Cuff Tears. JBJS 99:832-839.

10. Bialek P, Morris CA, Parkington J, Andre MS, Owens J, Yaworsky P, Seeherman H, Jelinsky SA. 2011. Distinct protein degradation profiles are induced by different disuse models of skeletal muscle atrophy. Physiological genomics.

11. Brooks NE, Myburgh KH. 2014. Skeletal muscle wasting with disuse atrophy is multi-dimensional: the response and interaction of myonuclei, satellite cells and signaling pathways. Frontiers in physiology 5:99.

12. Clark BC. 2009. In vivo alterations in skeletal muscle form and function after disuse atrophy. Medicine and science in sports and exercise 41:1869-1875.

13. Jones SW, Hill RJ, Krasney PA, O'CONNER B, Peirce N, Greenhaff PL. 2004. Disuse atrophy and exercise rehabilitation in humans profoundly affects the expression of genes associated with the regulation of skeletal muscle mass. The FASEB journal 18:1025-1027.

14. Reardon KA, Davis J, Kapsa RM, Choong P, Byrne E. 2001. Myostatin, insulin-like growth factor-1, and leukemia inhibitory factor mRNAs are upregulated in chronic human disuse muscle atrophy. Muscle & nerve 24:893-899.

15. Bonaldo P, Sandri M. 2013. Cellular and molecular mechanisms of muscle atrophy. Disease models & mechanisms 6:25-39.

16. Darr KC, Schultz E. 1987. Exercise-induced satellite cell activation in growing and mature skeletal muscle. Journal of Applied Physiology 63:1816-1821.

17. Schoenfeld BJ. 2012. Does exercise-induced muscle damage play a role in skeletal muscle hypertrophy? The Journal of Strength & Conditioning Research 26:1441-1453.

18. Lundgreen K, Lian ØB, Engebretsen L, Scott A. 2013. Lower muscle regenerative potential in full-thickness supraspinatus tears compared to partial-thickness tears. Acta orthopaedica 84:565-570.

19. Steinbacher P, Tauber M, Kogler S, Stoiber W, Resch H, Sänger A. 2010. Effects of rotator cuff ruptures on the cellular and intracellular composition of the human supraspinatus muscle. Tissue and Cell 42:37-41.

20. Zanotti RM, Carpenter JE, Blasier RB, Greenfield MLV, Adler RS, Bromberg MB. 1997. The low incidence of suprascapular nerve injury after primary repair of massive rotator cuff tears. Journal of Shoulder and Elbow Surgery 6:258-264.

21. Gerber C, Meyer D, Schneeberger A, Hoppeler H, Von Rechenberg B. 2004. Effect of tendon release and delayed repair on the structure of the muscles of the rotator cuff: an experimental study in sheep. The Journal of Bone & Joint Surgery 86:1973-1982.

22. Cardenas D, Stolov W, Hardy R. 1977. Muscle fiber number in immobilization atrophy. Archives of physical medicine and rehabilitation 58:423-426.

23. Petrof BJ. 1998. The molecular basis of activity-induced muscle injury in Duchenne muscular dystrophy. Molecular and cellular biochemistry 179:111-124.

24. McArdle A, Edwards R, Jackson M. 1995. How does dystrophin deficiency lead to muscle degeneration?—evidence from the mdx mouse. Neuromuscular Disorders 5:445-456.

25. Wallace GQ, McNally EM. 2009. Mechanisms of muscle degeneration, regeneration, and repair in the muscular dystrophies. Annual review of physiology 71:37-57.

26. Crameri RM, Langberg H, Magnusson P, Jensen CH, Schrøder HD, Olesen JL, Suetta C, Teisner B, Kjaer M. 2004. Changes in satellite cells in human skeletal muscle after a single bout of high intensity exercise. The Journal of physiology 558:333-340.

27. Friden J, Lieber R. 2001. Eccentric exercise-induced injuries to contractile and cytoskeletal muscle fibre components. Acta Physiologica Scandinavica 171:321-326.

28. Friden J, Lieber RL. 1992. Structural and mechanical basis of exercise-induced muscle injury. Medicine and science in sports and exercise 24:521-530.

29. Buford TW, MacNeil RG, Clough LG, Dirain M, Sandesara B, Pahor M, Manini TM, Leeuwenburgh C. 2014. Active muscle regeneration following eccentric contraction-induced

injury is similar between healthy young and older adults. Journal of Applied Physiology 116:1481-1490.

30. Palacios D, Mozzetta C, Consalvi S, Caretti G, Saccone V, Proserpio V, Marquez VE, Valente S, Mai A, Forcales SV. 2010. TNF/p38α/polycomb signaling to Pax7 locus in satellite cells links inflammation to the epigenetic control of muscle regeneration. Cell stem cell 7:455-469.

31. Sambasivan R, Yao R, Kissenpfennig A, Van Wittenberghe L, Paldi A, Gayraud-Morel B, Guenou H, Malissen B, Tajbakhsh S, Galy A. 2011. Pax7-expressing satellite cells are indispensable for adult skeletal muscle regeneration. Development 138:3647-3656.

32. Tatsumi R, Sheehan S, Iwasaki H, Hattori A, Allen R. 2001. Mechanical stretch induces activation of skeletal muscle satellite cells in vitro. Experimental cell research 267:107-114.

33. Porter JD, Khanna S, Kaminski HJ, Rao JS, Merriam AP, Richmonds CR, Leahy P, Li J, Guo W, Andrade FH. 2002. A chronic inflammatory response dominates the skeletal muscle molecular signature in dystrophin-deficient mdx mice. Human Molecular Genetics 11:263-272.

34. Gibbons MC, Singh A, Anakwenze O, Cheng T, Pomerantz M, Schenk S, Engler AJ, Ward SR. 2017. Histological Evidence of Muscle Degeneration in Advanced Human Rotator Cuff Disease. The Journal of Bone & Joint Surgery 99:190-199.

35. Bachasson D, Singh A, Shah SB, Lane JG, Ward SR. 2015. The role of the peripheral and central nervous systems in rotator cuff disease. Journal of Shoulder and Elbow Surgery 24:1322-1335.

36. Gibbons MC, Sato EJ, Bachasson D, Cheng T, Azimi H, Schenk S, Engler AJ, Singh A, Ward SR. 2016. Muscle architectural changes after massive human rotator cuff tear. Journal of Orthopaedic Research.

37. Sato EJ, Killian ML, Choi AJ, Lin E, Esparza MC, Galatz LM, Thomopoulos S, Ward SR. 2014. Skeletal muscle fibrosis and stiffness increase after rotator cuff tendon injury and neuromuscular compromise in a rat model. Journal of Orthopaedic Research 32:1111-1116.

38. Davis ME, Stafford PL, Jergenson MJ, Bedi A, Mendias CL. 2015. Muscle fibers are injured at the time of acute and chronic rotator cuff repair. Clinical Orthopaedics and Related Research® 473:226-232.

39. Gerber C, Meyer DC, Frey E, von Rechenberg B, Hoppeler H, Frigg R, Jost B, Zumstein MA. 2009. Neer Award 2007: Reversion of structural muscle changes caused by chronic rotator cuff tears using continuous musculotendinous traction. An experimental study in sheep. Journal of Shoulder and Elbow Surgery 18:163-171.

40. Silldorff MD, Choo AD, Choi AJ, Lin E, Carr JA, Lieber RL, Lane JG, Ward SR. 2014. Effect of Supraspinatus Tendon Injury on Supraspinatus and Infraspinatus Muscle Passive Tension and Associated Biochemistry. The Journal of Bone & Joint Surgery 96:e175.

41. Ward SR, Hentzen ER, Smallwood LH, Eastlack RK, Burns KA, Fithian DC, Friden J, Lieber RL. 2006. Rotator cuff muscle architecture: implications for glenohumeral stability. Clinical orthopaedics and related research 448:157-163.

42. Reddy GK. 2004. Cross-linking in collagen by nonenzymatic glycation increases the matrix stiffness in rabbit achilles tendon. Experimental Diabetes Research 5:143-153.

43. Bank RA, TeKoppele JM, Oostingh G, Hazleman BL, Riley GP. 1999. Lysylhydroxylation and non-reducible crosslinking of human supraspinatus tendon collagen: changes with age and in chronic rotator cuff tendinitis. Annals of the Rheumatic Diseases 58:35-41.

44. Hersche O, Gerber C. 1998. Passive tension in the supraspinatus musculotendinous unit after long-standing rupture of its tendon: a preliminary report. Journal of Shoulder and Elbow Surgery 7:393-396.

45. Safran O, Derwin KA, Powell K, Iannotti JP. 2005. Changes in rotator cuff muscle volume, fat content, and passive mechanics after chronic detachment in a canine model. J Bone Joint Surg Am 87:2662-2670.

46. Giambini H, Hatta T, Krzysztof GR, Widholm P, Karlsson A, Leinhard OD, Adkins MC, Zhao C, An KN. 2017. Intramuscular Fat Infiltration Evaluated by Magnetic Resonance Imaging Predicts the Extensibility of the Supraspinatus Muscle. Muscle & Nerve.

47. Meyer DC, Hoppeler H, von Rechenberg B, Gerber C. 2004. A pathomechanical concept explains muscle loss and fatty muscular changes following surgical tendon release. Journal of orthopaedic research 22:1004-1007.

48. Engler AJ, Griffin MA, Sen S, Bönnemann CG, Sweeney HL, Discher DE. 2004. Myotubes differentiate optimally on substrates with tissue-like stiffness. J Cell Biol 166:877-887.

49. Comley K, Fleck NA. 2010. A micromechanical model for the Young's modulus of adipose tissue. International Journal of Solids and Structures 47:2982-2990.

50. Mendias CL, Roche SM, Harning JA, Davis ME, Lynch EB, Enselman ERS, Jacobson JA, Claflin DR, Calve S, Bedi A. 2015. Reduced muscle fiber force production and disrupted myofibril architecture in patients with chronic rotator cuff tears. Journal of Shoulder and Elbow Surgery 24:111-119.

51. Tomioka T, Minagawa H, Kijima H, Yamamoto N, Abe H, Maesani M, Kikuchi K, Abe H, Shimada Y, Itoi E. 2009. Sarcomere length of torn rotator cuff muscle. Journal of Shoulder and Elbow Surgery 18:955-959.

52. Glass DJ. 2005. Skeletal muscle hypertrophy and atrophy signaling pathways. Int J Biochem Cell Biol 37:1974-1984.

53. Miller MK, Bang M-L, Witt CC, Labeit D, Trombitas C, Watanabe K, Granzier H, McElhinny AS, Gregorio CC, Labeit S. 2003. The muscle ankyrin repeat proteins: CARP, ankrd2/Arpp and DARP as a family of titin filament-based stress response molecules. Journal of molecular biology 333:951-964.

54. Peter AK, Cheng H, Ross RS, Knowlton KU, Chen J. 2011. The costamere bridges sarcomeres to the sarcolemma in striated muscle. Progress in pediatric cardiology 31:83-88.

55. Glass DJ. 2003. Molecular mechanisms modulating muscle mass. Trends in molecular medicine 9:344-350.

56. Bodine SC, Latres E, Baumhueter S, Lai VK-M, Nunez L, Clarke BA, Poueymirou WT, Panaro FJ, Na E, Dharmarajan K. 2001. Identification of ubiquitin ligases required for skeletal muscle atrophy. Science 294:1704-1708.

57. Mitch WE, Goldberg AL. 1996. Mechanisms of muscle wasting—the role of the ubiquitin–proteasome pathway. New England Journal of Medicine 335:1897-1905.

58. Bartoli M, Richard I. 2005. Calpains in muscle wasting. The international journal of biochemistry & cell biology 37:2115-2133.

59. Huang J, Forsberg NE. 1998. Role of calpain in skeletal-muscle protein degradation. Proceedings of the national academy of sciences 95:12100-12105.

60. Demiray H. 1972. A note on the elasticity of soft biological tissues. Journal of biomechanics 5:309-311.

61. McNeil PL, Steinhardt RA. 1997. Loss, restoration, and maintenance of plasma membrane integrity. The Journal of cell biology 137:1-4.

62. Trotter J. 1993. Functional morphology of force transmission in skeletal muscle. Cells Tissues Organs 146:205-222.

63. Bradley W, Fulthorpe J. 1978. Studies of sarcolemmal integrity in myopathic muscle. Neurology 28:670-670.

64. Turner PR, Fong P, Denetclaw WF, Steinhardt RA. 1991. Increased calcium influx in dystrophic muscle. The Journal of cell biology 115:1701-1712.

65. Turner PR, Westwood T, Regen CM, Steinhardt RA. 1988. Increased protein degradation results from elevated free calcium levels found in muscle from mdx mice. Nature 335:735-738.

66. Alderton JM, Steinhardt RA. 2000. Calcium influx through calcium leak channels is responsible for the elevated levels of calcium-dependent proteolysis in dystrophic myotubes. Journal of Biological Chemistry 275:9452-9460.

67. Squier MK, Miller AC, Malkinson AM, Cohen JJ. 1994. Calpain activation in apoptosis. Journal of cellular physiology 159:229-237.

68. Orrenius S, Zhivotovsky B, Nicotera P. 2003. Regulation of cell death: the calcium–apoptosis link. Nature reviews Molecular cell biology 4:552-565.

69. Spencer MJ, Mellgren RL. 2002. Overexpression of a calpastatin transgene in mdx muscle reduces dystrophic pathology. Human Molecular Genetics 11:2645-2655.

70. Wang X, Kawano F, Matsuoka Y, Fukunaga K, Terada M, Sudoh M, Ishihara A, Ohira Y. 2006. Mechanical load-dependent regulation of satellite cell and fiber size in rat soleus muscle. American Journal of Physiology-Cell Physiology 290:C981-C989.

71. Lepper C, Partridge TA, Fan C-M. 2011. An absolute requirement for Pax7-positive satellite cells in acute injury-induced skeletal muscle regeneration. Development 138:3639-3646.

72. Lee S-J, Huynh TV, Lee Y-S, Sebald SM, Wilcox-Adelman SA, Iwamori N, Lepper C, Matzuk MM, Fan C-M. 2012. Role of satellite cells versus myofibers in muscle hypertrophy induced by inhibition of the myostatin/activin signaling pathway. Proceedings of the National Academy of Sciences 109:E2353-E2360.

73. McCarthy JJ, Mula J, Miyazaki M, Erfani R, Garrison K, Farooqui AB, Srikuea R, Lawson BA, Grimes B, Keller C. 2011. Effective fiber hypertrophy in satellite cell-depleted skeletal muscle. Development 138:3657-3666.

74. Yin H, Price F, Rudnicki MA. 2013. Satellite cells and the muscle stem cell niche. Physiological reviews 93:23-67.

75. Mauro A. 1961. Satellite cell of skeletal muscle fibers. The Journal of biophysical and biochemical cytology 9:493-495.

76. Kuang S, Kuroda K, Le Grand F, Rudnicki MA. 2007. Asymmetric self-renewal and commitment of satellite stem cells in muscle. Cell 129:999-1010.

77. Quarta M, Brett JO, DiMarco R, De Morree A, Boutet SC, Chacon R, Gibbons MC, Garcia VA, Su J, Shrager JB. 2016. An artificial niche preserves the quiescence of muscle stem cells and enhances their therapeutic efficacy. Nature biotechnology.

78. Thomas K, Engler AJ, Meyer GA. 2015. Extracellular matrix regulation in the muscle satellite cell niche. Connective tissue research 56:1-8.

79. Hosoyama T, Ishiguro N, Yamanouchi K, Nishihara M. 2009. Degenerative muscle fiber accelerates adipogenesis of intramuscular cells via RhoA signaling pathway. Differentiation 77:350-359.

80. Urciuolo A, Quarta M, Morbidoni V, Gattazzo F, Molon S, Grumati P, Montemurro F, Tedesco FS, Blaauw B, Cossu G. 2013. Collagen VI regulates satellite cell self-renewal and muscle regeneration. Nature communications 4.

81. Sanes JR. 2003. The basement membrane/basal lamina of skeletal muscle. Journal of Biological Chemistry 278:12601-12604.

82. Carson JA, Wei L. 2000. Integrin signaling9s potential for mediating gene expression in hypertrophying skeletal muscle. Journal of applied physiology 88:337-343.

83. Hynes RO. 2009. The extracellular matrix: not just pretty fibrils. Science 326:1216-1219.

84. Bentzinger CF, Wang YX, von Maltzahn J, Soleimani VD, Yin H, Rudnicki MA. 2013. Fibronectin regulates Wnt7a signaling and satellite cell expansion. Cell stem cell 12:75-87.

85. Taipale J, Keski-Oja J. 1997. Growth factors in the extracellular matrix. The FASEB Journal 11:51-59.

86. Hinz B. 2015. The extracellular matrix and transforming growth factor-β1: Tale of a strained relationship. Matrix Biology 47:54-65.

87. Gilbert PM, Havenstrite KL, Magnusson KE, Sacco A, Leonardi NA, Kraft P, Nguyen NK, Thrun S, Lutolf MP, Blau HM. 2010. Substrate elasticity regulates skeletal muscle stem cell self-renewal in culture. Science 329:1078-1081.

88. Shefer G, Van de Mark DP, Richardson JB, Yablonka-Reuveni Z. 2006. Satellite-cell pool size does matter: defining the myogenic potency of aging skeletal muscle. Developmental biology 294:50-66.

89. Meyer GA, Farris AL, Sato E, Gibbons M, Lane JG, Ward SR, Engler AJ. 2015. Muscle progenitor cell regenerative capacity in the torn rotator cuff. Journal of Orthopaedic Research 33:421-429.

90. Kadi F, Schjerling P, Andersen LL, Charifi N, Madsen JL, Christensen LR, Andersen JL. 2004. The effects of heavy resistance training and detraining on satellite cells in human skeletal muscles. The Journal of physiology 558:1005-1012.

91. Choo A, McCarthy M, Pichika R, Sato EJ, Lieber RL, Schenk S, Lane JG, Ward SR. 2014. Muscle Gene Expression Patterns in Human Rotator Cuff Pathology. The Journal of Bone & Joint Surgery 96:1558-1565.

92. Davies MR, Liu X, Lee L, Laron D, Ning AY, Kim HT, Feeley BT. 2016. TGF-β Small Molecule Inhibitor SB431542 Reduces Rotator Cuff Muscle Fibrosis and Fatty Infiltration By Promoting Fibro/Adipogenic Progenitor Apoptosis. PloS one 11:e0155486.

93. De Giorgi S, Saracino M, Castagna A. 2013. Degenerative disease in rotator cuff tears: what are the biochemical and histological changes? Joints 2:26-28.

94. Flück M, Ruoss S, Möhl CB, Valdivieso P, Benn MC, von Rechenberg B, Laczko E, Hu J, Wieser K, Meyer DC. 2016. Genomic and lipidomic actions of nandrolone on detached rotator cuff muscle in sheep. The Journal of Steroid Biochemistry and Molecular Biology.

95. Gumucio JP, Davis ME, Bradley JR, Stafford PL, Schiffman CJ, Lynch EB, Claflin DR, Bedi A, Mendias CL. 2012. Rotator cuff tear reduces muscle fiber specific force production and induces macrophage accumulation and autophagy. Journal of Orthopaedic Research 30:1963-1970.

96. Perry SM, McIlhenny SE, Hoffman MC, Soslowsky LJ. 2005. Inflammatory and angiogenic mRNA levels are altered in a supraspinatus tendon overuse animal model. Journal of Shoulder and Elbow Surgery 14:S79-S83.

97. Morikawa D, Itoigawa Y, Nojiri H, Sano H, Itoi E, Saijo Y, Kaneko K, Shimizu T. 2014. Contribution of oxidative stress to the degeneration of rotator cuff entheses. Journal of Shoulder and Elbow Surgery 23:628-635.

98. Wang M-X, Wei A, Yuan J, Clippe A, Bernard A, Knoops B, Murrell GA. 2001. Antioxidant enzyme peroxiredoxin 5 is upregulated in degenerative human tendon. Biochemical and biophysical research communications 284:667-673.

99. Gumucio J, Rittman D, McDonagh B, Mendias C. 2016. Molecular mechanisms behind the accumulation of lipid that occurs after skeletal muscle injury. The FASEB Journal 30:1244.1248-1244.1248.

100. Kozakowska M, Pietraszek-Gremplewicz K, Jozkowicz A, Dulak J. 2015. The role of oxidative stress in skeletal muscle injury and regeneration: focus on antioxidant enzymes. Journal of muscle research and cell motility 36:377-393.

101. Chen S-E, Jin B, Li Y-P. 2007. TNF-α regulates myogenesis and muscle regeneration by activating p38 MAPK. American Journal of Physiology-Cell Physiology 292:C1660-C1671.

102. Ogura Y, Mishra V, Hindi SM, Kuang S, Kumar A. 2013. Proinflammatory cytokine TWEAK suppresses satellite cell self-renewal through inversely modulating Notch and NF-κB signaling pathways. Journal of Biological Chemistry:jbc. M113. 517300.

103. Arnold L, Henry A, Poron F, Baba-Amer Y, Van Rooijen N, Plonquet A, Gherardi RK, Chazaud B. 2007. Inflammatory monocytes recruited after skeletal muscle injury switch into antiinflammatory macrophages to support myogenesis. The Journal of experimental medicine 204:1057-1069.

104. Trendelenburg AU, Meyer A, Rohner D, Boyle J, Hatakeyama S, Glass DJ. 2009. Myostatin reduces Akt/TORC1/p70S6K signaling, inhibiting myoblast differentiation and myotube size. American Journal of Physiology-Cell Physiology 296:C1258-C1270.

105. Stitt TN, Drujan D, Clarke BA, Panaro F, Timofeyva Y, Kline WO, Gonzalez M, Yancopoulos GD, Glass DJ. 2004. The IGF-1/PI3K/Akt pathway prevents expression of muscle atrophy-induced ubiquitin ligases by inhibiting FOXO transcription factors. Molecular cell 14:395-403.

106. Rabinovsky ED, Gelir E, Gelir S, Lui H, Kattash M, DeMayo FJ, Shenaq SM, Schwartz RJ. 2003. Targeted expression of IGF-1 transgene to skeletal muscle accelerates muscle and motor neuron regeneration. The FASEB Journal 17:53-55.

107. Tonkin J, Temmerman L, Sampson RD, Gallego-Colon E, Barberi L, Bilbao D, Schneider MD, Musarò A, Rosenthal N. 2015. Monocyte/Macrophage-derived IGF-1 Orchestrates Murine Skeletal Muscle Regeneration and Modulates Autocrine Polarization. Molecular Therapy.

108. Bentzinger CF, Wang YX, Dumont NA, Rudnicki MA. 2013. Cellular dynamics in the muscle satellite cell niche. EMBO reports 14:1062-1072.

109. Charge SB, Rudnicki MA. 2004. Cellular and molecular regulation of muscle regeneration. Physiological reviews 84:209-238.

110. Meyer GA, Gibbons MC, Sato E, Lane JG, Ward SR, Engler AJ. 2015. Epimuscular Fat in the Human Rotator Cuff Is a Novel Beige Depot. Stem cells translational medicine:sctm. 2014-0287.

111. Asakura A, Rudnicki MA, Komaki M. 2001. Muscle satellite cells are multipotential stem cells that exhibit myogenic, osteogenic, and adipogenic differentiation. Differentiation 68:245-253.

112. Delaigle AlM, Jonas J-C, Bauche IB, Cornu O, Brichard SM. 2004. Induction of adiponectin in skeletal muscle by inflammatory cytokines: in vivo and in vitro studies. Endocrinology 145:5589-5597.

113. Starkey JD, Yamamoto M, Yamamoto S, Goldhamer DJ. 2011. Skeletal muscle satellite cells are committed to myogenesis and do not spontaneously adopt nonmyogenic fates. Journal of Histochemistry & Cytochemistry 59:33-46.

114. Shefer G, Wleklinski-Lee M, Yablonka-Reuveni Z. 2004. Skeletal muscle satellite cells can spontaneously enter an alternative mesenchymal pathway. Journal of cell science 117:5393-5404.

115. Yin H, Pasut A, Soleimani VD, Bentzinger CF, Antoun G, Thorn S, Seale P, Fernando P, van IJcken W, Grosveld F. 2013. MicroRNA-133 controls brown adipose determination in skeletal muscle satellite cells by targeting Prdm16. Cell metabolism 17:210-224.

116. Itoigawa Y, Kishimoto KN, Sano H, Kaneko K, Itoi E. 2011. Molecular mechanism of fatty degeneration in rotator cuff muscle with tendon rupture. Journal of orthopaedic research 29:861-866.

117. Beeler S, Ek ET, Gerber C. 2013. A comparative analysis of fatty infiltration and muscle atrophy in patients with chronic rotator cuff tears and suprascapular neuropathy. Journal of Shoulder and Elbow Surgery 22:1537-1546.

118. Judson RN, Zhang RH, Rossi F. 2013. Tissue-resident mesenchymal stem/progenitor cells in skeletal muscle: collaborators or saboteurs? FEBS Journal 280:4100-4108.

119. Birbrair A, Zhang T, Wang Z-M, Messi ML, Mintz A, Delbono O. 2014. Pericytes: multitasking cells in the regeneration of injured, diseased, and aged skeletal muscle. Frontiers in aging neuroscience 6:245.

120. Uezumi A, Fukada S-i, Yamamoto N, Takeda Si, Tsuchida K. 2010. Mesenchymal progenitors distinct from satellite cells contribute to ectopic fat cell formation in skeletal muscle. Nature cell biology 12:143-152.

121. Joe AW, Yi L, Natarajan A, Le Grand F, So L, Wang J, Rudnicki MA, Rossi FM. 2010. Muscle injury activates resident fibro/adipogenic progenitors that facilitate myogenesis. Nature cell biology 12:153-163.

122. Uezumi A, Ikemoto-Uezumi M, Tsuchida K. 2014. Roles of nonmyogenic mesenchymal progenitors in pathogenesis and regeneration of skeletal muscle. Frontiers in physiology 5.

123. Heredia JE, Mukundan L, Chen FM, Mueller AA, Deo RC, Locksley RM, Rando TA, Chawla A. 2013. Type 2 innate signals stimulate fibro/adipogenic progenitors to facilitate muscle regeneration. Cell 153:376-388.

124. Liu X, Ning AY, Chang NC, Kim H, Nissenson R, Wang L, Feeley BT. 2016. Investigating the cellular origin of rotator cuff muscle fatty infiltration and fibrosis after injury. Muscles, Ligaments and Tendons Journal 6:6.

125. Birbrair A, Zhang T, Wang Z-M, Messi ML, Enikolopov GN, Mintz A, Delbono O. 2013. Role of pericytes in skeletal muscle regeneration and fat accumulation. Stem cells and development 22:2298-2314.

126. Dellavalle A, Sampaolesi M, Tonlorenzi R, Tagliafico E, Sacchetti B, Perani L, Innocenzi A, Galvez BG, Messina G, Morosetti R. 2007. Pericytes of human skeletal muscle are myogenic precursors distinct from satellite cells. Nature cell biology 9:255-267.

127. Farrington-Rock C, Crofts N, Doherty M, Ashton B, Griffin-Jones C, Canfield A. 2004. Chondrogenic and adipogenic potential of microvascular pericytes. Circulation 110:2226-2232.

128. Lin S-L, Kisseleva T, Brenner DA, Duffield JS. 2008. Pericytes and perivascular fibroblasts are the primary source of collagen-producing cells in obstructive fibrosis of the kidney. The American journal of pathology 173:1617-1627.

129. Rajkumar VS, Howell K, Csiszar K, Denton CP, Black CM, Abraham DJ. 2005. Shared expression of phenotypic markers in systemic sclerosis indicates a convergence of pericytes and fibroblasts to a myofibroblast lineage in fibrosis. Arthritis research & therapy 7:R1113.

130. Schor AM, Canfield A, Sutton A, Arciniegas E, Allen TD. 1995. Pericyte differentiation. Clinical orthopaedics and related research 313:81-91.

131. Hinz B. 2009. Tissue stiffness, latent TGF-β1 activation, and mechanical signal transduction: implications for the pathogenesis and treatment of fibrosis. Current rheumatology reports 11:120-126.

132. Covas DT, Panepucci RA, Fontes AM, Silva WA, Orellana MD, Freitas MC, Neder L, Santos AR, Peres LC, Jamur MC. 2008. Multipotent mesenchymal stromal cells obtained from diverse human tissues share functional properties and gene-expression profile with CD146+ perivascular cells and fibroblasts. Experimental hematology 36:642-654.

133. Besson V, Smeriglio P, Wegener A, Relaix F, Oumesmar BN, Sassoon DA, Marazzi G. 2011. PW1 gene/paternally expressed gene 3 (PW1/Peg3) identifies multiple adult stem and progenitor cell populations. Proceedings of the National Academy of Sciences 108:11470-11475.

134. Mitchell KJ, Pannérec A, Cadot B, Parlakian A, Besson V, Gomes ER, Marazzi G, Sassoon DA. 2010. Identification and characterization of a non-satellite cell muscle resident progenitor during postnatal development. Nature cell biology 12:257-266.

135. Malecova B, Puri PL. 2012. "Mix of Mics"-phenotypic and biological heterogeneity of "Multipotent" muscle interstitial cells (MICs). Journal of stem cell research & therapy.

136. Millar NL, Hueber AJ, Reilly JH, Xu Y, Fazzi UG, Murrell GA, McInnes IB. 2010. Inflammation is present in early human tendinopathy. The American journal of sports medicine 38:2085-2091.

137. McWhorter FY, Davis CT, Liu WF. 2015. Physical and mechanical regulation of macrophage phenotype and function. Cellular and Molecular Life Sciences 72:1303-1316.

138. Lautenschläger F, Paschke S, Schinkinger S, Bruel A, Beil M, Guck J. 2009. The regulatory role of cell mechanics for migration of differentiating myeloid cells. Proceedings of the National Academy of Sciences 106:15696-15701.

139. Oak NR, Gumucio JP, Flood MD, Saripalli AL, Davis ME, Harning JA, Lynch EB, Roche SM, Bedi A, Mendias CL. 2014. Inhibition of 5-LOX, COX-1, and COX-2 Increases Tendon Healing and Reduces Muscle Fibrosis and Lipid Accumulation After Rotator Cuff Repair. The American journal of sports medicine 42:2860-2868.

140. Wang JH-C. 2006. Mechanobiology of tendon. Journal of biomechanics 39:1563-1582.

141. Kjaer M. 2004. Role of extracellular matrix in adaptation of tendon and skeletal muscle to mechanical loading. Physiological reviews 84:649-698.

142. Tidball JG, Dorshkind K, Wehling-Henricks M. 2014. Shared signaling systems in myeloid cell-mediated muscle regeneration. Development 141:1184-1196.

143. Kharraz Y, Guerra J, Mann CJ, Serrano AL, Muñoz-Cánoves P. 2013. Macrophage plasticity and the role of inflammation in skeletal muscle repair. Mediators of inflammation 2013.

144. Lawrence T, Natoli G. 2011. Transcriptional regulation of macrophage polarization: enabling diversity with identity. Nature reviews immunology 11:750-761.

145. Friedl P, Weigelin B. 2008. Interstitial leukocyte migration and immune function. Nature immunology 9:960-969.

146. Mantovani A, Sica A, Sozzani S, Allavena P, Vecchi A, Locati M. 2004. The chemokine system in diverse forms of macrophage activation and polarization. Trends in immunology 25:677-686.

147. Sugihara R, Kumamoto T, Ito T, Ueyama H, Toyoshima I, Tsuda T. 2001. Human muscle protein degradation in vitro by eosinophil cationic protein (ECP). Muscle & nerve 24:1627-1634.

148. Van Goethem E, Poincloux R, Gauffre F, Maridonneau-Parini I, Le Cabec V. 2010. Matrix architecture dictates three-dimensional migration modes of human macrophages: differential involvement of proteases and podosome-like structures. The journal of immunology 184:1049-1061.

149. Wolf K, Friedl P. 2011. Extracellular matrix determinants of proteolytic and non-proteolytic cell migration. Trends in cell biology 21:736-744.

150. Previtera ML, Sengupta A. 2015. Substrate stiffness regulates proinflammatory mediator production through TLR4 activity in macrophages. PloS one 10:e0145813.

151. Dorph C, Lundberg IE. 2002. Idiopathic inflammatory myopathies–myositis. Best Practice & Research Clinical Rheumatology 16:817-832.

152. Frontera WR, Meredith CN, O'reilly K, Knuttgen H, Evans W. 1988. Strength conditioning in older men: skeletal muscle hypertrophy and improved function. Journal of applied physiology 64:1038-1044.

153. Butt U, Rashid M, Temperley D, Crank S, Birch A, Freemont A, Trail I. 2016. Muscle regeneration following repair of the rotator cuff. Bone Joint J 98:1389-1394.

154. Galatz LM, Ball CM, Teefey SA, Middleton WD, Yamaguchi K. 2004. The outcome and repair integrity of completely arthroscopically repaired large and massive rotator cuff tears. The Journal of Bone & Joint Surgery 86:219-224.

155. Gerber C, Fuchs B, Hodler J. 2000. The Results of Repair of Massive Tears of the Rotator Cuff*†. The Journal of Bone & Joint Surgery 82:505-505.

156. Zumstein MA, Jost B, Hempel J, Hodler J, Gerber C. 2008. The clinical and structural long-term results of open repair of massive tears of the rotator cuff. J Bone Joint Surg Am 90:2423-2431.

157. Kim HM, Galatz LM, Lim C, Havlioglu N, Thomopoulos S. 2012. The effect of tear size and nerve injury on rotator cuff muscle fatty degeneration in a rodent animal model. Journal of shoulder and elbow surgery 21:847-858.

158. Liu X, Laron D, Natsuhara K, Manzano G, Kim HT, Feeley BT. 2012. A mouse model of massive rotator cuff tears. The Journal of Bone & Joint Surgery 94:e41.

159. Liu X, Manzano G, Kim HT, Feeley BT. 2011. A rat model of massive rotator cuff tears. Journal of orthopaedic research 29:588-595.

Chapter 2. Muscle Architectural Changes After Massive Human Rotator Cuff Tear

Abstract

Rotator cuff (RC) tendon tears lead to negative structural and functional changes in the associated musculature. The structural features of muscle that predict function are termed "muscle architecture". Although the architectural features of "normal" rotator cuff muscles are known, they are poorly understood in the context of cuff pathology. The purpose of this study was to investigate the effects of tear and repair on RC muscle architecture. To this end thirty cadaveric shoulders were grouped into one of four categories based on tear magnitude: Intact, Full-thickness tear (FTT), Massive tear (MT), or Intervention if sutures or hardware were present, and key parameters of muscle architecture were measured. We found that muscle mass and fiber length decreased proportionally with tear size, with significant differences between all groups. Conversely, sarcomere number was reduced in both FTT and MT with no significant difference between these two groups, in large part because sarcomere length was significantly reduced in MT but not FTT. The loss of muscle mass in FTT is due, in part, to subtraction of serial sarcomeres, which may help preserve sarcomere length. This indicates that function in FTT may be impaired, but there is some remaining mechanical loading to maintain "normal" sarcomere length-tension relationships. However, the changes resulting from MT suggest more severe limitations in force-generating capacity because sarcomere length-tension relationships are no longer normal. The architectural deficits observed in MT muscles may indicate deeper deficiencies in muscle adaptability to length change, which could negatively impact RC function despite successful anatomical repair.

Introduction

Rotator cuff tears have a lifetime prevalence of 20%, with the likelihood of tear increasing with age[1]. While many studies rightfully focus on the repair of the RC tendon itself, the fate of the RC muscle following tear is also clinically important (Goutallier[2], Patte[3], Warner[4]). Specifically, it is necessary to

understand, and ultimately through intervention change, the active and passive force-generating capacities of these muscles after prolonged RC injury.

Muscle function is dictated by a set of structural features that cumulatively define the muscle's distinct architecture. The critical parameters of muscle architecture include mass, muscle fiber length and pennation angle, and sarcomere length and number[5]. Fiber length determines muscle excursion and force-velocity relationships, where longer fibers permit a greater range of muscle lengths[6] for a given force output and lower muscle velocities for a given joint velocity[6]. Increased pennation angle allows for increased fiber number and physiological cross-sectional area (PCSA), and therefore increased force producing capacity in a given muscle volume[6]. Finally, sarcomere length and number play a major role in the position of the muscle-joint system on the sarcomere length-tension curve (Figure 1A), which ultimately determines the force generating capacity of the muscle at a given length[7]. This is referred to as the sarcomere length-operating range of the muscle.

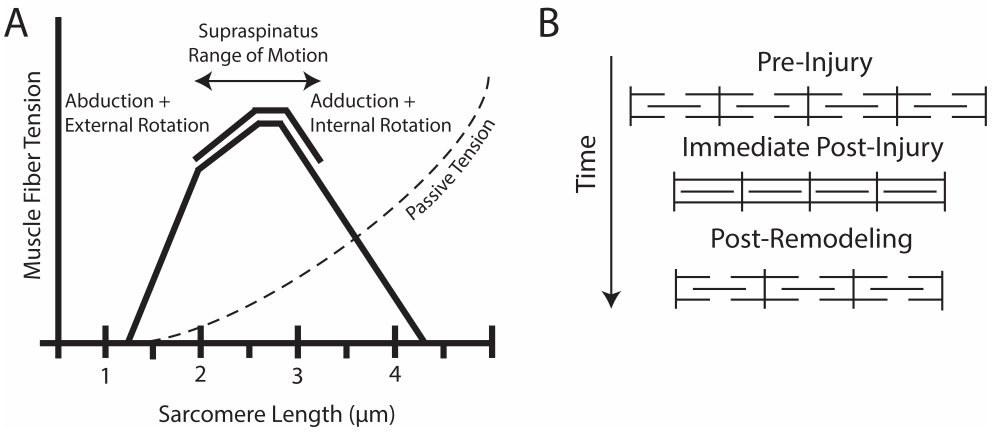

Figure 2.1 (A) Classical hypothesis of sarcomere subtraction and maintenance of sarcomere length after muscle shortening injury. (B) Sarcomere length-tension curve with normal sarcomere length-operating range (solid line) and passive tension curve (dashed line) of the supraspinatus muscle indicated[10].

When fiber lengths are chronically changed, the sarcomere length operating range is modulated by adding or subtracting sarcomeres in series[8; 9] (Figure 1B). In the case of torn RC's, muscle fibers become shorter as the muscle retracts and become longer when the tear is repaired. Whether or not sarcomere number is reduced or increased in response to tear or repair is of great clinical interest for two

reasons. First, this adaptation will have a direct impact on muscle passive tension, and therefore the forces acting on the repair site. Secondly, the preservation or disruption of the sarcomere length-operating range will ultimately impact the active force producing capacity of the muscle.

A previous study in human cadavers from Tomioka et al[10] demonstrated that in torn rotator cuffs, fiber lengths were reduced while sarcomere lengths were not significantly different between intact and torn cuffs[10]. These data suggest that the muscle is adapting normally. However, the effect of tear size/severity on architectural measurements was not considered. Therefore, goal of this study was to characterize the architectural features of rotator cuff muscles in the presence of different tendon tear severities in order to understand the biological adaptations that dictate muscle function.

We hypothesized that, in the presence of small tendon tears, sarcomere number and length are maintained within the normal length-operating range, but in the presence of chronic and massively retracted tears, sarcomere length and number are no longer normally maintained. Furthermore, we calculated the theoretical post-repair sarcomere length for each tear category, and documented the actual architectural changes in a small series of specimens with repaired rotator cuffs and reverse total shoulder arthroplasties.

Methods

Thirty cadaveric shoulders with an average age of 83.9±8.7 years were used in this study. All cadavers were fixed (10% formaldehyde) in approximately the same position, with the shoulder at approximately neutral flexion and abduction angles and internally rotated approximately 30 degrees with the elbow flexed to approximately 10 degrees.

The RC muscles were exposed by removing the trapezius and deltoid muscles, and the acromion was removed at the level of the spinoglenoid notch to expose the distal portion of the supraspinatus muscle and tendon. Where applicable, anterior-posterior tear dimensions and retraction distance of the tendon stump from its footprint on the humerus were measured with digital calipers (Mitutoyo, accuracy 0.01mm) before dissecting the rotator cuff muscles from the scapula. Each sample was assigned to a

group as being Intact (n=12), Full-Thickness (FTT, n=5), or Massive (MT, n=9). The distinction between FTT and Massive was made based on the size of the tear exceeding 5cm in any dimension. When evidence of repair was found in the form of sutures or hardware the integrity of the repair was noted based on the insertion of the tendon on the footprint of the humerus and the specimen was placed in a separate intervention group. The integrity of supraspinatus and infraspinatus repairs were graded independently (Table 1).

Table 2.1 Specimen Demographic Data

Tear State	Male	Female	Age (years)
Intact (N=12)	8	4	81.0±8.4
FTT (N=5)	3	2	84.6±15.5
MT (N=9)	5	4	86.7±5.6
Intervention	1	3	85.5±4.4

Architectural measurements of the supraspinatus and infraspinatus were made in accordance with previous studies[5]. Briefly, muscle mass, pennation angle, and length were recorded, and individual fascicles were dissected from distinct regions[5] and raw fiber lengths were measured with calipers before being stored in PBS for subsequent sarcomere length measurements. Bony measurements were also recorded, including scapular and humeral head dimensions, to normalize for differences in skeletal dimensions among subjects.

Sarcomere length measurements were carried out using a laser diffraction as previously described[11]. Individual muscle fibers were dissected from fascicles and mounted on glass slides. Sarcomere length was recorded for six individual muscle fibers to obtain the average sarcomere length for that region. Sarcomere number was determined by dividing fiber length by sarcomere length. Physiological cross-sectional area (PCSA), the standard metric for describing the force-generating capacity of a muscle, was calculated using the following formula:

$$PCSA = \frac{mass}{density * L_f} * \cos(Ø),$$

where density is assumed to be 1.06g/cm^3 [12], L_f is fiber length adjusted for sarcomere length, and Ø is the average pennation angle for the muscle[13]. Finally, we calculated the supraspinatus sarcomere length that would result from repair of the tendon to the footprint on the humeral head in FTT and MT using the following equation:

$$L_{s\_post} = L_{s\_pre} + \frac{Retraction\ Distance}{Sarcomere\ Number}$$

where L_{s_pre} and L_{s_post} are sarcomere length pre- and post-repair, respectively.

To adjust for differences in skeletal dimensions, comparisons of mass, fiber length, and sarcomere number were normalized by the length of the scapular spine from its most medial edge to the glenoid face (Figure 2). This method of normalization was used in analyzing the linear regression of architectural parameters to retraction distance. In four specimens, both shoulders were used. For the purpose of group comparisons, these shoulders were treated as separate samples due to the varying pathology and bony anatomy found on each side. Statistical comparisons between the intact, FTT and MT groups were carried out in GraphPad Prism 6 (GraphPad Software, Inc., La Jolla, CA, USA) software using linear regression to determine correlations and two-way repeated measures ANOVA by tear state and muscle region with post-hoc Tukey tests for significance ($p<0.05$). The intervention group is plotted for reference, but was excluded from statistical analysis due to the small sample size and heterogeneity of interventions within the group. Data are reported as mean±standard deviation, and p-values are indicated as follows: <0.1=#, <0.05=*, <0.01=**, <0.001=***, <0.0001=****.

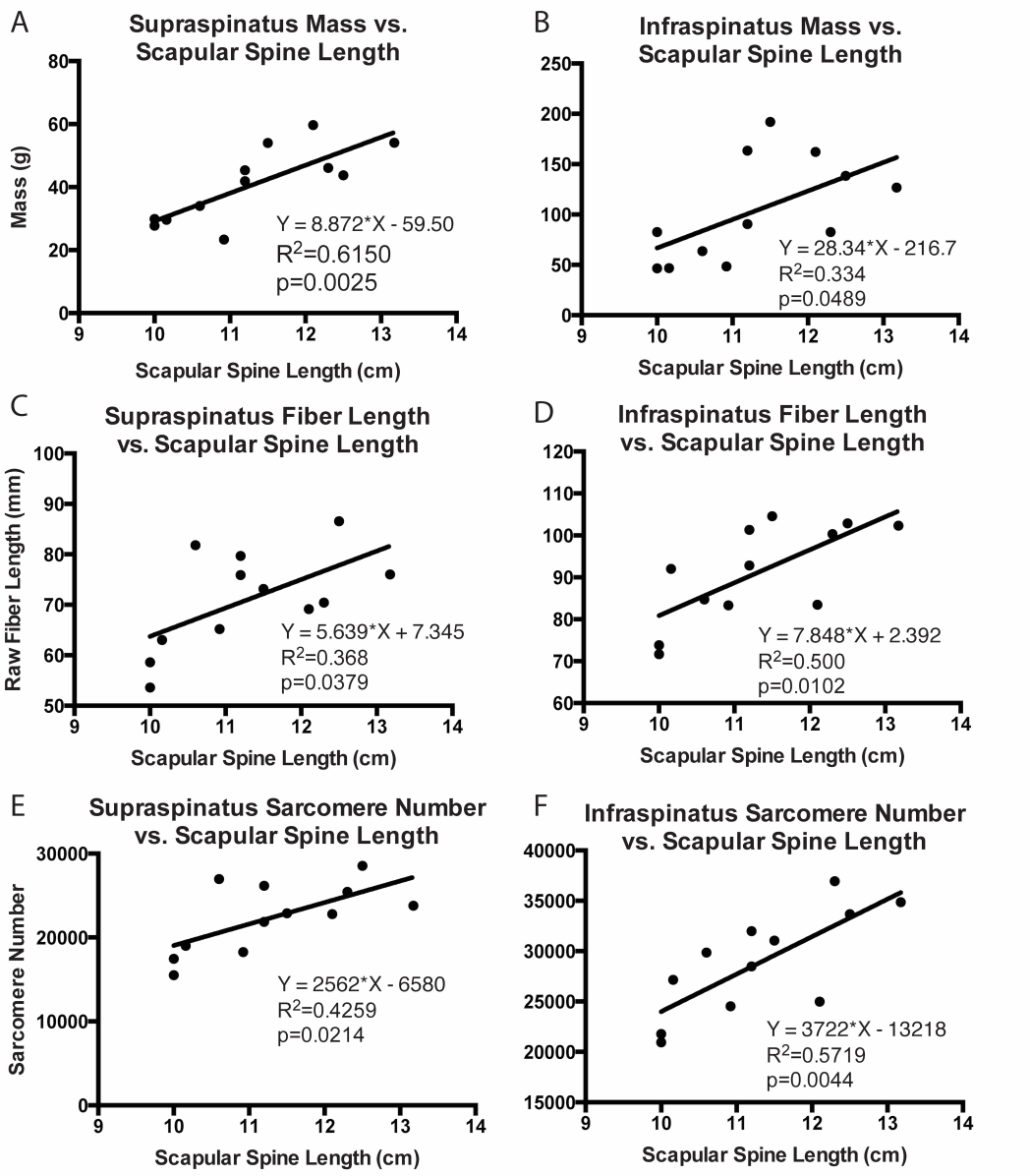

Figure 2.2 Linear regression of supraspinatus and infraspinatus muscle mass (A,B), muscle fiber length (C,D) and sarcomere number (E,F) with scapular spine length, demonstrating correlations between bony shoulder anatomy and muscle architecture parameters that accounts for inter-subject size variability. Equation of the regression line, the coefficient of determination, and the p-value are provided.

Results

No significant regional differences were found in muscle fiber or sarcomere lengths, nor were there any significant regional effects on these parameters in the presence of RC tear. Therefore, all architectural measurements were averaged and reported on a per-muscle basis.

Muscle mass was significantly reduced in both FTT and MT compared to intact, with a trend toward further mass reduction in MT and repaired cuffs compared to FTT (Figure 3A,B). Linear regression showed that mass was negatively correlated with retraction distance in the supraspinatus with a similar, though weaker, trend in the infraspinatus (Figure 4A,B). The weaker relationships found in the infraspinatus are likely due to our definition of MT, as some infraspinatus tendons in the MT group may retain some mechanical connection to the bone. Interestingly, mass was reduced to the level of MT in the intervention group regardless of the state of the repair (Figure 3A,B). The pennation angle was not significantly altered in either FTT or MT, though there was a trend toward larger supraspinatus pennation angles in MT (18.1 ± 8.0^{o}, $p=0.092$) and the intervention group compared to intact RCs (10.4 ± 4.5^{o}).

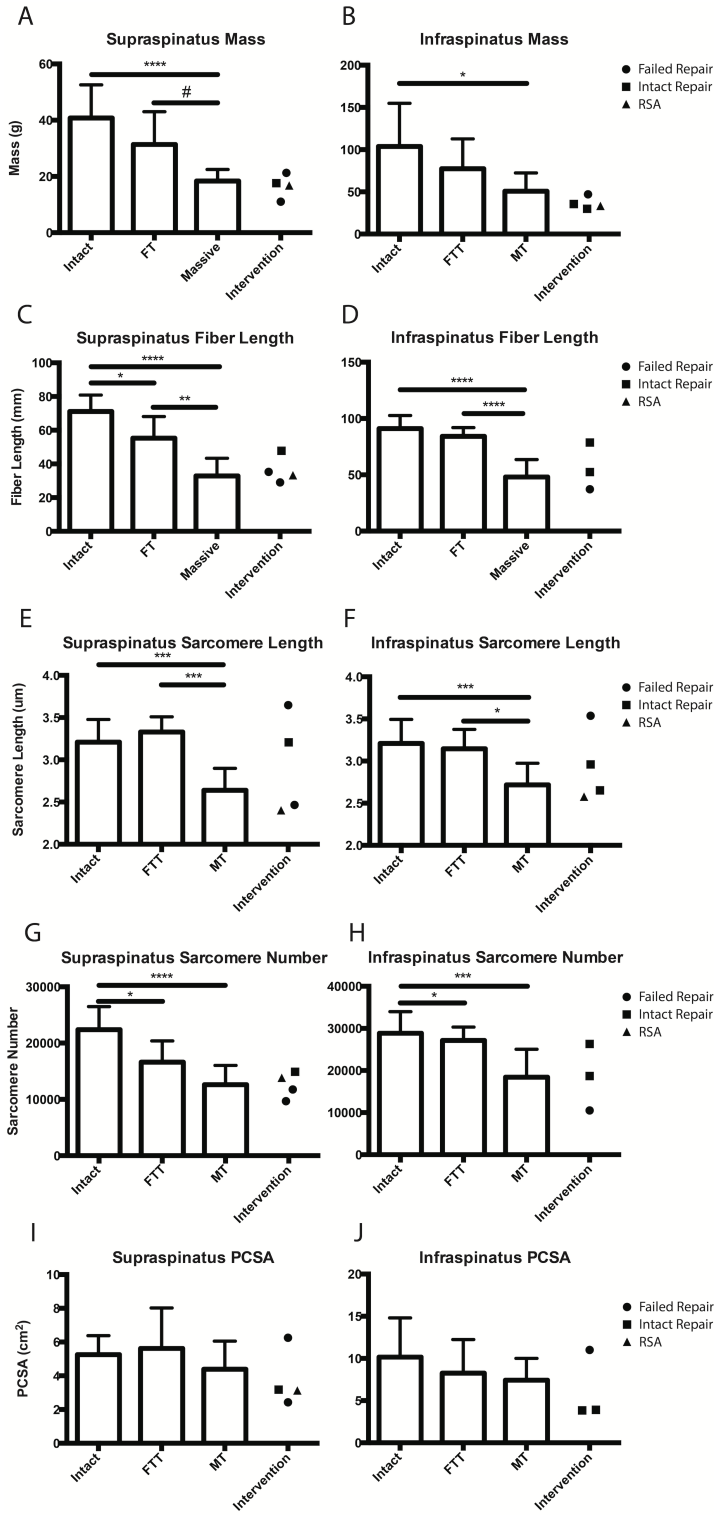

Figure 2.3 Average mass (A,B), raw muscle fiber length (C,D) sarcomere length (E,F), sarcomere number (G,H), and PCSA (I,J) of the supraspinatus and infraspinatus muscles grouped by tear state (Intact, FTT, MT), with samples demonstrating surgical intervention separated and indicated by symbol.

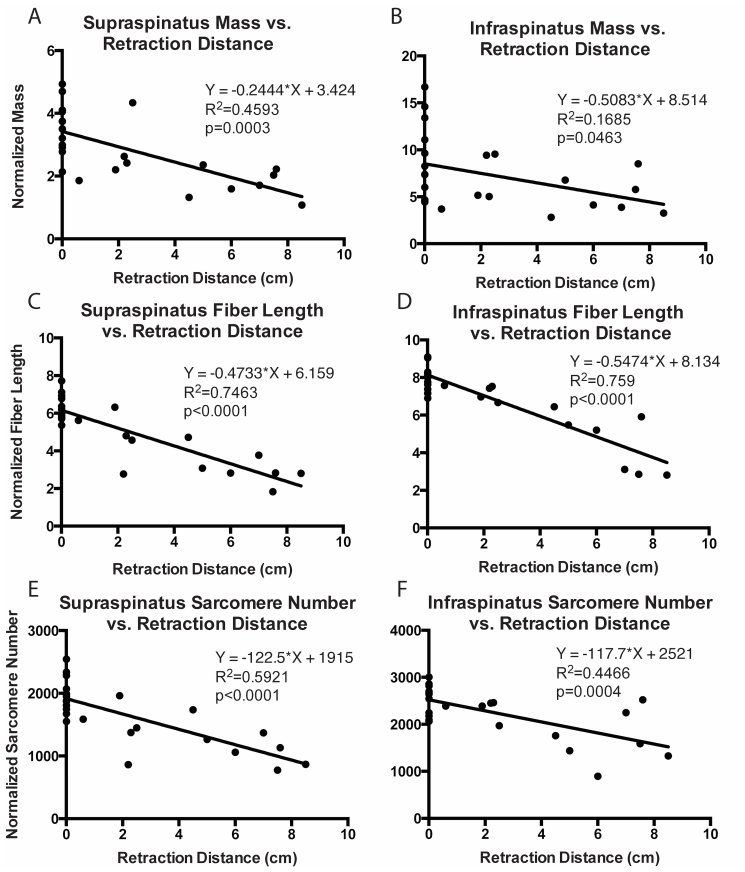

Figure 2.4 Linear regression of normalized supraspinatus and infraspinatus muscle mass (A,B), fiber length (C,D), and sarcomere number (E,F) demonstrating negative correlations between muscle retraction distance and architecture parameters. Equation of the regression line, the coefficient of determination, and the p-value are provided.

In a similar trend to mass, raw muscle fiber lengths were significantly shorter in the supraspinatus of both FTT and MT (Figure 3C), with fiber shortening significantly correlated to muscle retraction distance in both supraspinatus and infraspinatus (Figure 4C,D). In the infraspinatus, MT's presented with significantly shorter fibers. However, infraspinatus muscles with FTT did not demonstrate shorter fibers- likely due to localization of the tendon tear to the supraspinatus tendon (Figure 3D). Intervention did not increase muscle fiber length, as the samples from the intervention group were nearly identical to MT (Figure 3C,D).

Sarcomere length was significantly shorter in MT compared to intact and FTT in both the supraspinatus and infraspinatus (Figure 3E,F). Interestingly, the specimen with intact supraspinatus and infraspinatus repair contained normal sarcomere lengths in both muscles, while the remaining muscles

demonstrated either extremely long or short sarcomeres. In these latter cases, the extreme to which the sarcomere length was altered was similar in both RC muscles. The predicted supraspinatus sarcomere length at repair for the FTT group was 4.56±0.56µm, while the predicted MT repair length was an extreme 8.46±2.75µm (Figure 5A).

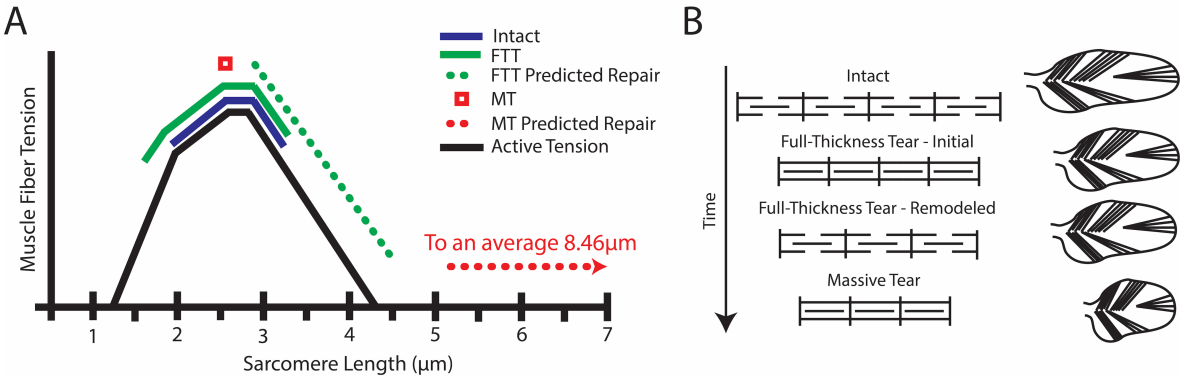

Figure 2.5 (A) Sarcomere length-tension curve demonstrating the approximate sarcomere operating range for each tear state (solid lines), using the operating ranges reported by Ward et. al[10], extrapolated in the case of FTT to account for diminished sarcomere number. MT is represented by a single point (red square), as this muscle is mechanically disconnected from the joint. The dotted lines demonstrate the theoretical, immediate post-repair sarcomere length operating ranges of FTT (green) and MT (red). (B) The proposed progression of sarcomere-length modulation in FTT and MT, where FTT demonstrates classical sarcomere subtraction and sarcomere length modulation while MT fails to subtract serial sarcomeres, resulting in shortened sarcomeres.

In contrast to the sarcomere length data, no significant differences in supraspinatus sarcomere number were found between FTT and MT, with significantly more sarcomeres found only in the intact muscles compared to both tear states (Figure 3G). In the infraspinatus, only the MT group had significantly fewer sarcomeres than both intact and FTT (Figure 3H). This discrepancy between muscles is likely due to our definition of FTT, where the infraspinatus tendon is largely intact and, therefore, the muscle remains relatively unaltered. As with the previous architectural measurements, sarcomere number was negatively correlated with the extent of retraction in both muscles (Figure 4E,F).

No significant differences were observed in PCSA across all tear states (Figure 3I,J). Although masses were significantly different between groups, the shorter fiber lengths associated with tears cancelled out any potential changes in PCSA. It is important to note that this calculation does not take in

to account changes in composition of the muscle, which detrimentally influences a key assumption of the PCSA calculation; that the total tissue volume is composed of functional contractile tissue.

Discussion

The purpose of this study was to determine the effect of tear severity on rotator cuff muscle architecture. Based on the high degree of muscle retraction and mechanical unloading observed in MT we hypothesized that unique architectural changes, particularly in terms of sarcomere length and number, would result from MT when compared to FTT and intact cuff muscle.

Muscle mass and fiber length were reduced with more severe RC tendon tears, similar to previous work[10]. We further demonstrated that these parameters are negatively correlated with tear size, where an increase in tear size leads to a decrease in mass and fiber length in a linear fashion. A secondary finding in this analysis was the correlation between scapular spine length and both mass and fiber length in the intact group (Figure 2), which combined with previous work[14] will allow for corrections based on differences in both muscle volume and skeletal dimensions between subjects.

Sarcomere lengths were significantly shorter in MT compared to either intact or FTT, both of which were found to be similar to previous studies[5; 10]. Importantly, the length of sarcomeres in intact cuffs is greater than the reported optimal length for human sarcomeres[15], suggesting that the sarcomeres of RC muscle are specifically maintained above optimal length. This is also consistent with previous findings[5], but remains unique among human muscles. In the case of MT, the observed sarcomere length of 2.64μm is slightly below the optimal predicted length of 2.8μm[15], which suggests that muscle retraction in MT has shortened sarcomeres to such an extent that MT muscle resides on the plateau of the length-tension curve, where passive tensions are minimal (Figure 5A). This is important because any muscle shortening would result in movement of the muscle down the ascending limb of the length tension curve, where active *and* passive tensions are low, which in turn will inhibit function. This finding contradicts previous reports, which showed maintenance of sarcomere length in the presence of tendon

tears and muscle fiber length shortening[10], and supports our hypothesis that maintenance of sarcomere length and number is in fact dependent on tear severity.

Of critical clinical importance is the effect of RC repair on sarcomere length and the subsequent location of the muscle on the length-tension curve. The predicted post-repair resting sarcomere length in the FTT group was just outside the range of active force generation, suggesting that on average complete anatomical repair to the tendon footprint is possible and unlikely to cause significant muscle damage due to sarcomere overstrain. However, the predicted repair length in the massive tears shows that anatomical repair to the footprint would overstretch sarcomeres, which would yield poor active force production, high passive tensions, and would likely result in damage to the contractile apparatus (Figure 5A). The importance of mechanical load in sarcomere length modulation is highlighted in the case of the repaired RC's, where only the anatomically intact repair demonstrated normal sarcomere lengths. In failed repairs, without the normal loading condition, sarcomere lengths appeared to be unregulated, and were found at both long and short extremes. Together, these data suggest that in the case of successful repair, normal sarcomere length may be restored. However, more evidence is required to confirm this hypothesis and determine the initial and final conditions under which sarcomere length is modulated in this manner.

Sarcomere number was significantly reduced in FTT compared to intact, which is the inevitable result of maintaining sarcomere length in a shorter muscle fiber[6]. Surprisingly, though there was a significant difference between fiber lengths in FTT and MT, the sarcomere numbers were not significantly different between the two. Mathematically, this is explained by the shorter sarcomeres in MT, as shorter sarcomeres allow for shorter fibers without loss of serial sarcomeres, but biologically it indicates that the muscle is no longer adapting appropriately to its changing mechanical environment (Figure 5B).

While PCSA is indicative of a normal muscle's force generating capacity and is expected to decrease in atrophic muscles[6], the PCSA data presented here must be viewed cautiously. At face value, it appears that PCSA is preserved across tear states. However, this interpretation is highly misleading based

on known compositional changes, such as fat accumulation and fibrosis[16; 17], that are unaccounted for in normal PCSA calculations.

The limitations of this study are similar to previous studies, in that minor alterations to muscle structure (<3%) are known to occur during and after fixation, namely that there may be slight contraction of the muscle fibers and overall shrinkage of the tissue[18]. While these effects are eliminated with in situ fixation of intact muscle, the presence of the unattached tendon in RC tear could lead to minor fixation-induced shortening. Though these are legitimate concerns, it has been shown that neither rigor mortis nor formalin fixation alter sarcomere length in a meaningful way[19; 20]. And, given the large discrepancies in fiber and sarcomere length observed, it is highly unlikely that the differences between tear states found here are due to fixation artifacts.

We speculate that the discrepancies in sarcomere length between intact and FTT muscle and MT muscle is the result of a deficiency in remodeling ability that only affects the more severely damaged MT muscle. Previous studies have shown that serial sarcomeres are added or subtracted in order to maintain a specific length[8; 9], which is thought to be determined by the muscle's physiological function and the relative length of the contractile proteins found in that muscle[5]. As such, the "set-point" sarcomere length may differ across muscles, though the optimal sarcomere length in terms of force-generating capacity is believed to be the same across all muscles within a species[7]. In the RC muscles, this type of remodeling appears to occur in FTT, where serial sarcomere subtraction maintains sarcomere length as fiber length is reduced by muscle retraction. But the cause for the disruption of this process in MT, where sarcomere lengths remain chronically short, is not clear (Figure 7B). One possibility is that the regulatory cues present in intact and FTT muscles are altered in MT due to the high degree of unloading and altered biological environment[21; 22] that they experience. Without the proper mechanical and biochemical cues, normal remodeling does not occur and sarcomeres shorten proportionally to the shortening of the fibers without subsequent sarcomere subtraction and sarcomere length maintenance. This hypothesis is further supported by the data from repaired shoulders. Specifically, sarcomere length was only maintained in the single specimen with and intact repair site. Since healthy RC muscle is maintained above optimal

sarcomere length in the anatomically neutral position, the shortened sarcomeres in MT may be construed as an inability to maintain non-optimal length, which results in sarcomeres returning to at or near slack sarcomere length.

In conclusion, we have demonstrated that MT leads to unique changes in muscle architecture. Both FTT and MT show decreased mass and fiber length proportional to the degree of muscle retraction. However, where FTT demonstrates serial sarcomere subtraction and maintained sarcomere length consistent with previous work, MT sarcomere lengths are shortened with a relative preservation of serial sarcomeres compared to FTT. This indicates a possible defect in the remodeling ability of the MT muscle, which may partially explain the irreversibility of many of the pathologic changes that occur in RC muscle with massive tendon tears. It is also possible that reconnecting the muscle mechanically would improve its ability to adapt, though both of these hypotheses require further investigation.

Acknowledgements

The authors gratefully acknowledge the UC San Diego Anatomical Gifts Program. Without the tissues donated by patients and families, this experiment would not have been possible. Funding for the project was provided by NIH R01HD073180 (Ward) and the UCSD Frontiers in Innovation Scholars Program.

This chapter, in full, is a reprint of the material as it appears in the Journal of Orthopedic Research 2016. Michael C. Gibbons, Eugene Sato, Damien Bachasson, Timothy Cheng, Hassan Azimi, Simon Schenk, Adam J. Engler, Anshu Singh, Samuel R. Ward. The dissertation/thesis author was the primary investigator of this material.

References

1. Yamamoto A, Takagishi K, Osawa T, Yanagawa T, Nakajima D, Shitara H, Kobayashi T. 2010. Prevalence and risk factors of a rotator cuff tear in the general population. Journal of Shoulder and Elbow Surgery 19:116-120.

2. Goutallier D, Postel J-M, Bernageau J, Lavau L, Voisin M-C. 1994. Fatty muscle degeneration in cuff ruptures: pre-and postoperative evaluation by CT scan. Clinical orthopaedics and related research 304:78-83.

3. PATTE D. 1990. Classification of rotator cuff lesions. Clinical orthopaedics and related research 254:81-86.

4. Warner JJ, Higgins L, Parsons I, Dowdy P. 2001. Diagnosis and treatment of anterosuperior rotator cuff tears. Journal of Shoulder and Elbow Surgery 10:37-46.

5. Ward SR, Hentzen ER, Smallwood LH, Eastlack RK, Burns KA, Fithian DC, Friden J, Lieber RL. 2006. Rotator cuff muscle architecture: implications for glenohumeral stability. Clinical orthopaedics and related research 448:157-163.

6. Lieber RL. 2002. Skeletal muscle structure, function, and plasticity: Lippincott Williams & Wilkins;

7. Gordon A, Huxley AF, Julian F. 1966. The variation in isometric tension with sarcomere length in vertebrate muscle fibres. The Journal of physiology 184:170-192.

8. Burkholder T. 1998. Sarcomere number adaptation after retinaculum transection in adult mice. Journal of Experimental Biology 201:309-316.

9. Friden J, Ponten E, Lieber RL. 2000. Effect of muscle tension during tendon transfer on sarcomerogenesis in a rabbit model. The Journal of hand surgery 25:138-143.

10. Tomioka T, Minagawa H, Kijima H, Yamamoto N, Abe H, Maesani M, Kikuchi K, Abe H, Shimada Y, Itoi E. 2009. Sarcomere length of torn rotator cuff muscle. Journal of Shoulder and Elbow Surgery 18:955-959.

11. Lieber RL, Yeh Y, Baskin RJ. 1984. Sarcomere length determination using laser diffraction. Effect of beam and fiber diameter. Biophysical journal 45:1007.

12. Ward SR, Lieber RL. 2005. Density and hydration of fresh and fixed human skeletal muscle. Journal of biomechanics 38:2317-2320.

13. Powell PL, Roy RR, Kanim P, Bello MA, Edgerton VR. 1984. Predictability of skeletal muscle tension from architectural determinations in guinea pig hindlimbs. Journal of Applied Physiology 57:1715-1721.

14. Holzbaur KR, Murray WM, Gold GE, Delp SL. 2007. Upper limb muscle volumes in adult subjects. Journal of biomechanics 40:742-749.

15. Lieber RL, Loren GJ, Friden J. 1994. In vivo measurement of human wrist extensor muscle sarcomere length changes. Journal of Neurophysiology 71:874-881.

16. Steinbacher P, Tauber M, Kogler S, Stoiber W, Resch H, Sänger A. 2010. Effects of rotator cuff ruptures on the cellular and intracellular composition of the human supraspinatus muscle. Tissue and Cell 42:37-41.

17. Lundgreen K, Lian ØB, Engebretsen L, Scott A. 2013. Lower muscle regenerative potential in full-thickness supraspinatus tears compared to partial-thickness tears. Acta orthopaedica 84:565-570.

18. Cutts A. 1988. Shrinkage of muscle fibres during the fixation of cadaveric tissue. Journal of anatomy 160:75.

19. Locker RH. 1959. Striation patterns of ox muscle in rigor mortis. The Journal of biophysical and biochemical cytology 6:419-422.

20. Bendall J. 1973. Postmortem changes in muscle. The structure and function of muscle 2:244-309.

21. De Giorgi S, Saracino M, Castagna A. 2013. Degenerative disease in rotator cuff tears: what are the biochemical and histological changes? Joints 2:26-28.

22. Choo A, McCarthy M, Pichika R, Sato EJ, Lieber RL, Schenk S, Lane JG, Ward SR. 2014. Muscle Gene Expression Patterns in Human Rotator Cuff Pathology. The Journal of Bone & Joint Surgery 96:1558-1565.

Chapter 3. Histological Assessment of Chronically Torn Human Rotator Cuff Muscles: Evidence of Degeneration, Regeneration and Remodeling

Abstract

Background: Cellular remodeling in rotator cuff (RC) muscles following massive RC tear is poorly understood. This study aimed to provide histological evidence to elucidate the mode of muscle loss in advanced human RC disease and to correlate interpretations of noninvasive imaging to tissue level changes.

Methods: Rotator cuff muscle biopsies taken from the scapular fossae were acquired from 23 consecutive patients undergoing reverse total shoulder arthroplasty in order to evaluate muscle composition in severe RC disease. Markers of vascularity, inflammation, fat distribution, and muscle atrophy, degeneration and regeneration were quantified.

Results: Biopsies primarily consisted of dense, organized connective tissue (48.2±19.1%) and disorganized, loose connective tissue (36.9±15.9%), with significantly smaller fractions of muscle (10.4±22.0%) and fat (6.5±11.6%). Only 25.8% of the biopsy pool contained any myofibers at all. Increased inflammatory cell counts (111.3±81.5 macrophages/mm^2) and increased vascularization (66.6±38.0 vessels/mm^2) was observed across biopsies. Myofiber degeneration was observed in 90.0±15.6% of observable muscle fascicles, and the percentage of centrally nucleated myofibers was pathologically elevated (11.3±6.3%). Lipid accumulation was noted in both interfascicular (60.7±41.4%) and intrafascicular (42.2±33.6%) spaces, with evidence that lipid may replace contractile elements without altering muscle organization.

Conclusion: Dramatic degeneration and inflammation of the RC muscles are characteristics of the most chronic and severe RC disease states, suggesting that muscle loss is more complicated than the simple atrophy found in less severe cases.

Clinical Significance: In order to address degenerative muscle loss, alternative therapeutic approaches directed at muscle regeneration must be considered if muscle function is to be restored in late stage RC disease.

Introduction

The lifetime prevalence of rotator cuff (RC) tear is estimated to be as high as one in every five people, where risk increases significantly with age[1]. Because RC tears may remain asymptomatic for years, and the onset of symptoms is often insidious, many patients do not seek treatment until the disease has progressed to a more chronic state. Along with other factors such as smoking, diabetes, and age, this late-stage intervention results in surgical failure rates as high as 50%[2]. The composition, quality, and function of the muscle in RC disease plays an important role in disease progression and recovery potential, but the biological features of the muscle are poorly defined on the cellular level, particularly in late-stage disease.

Compared to muscle, the response of the RC tendon to tear has been better studied biomechanically, biochemically, and histologically[3-5]. These studies suggest that while the tendon may look healthy macroscopically, at the cellular and molecular level the torn tendon is degenerated, with signs including increased vascularity, adipose content, inflammation and apoptosis[3-5]. We hypothesized that as RC disease progresses, muscle as well as tendon is lost to degenerative processes. Specifically, in advanced RC disease we expected to see a degenerative muscle phenotype demonstrating disrupted muscle fiber structure, myophagocytosis, and increased central nuclei, all signs of muscle degeneration-regeneration[6] not reported in earlier disease states.

While atrophy and degeneration are distinct mechanisms of muscle loss often involving different pathways and drivers[7-9], the terms “fatty atrophy”, “fatty degeneration” and the more generic “fatty infiltration” are consistently and interchangeably found in the literature. Muscle atrophy is a normal response to disuse, whether that disuse is caused by tenotomy-induced mechanical unloading[10] or inactivity[11], and under most conditions can be nearly reversed by muscle reloading[12]. In contrast, degeneration is an accumulation of muscle damage and cell death driven by multiple factors including inflammation, abnormal mechanical forces, and altered vascularization, and is classically seen in the inflammatory myopathies and dystrophies[8, 9]. It is indisputable that fat accumulates in diseased RC

muscle. Indeed, clinical and surgical decisions are often based on computed tomography (CT) or magnetic resonance imaging (MRI) evaluation of the RC muscles, with Goutallier scores being the primary clinical measure of RC muscle quality and overall disease severity[13, 14].

Regarding the remaining terms, "fatty atrophy" versus "fatty degeneration", previous studies of the relationship between muscle loss and fat accumulation are limited, and have focused primarily on early- to mid-stage RC disease. These studies have demonstrated decreased muscle fiber diameter[15] and specific force production[17], along with disrupted subcellular architecture including small (~1μm) lipid droplet accumulation in individual myofibers following tendon tear[16, 17]. No degenerative features such as myophagocytosis, disrupted myofiber membranes, split fibers, centralized nuclei, or other classic features of muscle degeneration[6] have been reported[15-17]. While these studies clearly demonstrate atrophic changes in the muscle, no clear evidence has emerged to suggest a degenerative mechanism of muscle loss.

To address these fundamental gaps in the literature regarding advanced RC disease, the aim of this study was to histologically characterize the tissues found in the muscular spaces of patients with chronic and severe RC disease in order to determine if degenerative processes are present in RC muscle. These data will provide evidence to challenge clinical assumptions about the state of muscle in RC disease and will broaden our understanding of the relationships between muscle and fat in advanced RC disease.

Methods

Twenty-three patients undergoing reverse total shoulder arthroplasty (Table 1) were consented for muscle biopsy under the approval of the appropriate Institutional Review Boards. A fellowship-trained shoulder surgeon assigned Goutallier scores[13] to each muscle based on clinically indicated T1-weighted MRI or CT arthrogram images in the coronal and sagittal-oblique planes.

Table 3.1 Patient Demographics.

				Average Goutallier Score			
All Patients	Age (years)	Gender	Massive Tear	*Supraspinatus*	*Infraspinatus*	*Teres Minor**	*Total*
23	73.9±8.3	10 Male 13 Female	16/20 (80%)	2.9 (18 Biopsies)	2.7 (11 Biopsies)	1.5 (2 Biopsy)	2.7 (31 Biopsies)
Muscle-Containing Samples Only							
8 (26% of Biopsies)	75.8±10.7	3 Male 3 Female	7/8 (88%)	3 (2 Biopsy)	2.8 (4 Biopsies)	1.5 (2 Biopsies)	2.5 (8 Biopsies)

**Biopsies taken from the intersection of infraspinatus and teres minor where the muscles are difficult to differentiate*

Using an anterosuperior approach, biopsies (30-500 mg, 5.3±2.0 mm diameter) were collected under direct visualization from the scapular fossae, in a region defined by the lateral edge of the glenoid and no more than 2 cm medial from that landmark. Muscle was specifically targeted, which was macroscopically defined as pink-red, organized fascicular tissues, avoiding obvious adipose or tendon tissue (Figure 1). Muscles without such tissue were not biopsied. The supraspinatus was always evaluated and biopsied if it met the above mentioned criteria, and in multiple cases the infraspinatus (including the infraspinatus/teres minor junction) was also biopsied. Immediately after biopsy, samples were pinned under tension along the medial-lateral axis, flash frozen in liquid nitrogen-cooled isopentane, transported on dry ice, and stored at -80^{O}C.

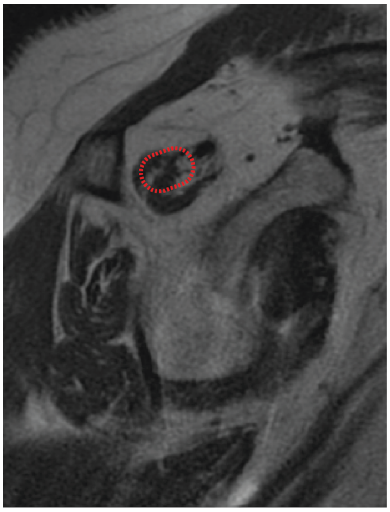

Figure 3.1 Representative T1-weighted MRI image showing the supraspinatus muscle biopsy region (red outline). In this image the supraspinatus was a Goutallier grade 3, and the biopsy did not contain identifiable muscle tissue.

Ten-micron OCT-embedded sections were generated on a Leica CM3050S cryostat. For each measurement, the entire area of a single cross-section (6-20 fields) was quantified by a single observer with four years of muscle histology experience who was blinded to Goutallier score and intraoperative appearance (Table 2). All quantification was performed using automated procedures in ImageJ[18] which required only minimal input from the operator. Hematoxylin and Eosin (H&E) and Gomori Trichrome stains were used to evaluate overall tissue composition and structure[19]. The relative fraction of organized, dense connective tissue, loose, disorganized tissue similar in appearance to granulation tissue, and muscle fibers was quantified based on manual thresholding of staining color and intensity, where loose connective tissue was similar in color but lighter in shade and intensity than dense connective tissue due to the relative packing of the ECM. The same program was also used to quantify areas of fat within the same sections.

Table 3.2 All quantification and manual screening performed by a single observer with 4 years experience in muscle histology. H&E and trichrome stains were mounted with Permount mounting medium and imaged on a Leica SCN400 slide scanner (**). Immunofluorescent stains were mounted with Vectamount mounting media with DAPI to visualize nuclei (***). All IF staining carried out on Leica DM6000B microscope with DCF365FX camera on 10x setting (100x total magnification). Tile image of entire cross-section section and manual background adjustment was performed before quantification of all immunofluorescent images in ImageJ (****).

Dye or 1° Ab (Dilution)	2° Ab (Dilution)	Staining Protocol	Quantification
Hematoxylin & Eosin	N/A	-4m Hematoxylin -1m LiCl soln. -3s Eosin -Dehydration -Citrate Clarifier -Mount	Fasicles identified and scored 1 or 0 for degeneration, intra- and inter-fascicular fat quantified at 10 and 20x in Leica Digital Image Hub **
Gomori Trichrome (In Distilled H_2O: 6g/ml Chromotrope 2R, 3g/ml Analine Blue, 0.1ml/ml Glacial Acetic Acid, 8g/ml Phosphotungstic Acid)	N/A	-1h fixation in Bouin's soln. -H_2O Wash -17.5m trichrome -10m Weigert's Hematoxylin -Dehydration -Mount**	ROI trace around sample area, manual thresholding of RGB channels (muscle = blue, loose ECM = green, dense ECM = red) used to calculate area fractions of each tissue type within ROI. Each pixel counted for each tissue type independently. **
CD68 (1:200) Leica/Novocastra, CD68-L-CE	Goat α-Mouse, AlexaFluor 488, Invitrogen A11029 (1:400)	-30m 1% BSA-PBS -Overnight 1° incubation in 0.1%BSA-PBS -Wash -45m 2° incubation -Wash -Mount	Particles in green channel with size range 10-200μm^2 automatically identified, with manual removal of non-cell particles preceding auto-quantification of macrophage density.***,****
αSMA (1:200) Diagnostic BioSystems, MoB 001	Goat α-Mouse, AlexaFluor 488, Invitrogen A11029	-30m 1% BSA-PBS -1h 1° incubation in 0.1%BSA-PBS -Wash -45m 2° incubation -Wash -Mount	Particles in green channel with area >20μm^2 automatically identified, with manual removal of non-vessel structures preceding auto- quantification of average vessel area and number ***,****
Perilipin (1:400) Abcam, ab3526	Goat α-Rabbit, AlexaFluor 488, Invitrogen A11008	Same as CD68	Used to confirm identity of lipid deposits in H&E and trichrome, and to evaluate the orientation of lipid relative to laminin myofiber borders ***,****
Laminin 211 (1:100) Vector Labs, VP-M648	Goat α-Mouse, AlexaFluor 594, Invitrogen A11032	Counterstain	Used to identify myofiber border to calculate myofiber area and centralized nuclei, counterstain for orientation in above stains ***,****
Laminin 111 (1:500) Sigma, L9393	Goat α-Rabbit, AlexaFluor 594, Invitrogen A11037	Counterstain	Used to identify myofiber border to calculate myofiber area and centralized nuclei, counterstain for orientation in above stains ***,****

To quantify the prevalence of degeneration and intrafascicular fat accumulation, each fascicle in an H&E-stained cross-section was scored for evidence of degenerating fibers and intrafascicular and perifascicular fat, with results reported as a percentage of total fascicles per sample. In this analysis, muscle degeneration was defined as the presence of hypercellular infiltration of muscle fibers (i.e. myophagocytosis), disrupted integrity of myofiber membranes, or split muscle fibers[6, 9]. Intrafascicular fat was defined as large, eosin-negative cells residing within the perimysium, while perifascicular fat was defined as similarly eosin-negative cells in contact with but not clearly within the fascicular border. Immunostaining for the adipocyte lipid droplet protein perilipin (Abcam) was used to confirm that such eosin-negative cells contained lipid.

The number and size of non-capillary blood vessels (alpha-smooth muscle actin, Diagnostic Biosystems) and number of macrophages (CD68, Novocastra) were quantified for whole biopsy cross-sections in ImageJ[20, 21]. Samples were counterstained with laminin-111 or -211 (LAMA1 (Sigma) or LAMA2 (Vector)) and 4',6-diamidino-2-phenylindole (DAPI).

Muscle fiber area and centralized nuclei were quantified via laminin and DAPI overlay using ImageJ[18]. Average muscle fiber area was weighted for total fiber area within each sample in order to account for varying amounts of muscle between samples. As a control group for muscle fiber area and central nuclei, four cadaveric supraspinatus muscles with no sign of RC disease were stained with H&E and quantified manually.

Data are reported as mean ± standard deviation. Due to the differences in disease state between muscles, no pairwise correction was applied when multiple muscles were biopsied from the same individual. One-way ANOVA's were used to compare measurements between different Goutallier scores, and Student's t-tests were used to compare human biopsies with cadaver data as well as muscle versus non-muscle regions within the same biopsies. Linear regression was used to assess correlations between compositional parameters. Significance thresholds were set at an alpha of 0.05.

Source of Funding:

Funding sources did not play a role in this investigation.

Results

Of the total biopsy pool, only 25.8% contained histologically identifiable muscle fibers. On average, biopsies were composed of 48.2±19.1% dense connective tissue, 36.9±15.9% disorganized and loose extracellular matrix (ECM) similar to granulation tissue, and only 10.4±22.0% muscle overall (Figure 2). Of those biopsies with any identifiable muscle tissue, the composition was 30.3±11.8% dense ECM, 26.7±17.4% loose ECM, and 40.1±26.5% muscle. There was a significant interaction between biopsy composition and Goutallier score ($p=0.0027$), with biopsies from lower Goutallier-scored muscles containing more muscle on average and muscle nearly absent in biopsies from muscles with a Goutallier

grade 4. The average fat composition for all biopsies was low (6.5±11.6%), which was likely due to our purposeful avoidance of macroscopic fat at biopsy collection.

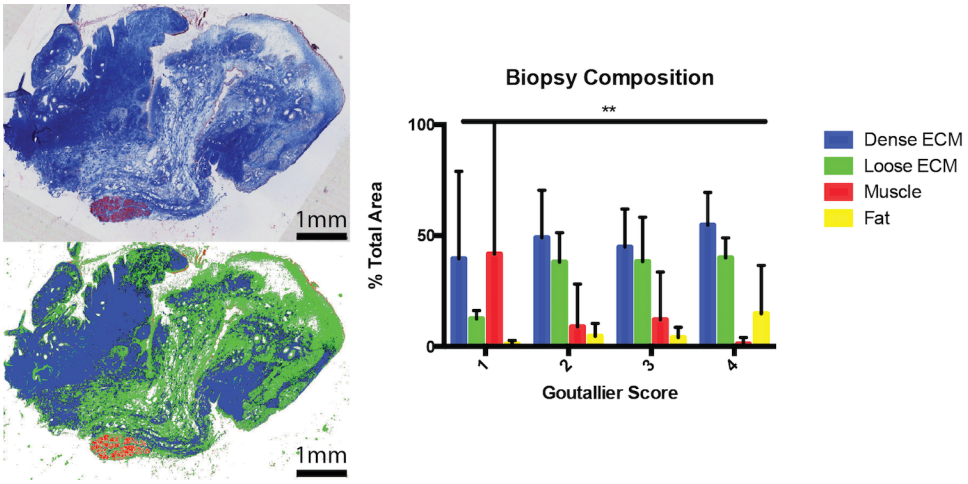

Figure 3.2 Gomori trichrome stained biopsy section demonstrating regions of dense collagen, loose collagen similar to granulation tissue, and muscle (Scale bar = 1mm) (upper left panel). Tissue fractions as classified by ImageJ, with muscle in red, organized collagen in blue and loose collagen in green (lower left panel. Biopsy composition grouped by Goutallier score, which demonstrate a significant interaction in 2-way ANOVA analysis (p=0.0027) (right panel).

Altered vascularization was prominent in the majority of biopsies, with a vessel density of 66.6±38.0 vessels/mm^2 and an average area per vessel of 448.7±204.3 μm^2 (Figure 3C,D). This represents a 4-[20] to 130-fold[22] increase in the normal vessel density of skeletal muscle (dashed line in Figure 3C, as measured in adult rat hindlimb muscle). No significant difference in vessel density was observed between samples with and without identifiable muscle tissue or between different Goutallier scores.

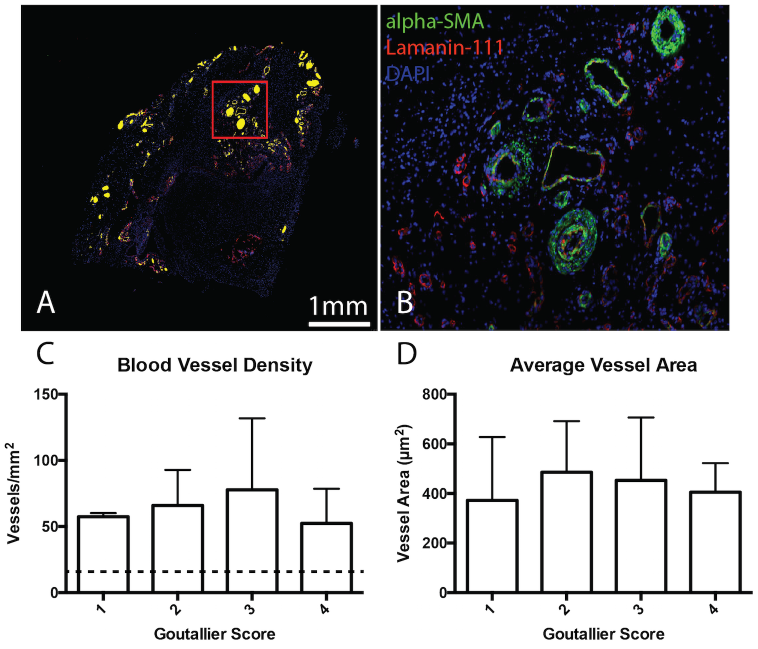

Figure 3.3 (A) Overview image of alpha-smooth muscle actin stain with positive vessels shaded in yellow. (B) 100x magnified image of the red outlined region in panel A showing alpha-SMA positive vessels (green). (C) Average blood vessel density grouped by Goutallier score, where the dotted line represents the vessel density reported for healthy muscle. (D) Average vessel area grouped by Goutallier Score.

Profound inflammation was observed in all biopsies (Figure 4). Across all samples there were 111.3±81.5 macrophages/mm^2, with 103.3±88.8 macrophages/mm^2 in muscle-containing samples. This is between 10- to 100-fold higher macrophage density than has been reported for either healthy muscle[23] or tendon[24] (1-10 macrophages/mm^2, dashed line in Figure 4C). No significant difference was found in macrophage content across Goutallier scores or between samples with and without histological evidence of muscle. Furthermore, macrophage content was not significantly different between biopsy regions composed primarily of muscle compared to the overall biopsy.

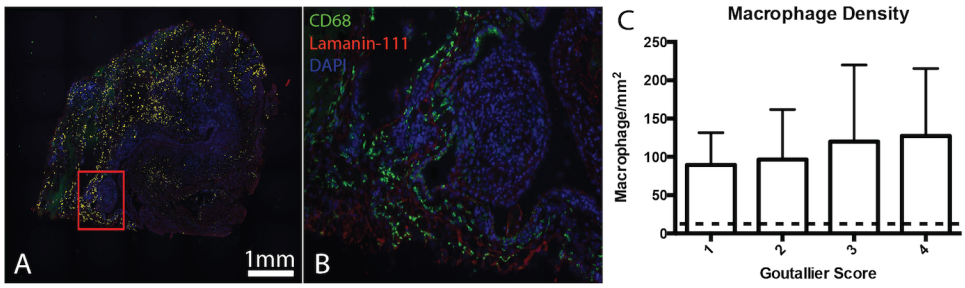

Figure 3.4 (A) Overview image of CD68 stain with positive macrophages shaded in yellow. (B) 100x magnified image of the red outlined region in panel A showing CD68-positive macrophages (green). (C) Density of macrophages reported by Goutallier score. The dotted line represents the normal threshold for macrophages in muscle tissue.

Within regions containing identifiable myofibers, signs of muscle degeneration were observed in 90.0±15.6% of all muscle fascicles (Figure 5A-E). These features qualitatively occurred more frequently around muscle/non-muscle interfaces and regions of high cellularity, though precise quantification of this phenomenon proved difficult. The percentage of centrally nucleated myofibers was also significantly elevated (11.3±6.3%) compared to both cadaveric controls (2.74±1.0%) and the clinical threshold for abnormal central nuclei (3%)[25] (Figure 6). Interestingly, no difference was found in average myofiber area between biopsies and cadaveric controls (Figure 5F), though this measurement was mildly underpowered (β=0.62).

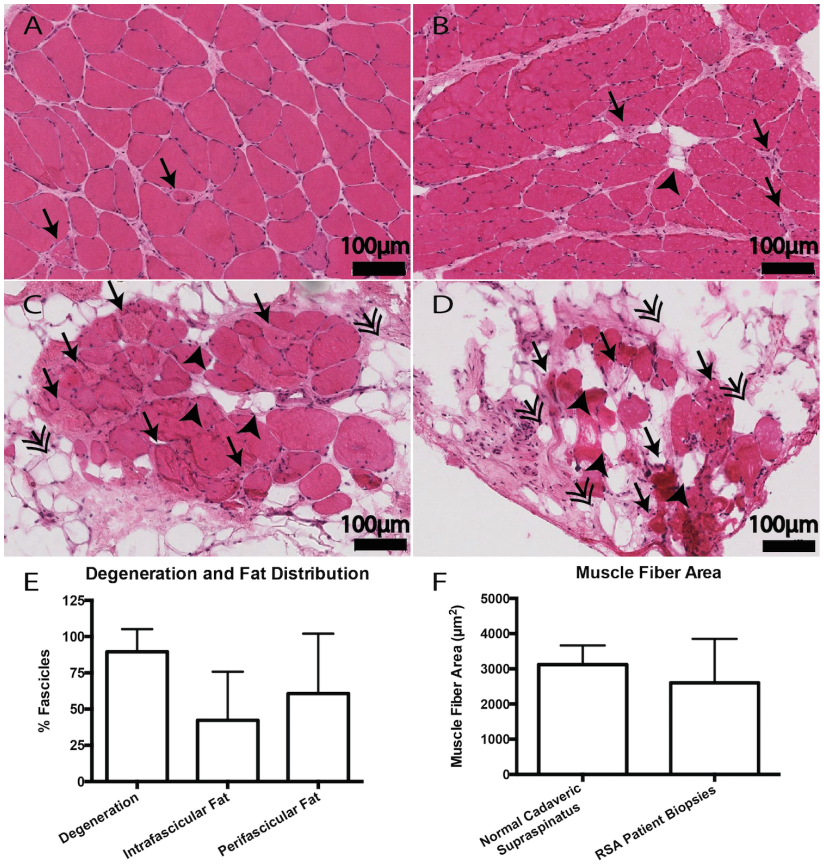

Figure 3.5 (A-D) Range of degenerative changes observed. (A) Limited degenerative signs (black arrows) and elevated central nuclei. (B) Increasing degenerative signs with limited fat accumulation within the fascicle (black arrowheads). (C) High levels of muscle degeneration and cellular invasion of myofibers (myophagocytosis), with greatly increased ECM and fat content both intrafascicularly (arrowheads) and perifascicularly (double arrowheads). (D) Nearly complete loss of muscle with replacement by fat and fibrous tissue. (E) Quantification of the percentage of total fascicles demonstrating muscle degeneration, intrafascicular fat, and perifascicular fat per sample. (F) Average muscle fiber area weighted by total muscle area, compared to cadaveric controls.

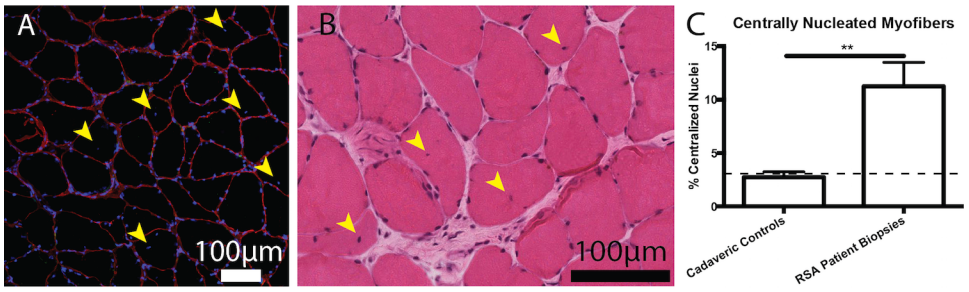

Figure 3.6 (A) Laminin-DAPI overlay image used to quantify central nuclei (yellow arrowheads). (B)Higher magnification H&E image of muscle fibers demonstrating centralized nuclei (yellow arrowheads). (C) Percentage of centrally-nucleated myofibers within a biopsy, demonstrating pathological elevation compared to both cadaveric controls and the clinical standard for pathology (dotted line).

On average, adipose tissue was dispersed throughout the biopsy and constituted only a small fraction (6.5±11.6%) of the total biopsy area. In samples containing myofibers, though total fat content remained low, fat was consistently concentrated at fascicular borders and between fascicles (perifascicular fat, 60.7±41.4% fascicles) as well as within fascicles (intrafascicular fat, 42.2±33.6% fascicles). Interestingly, intrafascicular fat was often seen in combination with degenerative signs, yet the endomysial and perimysial structures appeared intact (Figure 7,8A). In some cases, perilipin staining appeared to penetrate discontinuous laminin borders of muscle fibers (Figure 8B), though this phenomenon of fat infiltration of individual myofibers was rare and therefore difficult to quantify.

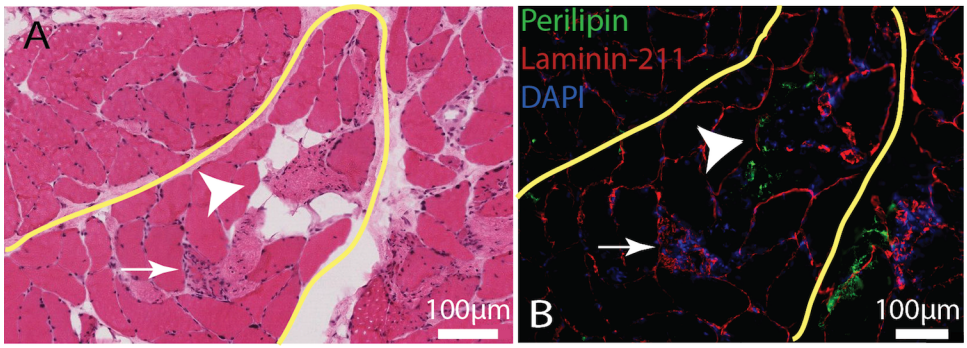

Figure 3.7 Serial sections of (A) H&E and (B) Perilipin counterstained with laminin and DAPI demonstrating a single muscle fascicle (yellow border) with a central region (white arrowhead) in which adipose tissue has directly replaced degenerating muscle (white arrow) without altering the structure of the fascicle (as quantified in Figure 5E).

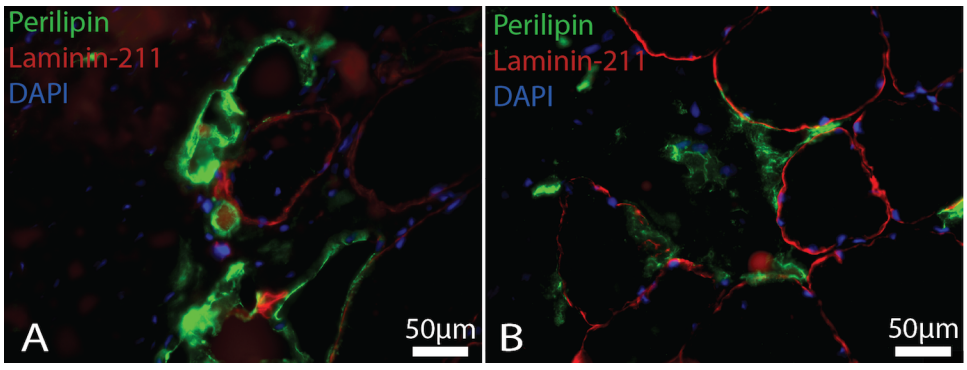

Figure 3.8 (A) Uniform perilipin positive regions (green) demonstrating adipose in a geometry and location similar to that of surround muscle fibers. (B) Disrupted muscle laminin border demonstrating positive perilipin staining suggestive of direct replacement of degenerating muscle by fat.

Discussion

In the presence of chronic and severe RC disease, the non-fatty tissues of the normally muscular supraspinatus and infraspinatus fossae are composed primarily of vascularized connective tissue. A large fraction of this tissue is similar in appearance to granulation tissue that forms in response to severe tissue damage, in that it is composed of vascular, loose ECM that has a high macrophage density[26]. This finding is not unprecedented given that chronic inflammation and muscle degeneration cause neovascularization while diminishing muscle volume[27, 28]. Though tissue composition was related to Goutallier score, the assumptions about tissue type and quality that are associated with each scoring level are called into question. Because our biopsy procedure targeted only non-fat tissue, low fat content relative to clinical images was expected. However, lack of muscle relative to what was observed on imaging and intraoperatively may relate to the hypervascularity of the disorganized connective tissue. Further research (high resolution, quantitative MRI and histology) on isolated biopsies is needed to test this idea. Combined with the large number of actively degenerating myofibers observed, these data suggest that imaging may create considerable over-estimation of the fraction of viable contractile tissue within the fossa.

While understanding the tissue composition is critical in interpreting clinical images and making surgical decisions, elucidating the source of muscle loss is potentially a more important question. Specifically, the distinction between the terms “fatty degeneration”, “fatty atrophy”, and “fatty infiltration” is rarely addressed in the literature. Though previously underappreciated, the implications of atrophy versus degeneration and fatty infiltration versus replacement are, in fact, critical in understanding disease progression on a cellular level.

The most appropriate term to describe previous studies in this area appears to be “fatty atrophy”. In evaluating the muscle of early-stage RC disease, Lundgreen et al.[15] reported decreased myofiber diameter and increased interfascicular adipose, but found no evidence of degeneration-regeneration cycling as evidenced by a normal percentage of centrally nucleated myofibers. Steinbacher et al.[16]

reported a similar increase in overall adipose and interfascicular ECM, with increased lipid content and decreased myofibrillar organization in affected myofibers. Mendias et al. corroborated these findings, and further showed diminished force production in myofibers isolated from chronic, full thickness tears[17]. Animal models of RC disease, particularly large animal models, are relatively effective in recapitulating this atrophic, fat accumulating phenotype of early and mid-stage disease[29-35]. However, no previous study in humans or animals has addressed the existence of degeneration or the higher order pattern of fat accumulation within the muscle in the most chronic and advanced stage of RC disease.

The data presented here provide clear evidence that muscle degeneration and regeneration occur in advanced RC disease. The level of muscle degeneration was profound, where 90% of fascicles displayed some degenerative features and 74% of biopsies contained no muscle tissue at all, despite intraoperative targeting of muscle tissue. Previous studies reported significant reductions in myofiber area between control and large tears[16], and though our mean myofiber areas were also lower on average, this was not statistically significant. Because our study was underpowered, we do not claim that atrophy is absent in these biopsies.

Cumulatively these data suggest that imbalanced degeneration-regeneration, possibly exacerbated by high levels of inflammation, is the primary driver of muscle loss in later stage RC disease. We speculate that this degenerative mechanism of muscle loss is somewhat similar to the inflammatory myopathies, and contrasts the atrophy-driven muscle loss reported in early stage disease[15]. Functionally, muscle loss from atrophy and degeneration will both result in impaired force production. The distinction between atrophy and degeneration has critical implications for recovery. An atrophic muscle may be rescued with renewed activation and mechanical reloading (i.e. tendon repair and exercise) even in older patients[12]. Conversely, a chronically degenerated muscle with cell loss and likely impaired regenerative capacity may be further damaged by the same treatment[36] , with limited capcity to increase myofiber number. In the latter case, treatment with anti-inflammatory and/or pro-myogenic (pharmacological or cellular) therapies may be appropriate.

Of interest was the presence of fat in structures that appeared to be previously filled with contractile tissue, indicative of a more chronic and possibly terminal stage of degeneration. In addition to the "fatty infiltration" described ubiquitously in the literature, we demonstrate the proximity of degenerative fibers and large adipocytes within architecturally preserved fascicles in over 40% of all fascicles. The origin of these adipocytes remains to be determined, but may be related to the lipid laden macrophages described by Mendias et al.[17], as it is possible that such macrophages could differentiate into adipocytes[39]. More detailed analysis demonstrated perilipin-postive membranes surrounded by or crossing laminin borders, suggesting that the lipid deposit had replaced the contractile apparatus while maintaining the original myofiber structure. To our knowledge this is the first human example of a muscle to fat transition that preserves the underlying muscle matrix architecture in what could be considered "fatty replacement". This phenomenon is not entirely unprecedented, as previous studies have shown adipogenic transition of both human myeloid cells[37] and resident muscle stem cells in rodent systems[38,39]. Further studies that specifically trace cell fate are required to identify the exact cell source or sources of the accumulating fat, as it is possible that the fat in different anatomical locations or in distinct stages of disease is derived from divergent cell depots.

As with many studies of this nature, obtaining the appropriate control data proved difficult. RC muscle-specific control data is absent in the literature, and due to limitations inherent to fixed tissue, specifically that extracellular and non-muscle tissues (especially loose connective and adipose tissue) are severely disrupted and often destroyed in processing, and that immunohistochemical assays are largely ineffective on fixed tissue, we could not obtain meaningful control data for many of our assays.

Another limitation of this study is the relatively low number of biopsies that actually contained identifiable muscle fibers, particularly in the supraspinatus. This low muscle fraction was startling, given the MRI and intraoperative appearance of muscle-like tissue in the region of the biopsy. Though we can correlate a biopsy region with an imaging-based region, we did not perform stereotactic biopsy (exact position). Nevertheless, the severe muscle degeneration measured here suggests that tissue quality is not well represented by current clinical imaging modalities. This in turn may help to explain the high number

of unsatisfactory clinical outcomes. If the extent of muscle degeneration and replacement by non-contractile tissue is systematically underestimated, which our data emphatically suggest, then standard treatments may insufficiently address the underlying pathology and functional deficits may persist even in the presence of an anatomically repaired cuff.

Conclusion

In this study, we demonstrate that RC muscle exhibits an active cycle of degeneration and regeneration in advanced RC disease, with degeneration potentially exacerbated by high levels of inflammation. Muscle loss in these samples was so profound that in a large majority of biopsies, muscle tissue was completely replaced by a disorganized, vascular ECM network with high macrophage density. It is possible that such tissue appears similar to muscle in clinical imaging, leading to gross underestimation of muscle degeneration. We also provide evidence for the existence of a process of "fatty replacement", whereby degenerating muscle is replaced by fat while maintaining the structure of the native muscle fiber ECM. Clinically, these results indicate that more careful staging of muscle quality may be important for surgical decision making, as the most severe forms of degeneration may not respond well to muscle reloading.

Acknowledgements

Financial support for this work was provided by the National Institutes of Health (NIH) R01 HD073180 (S.R.W.); the Orthopaedic Research and Education Foundation (OREF) Resident Research Grant (T.C.); and the University of California, San Diego Frontiers of Innovation Scholars Program Fellowship (M.C.G.).

This chapter, in full, is a reprint of the material as it appears in the Journal of Bone and Joint Surgery 2017. Michael C. Gibbons, Anshu Singh, Oke Anakwenze, Timothy Cheng, Maxwill Dylan Pomerantz, Simon Schenk, Adam J. Engler, Samuel R. Ward. The dissertation/thesis author was the primary investigator of this material.

References

1. Yamamoto A, Takagishi K, Osawa T, Yanagawa T, Nakajima D, Shitara H, Kobayashi T. 2010. Prevalence and risk factors of a rotator cuff tear in the general population. Journal of Shoulder and Elbow Surgery 19:116-120.

2. Bishop J, Klepps S, Lo IK, Bird J, Gladstone JN, Flatow EL. 2006. Cuff integrity after arthroscopic versus open rotator cuff repair: a prospective study. Journal of shoulder and elbow surgery 15:290-299.

3. Longo UG, Franceschi F, Ruzzini L, Rabitti C, Morini S, Maffulli N, Denaro V. 2008. Histopathology of the supraspinatus tendon in rotator cuff tears. The American journal of sports medicine 36:533-538.

4. Riley G, Goddard M, Hazleman B. 2001. Histopathological assessment and pathological significance of matrix degeneration in supraspinatus tendons. Rheumatology 40:229-230.

5. De Giorgi S, Saracino M, Castagna A. 2013. Degenerative disease in rotator cuff tears: what are the biochemical and histological changes? Joints 2:26-28.

6. Dubowitz V, Sewry CA, Oldfors A. 2013. Muscle Biopsy: A Practical Approach, Expert Consult; Online and Print, 4: Muscle Biopsy: A Practical Approach: Elsevier Health Sciences;

7. Bonaldo P, Sandri M. 2013. Cellular and molecular mechanisms of muscle atrophy. Disease models & mechanisms 6:25-39.

8. Wallace GQ, McNally EM. 2009. Mechanisms of muscle degeneration, regeneration, and repair in the muscular dystrophies. Annual review of physiology 71:37-57.

9. Preedy VR, Peters TJ. 2002. Skeletal muscle: pathology, diagnosis and management of disease: Cambridge University Press;

10. Thomason DB, Booth FW. 1990. Atrophy of the soleus muscle by hindlimb unweighting. Journal of Applied Physiology 68:1-12.

11. Levine S, Nguyen T, Taylor N, Friscia ME, Budak MT, Rothenberg P, Zhu J, Sachdeva R, Sonnad S, Kaiser LR. 2008. Rapid disuse atrophy of diaphragm fibers in mechanically ventilated humans. New England Journal of Medicine 358:1327-1335.

12. Frontera WR, Meredith CN, O'reilly K, Knuttgen H, Evans W. 1988. Strength conditioning in older men: skeletal muscle hypertrophy and improved function. Journal of applied physiology 64:1038-1044.

13. Goutallier D, Postel J-M, Bernageau J, Lavau L, Voisin M-C. 1994. Fatty muscle degeneration in cuff ruptures: pre-and postoperative evaluation by CT scan. Clinical orthopaedics and related research 304:78-83.

14. Fuchs B, Weishaupt D, Zanetti M, Hodler J, Gerber C. 1999. Fatty degeneration of the muscles of the rotator cuff: assessment by computed tomography versus magnetic resonance imaging. Journal of Shoulder and Elbow Surgery 8:599-605.

15. Lundgreen K, Lian ØB, Engebretsen L, Scott A. 2013. Lower muscle regenerative potential in full-thickness supraspinatus tears compared to partial-thickness tears. Acta orthopaedica 84:565-570.

16. Steinbacher P, Tauber M, Kogler S, Stoiber W, Resch H, Sänger A. 2010. Effects of rotator cuff ruptures on the cellular and intracellular composition of the human supraspinatus muscle. Tissue and Cell 42:37-41.

17. Mendias CL, Roche SM, Harning JA, Davis ME, Lynch EB, Enselman ERS, Jacobson JA, Claflin DR, Calve S, Bedi A. 2015. Reduced muscle fiber force production and disrupted myofibril architecture in patients with chronic rotator cuff tears. Journal of Shoulder and Elbow Surgery 24:111-119.

18. Abràmoff MD, Magalhães PJ, Ram SJ. 2004. Image processing with ImageJ. Biophotonics international 11:36-42.

19. Miller JL, Watkin KL, Chen MF. 2002. Muscle, adipose, and connective tissue variations in intrinsic musculature of the adult human tongue. Journal of Speech, Language, and Hearing Research 45:51-65.

20. Hansen-Smith F, Egginton S, Hudlicka O. 1998. Growth of arterioles in chronically stimulated adult rat skeletal muscle. Microcirculation 5:49-59.

21. Pulford KA, Sipos A, Cordell JL, Stross WP, Mason DY. 1990. Distribution of the CD68 macrophage/myeloid associated antigen. International immunology 2:973-980.

22. Laughlin MH, Cook JD, Tremble R, Ingram D, Colleran PN, Turk JR. 2006. Exercise training produces nonuniform increases in arteriolar density of rat soleus and gastrocnemius muscle. Microcirculation 13:175-186.

23. Dorph C, Englund P, Nennesmo I, Lundberg IE. 2006. Signs of inflammation in both symptomatic and asymptomatic muscles from patients with polymyositis and dermatomyositis. Annals of the rheumatic diseases 65:1565-1571.

24. Matthews T, Hand G, Rees J, Athanasou N, Carr A. 2006. Pathology of the torn rotator cuff tendon REDUCTION IN POTENTIAL FOR REPAIR AS TEAR SIZE INCREASES. Journal of Bone & Joint Surgery, British Volume 88:489-495.

25. Sorarù G, D'Ascenzo C, Polo A, Palmieri A, Baggio L, Vergani L, Gellera C, Moretto G, Pegoraro E, Angelini C. 2008. Spinal and bulbar muscular atrophy: skeletal muscle pathology in male patients and heterozygous females. Journal of the neurological sciences 264:100-105.

26. Clark R. 2013. The Molecular and Cellular Biology of Wound Repair: Springer US;

27. Jackson JR, Seed M, Kircher C, Willoughby D, Winkler J. 1997. The codependence of angiogenesis and chronic inflammation. The FASEB Journal 11:457-465.

28. Conn PM. 2013. Neurotoxins: Volume 8: Neurotoxins: Elsevier Science;

29. Liu X, Manzano G, Kim HT, Feeley BT. 2011. A rat model of massive rotator cuff tears. Journal of orthopaedic research 29:588-595.

30. Gerber C, Meyer D, Schneeberger A, Hoppeler H, Von Rechenberg B. 2004. Effect of tendon release and delayed repair on the structure of the muscles of the rotator cuff: an experimental study in sheep. The Journal of Bone & Joint Surgery 86:1973-1982.

31. Gumucio JP, Davis ME, Bradley JR, Stafford PL, Schiffman CJ, Lynch EB, Claflin DR, Bedi A, Mendias CL. 2012. Rotator cuff tear reduces muscle fiber specific force production and induces macrophage accumulation and autophagy. Journal of Orthopaedic Research 30:1963-1970.

32. Safran O, Derwin KA, Powell K, Iannotti JP. 2005. Changes in rotator cuff muscle volume, fat content, and passive mechanics after chronic detachment in a canine model. J Bone Joint Surg Am 87:2662-2670.

33. Kim HM, Galatz LM, Lim C, Havlioglu N, Thomopoulos S. 2012. The effect of tear size and nerve injury on rotator cuff muscle fatty degeneration in a rodent animal model. Journal of shoulder and elbow surgery 21:847-858.

34. Rowshan K, Hadley S, Pham K, Caiozzo V, Lee TQ, Gupta R. 2010. Development of fatty atrophy after neurologic and rotator cuff injuries in an animal model of rotator cuff pathology. J Bone Joint Surg Am 92:2270-2278.

35. Gerber C, Schneeberger AG, Perren SM, Nyffeler RW. 1999. Experimental Rotator Cuff Repair. A Preliminary Study*. The Journal of Bone & Joint Surgery 81:1281-1290.

36. Garrett WE, Kirkendall DT. 2000. Exercise and Sport Science: Lippincott Williams & Wilkins;

37. Majka SM, Fox KE, Psilas JC, Helm KM, Childs CR, Acosta AS, Janssen RC, Friedman JE, Woessner BT, Shade TR. 2010. De novo generation of white adipocytes from the myeloid lineage via mesenchymal intermediates is age, adipose depot, and gender specific. Proceedings of the National Academy of Sciences 107:14781-14786.

38. Asakura A, Rudnicki MA, Komaki M. 2001. Muscle satellite cells are multipotential stem cells that exhibit myogenic, osteogenic, and adipogenic differentiation. Differentiation 68:245-253.

39. Uezumi A, Ikemoto-Uezumi M, Tsuchida K. 2014. Roles of nonmyogenic mesenchymal progenitors in pathogenesis and regeneration of skeletal muscle. Frontiers in physiology 5.

Chapter 4. Heterogeneous muscle gene expression patterns in patients with massive rotator cuff tears

Abstract

Detrimental changes in the composition and function of rotator cuff (RC) muscles are hallmarks of RC disease progression. Previous studies have demonstrated both atrophic and degenerative muscle loss in advanced RC disease. However, the relationship between gene expression and RC muscle pathology remains poorly defined, in large part due to a lack of studies correlating gene expression to tissue composition. Therefore, the purpose of this study was to determine how tissue composition relates to gene expression in muscle biopsies from patients undergoing reverse shoulder arthroplasty (RSA). Gene expression related to myogenesis, atrophy and cell death, adipogenesis and metabolism, inflammation, and fibrosis was measured in 40 RC muscle biopsies, including 31 biopsies from reverse shoulder arthroplasty (RSA) cases that had available histology data and 9 control biopsies from patients with intact RC tendons. After normalization to reference genes, linear regression was used to identify relationships between gene expression and tissue composition. Hierarchical clustering and principal component analysis (PCA) identified unique clusters, and fold-change analysis was used to determine significant differences in expression between clusters. We found that gene expression profiles were largely dependent on muscle presence, with muscle fraction being the only histological parameter that was significantly correlated to gene expression by linear regression. Similarly, samples with histologically-confirmed muscle distinctly segregated from samples without muscle. However, two sub-groups within the muscle-containing RSA biopsies suggest distinct phases of disease, with one group expressing markers of both atrophy and regeneration, and another group not significantly different from either control biopsies or biopsies lacking muscle. In conclusion, this study provides context for the interpretation of gene expression in heterogeneous and degenerating muscle, and provides further evidence for distinct stages of RC disease in humans.

Key Words: Rotator Cuff, Muscle Degeneration, Muscle Atrophy, Gene Expression Analysis

Introduction

The progressive and irreversible loss of rotator cuff (RC) muscle that occurs in RC disease is a vexing clinical challenge[1]. Despite advances in surgical tools and techniques, outcomes of RC repair are often unsatisfactory, especially for those with large tendon tears and chronic, advanced disease[1]. These suboptimal outcomes include tendon re-tear and persistent functional limitations[2], and occur in a significant number of cases[3]. Compositional changes on a macroscopic scale can in part explain these outcomes, as muscle volume is displaced by fat[4]. Changes at the tissue level may also be responsible for poor outcomes, as muscle fiber organization and force production are reduced with tear[5], and patients with the most severe RC disease (those undergoing RSA) demonstrate widespread muscle fiber degeneration[6]. To better understand the biological processes that govern muscle loss and fatty infiltration in RC disease, several studies have evaluated gene expression in human RC muscle[7; 8]. Here, we aim to address a key limitation of previous studies by correlating gene expression to histological biopsy composition, and provide potential interpretations of our findings as they relate to progression of RC disease.

Two previous studies of human RC muscle gene expression showed that when compared to small tears, large or massive tears generally exhibit depressed expression of key myogenic, adipogenic, and fibrotic genes along with high myostatin expression[7; 8], suggestive of an anti-myogenic disease process[9; 10]. However, a major limitation of these and many other molecular studies of heterogeneous tissues is the difficulty of reconciling gene expression values with changes in tissue composition, which could influence measured transcript abundance[11]. Given the gross changes in muscle composition observed across the spectrum of RC diseases[6; 12; 13], it is reasonable to hypothesize that gene expression changes are driven as much by the composition (e.g. muscle content) of the tissue as by changes in gene expression that occur within a given tissue type or cell population, a measurement which itself remains difficult[14]. Despite this common assumption, that gene expression patterns are influenced by changes in the underlying tissue composition, no previous study has included both gene expression and compositional

data. Therefore, two major aims of this work were to 1) generate evidence to determine whether and to what extent tissue composition predicts gene expression patterns, and 2) use those findings to provide context for and caution against interpretation of gene expression data in the absence of compositional data.

Beyond the technical limitations of previous studies, we placed an emphasis on patients with advanced RC disease in this study, as these patients typically have the most severe muscle loss and the poorest outcomes among patients with cuff tears. We were particularly interested in genes and pathways involved in muscle atrophy and regeneration along with adipogenic and fibrotic genes, given the apparent irreversibility of muscle loss and fat and fibrotic tissue accumulation following chronic, massive RC tear. By providing insight into the relationship between gene expression and tissue composition, we hope to provide some perspective and context for previous studies while offering insight into the biological processes that govern the latter stages of RC disease.

Materials and Methods

Patients

Twenty-three patients undergoing reverse total shoulder arthroplasty (RSA) were consented for RC muscle biopsy. All biopsies were performed with informed written consent under the approval of the UC San Diego IRB (study #090829). In order to specifically target muscle, obvious regions of tendon and fat were avoided and only samples that macroscopically appeared vascular and organized in fascicular structures were retained (red circle in Fig. 1A). The supraspinatus was always biopsied if tissue meeting these criteria was present, otherwise the infraspinatus or teres minor were biopsied using the same criteria. In some cases both supraspinatus and infraspinatus were biopsied in order to increase the number of samples containing myofibers, leading to a total of 31 RSA biopsies, for which the histological data has been published[6]. Samples from patients with intact RC tendon were obtained arthroscopically from the superficial and lateral surface of the supraspinatus muscle during subacromial decompression

surgeries (n=9). After biopsy, samples were flash frozen in liquid nitrogen-cooled isopentane and stored at -80^{o}C for future processing.

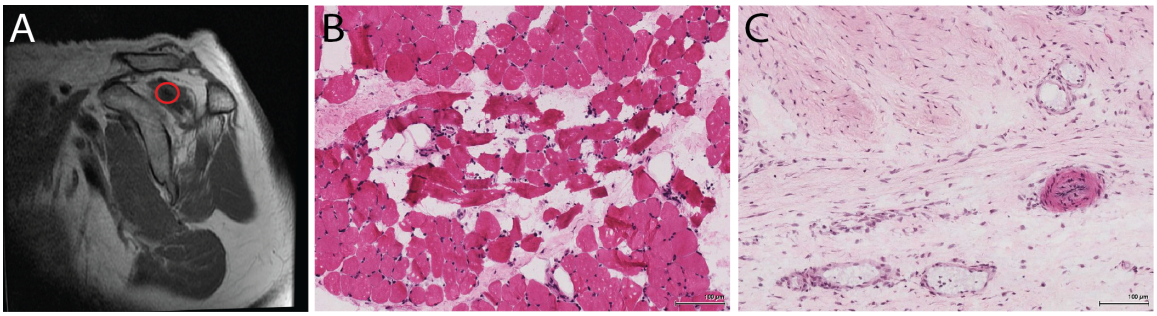

Figure 4.1 (A) MRI demonstrating the approximate biopsy region, where only regions of apparent muscle were targeted. (B) Representative H&E image of a muscle-containing biopsy, with high levels of muscle degeneration. (C) Representative H&E image of a biopsy that did not contain muscle, demonstrating high cellularity and presence of larger vascular structures.

RNA Isolation and Quantitative PCR

For gene expression analysis, biopsy cross-sections weighing approximately 30-50 mg were cut from the biopsy center and homogenized in bead tubes (Navy, NextAdvance) with TRIZOL (Ambion). RNeasy spin columns (Qiagen) were used to extract RNA using the manufacturer's protocol. One microgram of complimentary DNA (cDNA) was reverse transcribed with iScript cDNA Synthesis kits (Biorad). Quantitative PCR was carried out on custom plates on a BioRad CFX384 Touch qPCR analyzer for a panel of 42 genes associated with myogenic, atrophic, adipogenic, fibrotic and inflammatory pathways (Table 1), with cycle threshold determined using a SYBR green fluorophore. On-plate quality assessment was performed to assess gDNA contamination and RNA quality. Each sample was contained on a single plate, negating the need for inter-plate corrections.

Gene Expression Analysis

Raw cycle-threshold values (Ct values) were obtained from all samples and read into a qPCR expression set using the R Bioconductor package HTqPC, and were normalized using the delta-Ct normalization method to obtain gene expression values (*RPS18* and *ACTB* used as reference genes). Note

that a maximum Ct of 39 was applied to all genes of interest to allow for statistical comparisons, and that lower values indicate higher expression in this method[15].

To determine the effect of tissue composition on muscle gene expression, linear regression of normalized gene expression and previously measured and reported histological parameters[6] was implemented. The following histological parameters from the previous study[6] were evaluated here: relative tissue fractions of muscle, connective tissue, and fat, along with inflammation (macrophage density) and vasculature (α-SMA+ vessel density and size). Coefficients of determination were calculated for linear relationships between expression values and histological parameters, and were considered significantly predictive when $r^2 > 0.2$ and Bonferroni-corrected p-values were statistically significant ($\alpha = 0.05$).

Unsupervised hierarchical clustering using Euclidean distance was then applied to the normalized expression values to determine the ability of gene expression patterns to differentiate muscle-containing samples from those without muscle, and to identify potential sub-clustering of muscle-containing samples. Where appropriate, compositional parameters were compared using a two-tailed t-test ($\alpha < 0.05$) to determine significant differences in average composition of the sub-group versus the remaining biopsy pool. Additionally, principle component analysis (PCA) was performed on the normalized gene expression values using the R package prcomp[16], in order to better appreciate sample clustering and to identify the genes with the largest effect on variability between samples. Subsequent differential gene expression sub-analyses were performed based on the groups identified by hierarchical clustering and confirmed by PCA.

Differential expression values (delta-delta-Ct)[15] were calculated with the limmaCtData wrapper in HTqPCR for the Bioconductor package limma using a moderated *t*-test[17]. Based on the cluster analysis and histological data available for the RSA biopsies, the intact comparisons described below include only intact biopsies that clustered with muscle-containing RSA samples. Differential expression values were computed for: 1) RSA biopsies with muscle present vs. without muscle, 2) pooled RSA biopsies versus the intact group, and 3) each main RSA cluster compared to the intact group. Differential expression

values were also computed between clusters to determine if different sub-groups had significantly different gene expression. In all analyses, muscle content was included as a covariate to correct for the demonstrated effects of muscle content on expression profile, and genes with a Benjamini-Hochberg adjusted p-value < 0.05 were considered significantly differentially expressed. All raw data for this study can be found in the supplemental materials (Supplemental_Data.xlsx).

Results

As discussed in our previous publication[6], only 8/31 (26%) RSA samples contained histological evidence of skeletal muscle (Fig 1B). In samples lacking histologically identifiable muscle (Fig 1C), expression of muscle-specific genes was almost entirely absent (Fig 2, black dendrogram branches). Similarly, muscle content was significantly correlated to the expression of 11 muscle related genes (Table 1); there was no significant correlation between gene expression and any other histologic metric.

Table 4.1 Gene Categories, Linear Regression, and PCA Data. Genes categorized by most relevant category. Coefficient of determination (r^2) for normalized expression and muscle fraction calculated via histology. Gene weights for the first two principle components are reported. Note that directionality of gene weights indicates genes with opposing expression trends, and does not indicate positive or negative disease effects.

Gene Category	Gene Name (Abbreviation)	p-value	r^2	1st PC	2nd PC
Muscle structure/myogenesis	Embryonic Myosin Heavy Chain (MYH3)	n.s.	--	**0.194**	0.077
Muscle structure/myogenesis	Myosin Heavy Chain - Type I (MYH1)	6.24E-05	0.41	0.108	**0.211**
Muscle structure/myogenesis	Insulin-like Growth Factor 1 (IGF1)	n.s.	--	0.106	***-0.204***
Muscle structure/myogenesis	Cysteine and Glycine Rich Protein 3 / Muscle LIM Protein (CSRP3)	1.77E-07	0.602	0.131	**0.194**
Muscle structure/myogenesis	Ankyrin Repeat And SOCS Box Containing 15 (ASB15)	7.43E-10	0.726	0.144	**0.200**
Muscle structure/myogenesis	Ankyrin Repeat Domain 2-Stretch Responsive Muscle (ANKRD2)	7.88E-09	0.678	0.165	0.163
Muscle structure/myogenesis	Paired box 7 Transcription Factor (PAX7)	8.72E-09	0.676	0.168	**0.185**
Muscle structure/myogenesis	Myogenin/Myogenic Factor 4 (MYOG)	4.93E-08	0.635	0.154	**0.177**
Muscle structure/myogenesis	Myogenic Differentiation 1/Myogenic Factor 3 (MYOD1)	1.08E-07	0.615	0.128	**0.172**
Muscle structure/myogenesis	Myogenic Factor 5 (MYF5)	6.88E-07	0.564	0.160	0.153
Atrophy/Myogenic Inhibition	Myostatin/Growth Differentiation Factor 8 (MSTN)	1.28E-05	0.469	**0.212**	0.108
Atrophy/Myogenic Inhibition	Activin Receptor 2B (ACVR2B)	n.s.	--	**0.217**	0.002
Atrophy/Myogenic Inhibition	Tripartite Motif Containing 63/E3 Ubiquitin Ligase (TRIM63)	n.s.	--	0.169	0.144
Atrophy/Myogenic Inhibition	Forkhead Box O3 (FOXO3)	n.s.	--	**0.233**	*-0.068*
Atrophy/Myogenic Inhibition	F-box Protein 32/Atrogin-1/Muscle Atrophy Fbx32 (FBXO32)	3.23E-09	0.697	**0.218**	0.111
Atrophy/Myogenic Inhibition	Caspase-3 (CASP3)	n.s.	--	**0.208**	*-0.127*
Atrophy/Myogenic Inhibition	Caspase-1 (CASP1)	n.s.	--	**0.175**	*-0.155*
Metabolism	Protein Tyrosine Phosphatase, non-Receptor Type 4 (PTPN4)	n.s.	--	**0.236**	0.018
Metabolism	Mammalian Target of Rapamycin (MTOR)	n.s.	--	**0.227**	*-0.055*
Adipogenic	PPARG Coactivator 1 Alpha (PPARGC1A)	1.13E-06	0.549	**0.209**	0.098
Adipogenic	Peroxisome Proliferator-Activated Receptor Gamma (PPARG)	n.s.	--	**0.200**	*-0.073*
Adipogenic	Peroxisome Proliferator-Activated Receptor Delta (PPARD)	n.s.	--	**0.223**	*-0.071*
Adipogenic	Fatty Acid Binding Protein 4 (Adipcyte-Specific) (FABP4)	n.s.	--	**0.201**	0.007
Adipogenic	CCATT/Enhancer Binding Protein Alpha (CEBPA)	n.s.	--	**0.193**	*-0.048*
Adipogenic	Adiponectin (ADIPOQ)	n.s.	--	**0.183**	0.021
Adipogenic	Wnt Family Member 10B (WNT10B)	n.s.	--	*-0.060*	0.106
Inflammation	Tumor Necrosis Factor (TNF)	n.s.	--	0.119	*-0.038*
Inflammation	Interleukin-6 (IL6)	n.s.	--	0.093	*-0.169*
Inflammation	Interleukin-10 (IL10)	n.s.	--	0.047	***-0.195***
Inflammation	Interleukin-1 Beta (IL1B)	n.s.	--	0.051	*-0.162*
Fibrosis	Platelet-Derived Growth Factor Receptor Alpha (PDGFRA)	n.s.	--	0.140	***-0.194***
Fibrosis	Tissue Inhibitor of Metalloproteinase 3 (TIMP3)	n.s.	--	***-0.177***	0.128
Fibrosis	Tissue Inhibitor of Metalloproteinase 1 (TIMP1)	n.s.	--	0.093	***-0.229***
Fibrosis	Matrix Metalloproteinase 9 (MMP9)	n.s.	--	0.004	*-0.154*
Fibrosis	Matrix Metalloproteinase 3 (MMP3)	n.s.	--	*-0.026*	*-0.148*
Fibrosis	Matrix Metalloproteinase 1 (MMP1)	n.s.	--	*-0.023*	*-0.135*
Fibrosis	Lysyl Oxidase (LOX)	n.s.	--	0.070	***-0.224***
Fibrosis	Fibronectin 1 (FN1)	n.s.	--	*-0.016*	***-0.219***
Fibrosis	Connective Tissue Growth Factor (CTGF)	n.s.	--	0.113	***-0.209***
Fibrosis	Collagen Type III Alpha 1 Chain (COL3A1)	n.s.	--	0.012	***-0.228***
Fibrosis	Collagen Type I Alpha 1 Chain (COL1A1)	n.s.	--	0.011	***-0.230***
Fibrosis	Transforming Growth Factor Beta 1 (TGFB1)	n.s.	--	0.151	***-0.217***

Hierarchical cluster analysis of normalized expression values (noting that with the delta-Ct method, greater expression is denoted by negative values) resulted in two primary clusters, with all muscle-containing RSA samples contained in one primary cluster that also included 5/9 intact samples (Fig 2). Within this muscle-containing cluster, samples were further segregated into two groups: a group with higher expression of myogenic, adipogenic, and metabolic genes and lower expression of fibrotic genes which will be referred to as the HIGH cluster (Fig 2, red), and a second group with lower expression of myogenic and atrophic genes and higher expression of fibrotic genes which will be referred to as the LOW cluster (Fig 2, orange). Based on the exclusivity of the main muscle cluster, only intact samples that co-segregated with muscle-containing RSA samples were used for differential expression comparisons between INTACT and RSA sub-clusters.

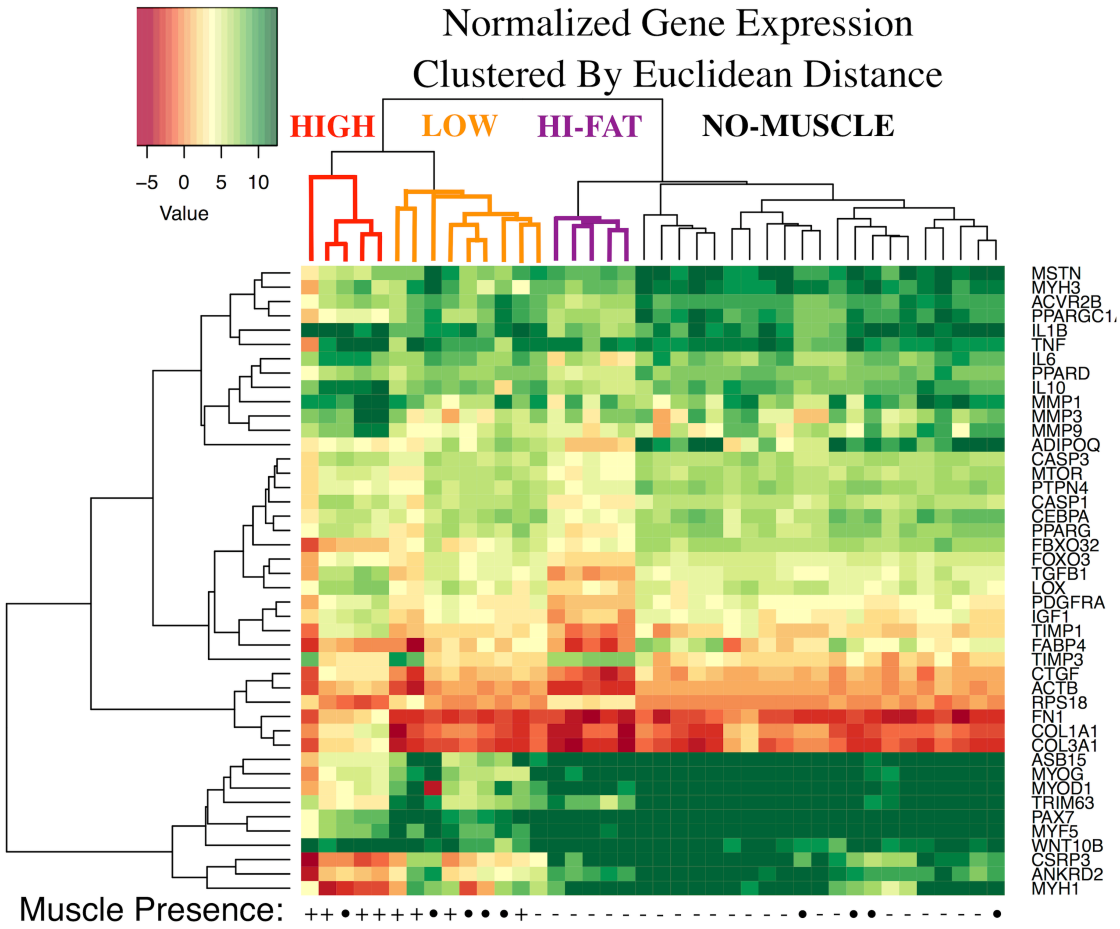

Figure 4.2 Hierarchical cluster analysis of all muscle biopsies, using Euclidean distance as the similarity metric. The histological presence or absence of muscle is noted on the bottom edge of the heatmap, with INTACT samples indicated by filled circles. Distinct biopsy clusters are denoted by coloring of the dendrogram leaves—the high-expression group (HIGH) is red, low-expression group (LOW) is orange, and high fat group (HI-FAT) is purple.

The strong effect of muscle presence and relative expression of muscle-related genes was observed in PCA as well. PCA analysis showed a high degree of separation between muscle-containing RSA samples and RSA biopsies without muscle (Fig 3). While the muscle-containing RSA samples tended to be the most variable, RSA samples without muscle formed two clear clusters in the PCA analysis. The smaller cluster (lower center) was found to contain significantly increased fat content via histology when compared to other non-muscle RSA samples (~4 fold, 17.8% vs. 4.3% fat), and will be referred to as the HI-FAT cluster (purple in Fig 2). The remaining samples lacking histological muscle

formed a larger cluster defined primarily by expression of fibrotic genes (NO-MUSCLE, black in Fig 2). Similarly, the weighting of the principal components (PCs) reflected these differences across samples, where the first PC (37.9% overall variance) was weighted primarily by myogenic inhibition, apoptotic, and adipogenic genes, while the second PC (28.7% overall variance) was weighted primarily by pro-myogenic and fibrotic genes (Table 1). No clear trend in gene families was observed in subsequent PCs.

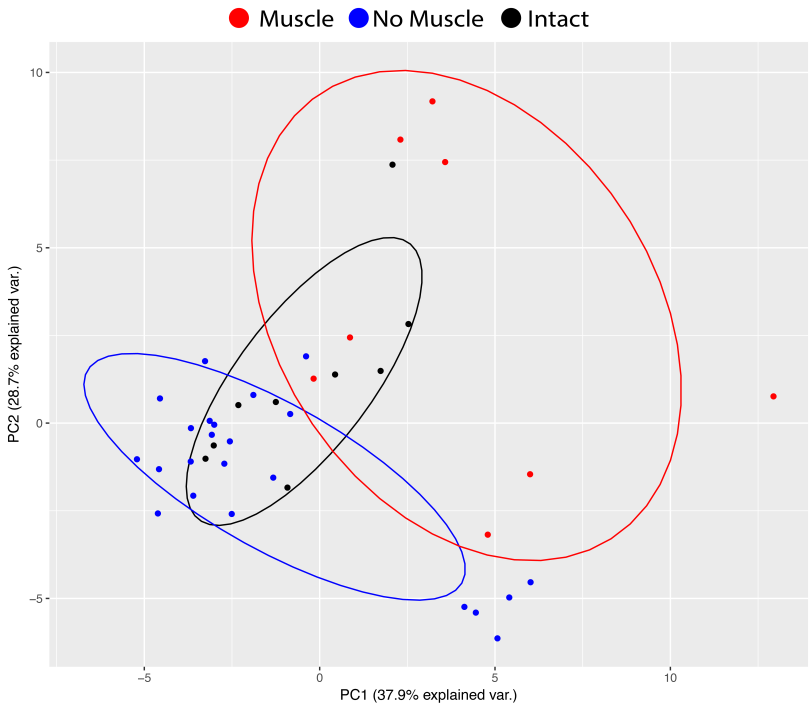

Figure 4.3 Principal component analysis employed to visualize variability between biopsies. Samples containing histological muscle are red, samples without muscle are blue, and controls are black. Of particular note are the cluster of blue samples in the lower center which correspond to the HI-FAT group in Fig 2, and the high variability in expression among the muscle-containing samples.

Differential expression analysis within the RSA biopsy pool showed that all but three of the analyzed genes (93%) were differentially expressed in samples with muscle compared to those without, with the majority of genes up-regulated in muscle containing samples (Fig 4). In stark contrast, when pooled RSA samples were compared to INTACT, there were no significant differences in expression of any genes, though 8/9 pro-myogenic genes trended toward reduced expression (Fig 5).

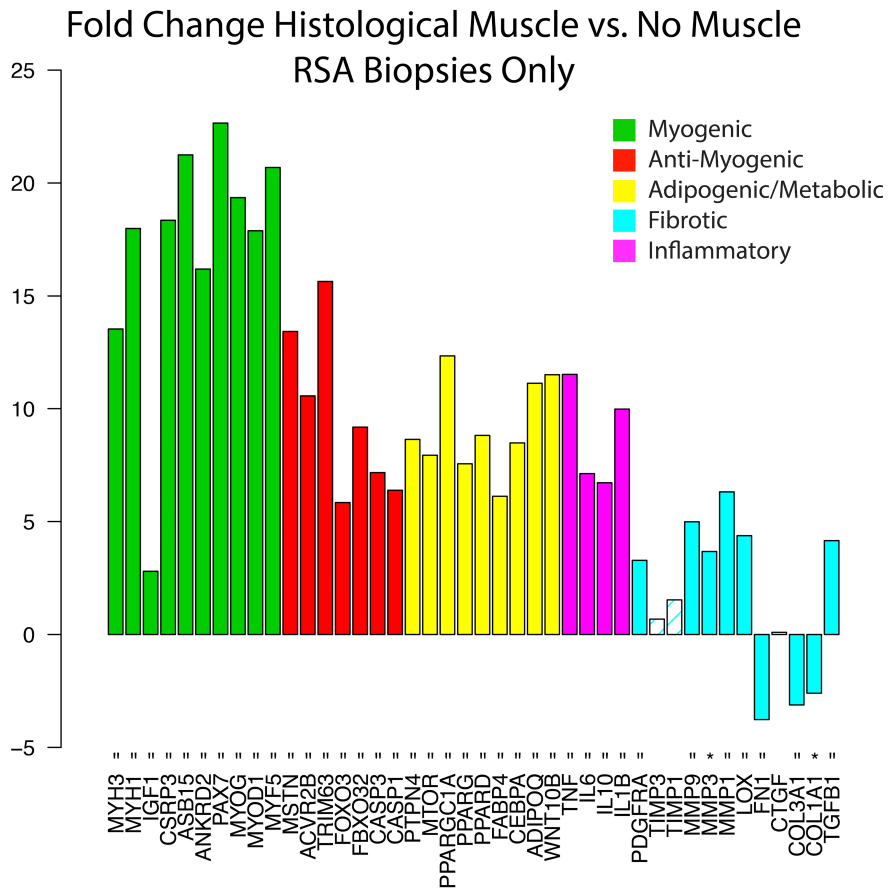

Figure 4.4 Fold change in expression between the RSA biopsies that contain muscle compared to those without muscle. Solid bars indicate significant up- or down-regulation ($p<0.01$ and $p<0.05$ indicated by ' = ', and ' * ', respectively). With muscle present, nearly all genes of interest are significantly differentially regulated, with increased expression of muscle- and fat-related genes and decreased expression of fibrosis-related genes.

These contrasting results highlight the need for a more detailed segregation and comparison of samples. Compared to INTACT, the HIGH group (red in Fig 2) demonstrated increased expression of both pro- and anti-myogenic genes, with reduced gene expression of three extracellular matrix proteins (Fig 6). However, in the LOW group (orange in Fig 2) no genes were significantly different compared to INTACT. Unsurprisingly, the HI-FAT group demonstrates increased expression of adipogenic genes and decreased muscle-related genes compared to INTACT, while the NO-MUSCLE group shows significant reduction of both pro- and anti-myogenic genes.

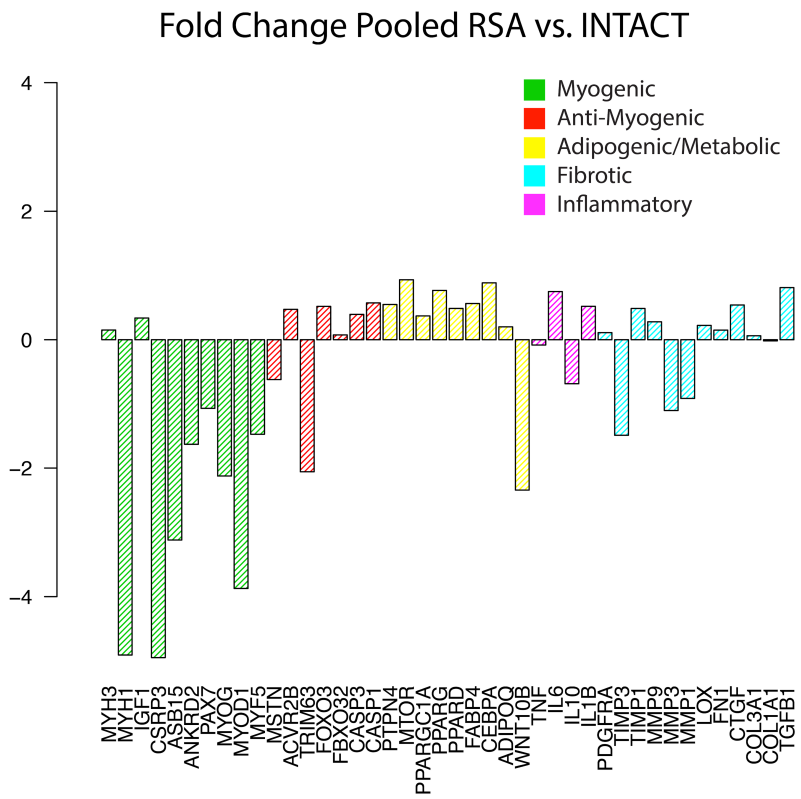

Figure 4.5 Fold change in expression between pooled RSA biopsies and controls. As a single pool, RSA biopsies are not significantly different from controls, though expression of pro-myogenic genes trended down while atrophic, adipogenic, and fibrotic genes trended up.

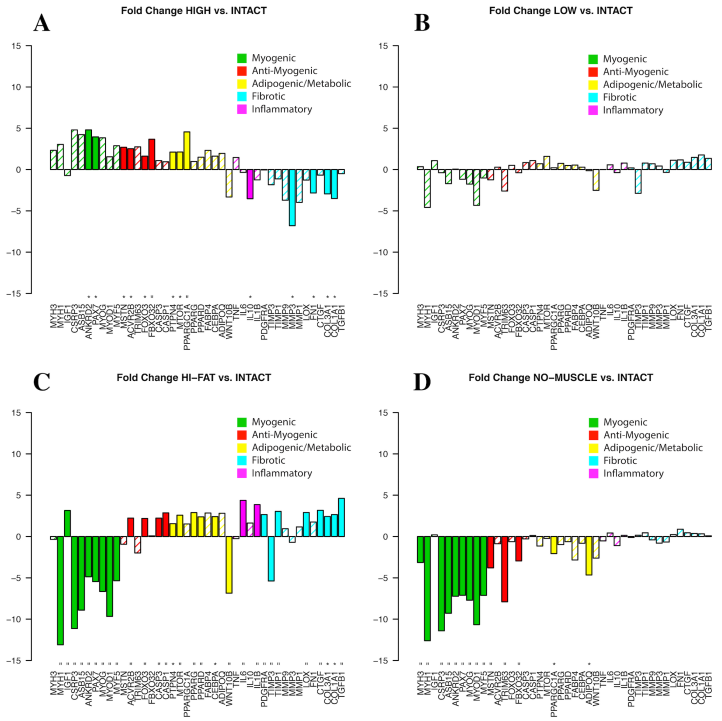

Figure 4.6 Fold changes in expression relative to INTACT for (A) HIGH muscle group (red in Fig 2), (B) LOW muscle group (orange in Fig 2), (C) HI-FAT group (purple in Fig 2), and (D) NO-MUSCLE group (black in Fig 2). Solid bars indicate significant up- or down-regulation ($p<0.01$ and $p<0.05$ indicated by ' = ', and ' * ', respectively).

Finally, fold-change expression was calculated between each sub-group (high muscle expression, low muscle expression, high fat content/expression, and the remaining samples without histological muscle or high fat). Compared to LOW group, the HIGH group demonstrated significantly increased expression of both pro- and anti-myogenic genes, with a similar but higher magnitude pattern observed between the HIGH and NO-MUSCLE groups (Fig 7A,B). This pattern was also repeated in comparing the HIGH and HI-FAT groups, though additionally the HIGH group showed significantly decreased ECM-related gene expression (Fig 7C). Similar to the analysis relative to INTACT, the LOW group did not show significant differences in expression of any genes compared to either the HI-FAT or NO-MUSCLE groups (Fig 7D,E). Compared to the NO-MUSCLE group, the HI-FAT group demonstrated increased expression of both adipogenic and fibrotic genes.

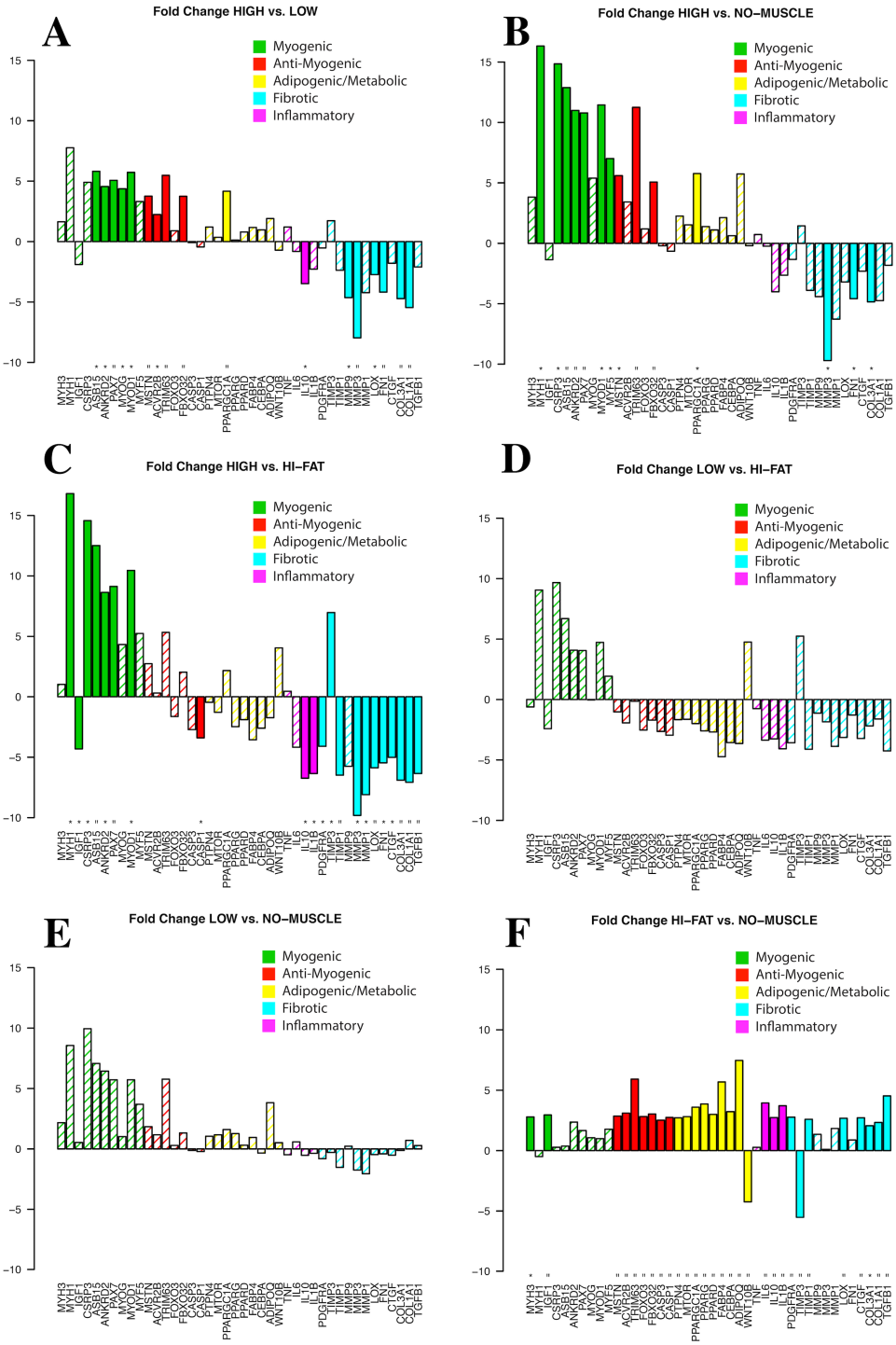

Figure 4.7 Fold changes in expression between (A) HIGH and LOW expression muscle groups, (B) HIGH and NO-MUSCLE groups, (C) HIGH muscle and HI-FAT groups, (D) LOW muscle and HI-FAT groups, (E) LOW muscle and NO-MUSCLE groups, and (F) HI-FAT and NO-MUSCLE groups. Solid bars indicate significant up- or down-regulation ($p<0.01$ and $p<0.05$ indicated by ' = ', and ' * ', respectively).

Discussion

This study highlights the importance of understanding tissue composition, and in particular muscle content, when evaluating gene expression in human muscle biopsies taken from patients with chronic, degenerative disease. Even when screened at the time of surgery and harvested to avoid non-muscle tissue, biopsies are highly heterogeneous and often do not contain any muscle fibers[6]. This poses significant problems in the context of studying how and why muscle is irreversibly lost in RC disease[1] (and diseases with similar chronic and degenerative muscle loss, such as lumbar spine pathology[18] and muscular dystrophy[19-21]). When biopsies are taken from the muscle belly and appear to be muscle both via non-invasive imaging and direct visualization, confirmation of muscle content, let alone broad analysis of biopsy composition, is rarely performed. This data highlights the potential pitfalls of omitting compositional data, where the conclusions reached with and without the context of histology are often drastically different.

The first broad aim of this study, to determine whether and to what extent the composition of a biopsy predicts its measured gene expression, demonstrated mixed results. Perhaps unsurprisingly, linear regression did demonstrate significant predictive capacity of muscle content for 10/17 genes expected to be expressed either solely or primarily by muscle fibers or muscle stem cells. However, the same analysis did not find any significant relationship between fat or fibrous tissue content and any gene family, suggesting that gene expression levels are not necessarily reflective of underlying tissue composition, as is often assumed. At a high level, this suggests that even when accounting for tissue composition, the mechanical and biochemical milieu of the torn RC effect gene expression in multiple cell and tissue types relevant to RC disease progression[22] independent of their relative quantity.

When taken as a single pool, there are no significant differences in the expression profile between RSA and INTACT biopsies. Alone, this finding could either be interpreted as RSA biopsies lacking a distinct gene expression signature compared to ‘healthy’ muscle, or as the INTACT biopsies possessing a ‘pathologic’ expression pattern (as the INTACT samples, while lacking tendon tears, nonetheless came

from patients with shoulder pathology). With a more liberal approach, the trends (though insignificant) toward diminished signaling from muscle-related genes and pro-myogenic genes in RSA biopsies could be interpreted as diminished muscle maintenance overall, and indeed would align with previous studies[7; 8]. On the surface this does explain the macroscopic phenomenon; myogenic genes are diminished and muscle is lost over time[23; 24]. But this analysis is based on a highly heterogeneous biopsy pool in which the majority of biopsies *do not contain any muscle*, and therefore would not be expected to express muscle-specific myogenic genes. Indeed, the lack of a significant signal in the pooled RSA analysis appears to be due to high variability across RSA samples, and it is clear that any conclusions reached from this particular analysis, without the context of histology would, at best, be right for the wrong (or at least incomplete) reasons.

A clearer picture begins to emerge when biopsy composition is taken into account. Despite no significant difference in muscle fraction, muscle-containing biopsies segregate into two distinct groups (HIGH and LOW). Compared to INTACT, the HIGH group demonstrated increased expression of both atrophic/anti-myogenic and, to a lesser extent, pro-myogenic genes. This suggests that the HIGH biopsies are still responding to the atrophy pressure of mechanical unloading[25], and are mounting a regenerative response to the muscle fiber damage and degeneration observed histologically[6; 26-28]. Importantly, this interpretation directly refutes the conclusion reached from the pooled analysis, suggesting that continued muscle loss may be attributed to some combination of muscle atrophy and an inability of regenerative processes to match the rate of muscle degeneration, rather than a general reduction in myogenesis.

In contrast, the LOW group did not have any differentially expressed genes compared to INTACT, though myogenic gene expression trended downward. To better understand this finding, we looked to the sub-group comparisons. Surprisingly, the low-expression muscle group did not differentially express any genes compared to either the high fat or no muscle groups, but had increased expression of inflammatory and fibrotic markers compared to the high-expression muscle group. Two competing explanations may account for this finding. One possibility is that this group is more 'terminally degenerated', evidenced by its similarity to the high-fat and no-muscle sub-groups. In this

case, the similarity of expression to the INTACT group is indicative of pathology—the muscle is mechanically unloaded and contains degenerating fibers, but is not expressing the atrophic genes that are expressed in otherwise healthy unloaded muscle[25; 29; 30], nor is it mounting a normal regenerative response to muscle fiber damage[26; 27; 31-33]. However it is also possible that, based on its similarity to INTACT, the LOW group is in a less advanced stage of disease. Given the difficulty of resolving the time course of disease clinically, a definitive answer to this question from any clinical data set is unlikely; to satisfactorily determine the course of gene expression changes over time will likely require an animal model that adequately represents human disease.

Together, the segregation and interpretation of expression results for the HIGH and LOW groups provide further evidence for the existence of a biological spectrum of RC disease[6], though our understanding of how disease progresses through different stages, how these biological changes relate to clinical scoring systems[4; 34], and the processes that underlie the transition from active to terminal muscle degeneration, remains limited. While strategies have been developed for deconvolution of gene expression data, they rely on accurate understanding of both sample composition and expression in each individual cell population[35]. Even in healthy muscle this strategy would be complicated; fluorescence assisted cell sorting (FACS) could isolate and assay the subset of mononuclear cells expected to be found in the muscle, but there is often debate regarding the relationship between cell surface markers and specific cell populations[22; 36-38] and the isolation process itself may alter expression profiles in the cells of interest. Beyond that, the arguably most important cells, the multi-nucleated muscle fibers, would be lost in this process, as FACS cannot isolate myonuclei. In pathological muscle, where the relative cell fractions for known cell populations change dramatically and there remains the possibility of unexpected and potentially unidentified cell populations, this strategy may miss critical contributors to muscle pathology. Furthermore, though highly prevalent, the number of degenerating fibers in a given biopsy relative to the number of non-degenerating fibers at any single point in time is relatively low. One possible strategy to overcome this limitations is physical isolation of specific regions within the muscle biopsy using laser capture microscopy (LCM), which may allow for more targeted investigation of

degenerative mechanisms without the confounding signal of surrounding fat, connective tissue, and non-degenerative muscle fibers. Indeed, LCM and associated downstream analytic techniques to hone in on mechanisms of muscle degeneration are a current focus in our lab.

Despite the fact that histological parameters other than muscle content are not linear predictors of gene expression, which may be explained by the chronicity of disease[23; 39] relative to the phase of active remodeling[40], these data nonetheless demonstrate the importance of interpreting gene expression data in the context of biopsy composition[11; 14]; without definitive evidence for the presence of muscle, there would be no basis for even the broad interpretations presented above. More generally, the disconnect between gene expression and histological findings (where even muscle presence and fat content are only modest predictors of expression levels and sample clustering) further complicates the interpretation of gene expression data not only in this and previous studies[7; 8], but throughout the RC disease literature, where complex interactions of the mechanical and biological environment have a significant impact on several of the tissue types central to RC muscle pathology[22].

A major remaining limitation of this work lies in our inability to histologically characterize our INTACT samples. Because the INTACT patients did have sufficient shoulder symptoms to warrant surgery, it is possible that these samples are not representative of normal, healthy muscle. Supporting this, 44% of INTACT biopsies were excluded from the differential expression analysis based on cluster analysis, though it is important to note that trends in gene expression fold-change were not altered when normalized to the entire pool of INTACT samples. In the same vein, the relatively poor predictive ability of histological parameters outside of muscle content remains a limitation, and points to one of the overarching limitations of studying clinical samples, which is an inherent inability to resolve the time course of disease in the majority of patients[41]. To adequately address these limitations will require either development of a new animal model or validation of an existing model that adequately recapitulates both the atrophic and degenerative phases of human disease[22]. Such a model may then be employed to more accurately define the time course of disease, including the relationship between observed changes in gene expression as they relate to sample composition over time.

Conclusion

As a group, pooled RSA muscle biopsies provide little insight into gene expression patterns in RC disease, with only trends toward down-regulation of muscle-related genes and up-regulation of a limited number of inflammatory and adipogenic genes. But when muscle content determined via histology is considered, much of the variation in RSA gene expression can be explained—samples containing muscle fibers are unanimously separated from samples without muscle, and further segregate into two categories: one with increased expression of both myogenic and atrophic genes indicative of a responsive muscle undergoing active muscle turnover[42; 43], and another with an expression pattern not significantly different from control samples or samples without muscle, indicating potentially diminished responsiveness to both atrophic and degenerative stimuli. These categories may help explain the variability in rehabilitation found in the patient population; while the first category may represent a patient subset with some potential to respond to intervention[44; 45], the remaining patients (both with and without histological muscle) may represent a terminally degenerated muscle with limited regenerative capacity[1; 46; 47]. Future work in this area should focus on two areas: combining histology-informed interpretations of data with better controlled time series data from clinically relevant animal models, and employing advanced biological tools including FACS and LCM to physically separate and assay specific cell types and degenerative muscle fibers to better characterize the molecular mechanisms that govern progression of muscle loss and fat accumulation. The former strategy will allow for improved understanding of the temporal and spatial relationship between gene expression and tissue composition generally. However, the latter, more targeted approach will allow for a deeper understanding of the processes that govern irreversible muscle loss in chronic musculoskeletal conditions, including a more definitive understanding of the phases that define RC disease. Only by separating the highly heterogeneous mix of cell and tissue types[11; 14] will the cellular and molecular processes that govern RC disease progression from reversible, atrophic muscle loss to terminal muscle degeneration be elucidated. Ultimately, understanding the relationships between gene expression, disease state, and patient outcomes

will aid in identifying optimal interventions on a more individualized basis, which will in turn lead to improved patient outcomes.

Acknowledgements

This work was funded by the University of California, San Diego Frontiers of Innovation Program (M.C.G.), the Orthopedic Research and Education Foundation (T.C.), and the National Institute of Child Health and Human Development (S.R.W.).

This chapter, in full, is a reprint of the material as it appears in PLOS One 2018. Michael C. Gibbons, Kathleen Fisch, Rajeswari Pichika, Timothy Cheng, Adam J. Engler, Simon Schenk, John G. Lane, Anshu Singh, Samuel R. Ward. The dissertation/thesis author was the primary investigator of this material.

References

1. Gladstone JN, Bishop JY, Lo IK, Flatow EL. 2007. Fatty infiltration and atrophy of the rotator cuff do not improve after rotator cuff repair and correlate with poor functional outcome. The American journal of sports medicine 35:719-728.

2. Bishop J, Klepps S, Lo IK, Bird J, Gladstone JN, Flatow EL. 2006. Cuff integrity after arthroscopic versus open rotator cuff repair: a prospective study. Journal of shoulder and elbow surgery 15:290-299.

3. Galatz LM, Ball CM, Teefey SA, Middleton WD, Yamaguchi K. 2004. The outcome and repair integrity of completely arthroscopically repaired large and massive rotator cuff tears. The Journal of Bone & Joint Surgery 86:219-224.

4. Goutallier D, Postel J-M, Bernageau J, Lavau L, Voisin M-C. 1994. Fatty muscle degeneration in cuff ruptures: pre-and postoperative evaluation by CT scan. Clinical orthopaedics and related research 304:78-83.

5. Mendias CL, Roche SM, Harning JA, Davis ME, Lynch EB, Enselman ERS, Jacobson JA, Claflin DR, Calve S, Bedi A. 2015. Reduced muscle fiber force production and disrupted myofibril architecture in patients with chronic rotator cuff tears. Journal of Shoulder and Elbow Surgery 24:111-119.

6. Gibbons MC, Singh A, Anakwenze O, Cheng T, Pomerantz M, Schenk S, Engler AJ, Ward SR. 2017. Histological Evidence of Muscle Degeneration in Advanced Human Rotator Cuff Disease. The Journal of Bone & Joint Surgery 99:190-199.

7. Choo A, McCarthy M, Pichika R, Sato EJ, Lieber RL, Schenk S, Lane JG, Ward SR. 2014. Muscle Gene Expression Patterns in Human Rotator Cuff Pathology. The Journal of Bone & Joint Surgery 96:1558-1565.

8. Shah SA, Kormpakis I, Cavinatto L, Killian ML, Thomopoulos S, Galatz LM. 2017. Rotator cuff muscle degeneration and tear severity related to myogenic, adipogenic, and atrophy genes in human muscle. Journal of Orthopaedic Research.

9. Reardon KA, Davis J, Kapsa RM, Choong P, Byrne E. 2001. Myostatin, insulin-like growth factor-1, and leukemia inhibitory factor mRNAs are upregulated in chronic human disuse muscle atrophy. Muscle & nerve 24:893-899.

10. Zimmers TA, Davies MV, Koniaris LG, Haynes P, Esquela AF, Tomkinson KN, McPherron AC, Wolfman NM, Lee S-J. 2002. Induction of cachexia in mice by systemically administered myostatin. Science 296:1486-1488.

11. Rodrıguez-Gonzalez FG, Mustafa DA, Mostert B, Sieuwerts AM. 2013. The challenge of gene expression profiling in heterogeneous clinical samples. Methods 59:47-58.

12. Steinbacher P, Tauber M, Kogler S, Stoiber W, Resch H, Sänger A. 2010. Effects of rotator cuff ruptures on the cellular and intracellular composition of the human supraspinatus muscle. Tissue and Cell 42:37-41.

13. Lundgreen K, Lian ØB, Engebretsen L, Scott A. 2013. Lower muscle regenerative potential in full-thickness supraspinatus tears compared to partial-thickness tears. Acta orthopaedica 84:565-570.

14. Jung J, Jung H. 2016. Methods to analyze cell type-specific gene expression profiles from heterogeneous cell populations. Animal Cells and Systems 20:113-117.

15. Dvinge H, Bertone P. 2009. HTqPCR: high-throughput analysis and visualization of quantitative real-time PCR data in R. Bioinformatics 25:3325-3326.

16. Team RC. 2014. R: A language and environment for statistical computing. R Foundation for Statistical Computing, Vienna, Austria. 2013.

17. Ritchie ME, Phipson B, Wu D, Hu Y, Law CW, Shi W, Smyth GK. 2015. limma powers differential expression analyses for RNA-sequencing and microarray studies. Nucleic acids research:gkv007.

18. Shahidi B, Hubbard JC, Gibbons MC, Ruoss S, Zlomislic V, Allen RT, Garfin SR, Ward SR. 2017. Lumbar multifidus muscle degenerates in individuals with chronic degenerative lumbar spine pathology. Journal of Orthopaedic Research.

19. Petrof BJ. 1998. The molecular basis of activity-induced muscle injury in Duchenne muscular dystrophy. Molecular and cellular biochemistry 179:111-124.

20. Haslett JN, Sanoudou D, Kho AT, Bennett RR, Greenberg SA, Kohane IS, Beggs AH, Kunkel LM. 2002. Gene expression comparison of biopsies from Duchenne muscular dystrophy (DMD) and normal skeletal muscle. Proceedings of the National Academy of Sciences 99:15000-15005.

21. Wren TA, Bluml S, Tseng-Ong L, Gilsanz V. 2008. Three-point technique of fat quantification of muscle tissue as a marker of disease progression in Duchenne muscular dystrophy: preliminary study. American Journal of Roentgenology 190:W8-W12.

22. Gibbons MC, Singh A, Engler AJ, Ward SR. 2017. The Role of Mechanobiology in Progression of Rotator Cuff Muscle Atrophy and Degeneration. Journal of Orthopaedic Research.

23. Hebert-Davies J, Teefey SA, Steger-May K, Chamberlain AM, Middleton W, Robinson K, Yamaguchi K, Keener JD. 2017. Progression of Fatty Muscle Degeneration in Atraumatic Rotator Cuff Tears. JBJS 99:832-839.

24. Sakuma K, Yamaguchi A. 2010. Molecular mechanisms in aging and current strategies to counteract sarcopenia. Current Aging Science 3:90-101.

25. Bonaldo P, Sandri M. 2013. Cellular and molecular mechanisms of muscle atrophy. Disease models & mechanisms 6:25-39.

26. Charge SB, Rudnicki MA. 2004. Cellular and molecular regulation of muscle regeneration. Physiological reviews 84:209-238.

27. Ciciliot S, Schiaffino S. 2010. Regeneration of mammalian skeletal muscle: basic mechanisms and clinical implications. Current pharmaceutical design 16:906-914.

28. Goetsch SC, Hawke TJ, Gallardo TD, Richardson JA, Garry DJ. 2003. Transcriptional profiling and regulation of the extracellular matrix during muscle regeneration. Physiological genomics 14:261-271.

29. Bialek P, Morris CA, Parkington J, Andre MS, Owens J, Yaworsky P, Seeherman H, Jelinsky SA. 2011. Distinct protein degradation profiles are induced by different disuse models of skeletal muscle atrophy. Physiological genomics.

30. Bodine SC, Latres E, Baumhueter S, Lai VK-M, Nunez L, Clarke BA, Poueymirou WT, Panaro FJ, Na E, Dharmarajan K. 2001. Identification of ubiquitin ligases required for skeletal muscle atrophy. Science 294:1704-1708.

31. Czerwinska AM, Streminska W, Ciemerych MA, Grabowska I. 2012. Mouse gastrocnemius muscle regeneration after mechanical or cardiotoxin injury. Folia Histochem Cytobiol 50:144-153.

32. Lepper C, Partridge TA, Fan C-M. 2011. An absolute requirement for Pax7-positive satellite cells in acute injury-induced skeletal muscle regeneration. Development 138:3639-3646.

33. Wallace GQ, McNally EM. 2009. Mechanisms of muscle degeneration, regeneration, and repair in the muscular dystrophies. Annual review of physiology 71:37-57.

34. Fuchs B, Weishaupt D, Zanetti M, Hodler J, Gerber C. 1999. Fatty degeneration of the muscles of the rotator cuff: assessment by computed tomography versus magnetic resonance imaging. Journal of Shoulder and Elbow Surgery 8:599-605.

35. Shen-Orr SS, Tibshirani R, Khatri P, Bodian DL, Staedtler F, Perry NM, Hastie T, Sarwal MM, Davis MM, Butte AJ. 2010. Cell type–specific gene expression differences in complex tissues. Nature methods 7:287-289.

36. Porpiglia E, Samusik N, Van Ho AT, Cosgrove BD, Mai T, Davis KL, Jager A, Nolan GP, Bendall SC, Fantl WJ. 2017. High-resolution myogenic lineage mapping by single-cell mass cytometry. Nature Cell Biology.

37. Rajkumar VS, Howell K, Csiszar K, Denton CP, Black CM, Abraham DJ. 2005. Shared expression of phenotypic markers in systemic sclerosis indicates a convergence of pericytes and fibroblasts to a myofibroblast lineage in fibrosis. Arthritis research & therapy 7:R1113.

38. Mackey AL, Kjaer M, Charifi N, Henriksson J, Bojsen-Moller J, Holm L, Kadi F. 2009. Assessment of satellite cell number and activity status in human skeletal muscle biopsies. Muscle & nerve 40:455-465.

39. Essman JA, Bell RH, Askew M. 1991. Full-Thickness Rotator-Cuff Tear: An Analysis of Results. Clinical orthopaedics and related research 265:170-177.

40. Jun J-I, Lau LF. 2010. Cellular senescence controls fibrosis in wound healing. Aging (Albany NY) 2:627-631.

41. Bartolozzi A, Andreychik D, Ahmad S. 1994. Determinants of outcome in the treatment of rotator cuff disease. Clinical orthopaedics and related research 308:90-97.

42. Raue U, Slivka D, Jemiolo B, Hollon C, Trappe S. 2006. Myogenic gene expression at rest and after a bout of resistance exercise in young (18–30 yr) and old (80–89 yr) women. Journal of Applied Physiology 101:53-59.

43. Kim J-s, Kosek DJ, Petrella JK, Cross JM, Bamman MM. 2005. Resting and load-induced levels of myogenic gene transcripts differ between older adults with demonstrable sarcopenia and young men and women. Journal of applied physiology 99:2149-2158.

44. Jones SW, Hill RJ, Krasney PA, O'CONNER B, Peirce N, Greenhaff PL. 2004. Disuse atrophy and exercise rehabilitation in humans profoundly affects the expression of genes associated with the regulation of skeletal muscle mass. The FASEB journal 18:1025-1027.

45. Butt U, Rashid M, Temperley D, Crank S, Birch A, Freemont A, Trail I. 2016. Muscle regeneration following repair of the rotator cuff. Bone Joint J 98:1389-1394.

46. Warren GL, Summan M, Gao X, Chapman R, Hulderman T, Simeonova PP. 2007. Mechanisms of skeletal muscle injury and repair revealed by gene expression studies in mouse models. The Journal of physiology 582:825-841.

47. Yan Z, Choi S, Liu X, Zhang M, Schageman JJ, Lee SY, Hart R, Lin L, Thurmond FA, Williams RS. 2003. Highly coordinated gene regulation in mouse skeletal muscle regeneration. Journal of Biological Chemistry 278:8826-8836.

Chapter 5. The Relative Effects of Tenotomy, Neurotomy, and Combined Injury on Mouse Rotator Cuff Muscles: Consequences for the Mouse as a Pre-Clinical Model

Abstract

A commonly employed animal model of muscle pathology following rotator cuff tear (RCT) is tenotomy of the supraspinatus and infraspinatus, often combined with neurotomy of the suprascapular nerve. However, the utility of this model depends on its similarity to human muscle pathology in terms of the disease phenotype and the mechanisms by which muscle volume is reduced and fat volume increases. Here, we evaluated the individual and combined effect of tenotomy and neurotomy at acute and chronic time points in the mouse in order to determine the relevance of each injury mechanism for modeling human RCT as it relates to muscle atrophy, degeneration, fat accumulation, and fibrosis. We found that tenotomy alone caused small, transient changes in these pathological features that resolved over the course of the study, while neurotomy alone caused a significant atrophy and fat distribution phenotype. The dual injury group had a similar atrophy phenotype to the neurotomy group alone, though the addition of tenotomy did marginally enhance the fatty and fibrotic phenotype. Overall, this demonstrated that the most clinically relevant injury model, tenotomy alone, does not produce a clinically relevant phenotype, and while the dual injury model partially recapitulates the human condition, it does so primarily through a nerve injury that is not well justified clinically.

Introduction

Chronic RCTs affect upwards of 20% of the population, and are characterized by persistent functional defects and high rates of repair failure and reoperation[1-3]. Along with defects in the tendon itself[4], detrimental changes in the RC muscles have been implicated in the clinical intractability of RC disease, with the degree of muscle loss and fat accumulation in the RC muscles serving as a key marker of disease progression[5]. However, the reason that muscle loss is irreversible is not clear. Several studies have demonstrated muscle fiber atrophy in RC disease[6,7], but while disuse and mechanical unloading

undoubtedly contribute to atrophic pressure and loss of muscle mass, these processes are normally reversible[8-10]. In RC disease, muscle loss persists even after successful anatomical repair, suggesting a distinct biological driver of irreversible muscle loss. In support of this hypothesis, recent studies in human RC muscle have demonstrated dysfunctional sarcomere remodeling[11] and organization[12] along with high levels of muscle fiber degeneration, in which muscle fibers are damaged and degraded, myophagocytosis is evident, and fat appears to inhabit the spaces vacated by degenerated fibers[13]. Because muscle fibers are lost in this process, and because it is likely that the environment of the torn RC has a detrimental effect on muscle regeneration[14], this degenerative rather than atrophic mechanism of muscle loss may better explain the irreversibility of muscle pathology with RC tear.

While the existence of atrophic and degenerative processes of muscle loss and fat accumulation resulting from RCT are clear, understanding the underlying biology and physiology of these pathological processes in humans is difficult; RCT initiation and progression are often insidious, and genetic, phenotypic and demographic variability in the patient population create significant challenges to studying these processes in humans. Based on these challenges, and the need for a preclinical model in which to evaluate potential interventions, much effort has been dedicated to developing and implementing animal models of RC disease. While large animal models have been developed that effectively recapitulate the whole-muscle fat infiltration found in humans[15,16], logistical factors and the diversity of molecular and genetic tools available in mice have led to a proliferation of studies employing a murine model of RC disease.

In its most common form, the mouse RC model involves tenotomy of the supraspinatus and infraspinatus muscles to simulate a massive RC tear, as well as transection of the suprascapular nerve[17-20]. While the addition of a nerve injury induces a more robust atrophy response in the muscle than tenotomy alone[17,18], the clinical prevalence of nerve injury, and denervation specifically, is low[21,22]. This is potentially problematic, as the muscular response to denervation, including the molecular mediators of atrophy, are distinct from the response to mechanical unloading or disuse[22-31]. Therefore, understanding the relative influence of the nerve injury in concert with the mechanical injury of tenotomy is critical in

evaluating the clinical relevance of this particular model of RC disease, and in interpreting the results of published studies utilizing this dual injury model.

The goal of this study was to evaluate the relative effects of tenotomy and denervation, both alone and in combination, in the mouse supraspinatus at acute and chronic time points. By constructing robust time-series data including compositional, histological, and gene expression data related to muscle atrophy, degeneration-regeneration, fatty infiltration and fibrosis, we can definitively determine the independent and combinatorial effects of tenotomy and denervation on mouse supraspinatus in the short- and long-term, and better appreciate the strengths and weaknesses of the mouse RC as a model of human RC disease.

Methods

Animals

One hundred fifty C57/Bl6 mice were randomly assigned to one of five injury groups: non-operated control (NC), sham surgery (SS), tenotomy only (TT), neurotomy only (NT), or dual injury (DI) consisting of TT combined with NT. All surgeries were performed under approval of the University of California San Diego IACUC. The approach for all surgeries included a 2cm lateral skin incision followed by a transverse incision through the deltoid to visualize the RC tendon. TT was performed by sharp dissection of the supraspinatus and infraspinatus tendons from their insertions on the humeral head. For NT, the suprascapular nerve was identified anterior to the supraspinatus and superior to the brachial plexus, and a 1-2mm section of nerve was removed. TT was performed immediately prior to NT in the DI group, while SS consisted of the approach and palpation of the RC tendon complex and suprascapular nerve with a blunt probe. The deltoid and skin were then closed with 6-0 Vicryl, and surgical glue was additionally used on the skin incision, and a cocktail of bupivacaine (2ml/kg) and buprenorphine (0.1mg/kg) were administered subcutaneously as anesthetic and analgesic agents, respectively. All mice were 3 months of age at the start of the experiment. Within each group, mice were sacrificed at 1, 3, 7, 14, and 28 days, with an additional group at 12 weeks (n=5 mice/timepoint). Supraspinatus muscles were

dissected from the scapula, weighed, flash frozen in liquid nitrogen and stored at -80^{o}C prior to processing.

Histology

The supraspinatus muscle was cut axially into thirds at -20^{o}C, and the middle third was blocked in OCT while the proximal and distal thirds were retained for gene expression analysis (see below). Ten-micron axial sections were generated at -20^{o}C on a Leica cryostat. To quantify muscle fiber cross-sectional area (CSA) as a measure of atrophy and the percentage of centralized nuclei (CN) as a measure of muscle fiber regeneration, laminin-DAPI stained cross sections were quantified using a custom ImageJ macro[32]. Hematoxylin and eosin (H&E) was used to quantify the incidence of degeneration (myophagocytosis, disrupted myofiber membranes, split muscle fibers), and intra- and inter-fascicular fat (fat within the structure of a fascicle and fat between muscle fascicles, respectively), reported as the percentage of 250μm^2 grid elements positive for each pathologic feature[13]. Gomori trichrome staining was used to visualize the relative fraction of muscle fibers and connective tissue across the muscle cross-section, and Oil Red-O staining was employed to visualize the relative fraction of fat. The relative fractions of muscle, fibrous tissue, and fat were quantified using MetaMorph image analysis software (Molecular Devices).

Two-way ANOVA (alpha = 0.05) with Tukey post-hoc significance testing was used to analyze differences between groups over time. For simplicity, only post-hoc comparisons involving SS are represented in figures, while other relevant comparisons are discussed in the text and figure captions.

Gene Expression

The proximal and distal thirds of each supraspinatus muscle were pulverized in liquid nitrogen and nucleic acid was extracted in TRIzol (Ambion). RNA was isolated using RNeasy affinity columns (Qiagen), followed by cDNA synthesis using the SuperScript III reverse transcription kit (Thermo-Fisher). Quantitative PCR was then performed in custom 394-well plates on a BioRad CFX394 anlayzer

(Biorad) using a SYBR green detection method, and relative quantity of 87 genes was calculated using a multiple-reference gene delta-Ct method[33], with *Actb, Gapdh, Rps18,* and *Hprt* used as references. Subsequent analysis of relative expression was performed using the delta-delta-Ct method[33]. Genes for which the Ct values were inconsistent (>1 cycle apart) and samples missing any reference genes or failing screens for gDNA contamination were excluded from the analysis. After low-quality sample exclusion at least three samples remained in each group.

To establish the effect of time and surgery independent of TT or NT, expression analysis was performed for the NC and SS muscles prior to analysis of TT, NT, or DI groups. Cluster analysis of relative transcript quantity in the NC group was performed to determine whether the gene expression profile changed as a function of age over the course of the study, with missing data imputed using a nearest-neighbor approach (*knnimpute* function in Matlab). On the basis of this result, cluster analysis was performed on the expression of the SS group relative to the average of the pooled NC group in order to determine the effect of surgery (absent TT or NT) on gene expression over the time course. Based on the results from the NC and SS control groups, the relative expression values for the three treatment groups were normalized (using the delta-delta-Ct method) to their time point-matched SS values, in order to correct for the demonstrated effects of surgery (without TT or NT) on gene expression.

Results

Muscle mass and fiber area analysis both demonstrated a trend toward continuous muscle fiber hypertrophy in the NC group (28.6% mass increase, p=0.014; 36.1% CSA increase, p=0.06 from day 1 to week 12) (Fig. 1). In the SS group, mass and CSA were not significantly different from NC at any time point, though CSA did trend downward at 7 days. Muscle mass was significantly reduced in the TT group compared to both NC and SS at days 14 and 28, but had recovered to SS (but not NC) levels by 12 weeks. A trend similar to the SS group was observed for CSA in the TT group, where the degree of fiber atrophy at 14 days was significant compared to both NC and SS groups, but returned to NC and SS levels by day 28. NT showed significant mass reduction relative to SS by day 7, and both mass and CSA reduction

relative to NC and SS by day 14, progressing throughout the time course to a mere 29.6% of the NC group CSA and 53.7% of NC mass by 12 weeks post-injury. In the DI group, whole-muscle and muscle fiber atrophy progressed more rapidly than NT alone, with significant decreases observed as early as 7 days post-injury, at which point the DI group had significantly smaller fibers than the NT group. By 12 weeks, muscle mass in the DI group was significantly lower than NT, though from 14 days and onward there was no difference in CSA between DI and NT groups.

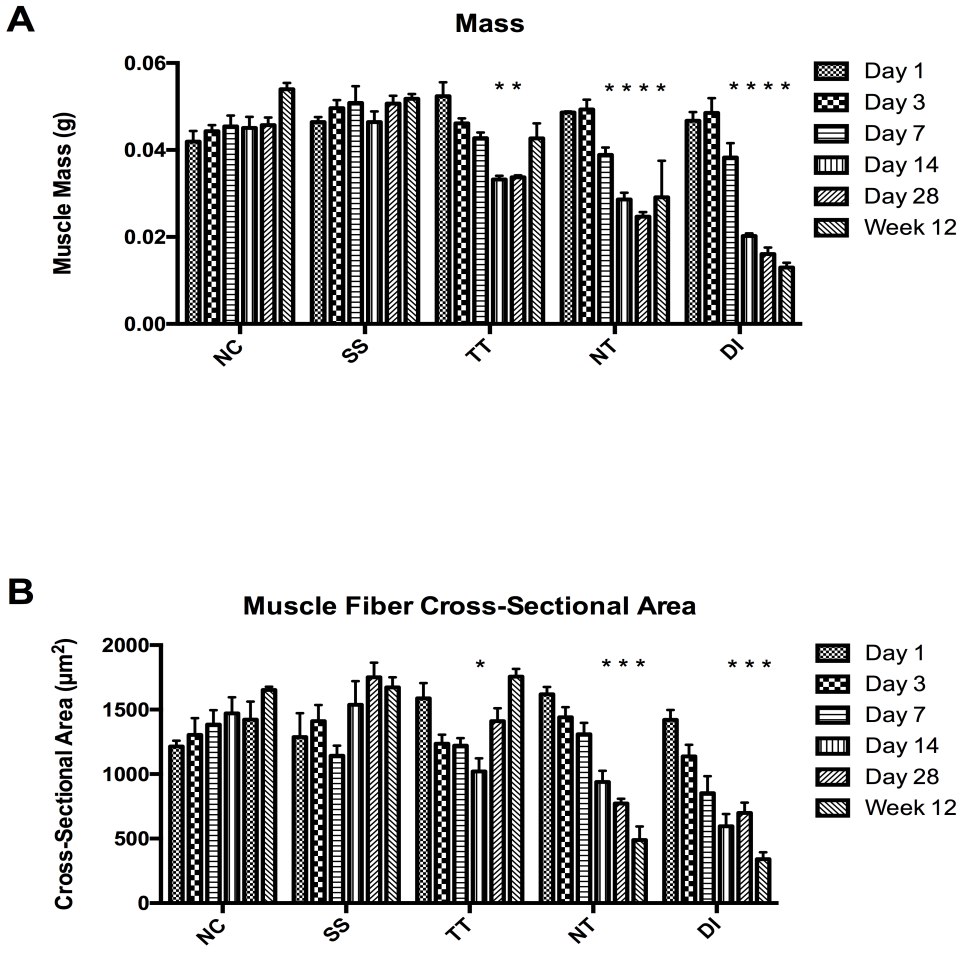

Figure 5.1 (A) Muscle mass and (B) fiber cross-sectional area were significantly reduced in NT and DI by one week post-intervention, and in TT by two weeks. Mass and CSA recovered in the TT group to SS values, while in NT and DI whole muscle and muscle fiber atrophy progressed through week 12.

Muscle degeneration, defined by disrupted muscle fiber membranes, hypercellular or myophagocytic muscle fibers, or split muscle fibers, was not a prevalent feature in NC or SS at any time points (Fig. 2). In contrast, by day 14 the TT, NT and DI groups all had significantly increased signs of degeneration. The prevalence of degeneration in the TT group returned to baseline levels by day 28, while degeneration levels persisted but did not progress in the NT group through 12 weeks. However, the prevalence of degenerative features in the DI muscle progressed significantly through 12 weeks, suggesting a compounding effect of TT and NT on degeneration progression but not initiation (Fig. 2).

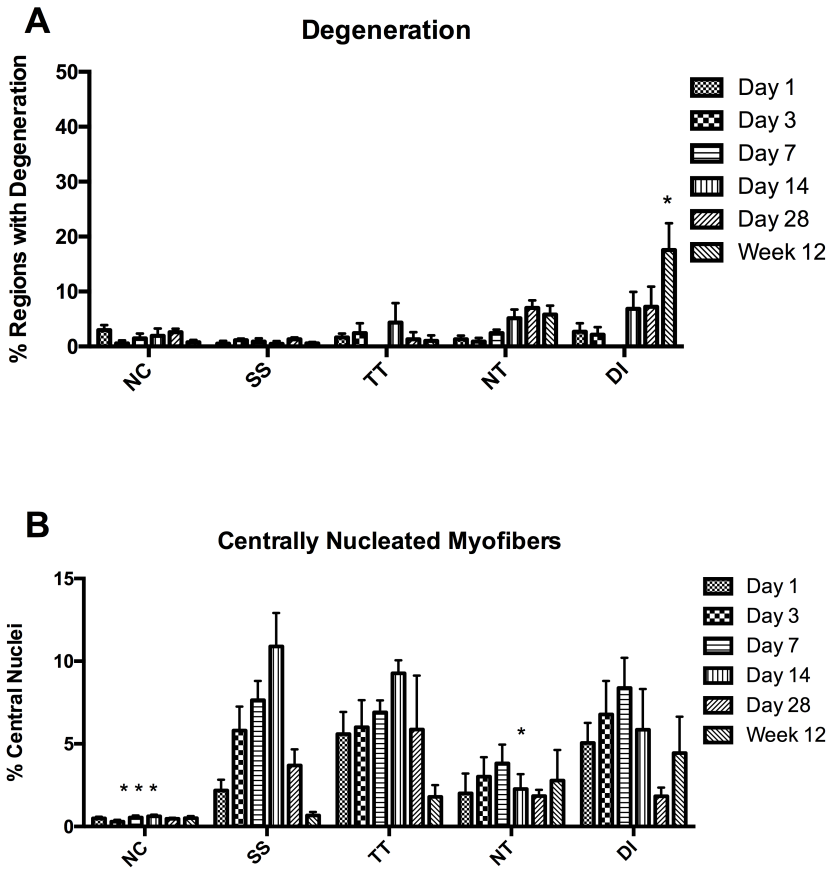

Figure 5.2 (A) The prevalence of muscle degeneration was not significantly different between NC, SS, TT, or NT at any time point. Twelve weeks post-DI, degeneration was found in significantly more regions than any other group or time point. (B) Centralized nuclei were significantly increased in SS relative to NC from day 3 to day 14, while with the exception of NT relative to SS at day 14 there was no significant difference in regenerated fibers among any of the operated groups.

Regeneration, as measured by the percentage of CN fibers, was significantly increased in the acute time points (days 3, 7, and 14) of the SS group compared to the NC group, with no difference by 12 weeks post-surgery (Fig. 2). Similarly, TT led to increased CN from 3 to 28 days compared to the NC group; however, TT and SS had similar percentages of CN at all time points. The percentage of CN in the NT group was significantly lower than SS at day 14, suggesting a blunted degeneration-regeneration response following NT. CN in the DI group followed a similar pattern as the SS and TT groups, with increased CN relative to NC in the acute (3 through 14 day) time points and no differences at chronic time points.

The overall fat fraction of the NC and SS muscles as measured by Oil-Red O was close to zero, and did not change over the course of the experiment (Fig. 3A). However, the TT group showed a small but significant peak in fat at day 14, which returned to NC values by day 28. While fat content in NT was similar to NC and SS throughout the experiment, the DI grouped demonstrated strong and persistent fat accumulation over time, with a significant increase as early as 1 week post-injury that persisted through 12 weeks, though notably at 28 days fat content in DI was not different from NC.

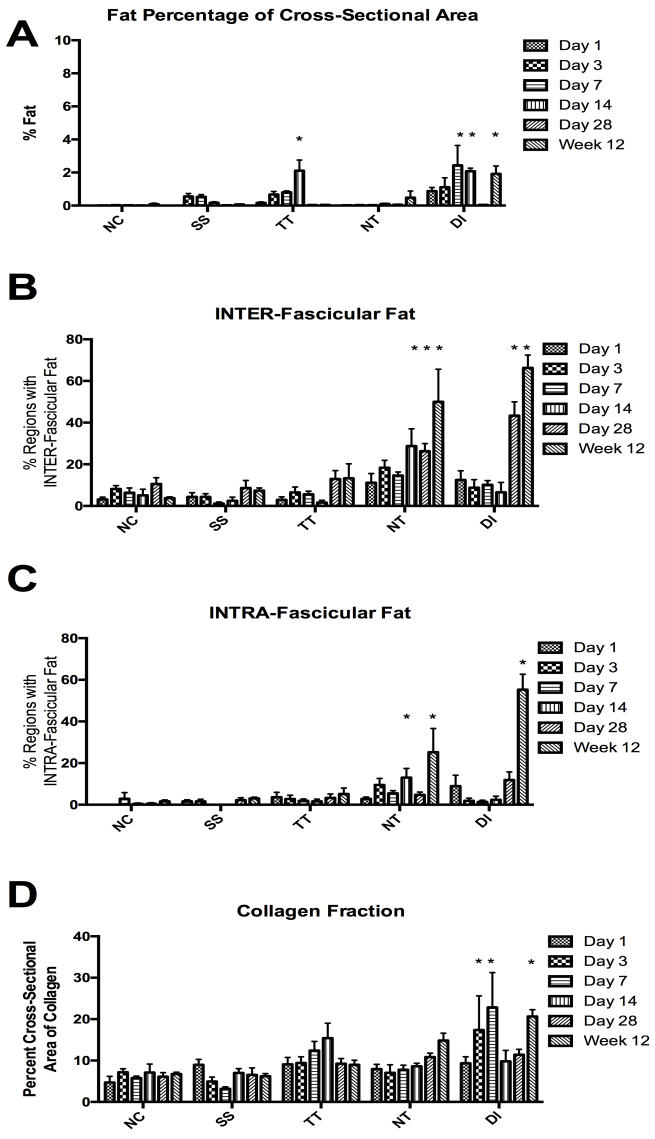

Figure 5.3 (A) The area fraction of fat determined by Oil-Red-O showed that overall fat content was low, with no group containing more than 5% fat area. While fat content was not significantly altered in the majority of time-point groups, a significant spike was observed in TT at 14 days that resolved by day 28, while DI showed increased fat content at one, two and twelve weeks, but interesting not at four weeks. Neither SS nor TT affected the prevalence or distribution of fat in either the inter-fascicular (B) or intra-fascicular (C) space, while NT and DI increased the presence of fat in both locations at chronic time points. (D) Collagen area fraction was significantly increased at 3 and 7 days as well as 12 weeks in DI, while no other group showed a significant change in collagen at any time point. While the acute increase may be due to rapid atrophy, the chronic increase suggests a true fibrotic process.

Few regions contained either intra- or inter-fascicular fat in the NC, SS, or TT groups, which is unsurprising given the low total fat fractions in these groups (Fig. 3B,C, Fig. 4). Interestingly, though the overall fat fraction for NT was significantly less than TT and not different from NC or SS, significantly

more regions in NT were scored for both inter- and intra-fascicular fat, suggesting that NT causes a change in distribution but not total fat content. Fat distribution in both the inter- and intra-fascicular spaces was similarly increased in DI, which combined with the small but persistent significant increase in total fat implies that in DI, nerve injury drives distribution while tenotomy causes the increase in total fat (Fig. 3, Fig.4).

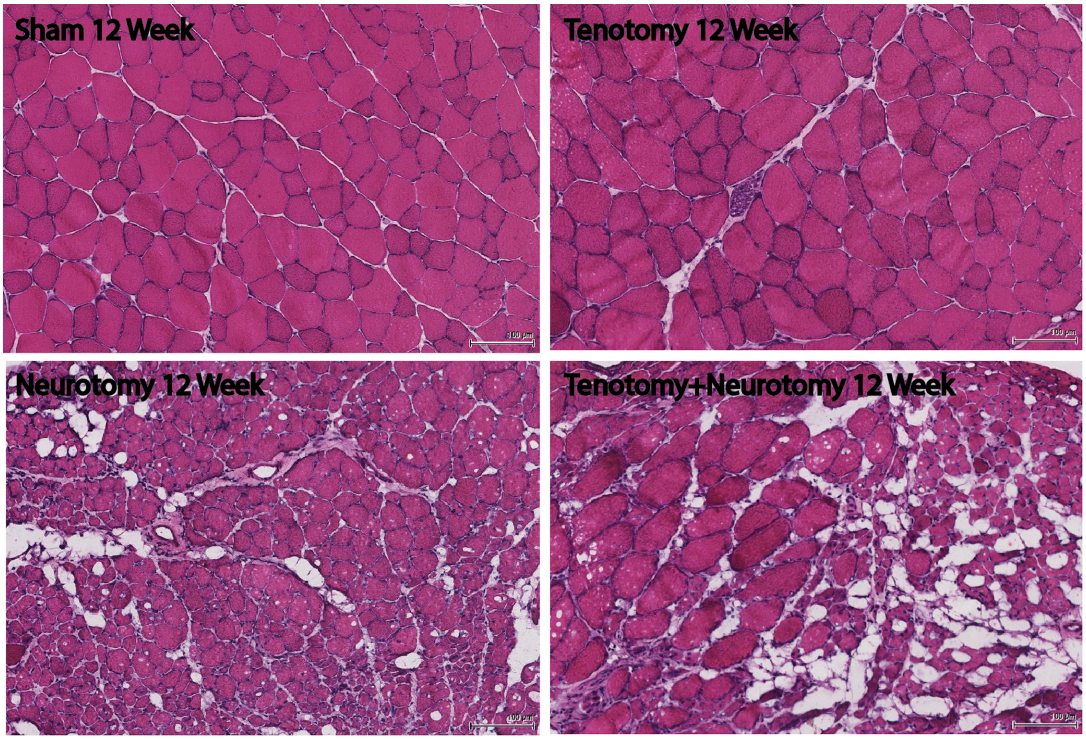

Figure 5.4 Representative Hematoxylin and Eosin images of (clockwise from top left) SS, TT, NT, and DI treatments 12 weeks after intervention. SS and TT do not have any obvious histopathological features, while decreased fiber size, increased and altered distribution of fat, and increased fibrosis consistent with the preceding assays can be appreciated in the NT and DI images.

The collagen fraction of NC, SS, TT, and NT were not significantly different at any time point (Fig. 3D). DI demonstrated significantly increased collagen area fractions at acute 3- and 7-day time points, possibly the result of rapid muscle atrophy leading to a relative increase in collagen area (particularly in the central tendon) rather than de novo collagen deposition in the acute phase. However, the increased collagen content at 12 weeks of DI represents a potentially chronic fibrotic process.

Cluster analysis of gene expression relative quantity values for the NC group alone suggests that there is no independent effect of time/aging on gene expression patterns in the RC muscle, as there was no pattern of samples clustering by time point (Fig. 5). On this basis, the average across all NC samples was collapsed to a single reference RQ value to calculate expression fold change in the SS group. Clustering of expression values in the SS group suggests that, unlike the NC group, there is an effect of intervention on gene expression particularly in the acute phase, with early 1- and 3-day time points tending to segregate into clusters with higher variability while later time points were generally more tightly clustered (Fig. 6). Therefore, to correct for this surgical effect in our TT, NT, and DI groups, gene expression data was normalized to the average time point-matched quantity in the SS group in the subsequent analysis.

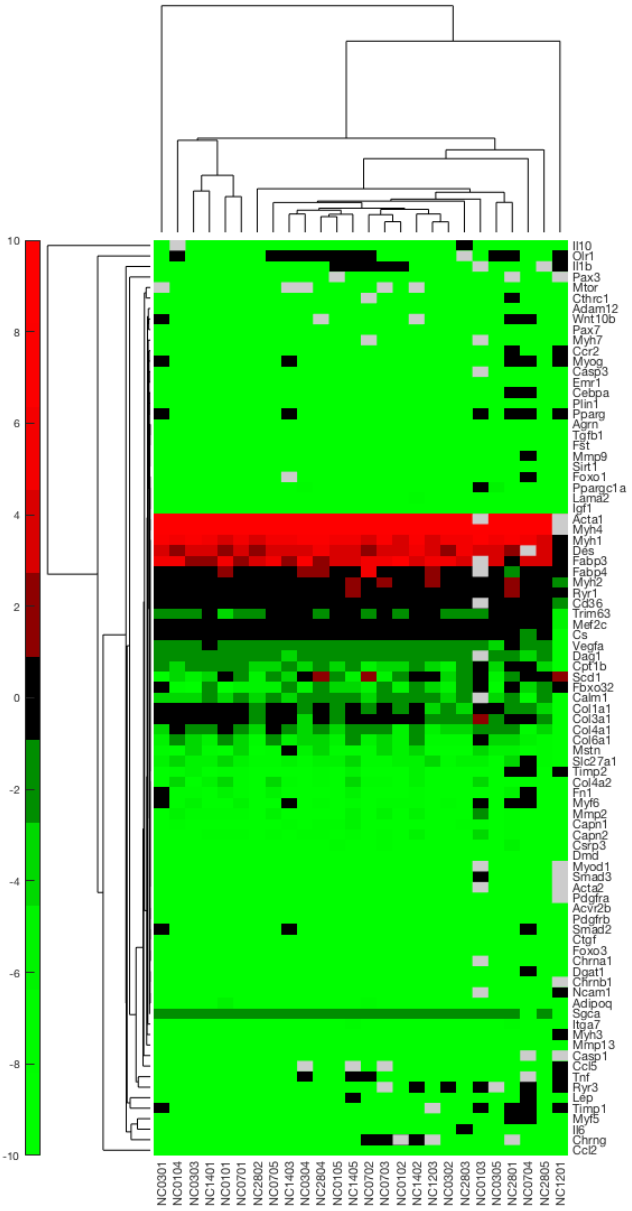

Figure 5.5 Cluster analysis of relative expression values in the NC group did not show any clustering by time point, suggesting that in un-operated shoulders there is not an age affect relevant to the time course of this experiment. On this basis, analysis of the time effect in the SS group was normalized to the pooled NC values.

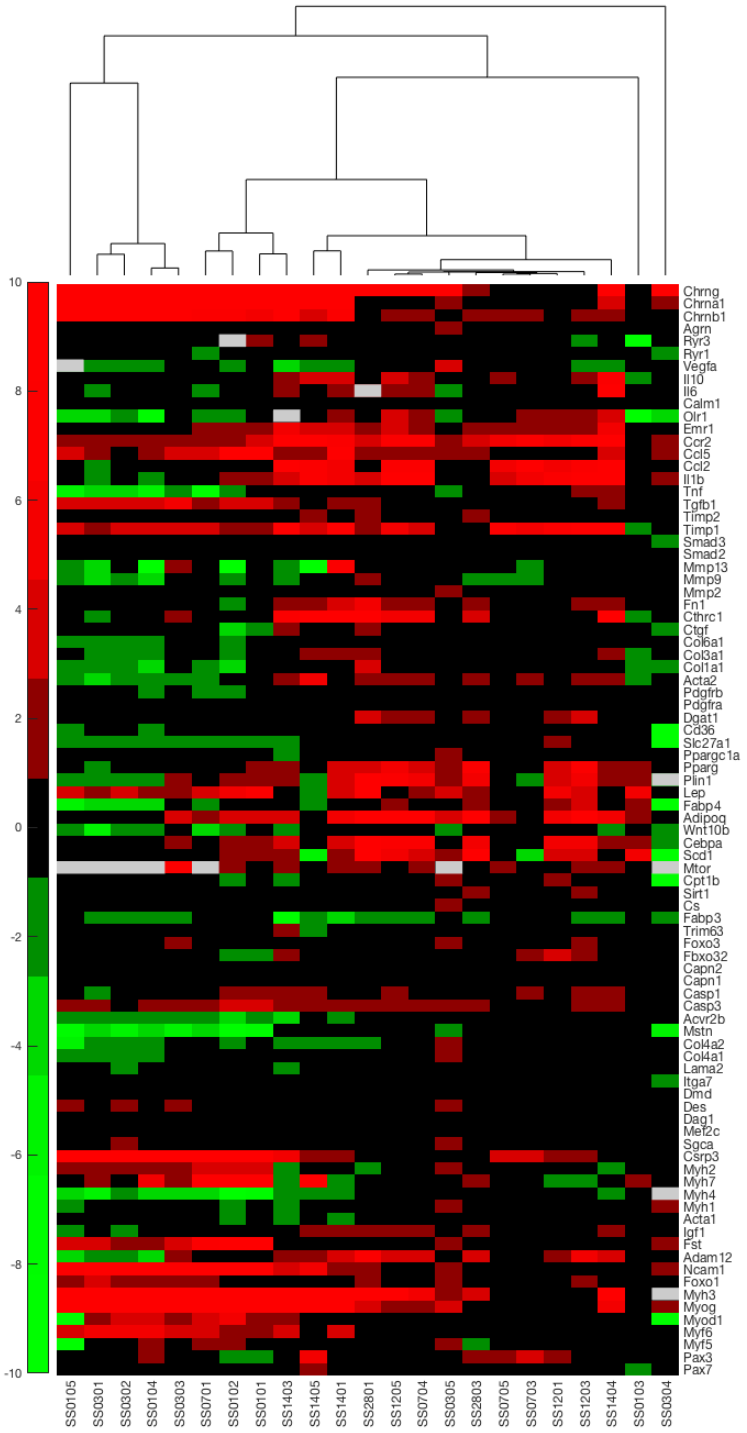

Figure 5.6 Clustering of SS gene expression represented by fold-change relative to pooled relative NC expression values suggested a time-course bias in the SS group, as samples from the same and adjacent time points tended to cluster together. This motivated the use of time point-matched SS normalization for expression in the TT, NT, and DI groups, in order to correct for the pure surgical effects on gene expression in these groups.

The effect of TT on gene expression in the acute phase included an increase in inflammatory expression at 1 day, and fibrotic expression from 3 to 14 days post-TT (Fig. 7). Adipogenic genes were generally up-regulated at day 14, but expression was subsequently reduced at 28 days and 12 weeks. Expression of metabolic, atrophic, neuromuscular junction, and muscle structural genes were generally unaffected by TT, while expression of pro-regenerative genes appear to peak between 7 and 14 days, with little difference between SS and TT by 12 weeks.

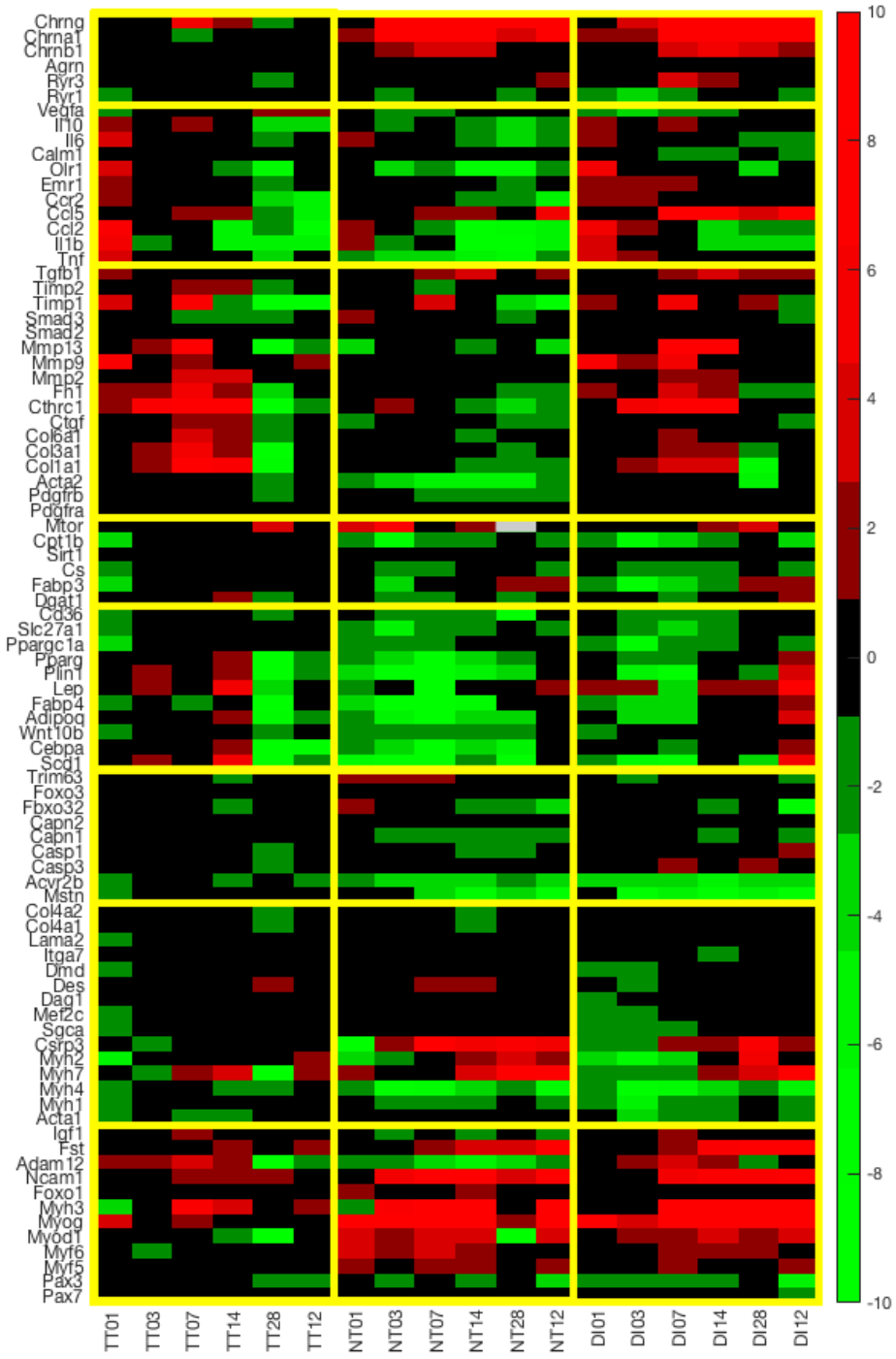

Figure 5.7 Gene expression represented as fold-change relative to SS for, from top to bottom, neurogenic, inflammatory, fibrotic, metabolic, adipogenic, atrophic, muscle-structural, and pro-myogenic genes, with gene families separated by yellow lines. Note that several genes have functions in multiple families, and are grouped here by their most relevant function to disease processes.

In NT, genes associated with muscle regeneration as well as neurogenesis were up-regulated beginning as early as 1 days post intervention and persisting through the 12 week time point, though overlap between myogenic regenerative genes and genes that regulate denervation atrophy complicate interpretation to a degree. Similarly, a subset of muscle structural genes was up-regulated beginning after 14 days of NT and remaining elevated at 12 weeks. Aside from *Trim63* in the acute (1-7 days) phase, atrophic genes tended to either be decreased or not different from SS. Inflammatory, fibrotic, adipogenic, and metabolic genes all tended to decrease with NT, suggesting an overall reduction in anabolic processes.

Gene expression in the DI group demonstrated trends consistent with a compound injury model, with a gene expression signature that is in large part an amalgamation of the TT and NT groups. Trends in expression of myogenic, muscle structural, metabolic, atrophic, and neurogenic genes in the DI group was consistent with the NT group. Meanwhile, inflammatory and fibrotic gene expression was similar to the TT group, and adipogenic gene expression (up-regulated at day 14 in TT) was increased at 12 weeks in the DI group. Together, these suggest that the gene expression signatures of both TT and NT are preserved in DI, and possibly have a synergistic effect on adipogenesis at the most chronic 12 week time point.

Discussion

The prevalence and clinical intractability of human RC tear necessitate a reproducible, clinically relevant animal model in which to explore both basic disease mechanisms as well as potential therapies. Based on its size, ease of use, and range of available molecular and genetic tools, the mouse has become a frequently implemented model of RCT. In order to generate a more robust response in the muscle, a suprascapular nerve injury is often implemented in addition to mechanical unloading. As nerve injury represents an insult to the muscle distinct from disuse/unloading[24], and as nerve injuries (and denervation especially) are not common findings in human RCT, it is imperative to contextualize the separate and combined impact of these injuries in the mouse RC. Therefore, in this study we sought to quantify the

relative effects of tenotomy, denervation, and combined tenotomy and denervation on key muscle parameters in order to better understand the strengths and limitations of the mouse as a pre-clinical model of RC disease.

The most clinically relevant injury, TT alone, did not induce significant chronic atrophy at the whole muscle or muscle fiber level, with limited evidence of long-term activation of the atrophic pathway[24] at the molecular level. Based on its similarity to the SS group, the atrophy observed in TT appears to be as much a function of surgery in general as TT specifically. As expected, NT alone and in combination with TT (i.e. DI) caused rapid and significant atrophy at the whole muscle and muscle fiber level, though surprisingly the gene expression of many known molecular regulators of atrophy were not altered in either NT or DI. One possible explanation for this may be found in the persistently reduced expression of genes central to metabolism. Whereas no changes in the expression of metabolic genes are found after day 1 in TT muscles, expression of key mitochondrial constituents is reduced at both acute and chronic time points in NT and DI, suggesting that reduced biogenesis/anabolism may be an important driver of muscle atrophy after nerve injury. While clinical data is sparse, there is some indication that reduced metabolism contributes to muscle loss in human RCT[34], though it is unclear whether the metabolic and physiological changes brought about by mechanical unloading and denervation are equivalent. Furthermore, while atrophic genes are increased in torn human RC muscle biopsies[35], the atrophy found in NT and DI is far more extreme than that reported in even the most advanced clinical cases[6,13], with 12 week average CSA's in these groups less than 30% of either NC or SS. As the mechanisms of injury, gene expression patterns, and extremity of injury do not recapitulate the clinical RC atrophy phenotype, the suitability of the mouse as a model of torn RC muscle atrophy is doubtful.

Degenerative muscle loss, which has recently been established as a key feature of advanced human RC disease[13], has not previously been explored in murine models of RC tear. As expected, baseline levels of muscle degeneration are low in both NC and SS muscles. TT and NT alone also failed to generate a significant degenerative response, and as such are not relevant to modeling the chronic, clinical phenotype. However, when TT and NT were combined in DI there was progressive degeneration.

This compounding effect is consistent with the overall expression trends where DI broadly represents a combination of the TT and NT expression signatures, and may explain why the DI group shows progressive degeneration—only when the muscle is mechanically and electrochemically unloaded is there sustained degenerative pressure on the mouse RC muscle. Whether this degenerative mechanism is transcriptionally similar to human is difficult to determine, as the molecular signature of degeneration across species is still largely unknown. However, as the prevalence of degeneration is lower even in DI when compared to clinical values[13], and the effect of the extreme atrophy found in DI (but not human RC muscles) on degenerative processes is also unknown, caution against over-interpretation of degeneration-related metrics in the mouse is warranted.

On the regenerative side, the finding that SS, TT, and DI all significantly increased the percentage of CN fibers suggests that intervention generally, and not necessarily a specific injury, produce a regenerative response in the RC muscle. All three of these groups displayed increased expression of myogenic genes to various degrees, though overlap between genes involved in muscle regeneration and those known to be activated by and involved in denervation-induced atrophy make interpretation of this gene expression data alone difficult[27,28]. In contrast, NT appeared to suffer an impairment of regeneration in response to intervention, which was 'rescued' with the addition of TT in DI. From a clinical modeling perspective, it is troubling that the degeneration-regeneration cycle seems to be driven as much or more by the act of intervention (i.e. the SS group) rather than the mechanical unloading of TT. More encouraging was that while the regenerative levels of SS, TT, and DI at day 14 were similar to chronic human RCT[13], CN were subsequently reduced by half or more by 12 weeks in all three groups (despite increased evidence of degeneration and maintained elevation of regenerative gene expression). This suggests that, as has been proposed in human disease, muscle loss in DI mouse is in part the result of reduced regeneration in the face of increased degeneration[13]. However, because CSA of fibers in NT and DI are so extremely diminished, it is also possible that regenerative rates are not reduced, and that this measurement is instead an artifact of severe atrophy where distinguishing between a central and peripheral nucleus becomes increasingly difficult as fiber CSA is reduced.

Aside from muscle loss, fatty infiltration and fibrosis are key clinical indicators of RC disease progression[5,36,37]. Across all groups, the fat fraction never exceeded 5%, suggesting that even in the DI group fat accumulation in the mouse does not approach the magnitude of fat infiltration found clinically[5]. Even so, there does appear to be an emergent effect of DI on fat accumulation and fibrosis at the expression and tissue level. In TT, fat and collagen content (and related gene expression) peaked early (14 days), but returned to baseline (and reduced expression) by 28 days. In contrast, fat, fibrosis, and related gene expression in NT was low and stable throughout the experiment, though NT did appear to alter the distribution of fat over time. DI increased fat and collagen content similar to TT in the acute phase, despite a general reduction in adipogenic gene expression early (<7 days). However, the increased adipogenic expression and persistence of fat infiltration and fibrosis at 12 weeks in the DI group suggests that, unlike the findings in other gene programs, the adipogenic and fibrotic phenotype in DI cannot be explained by a simple compounding effect of two injuries, and is instead the result of a specific but unknown chronic interaction of TT and NT. Again, this is problematic from a modeling perspective as NT (and particularly complete denervation) is not typically found in patients with RC tear[21,22,38]. Without understanding why the combined injury leads to a more clinically relevant phenotype of fatty infiltration and fibrosis, it is possible that despite phenotypic similarity the mechanisms of fat accumulation and fibrosis in the DI mouse RC and chronically torn human RC are biologically distinct. Combined with the low overall fat content found here, findings from the mouse, particularly as they relate to the processes of fat accumulation and fibrosis, should be interpreted and applied with caution, at least until the relationship between these compositional changes and injury mechanisms are better understood.

Conclusion

Understanding the cellular and molecular mechanisms of muscle atrophy, degeneration, fat accumulation, and fibrosis in RC muscles following RC tendon tear is of great clinical importance. To this end, several animal models have been developed, including a mouse model that combines suprascapular neurotomy with tenotomy of the supraspinatus and infraspinatus. However, based on

established differences in atrophic machinery between denervation and mechanical unloading, the unknown degenerative phenotype in the mouse, and the lack of clinical relevance of denervation, this study set out to determine the relative effects of TT, NT, and DI on mouse RC muscle as they relate to clinically meaningful histological and transcriptional parameters. Many of the effects observed in TT appear to be as much an effect of general intervention as mechanical unloading specifically, as outside of small, transient changes at the gene expression and tissue level, TT was similar to SS. As such, the TT model does appear to have significant clinical value, which explains the addition of NT by many previous works. The atrophic phenotype in DI appeared to be driven primarily by NT, while the accumulation degenerative fibers, fat, and fibrosis in the combined injury group suggests that pathological changes in this group are the result of an emergent phenotype that cannot be explained by simple additive effects of TT and NT alone. Despite DI appearing more histologically similar to torn human RC muscle, the low magnitude of degenerative, fatty, and fibrotic changes relative to those found in human muscles are problematic; combined with the limited clinical evidence for neuropathy (and especially complete denervation) in the clinical population, the application and generalization of results from either the TT or DI mouse model of RC tear must be made with great care.

Acknowledgements

This work was funded in part by an Orthopedic Research Education Foundation Resident Research project grant (MS).

This chapter, in part, is currently being prepared for submission for publication of the material. Michael C. Gibbons, Morgan Silldorff, Hiroshi Okuno, Mary C. Esparza, Christopher Migdal, Seth Johnson, Matthew MacEwen, Simon Schenk, Samuel R. Ward. The dissertation/thesis author was the primary investigator of this material.

References

1. Yamamoto A, Takagishi K, Osawa T, Yanagawa T, Nakajima D, Shitara H, Kobayashi T. 2010. Prevalence and risk factors of a rotator cuff tear in the general population. Journal of Shoulder and Elbow Surgery 19:116-120.

2. Gladstone JN, Bishop JY, Lo IK, Flatow EL. 2007. Fatty infiltration and atrophy of the rotator cuff do not improve after rotator cuff repair and correlate with poor functional outcome. The American journal of sports medicine 35:719-728.

3. Bishop J, Klepps S, Lo IK, Bird J, Gladstone JN, Flatow EL. 2006. Cuff integrity after arthroscopic versus open rotator cuff repair: a prospective study. Journal of shoulder and elbow surgery 15:290-299.

4. Longo UG, Franceschi F, Ruzzini L, Rabitti C, Morini S, Maffulli N, Denaro V. 2008. Histopathology of the supraspinatus tendon in rotator cuff tears. The American journal of sports medicine 36:533-538.

5. Goutallier D, Postel J-M, Bernageau J, Lavau L, Voisin M-C. 1994. Fatty muscle degeneration in cuff ruptures: pre-and postoperative evaluation by CT scan. Clinical orthopaedics and related research 304:78-83.

6. Steinbacher P, Tauber M, Kogler S, Stoiber W, Resch H, Sänger A. 2010. Effects of rotator cuff ruptures on the cellular and intracellular composition of the human supraspinatus muscle. Tissue and Cell 42:37-41.

7. Lundgreen K, Lian ØB, Engebretsen L, Scott A. 2013. Lower muscle regenerative potential in full-thickness supraspinatus tears compared to partial-thickness tears. Acta orthopaedica 84:565-570.

8. Glass DJ. 2005. Skeletal muscle hypertrophy and atrophy signaling pathways. Int J Biochem Cell Biol 37:1974-1984.

9. Jones SW, Hill RJ, Krasney PA, O'CONNER B, Peirce N, Greenhaff PL. 2004. Disuse atrophy and exercise rehabilitation in humans profoundly affects the expression of genes associated with the regulation of skeletal muscle mass. The FASEB journal 18:1025-1027.

10. Frontera WR, Meredith CN, O'reilly K, Knuttgen H, Evans W. 1988. Strength conditioning in older men: skeletal muscle hypertrophy and improved function. Journal of applied physiology 64:1038-1044.

11. Gibbons MC, Sato EJ, Bachasson D, Cheng T, Azimi H, Schenk S, Engler AJ, Singh A, Ward SR. 2016. Muscle architectural changes after massive human rotator cuff tear. Journal of Orthopaedic Research.

12. Mendias CL, Roche SM, Harning JA, Davis ME, Lynch EB, Enselman ERS, Jacobson JA, Claflin DR, Calve S, Bedi A. 2015. Reduced muscle fiber force production and disrupted myofibril architecture in patients with chronic rotator cuff tears. Journal of Shoulder and Elbow Surgery 24:111-119.

13. Gibbons MC, Singh A, Anakwenze O, Cheng T, Pomerantz M, Schenk S, Engler AJ, Ward SR. 2017. Histological Evidence of Muscle Degeneration in Advanced Human Rotator Cuff Disease. The Journal of Bone & Joint Surgery 99:190-199.

14. Gibbons MC, Singh A, Engler AJ, Ward SR. 2017. The Role of Mechanobiology in Progression of Rotator Cuff Muscle Atrophy and Degeneration. Journal of Orthopaedic Research.

15. Farshad M, Meyer DC, Nuss KM, Gerber C. 2012. A modified rabbit model for rotator cuff tendon tears: functional, histological and radiological characteristics of the supraspinatus muscle. Shoulder & Elbow 4:90-94.

16. Gerber C, Schneeberger AG, Perren SM, Nyffeler RW. 1999. Experimental Rotator Cuff Repair. A Preliminary Study*. The Journal of Bone & Joint Surgery 81:1281-1290.

17. Kim HM, Galatz LM, Lim C, Havlioglu N, Thomopoulos S. 2012. The effect of tear size and nerve injury on rotator cuff muscle fatty degeneration in a rodent animal model. Journal of shoulder and elbow surgery 21:847-858.

18. Liu X, Laron D, Natsuhara K, Manzano G, Kim HT, Feeley BT. 2012. A mouse model of massive rotator cuff tears. The Journal of Bone & Joint Surgery 94:e41.

19. Davies MR, Liu X, Lee L, Laron D, Ning AY, Kim HT, Feeley BT. 2016. TGF-β Small Molecule Inhibitor SB431542 Reduces Rotator Cuff Muscle Fibrosis and Fatty Infiltration By Promoting Fibro/Adipogenic Progenitor Apoptosis. PloS one 11:e0155486.

20. Liu X, Ning AY, Chang NC, Kim H, Nissenson R, Wang L, Feeley BT. 2016. Investigating the cellular origin of rotator cuff muscle fatty infiltration and fibrosis after injury. Muscles, Ligaments and Tendons Journal 6:6.

21. Zanotti RM, Carpenter JE, Blasier RB, Greenfield MLV, Adler RS, Bromberg MB. 1997. The low incidence of suprascapular nerve injury after primary repair of massive rotator cuff tears. Journal of Shoulder and Elbow Surgery 6:258-264.

22. Beeler S, Ek ET, Gerber C. 2013. A comparative analysis of fatty infiltration and muscle atrophy in patients with chronic rotator cuff tears and suprascapular neuropathy. Journal of Shoulder and Elbow Surgery 22:1537-1546.

23. Gerber C, Meyer DC, Flück M, Valdivieso P, von Rechenberg B, Benn MC, Wieser K. 2016. Muscle Degeneration Associated With Rotator Cuff Tendon Release and/or Denervation in Sheep. The American Journal of Sports Medicine:0363546516677254.

24. Bonaldo P, Sandri M. 2013. Cellular and molecular mechanisms of muscle atrophy. Disease models & mechanisms 6:25-39.

25. Clark BC. 2009. In vivo alterations in skeletal muscle form and function after disuse atrophy. Medicine and science in sports and exercise 41:1869-1875.

26. Jackman RW, Kandarian SC. 2004. The molecular basis of skeletal muscle atrophy. American Journal of Physiology-Cell Physiology 287:C834-C843.

27. Macpherson PC, Wang X, Goldman D. 2011. Myogenin regulates denervation-dependent muscle atrophy in mouse soleus muscle. Journal of cellular biochemistry 112:2149-2159.

28. Moresi V, Williams AH, Meadows E, Flynn JM, Potthoff MJ, McAnally J, Shelton JM, Backs J, Klein WH, Richardson JA. 2010. Myogenin and class II HDACs control neurogenic muscle atrophy by inducing E3 ubiquitin ligases. Cell 143:35-45.

29. Reardon KA, Davis J, Kapsa RM, Choong P, Byrne E. 2001. Myostatin, insulin-like growth factor-1, and leukemia inhibitory factor mRNAs are upregulated in chronic human disuse muscle atrophy. Muscle & nerve 24:893-899.

30. Stein T, Wade C. 2005. Metabolic consequences of muscle disuse atrophy. The Journal of nutrition 135:1824S-1828S.

31. Stitt TN, Drujan D, Clarke BA, Panaro F, Timofeyva Y, Kline WO, Gonzalez M, Yancopoulos GD, Glass DJ. 2004. The IGF-1/PI3K/Akt pathway prevents expression of muscle atrophy-induced ubiquitin ligases by inhibiting FOXO transcription factors. Molecular cell 14:395-403.

32. Minamoto VB, Hulst JB, Lim M, Peace WJ, Bremner SN, Ward SR, Lieber RL. 2007. Increased efficacy and decreased systemic-effects of botulinum toxin A injection after active or passive muscle manipulation. Developmental Medicine & Child Neurology 49:907-914.

33. Livak KJ, Schmittgen TD. 2001. Analysis of relative gene expression data using real-time quantitative PCR and the $2^{-\Delta\Delta CT}$ method. methods 25:402-408.

34. Shah SA, Kormpakis I, Cavinatto L, Killian ML, Thomopoulos S, Galatz LM. 2017. Rotator cuff muscle degeneration and tear severity related to myogenic, adipogenic, and atrophy genes in human muscle. Journal of Orthopaedic Research.

35. Gibbons MC, Fisch KM, Pichika R, Cheng T, Engler AJ, Schenk S, Lane JG, Singh A, Ward SR. 2018. Heterogeneous muscle gene expression patterns in patients with massive rotator cuff tears. PloS one 13:e0190439.

36. Goutallier D, Postel J-M, Gleyze P, Leguilloux P, Van Driessche S. 2003. Influence of cuff muscle fatty degeneration on anatomic and functional outcomes after simple suture of full-thickness tears. Journal of Shoulder and Elbow Surgery 12:550-554.

37. Silldorff MD, Choo AD, Choi AJ, Lin E, Carr JA, Lieber RL, Lane JG, Ward SR. 2014. Effect of Supraspinatus Tendon Injury on Supraspinatus and Infraspinatus Muscle Passive Tension and Associated Biochemistry. The Journal of Bone & Joint Surgery 96:e175.

38. Shi LL, Boykin RE, Lin A, Warner JJ. 2014. Association of suprascapular neuropathy with rotator cuff tendon tears and fatty degeneration. Journal of shoulder and elbow surgery 23:339-346.

Chapter 6. Muscle Degeneration, Fat Accumulation, and Fibrosis in a Rabbit Model of Massive Rotator Cuff Tear

Introduction

The prevalence of rotator cuff (RC) tears in the general population, and particularly in the aged population[1], represents a substantial burden to the healthcare system and patient quality of life [2]. Despite advances in surgical techniques and technology, rotator cuff tears remain one of the most difficult orthopedic injuries to treat. Surgical intervention is generally successful at reducing pain and improving function[3]. However, reversing negative changes in the muscle, avoiding re-tear, and restoring function remain significant clinical challenges, particularly in patients with chronic, massive tears[3-5]. Although contemporary research is attempting to identify the cellular and molecular mechanisms that drive muscle loss and fat accumulation in human RC muscles, several hurdles still remain. Differences in patient demographics, risk factors, injury mechanism, and chronicity complicate mechanistic studies in human biopsies, and there remains a paucity of data in well-characterized, cost effective preclinical models that recapitulate the spectrum of relevant clinical disease features. This in turn hinders our ability to study the underlying biological mechanisms of RC disease, as well as our ability to evaluate new therapeutic approaches aimed at reversing muscle loss following RC tear.

To this end, several animal models, including mouse[6; 7], rat[7], rabbit[8-10], and sheep[11; 12], have been developed to study pathophysiological mechanisms of RC disease, and a limited number of studies have evaluated potential therapeutic approaches in these models[9; 13-16]. However, as our clinical understanding of RC disease evolves, the suitability of these models for a given research question must be re-evaluated. Recent evidence from a cohort of patients (human) with advanced RC disease suggests that not just muscle atrophy and pericellular fat deposition, but muscle degeneration[17], in which muscle fibers are damaged[18] and possibly replaced by fat[17], is a key feature of the most intractable cases of RC tear – to date, this phenomenon has not been explicitly described in any animal model. Based on existing studies, the mouse and rat models do not seem to develop the degree of muscle atrophy, degeneration, or cell-level fat replacement found clinically, even with the controversial addition of a nerve injury[6; 7; 19]. At the

other end of the spectrum, the sheep does seem to lose muscle and accumulate fat similar to humans[11; 20], but the size of the sheep and its associated costs limit its widespread use. Therefore, the rabbit is an attractive alternative at an intermediate size and cost, provided it adequately recapitulates the pathological phenotype found in human disease.

Indeed, rabbit models of RC disease have been previously developed and deployed for both basic science[8; 10] and translational[9; 15] purposes. These studies have demonstrated robust muscle atrophy and accumulation of fat in rabbit RC, but the development of muscle degeneration/regeneration and the relative localization of accumulated adipocytes in the rabbit RC has yet to be explored in detail. As such, the purpose of this study was to generate a repeatable tenotomy model of RC tear in the rabbit, in order to characterize the time course of atrophy, degeneration, fat accumulation, and fibrosis that occur at sub-chronic and chronic time points. Having confirmed the presence of clinically relevant degenerative features in torn rabbit RC (as well as previously reported atrophy and bulk fat accumulation), the short-term goal is to implement this model for the exploration of biological mechanisms of irreversible muscle loss (i.e. muscle cell degeneration), and testing of therapeutic interventions.

Methods

Animals

A total of twenty-nine female New Zealand White rabbits were used for this study. All protocols were approved by the UCSD Institutional Animal Care and Use Committee. All animals were approximately 6 months of age at the start of the study as this is the age of skeletal maturity in NZW rabbits[21]. Anesthesia was induced with a subcutaneous injection of ketamine and xylazine, and rabbits were then intubated and anesthesia was maintained with a 2-4% isoflurane vapor. For the five animals assigned to the architecture portion of the study, tenotomy of the supraspinatus was performed unilaterally by sharp transection of the supraspinatus tendon at its footprint on the greater tubercle of the humerus followed by blunt dissection of surrounding soft tissue connections to allow unhindered retraction of the tendon stump and distal pole of the muscle. The contralateral shoulder remained un-

operated and served as an internal control. Euthanasia was performed immediately following tenotomy via intravenous pentobarbital (Beuthanasia) overdose. The remaining 24 animals underwent a similar tenotomy on the left side, where a Penrose drain was secured to the tendon stump to prevent scar formation between the tendon and surrounding soft tissue, while a sham operation was performed on the contralateral side. These animals were allowed to recover and were then euthanized as previously described at 2, 4, 8, or 16 weeks to study the time course of pathological changes in the RC muscle following tenotomy.

Architecture

To preserve the architecture of the muscle, immediately after sacrifice the humerus was transected and the scapula and associated musculature was removed in order to preserve the native configuration of the glenohumeral joint. The joint was pinned with the humerus at a 90^{o} angle to the scapular spine and submersion fixed in 10% formalin for one week. Prior to dissection, the retraction distance was measured as the distance from the footprint of the supraspinatus tendon on the greater tubercle of the humerus to the tendon stump, and pennation angle was measured for each of four regions: anterior lateral (A1), anterior medial (A2), posterior lateral (P1), and posterior medial (P2), where the central tendon was used to demarcate the muscle midline and the division between anterior and posterior regions. The supraspinatus muscle was then harvested from scapula, and fascicles were dissected from the superior aspect of each region of the muscle as a proxy for fiber length. Fiber bundles were dissociated from these fascicles and sarcomere length was measured using established laser diffraction techniques[22].

Histology

At each time point, both the operated and sham shoulders were resected, and the retraction distance (with the joint in a similar 90^{o} position) was recorded for the tenotomized muscle. Both supraspinatus muscles were harvested, and a full-muscle thickness segment was dissected from each of the regions described above. These segments were then pinned to *in vivo* length and snap frozen in liquid

nitrogen-cooled isopentane before being stored at -80^{o}C. Frozen muscle segments were then embedded in OCT and sectioned in a cryostat to obtain both axial and longitudinal sections.

To evaluate muscle fiber cross-sectional area (CSA) and the percentage of centralized nuclei (CN), as measures of atrophy and regeneration, respectively, sections were stained with laminin (Vector, VP-M648) and DAPI (Vector Vectashield with DAPI, H-1500). CSA and CN were then quantified using a custom ImageJ macro[23]. The frequency of muscle fiber degeneration, quantified by overlaying a 500μm^2 grid over an entire Hematoxylin and Eosin-stained section, and scoring each grid element as either positive or negative for signs of muscle fiber degeneration[17; 24].

Fat accumulation was quantified using two methods, one to approximate total fat content, and a second to determine the localization of fat relative to fascicular structures. The overall fat fraction of each region was quantified as the percentage of the entire muscle segment staining positive for Oil Red-O, as determined by a semi-automated thresholding protocol (Metamorph). Localization of fat was quantified using a similar strategy as used to quantify muscle fiber degeneration, reported as a percentage of grid elements containing either intra-fascicular or peri-fascicular fat. The incidence of intra-fascicular fat adjacent to degenerating muscle fibers (i.e. contained within the same grid element) was also measured as a potential marker of more 'terminal' degeneration, as muscle fibers replaced by fat within the lattice of the fascicles are likely irreversibly degenerated. Fibrosis was quantified using a bulk tissue, hydroxyproline assay as well as histology. Hydroxyproline content was calculated and converted to bulk collagen content using established methods[26].

Each region was analyzed for each histological parameter to determine whether or not there were regional effects of tenotomy using a two-way, repeated measures ANOVA ($\alpha = 0.05$). Additionally, for simplicity and in order to compare these data to previously published work (where information on the muscle region evaluated is often omitted), we report the average of all four regions as the whole-muscle average for each parameter using a similar statistical analysis. In cases where power analysis was warranted, G*Power[27] was used to calculate post-hoc power based on experimental effect sizes.

Results

In the five animals sacrificed immediately following tenotomy, architectural changes confirmed a robust mechanical unloading of the supraspinatus muscle as the total muscle length was significantly shortened, corresponding to an average initial retraction distance of 7.3 millimeters (Fig 1A). This muscle shortening corresponded to a significant decrease in fiber length in P1, and a trend toward shortening in A2 and P2 (Fig 1B). Pennation angle was significantly increased as a function of tenotomy, though the effect was not significant for any individual region. All regions demonstrated significant sarcomere shortening with tenotomy (Fig 1C).

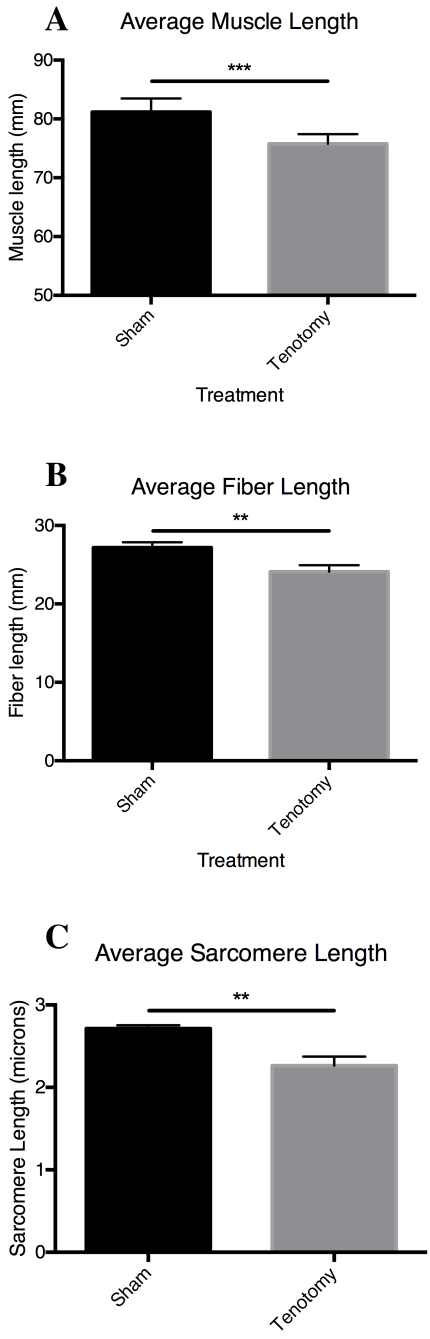

Figure 6.1 Average muscle length (A), fiber length (B) and sarcomere length (C) decrease significantly immediately following tenotomy of the supraspinatus.

In the time course group, retraction distance was significantly increased over time, with the largest increase found between 2 and 16 weeks (Fig 2A). Muscle mass was significantly reduced by 2 weeks post-tenotomy, with persistent mass reduction of 24.2% at 16 weeks (Fig 2B). Similar to muscle

mass, muscle fiber atrophy was significant by two weeks post-tenotomy and remained 26.5% smaller than contralateral at 16 weeks (Fig 2C).

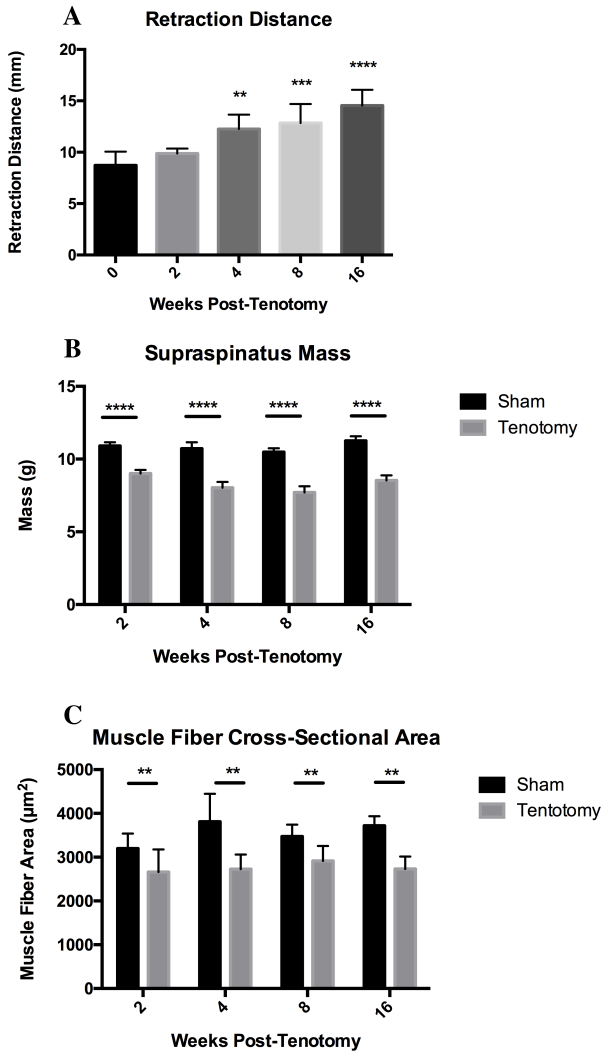

Figure 6.2 (A) Retraction distance increases significantly over time. Significant atrophy at the whole muscle level (B) and the muscle fiber-cross sectional level (C) occurs by two weeks post-tenotomy, and does not progress from 2 to 16 weeks.

Muscle degeneration was significantly increased with tenotomy (Fig 3) after 2 weeks, after which tenotomized muscles only trended toward increased degeneration. Despite increased degeneration found in tenotomized muscles, there was no increase in regeneration as measured by the percentage of centralized nuclei at any time point.

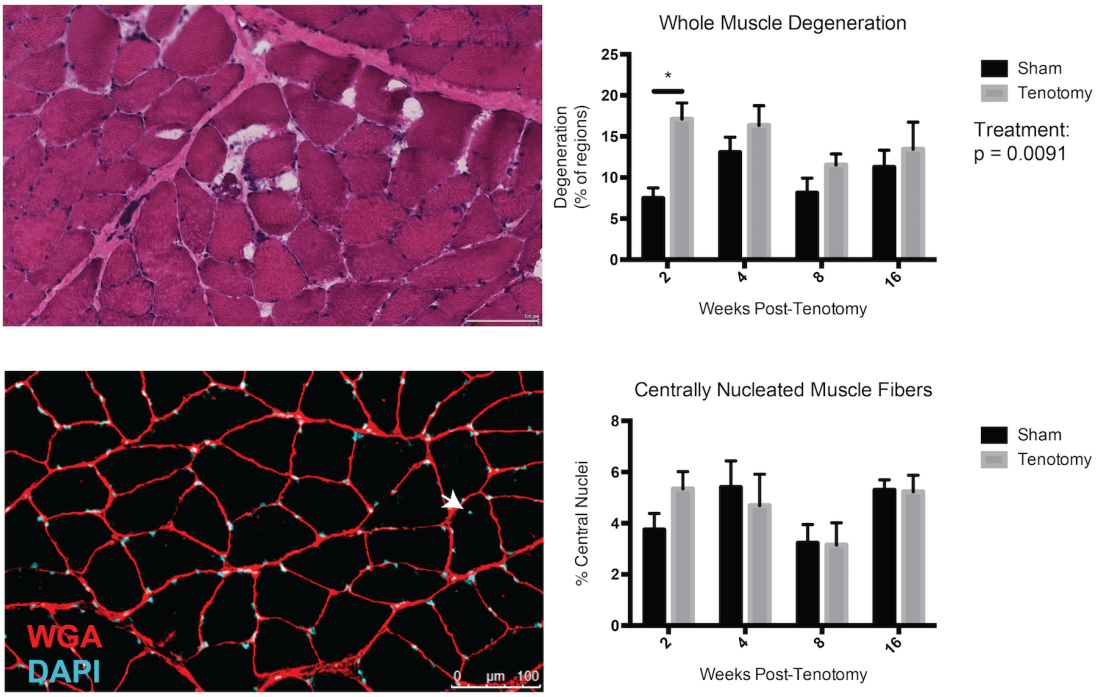

Figure 6.3 (A) Representative H&E image of a degenerating muscle fiber. (B) At 2 weeks, the prevalence of degeneration was significantly increased in the tenotomized shoulder, with a trend toward increased degeneration at subsequent time points. (C) Representative image of centrally nucleated muscle fibers (arrows) indicative of a regenerated fiber. (D) Centralized nuclei were not significantly different between tenotomy and sham at any time point.

Along with muscular changes, fat and fibrosis are key characteristics of RC muscle pathology. There was a significant increase in collagen content with tenotomy (main effect), with an approximately 50% increase in tenotomized shoulders at 4 and 8 weeks that through 16 weeks (Fig 4A). Post-hoc power analysis suggested that while adequately powered for main-effect testing, the experiment was underpowered for post-hoc testing in this assay ($\beta < 0.8$), which may explain why changes in collagen content were not statistically significant at any individual time point.

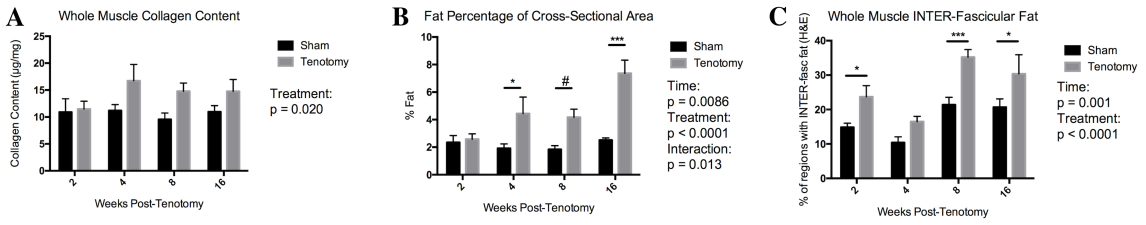

Figure 6.4 A) Whole muscle collagen was not significantly different at any time point. (B) The overall fat fraction was significantly increased by 4 weeks post-tenotomy, and progressed through 16 weeks. (C) The prevalence of inter-fascicular fat was significantly increased by 2 weeks of tenotomy, and progressed through week 16.

Overall fat accumulation, as measured by whole-cross section ORO staining, showed a significant increase in fat beginning at week 4 and progressing through week 16, where fat content was nearly tripled compared to the contralateral control (Fig 4B). In terms of localization, fat was more often found between fascicles (inter-fascicular) in both the tenotomized muscle as well as the contralateral. Tenotomy significantly increased the incidence of inter-fascicular fat by approximately 50% at later 8- and 16-week time points (Fig 4C). Furthermore, though the main effect of tenotomy on the incidence of intra-fascicular fat was significant, statistical under-powering similar to the collagen content assay ($\beta < 0.80$ for post-hoc testing) likely contributes to the lack of significant differences at any individual time points (Fig 5A). Finally, while there was virtually no incidence of intra-fascicular fat adjacent to degenerating muscle fibers in contralateral muscles, tenotomized muscles showed a significant increase in this indicator of terminal degeneration at the most chronic 16 week time point (Fig 5B).

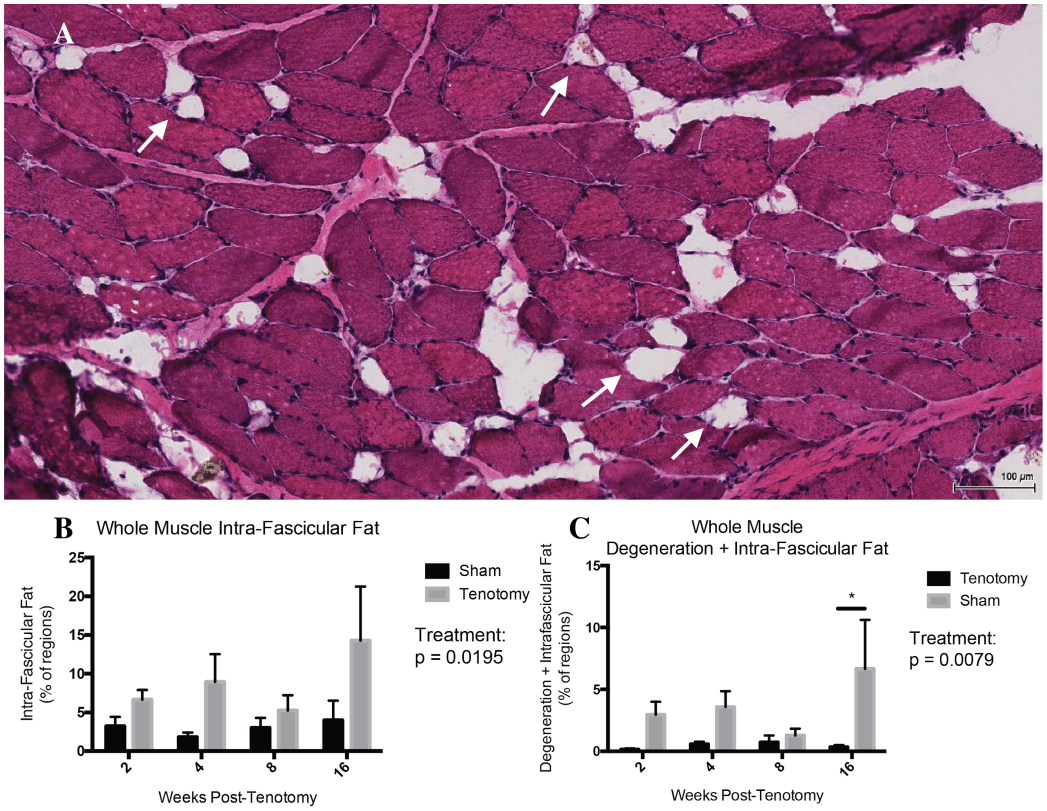

Figure 6.5 (A) Representative image of intra-fascicular fat (arrows). (B) While there was a treatment effect of tenotomy on intra-fascicular fat, this study was underpowered to detect significant differences within time points. (C) The occurrence of intra-fascicular fat adjacent to degenerating fibers was significantly increased after 16 weeks of tenotomy.

Discussion

There is a current need for a clinically relevant, cost-effective animal model of RC disease to study the biology of muscle loss after RC tear as well as to evaluate new biological interventions aimed at improving or restoring function to the RC complex[28; 29]. While rodent models are often employed for these purposes, the applicability of findings from the mouse and rat to clinical practice is often unclear, as these models exhibit key differences in the injury mechanisms[30], biological scale, and presence of degenerative features that define human RC disease. The rabbit, which has historically been used as a model of RC tear[31], has recently garnered attention as a potential model that may address the shortcomings of the rodent models without the restrictive time, space and cost considerations of larger animal models[8]. Therefore, the purpose of this study was to determine the suitability of the rabbit as a pre-

clinical model that recapitulates the relevant mechanical and biological features of human RC disease, specifically related to muscle cell degeneration and replacement of muscle fibers by fat[29].

Immediately after RC tear, the muscle length, fiber length, and sarcomere length are all significantly reduced, confirming that the muscle can be released from surrounding soft-tissue structures and retract and remodel to a comparable degree as a massive human RC tear[32]. Importantly, the muscle continues to retract over time, suggesting that 1) the muscle does not scar down and become reloaded (a persistent problem in rodent models), and 2) the muscle atrophies longitudinally in response to chronic retraction and unloading over the time course investigated here - a feature also observed in human muscles[32].

Longitudinal and radial muscle fiber atrophy occurs primarily in the first two weeks following tear, and persists throughout the time course studied here. This time course likely differs from the insidious onset of many chronic human tears[33], which are presumed to become unloaded over a period of time as tendon tears enlarge. As a result, it is likely that radial muscle atrophy following RC tear in humans[34; 35] occurs over longer periods of time, while the immediate unloading of this model generates a maximum atrophic stimulus in the acute phase without a continuous atrophic pressure over the time course. Because the magnitude of muscle fiber atrophy is similar between human and rabbit, it is likely that the classic atrophic mechanisms[36] apparent in human disease[37] are similarly responsible for atrophy in the rabbit (despite differences in time course), though this must be confirmed in future studies.

Whereas muscle loss via atrophy is generally reversible in the context of disuse and unloading[38-41], muscle volume in human and animal models of RCT is not restored with mechanical repair and reloading alone[5; 11]. These observations together with recent descriptions of muscle fiber disorganization and degeneration in human biopsies suggesting muscle cell dysfunction and death, and not simple atrophy, are responsible for the persistent muscle loss and functional deficits found clinically. This necessitates an animal model that recapitulates not only atrophic but also degenerative muscle loss to study degenerative mechanisms and regenerative therapies. Unlike the mouse and rat, which demonstrate very mild atrophy without concomitant nerve transection, and no degeneration, the rabbit does show

significant incidence of degeneration after tenotomy. Furthermore, the rabbit shows increased incidence of intra-fascicular fat and degeneration adjacent to intra-fascicular fat over time, which may indicate irreversibly degenerated muscle fibers. Interestingly, though degeneration is significantly increased in the rabbit, there is no indication of increased regeneration as measured by the percentage of centrally nucleated fibers. This is not necessarily detrimental from a modeling perspective, as diminished regenerative capacity is thought to be a feature of irreversible muscle loss in humans[29], and in an environment that appears to favor replacement of muscle fibers by fat and fibrosis over regeneration[29] it may take longer than 16 weeks for the percentage of regenerated fibers to reach a detectable level even when rates of muscle degeneration are increased. Overall, the similarity of the atrophic and degenerative phenotypes found in rabbit and man support the use of the rabbit as a clinically relevant model of both mechanisms of muscle loss.

Beyond muscle loss, the development of fatty infiltration and fibrosis are important from a clinical perspective. Not only is fat accumulation a potential contributor to the irreversibility of muscle loss[17; 29], it is also an important clinical diagnostic feature[42; 43]. Previous work has demonstrated infiltration of fat at a whole-muscle level in the rabbit[8], and here we find a preponderance of fat accumulation in the inter-fascicular space. Similar to human, fat accumulation at both the tissue and whole-muscle level is progressive and occurs primarily between fascicles. Equally important is the finding detailed above regarding the accumulation of fat within fascicles which, though less prevalent than inter-fascicular fat, may represent a more biologically significant fat depot that should be considered a necessary feature of a pre-clinical model given it's currently unknown role in the development and progression of RC pathology. Collagen content, as a metric of fibrosis, also showed a modest increase beginning at four weeks. However, as the hydroxyproline assay determines collagen on a per-weight basis it is unclear to what degree this result is a function of de novo collagen synthesis versus a relative increase due to a reduction in muscle content. In future experiments, fractional synthetic rates of collagen should be examined.

On the basis of the data presented here and in other recent work[8], the rabbit is a strong preclinical model for both basic science and translational research related to RC disease. Unlike smaller animal models, the rabbit demonstrates robust atrophy and significant muscle degeneration. This muscle loss is also accompanied by two key clinical markers of disease progression: significant and progressive fatty infiltration, and apparent fibrosis. Finally, though the incidence is lower than in chronic human tears, the progressive increase in degenerating muscle fibers adjacent to intra-fascicular fat suggests that this model could serve to answer the pressing questions surrounding the cellular and molecular mechanisms of irreversible muscle loss in human RC disease – including mechanisms of muscle degeneration as well as potential inhibitors of normal muscle regeneration in the context of RC tear. Beyond these mechanistic questions, the size of the rabbit combined with the similarity of human and rabbit response to RC tear provide an ideal platform for investigating the safety, efficacy, and mechanism of action of emerging therapies, particularly those targeted toward promoting regeneration and restoring mechanical function of the RC muscle-tendon complex.

Conclusion

The challenges of studying RC disease in humans, including variability caused by different tear modalities and sizes, indeterminate duration of injury, and comorbidities, necessitate an animal model that faithfully recapitulates the muscle phenotype found in humans. In this study, we demonstrate that tenotomy leads to significant acute muscle retraction which progresses through 16 weeks. Similar to human RC, both atrophic and degenerative mechanisms of muscle loss are present in the rabbit following RC tear. Furthermore, fat accumulates in both inter- and intra-fascicular spaces, suggesting that the rabbit is a suitable model for studying both bulk fatty infiltration as well as the potentially more terminal process of fat replacing muscle fibers within the fascicular structure. On this basis, we believe the rabbit is an appropriate preclinical model for studying biological questions as well as evaluating new regenerative therapies aimed toward restoring RC function.

Acknowledgements

This work was funded in part by an Orthopedic Research Education Foundation Resident Research Project grant (MVV).

This chapter, in part, is currently being prepared for submission for publication of the material. Mario Vargas-Vila, Michael C. Gibbons, Mary C. Esparza, Shingo Miyazaki, Seth Johnson, Koichi Masuda, Anshu Singh, Samuel R. Ward. The dissertation/thesis author was a primary investigator of this material.

References

1. Yamamoto A, Takagishi K, Osawa T, Yanagawa T, Nakajima D, Shitara H, Kobayashi T. 2010. Prevalence and risk factors of a rotator cuff tear in the general population. Journal of Shoulder and Elbow Surgery 19:116-120.

2. MacDermid JC, Ramos J, Drosdowech D, Faber K, Patterson S. 2004. The impact of rotator cuff pathology on isometric and isokinetic strength, function, and quality of life. Journal of Shoulder and Elbow Surgery 13:593-598.

3. Galatz LM, Ball CM, Teefey SA, Middleton WD, Yamaguchi K. 2004. The outcome and repair integrity of completely arthroscopically repaired large and massive rotator cuff tears. The Journal of Bone & Joint Surgery 86:219-224.

4. Deniz G, Kose O, Tugay A, Guler F, Turan A. 2014. Fatty degeneration and atrophy of the rotator cuff muscles after arthroscopic repair: does it improve, halt or deteriorate? Archives of orthopaedic and trauma surgery 134:985-990.

5. Gladstone JN, Bishop JY, Lo IK, Flatow EL. 2007. Fatty infiltration and atrophy of the rotator cuff do not improve after rotator cuff repair and correlate with poor functional outcome. The American journal of sports medicine 35:719-728.

6. Liu X, Laron D, Natsuhara K, Manzano G, Kim HT, Feeley BT. 2012. A mouse model of massive rotator cuff tears. The Journal of Bone & Joint Surgery 94:e41.

7. Kim HM, Galatz LM, Lim C, Havlioglu N, Thomopoulos S. 2012. The effect of tear size and nerve injury on rotator cuff muscle fatty degeneration in a rodent animal model. Journal of shoulder and elbow surgery 21:847-858.

8. Farshad M, Meyer DC, Nuss KM, Gerber C. 2012. A modified rabbit model for rotator cuff tendon tears: functional, histological and radiological characteristics of the supraspinatus muscle. Shoulder & Elbow 4:90-94.

9. Oh JH, Chung SW, Kim SH, Chung JY, Kim JY. 2014. 2013 Neer Award: Effect of the adipose-derived stem cell for the improvement of fatty degeneration and rotator cuff healing in rabbit model. Journal of Shoulder and Elbow Surgery 23:445-455.

10. Rubino LJ, Stills Jr HF, Sprott DC, Crosby LA. 2007. Fatty infiltration of the torn rotator cuff worsens over time in a rabbit model. Arthroscopy: The Journal of Arthroscopic & Related Surgery 23:717-722.

11. Gerber C, Meyer D, Schneeberger A, Hoppeler H, Von Rechenberg B. 2004. Effect of tendon release and delayed repair on the structure of the muscles of the rotator cuff: an experimental study in sheep. The Journal of Bone & Joint Surgery 86:1973-1982.

12. Luan T, Liu X, Easley JT, Ravishankar B, Puttlitz C, Feeley BT. 2015. Muscle atrophy and fatty infiltration after an acute rotator cuff repair in a sheep model. Muscles, ligaments and tendons journal 5:106.

13. Gerber C, Meyer DC, Flück M, Benn MC, von Rechenberg B, Wieser K. 2015. Anabolic steroids reduce muscle degeneration associated with rotator cuff tendon release in sheep. The American journal of sports medicine 43:2393-2400.

14. Davies MR, Liu X, Lee L, Laron D, Ning AY, Kim HT, Feeley BT. 2016. TGF-β Small Molecule Inhibitor SB431542 Reduces Rotator Cuff Muscle Fibrosis and Fatty Infiltration By Promoting Fibro/Adipogenic Progenitor Apoptosis. PloS one 11:e0155486.

15. Gerber C, Meyer D, Nuss K, Farshad M. 2011. Anabolic steroids reduce muscle damage caused by rotator cuff tendon release in an experimental study in rabbits. J Bone Joint Surg Am 93:2189-2195.

16. Gerber C, Meyer DC, Frey E, von Rechenberg B, Hoppeler H, Frigg R, Jost B, Zumstein MA. 2009. Neer Award 2007: Reversion of structural muscle changes caused by chronic rotator cuff tears using continuous musculotendinous traction. An experimental study in sheep. Journal of Shoulder and Elbow Surgery 18:163-171.

17. Gibbons MC, Singh A, Anakwenze O, Cheng T, Pomerantz M, Schenk S, Engler AJ, Ward SR. 2017. Histological Evidence of Muscle Degeneration in Advanced Human Rotator Cuff Disease. The Journal of Bone & Joint Surgery 99:190-199.

18. Mendias CL, Roche SM, Harning JA, Davis ME, Lynch EB, Enselman ERS, Jacobson JA, Claflin DR, Calve S, Bedi A. 2015. Reduced muscle fiber force production and disrupted myofibril architecture in patients with chronic rotator cuff tears. Journal of Shoulder and Elbow Surgery 24:111-119.

19. Liu X, Manzano G, Kim HT, Feeley BT. 2011. A rat model of massive rotator cuff tears. Journal of orthopaedic research 29:588-595.

20. Gerber C, Meyer DC, Flück M, Valdivieso P, von Rechenberg B, Benn MC, Wieser K. 2016. Muscle Degeneration Associated With Rotator Cuff Tendon Release and/or Denervation in Sheep. The American Journal of Sports Medicine:0363546516677254.

21. Ravanetti F, Scarpa E, Farina V, Zedda M, Galli C, Borghetti P, Cacchioli A. 2015. The effect of age, anatomical site and bone structure on osteogenesis in New Zealand White rabbit. Journal of Biological Research-Bollettino della Società Italiana di Biologia Sperimentale 88.

22. Lieber RL, Yeh Y, Baskin RJ. 1984. Sarcomere length determination using laser diffraction. Effect of beam and fiber diameter. Biophysical journal 45:1007.

23. Minamoto VB, Hulst JB, Lim M, Peace WJ, Bremner SN, Ward SR, Lieber RL. 2007. Increased efficacy and decreased systemic-effects of botulinum toxin A injection after active or passive muscle manipulation. Developmental Medicine & Child Neurology 49:907-914.

24. Dubowitz V, Sewry CA, Oldfors A. 2013. Muscle Biopsy: A Practical Approach, Expert Consult; Online and Print, 4: Muscle Biopsy: A Practical Approach: Elsevier Health Sciences;

25. Edwards C, O'brien W. 1980. Modified assay for determination of hydroxyproline in a tissue hydrolyzate. Clinica chimica acta 104:161-167.

26. Faul F, Erdfelder E, Lang A-G, Buchner A. 2007. G* Power 3: A flexible statistical power analysis program for the social, behavioral, and biomedical sciences. Behavior research methods 39:175-191.

27. Lebaschi A, Deng XH, Zong J, Cong GT, Carballo CB, Album ZM, Camp C, Rodeo SA. 2016. Animal models for rotator cuff repair. Annals of the New York Academy of Sciences.

28. Gibbons MC, Singh A, Engler AJ, Ward SR. 2017. The Role of Mechanobiology in Progression of Rotator Cuff Muscle Atrophy and Degeneration. Journal of Orthopaedic Research.

29. Beeler S, Ek ET, Gerber C. 2013. A comparative analysis of fatty infiltration and muscle atrophy in patients with chronic rotator cuff tears and suprascapular neuropathy. Journal of Shoulder and Elbow Surgery 22:1537-1546.

30. Fabis J, Kordek P, Bogucki A, Synder M, Kolczynska H. 1998. Function of the rabbit supraspinatus muscle after detachment of its tendon from the greater tubercle: Observations up to 6 months. Acta orthopaedica Scandinavica 69:570-574.

31. Gibbons MC, Sato EJ, Bachasson D, Cheng T, Azimi H, Schenk S, Engler AJ, Singh A, Ward SR. 2016. Muscle architectural changes after massive human rotator cuff tear. Journal of Orthopaedic Research.

32. Bigliani LU, Cordasco FA, Mcllveen SJ, Musso ES. 1992. Operative repair of massive rotator cuff tears: long-term results. Journal of shoulder and elbow surgery 1:120-130.

33. Lundgreen K, Lian ØB, Engebretsen L, Scott A. 2013. Lower muscle regenerative potential in full-thickness supraspinatus tears compared to partial-thickness tears. Acta orthopaedica 84:565-570.

34. Steinbacher P, Tauber M, Kogler S, Stoiber W, Resch H, Sänger A. 2010. Effects of rotator cuff ruptures on the cellular and intracellular composition of the human supraspinatus muscle. Tissue and Cell 42:37-41.

35. Bonaldo P, Sandri M. 2013. Cellular and molecular mechanisms of muscle atrophy. Disease models & mechanisms 6:25-39.

36. Gibbons MC, Fisch KM, Pichika R, Cheng T, Engler AJ, Schenk S, Lane JG, Singh A, Ward SR. 2018. Heterogeneous muscle gene expression patterns in patients with massive rotator cuff tears. PloS one 13:e0190439.

37. Frontera WR, Meredith CN, O'reilly K, Knuttgen H, Evans W. 1988. Strength conditioning in older men: skeletal muscle hypertrophy and improved function. Journal of applied physiology 64:1038-1044.

38. Jones SW, Hill RJ, Krasney PA, O'CONNER B, Peirce N, Greenhaff PL. 2004. Disuse atrophy and exercise rehabilitation in humans profoundly affects the expression of genes associated with the regulation of skeletal muscle mass. The FASEB journal 18:1025-1027.

39. Raue U, Slivka D, Jemiolo B, Hollon C, Trappe S. 2006. Myogenic gene expression at rest and after a bout of resistance exercise in young (18–30 yr) and old (80–89 yr) women. Journal of Applied Physiology 101:53-59.

40. Schoenfeld BJ. 2012. Does exercise-induced muscle damage play a role in skeletal muscle hypertrophy? The Journal of Strength & Conditioning Research 26:1441-1453.

41. Goutallier D, Postel J-M, Bernageau J, Lavau L, Voisin M-C. 1994. Fatty muscle degeneration in cuff ruptures: pre-and postoperative evaluation by CT scan. Clinical orthopaedics and related research 304:78-83.

42. Goutallier D, Postel J-M, Gleyze P, Leguilloux P, Van Driessche S. 2003. Influence of cuff muscle fatty degeneration on anatomic and functional outcomes after simple suture of full-thickness tears. Journal of Shoulder and Elbow Surgery 12:550-554.

Chapter 7. Muscle Degeneration and Patterns of Fat Accumulation in Chronically Unloaded Sheep Infraspinatus: Comparisons to Human Rotator Cuff Disease

Abstract

Background and Hypothesis: Chronic human rotator cuff (RC) disease remains an intractable clinical problem. While small and large animal models have been developed, there is controversy about how well these models represent the clinical muscle phenotype, particularly in cases of advanced disease. Here, we present and compare new muscle atrophy, degeneration-regeneration, characteristic fat infiltration, and accompanying gene expression data in an ovine model to data from patients with advanced RC disease.

Methods: Mechanically unloaded sheep infraspinatus biopsies were collected at acute (2 week), chronic (16 week), and post-repair (16+6 week) time points. Laminin-DAPI staining was used to quantify muscle fiber area and centralized nuclei, and H&E staining was used to manually quantify the incidence of muscle fiber degeneration and inter- and intra-fascicular fat accumulation. Gene expression values were obtained from RNA-sequencing data to identify gene ontologies enriched in up- and down-regulated genes after tear and repair. These results were compared to previously published values from human RC biopsies.

Results: Muscle fiber atrophy was limited in the sheep model. However, muscle fiber degeneration was significantly increased by 16 weeks. Furthermore, the incidence of fat accumulation both around and within fascicles, and importantly the co-localization of muscle degeneration with intra-fascicular fat, was similar between the sheep and human RC muscle. Similar to human disease, there was little sign of tissue-level recovery in the sheep after six weeks of repair, suggesting that these degenerative changes may be irreversible. *Conclusion:* These data provide a strong case for the ovine model of RC disease as a platform for exploring the structural, cellular and molecular mechanisms driving these degenerative processes as well as for developing new interventions to reverse and prevent them.

Basic Science Study

Key Words: Rotator Cuff, Muscle Atrophy, Muscle Degeneration, Fat Infiltration

Introduction

Rotator cuff (RC) tendon tears lead to muscle unloading, reduced muscle length and volume, and fatty infiltration. While surgical options continually improve, patient outcomes in advanced disease and or more active patients do not. A key issue in recovery is the persistence of muscle "fatty infiltration" even when tendon repairs are successful[19]. To better understand the underlying muscle biology that results from RC disease, and to evaluate potential therapeutic agents, a number of animal models have been developed[6, 10, 23, 27, 28, 36, 39]. However, the lack of robust human data has made validation of these models difficult. As our understanding of the human disease increases, it is imperative to continually reevaluate our animal models to ensure that these models are in fact representative of the clinical problems that we are aiming to solve.

To this end, mouse[27, 48], rat[1, 28, 42], rabbit[6, 39], dog[41], and sheep[10, 14, 29] have all been explored as possible models of RC disease. Each of these models has demonstrated some degree of muscle atrophy and fat accumulation. In small animals, however, tenotomy must be combined with neurotomy to produce these changes[23, 27]. Yet in man[2] as in larger animals[12] the pathology resulting from suprascapular nerve transection is distinct from those resulting from RC tear alone. As the relative advantages and disadvantages of each model have been reviewed elsewhere[25], we will only summarize the relevant attributes of the sheep model. The most common unloading strategy in the sheep involves osteotomy of the greater tuberosity to release the *infraspinatus* (ISP) tendon[10], because of its similarities to the human supraspinatus[15]. This model has consistently demonstrated robust whole muscle atrophy and fat accumulation in response to unloading[10], consistent with human RC disease[20, 43]. The most commonly used chronic time point in the sheep is sixteen weeks[13, 14], at which point the muscle is considered acceptably pathological for evaluation of various interventions[7, 13], though pathology does continue to progress after these time points[10].

In advanced human disease, loss of muscle volume appears to be at least partially driven by a degenerative process that is characterized by the accumulation of muscle fiber damage, ultimately leading to fiber death[18]. This muscle loss is coupled to irreversible fatty infiltration at the organ (muscle) level, which has implications for disease staging[21] and interventional outcomes[19]. Though organ level fat accumulation is a key clinical variable, studies regarding the mechanisms of fatty infiltration in human RC muscle are limited. While previous human studies demonstrate an accumulation of small lipid droplets within muscle fibers[30] and a possible whitening of the fat depots around the RC muscle[33], our understanding of the cellular and molecular mechanisms of muscle degeneration and fat accumulation are based primarily on data from small animal studies, which, based on their failure to recapitulate the whole-muscle level changes in muscle degeneration and fat accumulation seen in humans, may not represent the clinical disease processes. More recent evidence has shown that some of the accumulated fat appears within the fascicular structure, often adjacent to degenerating muscle fibers, indicating that degenerating muscle cells may be replaced directly by fat[18]. Again, the mechanisms involved in this process remain unknown, due largely to the lack of appropriate animal models recapitulating this degenerative phenotype.

Studying these processes in humans is complex because of the high variability in disease severity and chronicity, which is often exacerbated by comorbidities in the patient population, and substantial difficulty obtaining biopsies that contain identifiable muscle in patients with advanced disease[18]. These impediments underscore the need for an animal model that recapitulates not only the atrophic phenotype, but then goes on to develop the degenerative phenotype of muscle loss after prolonged tendon tear. Based on their similarity to human muscle in terms of gross muscle loss and fat accumulation in response to mechanical unloading, the sheep represents the most promising model of advanced rotator cuff disease to date[10, 13-15]. Here, we aim to confirm and quantify the presence of degeneration and intra-fascicular fat accumulation in the sheep model, and compare both histological and transcriptional responses in human and sheep to chronic unloading, in order to validate the use of the sheep model in studying and developing therapies related to muscle pathology in advanced RC disease.

Materials and Methods

Human data were derived from biopsies obtained during reverse total shoulder arthroplasty (RSA) in patients with advanced RC disease (n=31 biopsies)[16, 18]. Histological sheep data were derived from biopsies obtained in two separate cohorts of sheep described in previous studies[7, 40]. Briefly, the infraspinatus was surgically unloaded via osteotomy of the greater tuberosity and allowed to retract for 2 or 16 weeks (n=6/group). In the latter group, the osteotomy was repaired to the original footprint after 16 weeks, with a final evaluation 6 weeks post-repair[7]. At each stage of the protocol (pre-release, 2 or 16 weeks, and 6 weeks post-repair) a Bergstrom needle muscle biopsy was obtained and fresh frozen in liquid nitrogen for subsequent evaluation. CT and MRI scans were performed immediately after tendon release, at 6 weeks, before repair (16 weeks) and finally 6 weeks thereafter. On transverse MR images, the cross-sectional area of the ISP muscles was marked along their whole length, including the central tendon, and the respective muscle volume was calculated in percentage of the volume immediately after tenotomy. Transverse fat- and water-only Dixon images were used for measuring the fat fraction of the ISP muscles. On CT scans, myotendinous retraction and the density (HU) of the muscle tissue were measured on complete transverse cross-sectional area at the level of the central tendon of the infraspinatus muscle.

Because the purpose of this study was to compare the natural history of pathology in sheep and humans, this study does not include animals that received treatment other than mechanical tendon repair.

Histological assessment of muscle biopsies was performed for model comparisons. Muscle fiber cross-sectional area (CSA) and the percentage of centrally nucleated, regenerating muscle fibers were quantified with wheat germ agglutitin-DAPI immunohistochemical staining in six 10x fields using a custom ImageJ macro[34]. Sections were subsequently stained with Hematoxylin and Eosin (H&E) for quantification of the incidence of muscle degeneration. Degeneration was defined by the presence of myophagocytic or hypercellular muscle fibers, split fibers, or fibers with obvious signs of sarcolemma disruption[5], and was quantified in the sheep biopsies by overlaying a 500x500μm grid over the entire

H&E stained biopsy cross-sections and scoring all grid elements with greater than 50% muscle content as either containing or not containing degeneration. A similar scoring scheme was employed in parallel to quantify the incidence of inter- and intra-fascicular fat, including a score for grid elements containing both degenerative signs and intra-fascicular fat indicative of an important degenerative feature found in human RC disease[18]. For each measurement the fraction of grid elements containing the pathological phenotype (muscle fiber degeneration, inter- and intra-fascicular fat) was compared to the total number of grid elements, and is reported as the percentage of grid elements containing each degenerative phenotype.

Levels of muscle fiber atrophy, degeneration, and regeneration were compared using one-way ANOVA and post-hoc Tukey tests to determine significant differences between groups and time points in the sheep model (asterisks in figures). A separate one-way ANOVA was used to compare atrophy and degeneration-regeneration parameters between sheep and human data (number sign in figures). The significance threshold was defined as a p-value less than 0.05 for all analyses.

While gene expression data was available for both sheep and human biopsies, direct statistical comparisons were not made as RNA sequencing and quantitative PCR were used to generate the two data sets, respectively. Differentially expressed genes were identified in the sheep data set[7] using a limma-voom pipeline[38], followed by gene-ontology enrichment analysis (GOEA) to identify ontologies that were differentially regulated following 16 weeks of unloading and 6 weeks of repair. Genes were considered up-regulated if the log fold-change (logFC) was greater than 0.5 (<0.5 for down-regulated genes) and the adjusted p-value was less than 0.05. Due to limited GO annotation of the sheep genome specifically, gene symbols were input in the PANTHER GO pipeline and human annotations were used to categorize gene function, where ontologies with an FDR < 0.05 considered significantly enriched. For a more direct comparison, the logFC in expression in the sheep data set was reported for the subset of available human gene expression results[16]. For both analyses, it should be noted that not all human genes have orthologs in sheep.

Results

Muscle Atrophy and Degeneration

In the sheep, myotendinous retraction, as measured on the CT scan, was 2.9±0.4mm immediately after tendon release, and increased to 4.9±0.5mm after 6 weeks and 5.8±1mm after 16 weeks. The volume of the sheep infraspinatus muscle, as measured on the MRI, decreased to 80±8% after 6 weeks, remained stable at 78±11% after 16 weeks, and decreased further to 69±9% 6 weeks after the repair[7] (Fig. 1A). The mean muscle fibers length changed from 3.5±1 cm to 1.8±0.7 cm after 6 weeks and to 2.1±0.8 cm after 16 weeks. At the tissue level, fiber area analysis indicated that muscle fiber area was significantly increased at two weeks ($p \leq 0.029$, Fig. 2C), possibly due to muscle retraction. By 16 weeks post-injury, muscle fiber area returns to pre-injury levels, with no change after six weeks of repair. Furthermore, there was no significant difference between fiber area six weeks post-repair and the unoperated contralateral control. There was also no significant difference between muscle fiber CSA in human RC muscle compared to sheep at any time point.

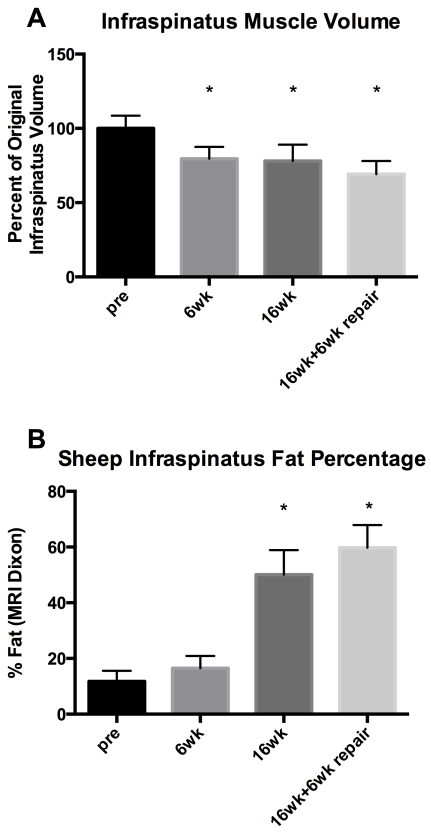

Figure 7.1 Changes in whole muscle volume (A) and fat percentage (B). Infraspinatus muscle volume is reduced after 6 weeks of unloading and remains so after 6 weeks of repair, while fat volume is significantly increased after 16 weeks of unloading and continues to trend upward (p=0.086) after 6 weeks of repair.

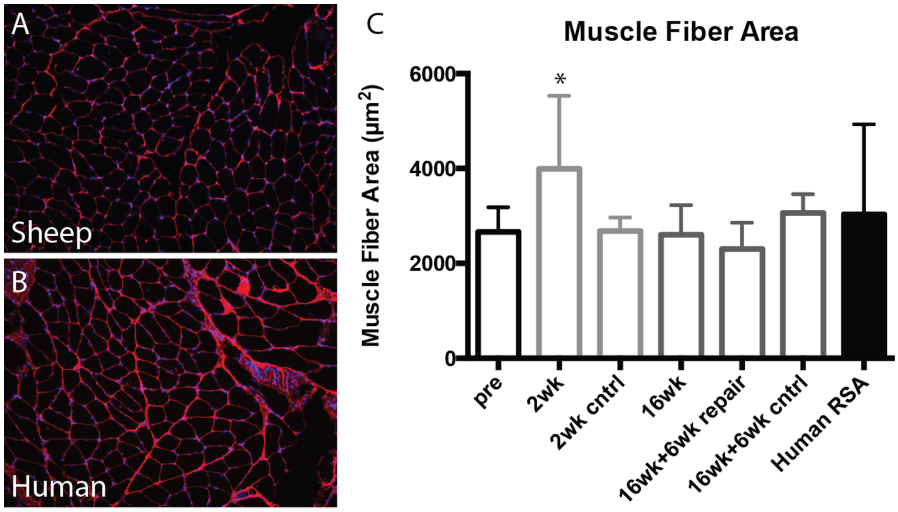

Figure 7.2 Example laminin-DAPI staining for sheep (A) and human (B) muscle biopsy sections. (C) Muscle fiber CSA for sheep muscle over time (hollow bars) and human muscle from RSA patient biopsies (black bar). Muscle fiber CSA was significantly elevated at two weeks compared to pre, 2 week contralateral, 16 weeks, and 6 weeks post-repair time points (*, $p \leq 0.029$). No significant differences were found between sheep and human data at any time point.

Prior to injury, 19.8±14.3% of biopsy regions (22.3±10.3 regions/biopsy) in the sheep contained degenerating muscle fibers (Fig. 3C). No significant increase in degeneration was found two weeks post-injury, though centrally nucleated fibers indicative of regeneration was significantly increased from 6.2±3.4% to 15.1±6.0% ($p=0.045$) (Fig 3D). After sixteen weeks of unloading the level of degeneration is significantly increased (55.0±12.0% biopsy regions) and remains elevated after six weeks of repair (51.3±21.6%) ($p \leq 0.005$). Centrally nucleated fibers were not significantly elevated at these later time points, though a subset of samples (3/6) displayed a large increase in centralized nuclei after sixteen weeks of unloading (21.2±4.7%) (Fig 3). Because baseline levels of degeneration for untorn human RC muscle are unknown, it is difficult to interpret the clinical significance of the pre-injury degeneration levels in sheep. At the chronic sixteen-week and six-week post-repair time points, sheep biopsy regions contained fewer regions with degenerative fibers compared to human biopsies ($p \leq 0.005$), but remain markedly increased compare to baseline levels.

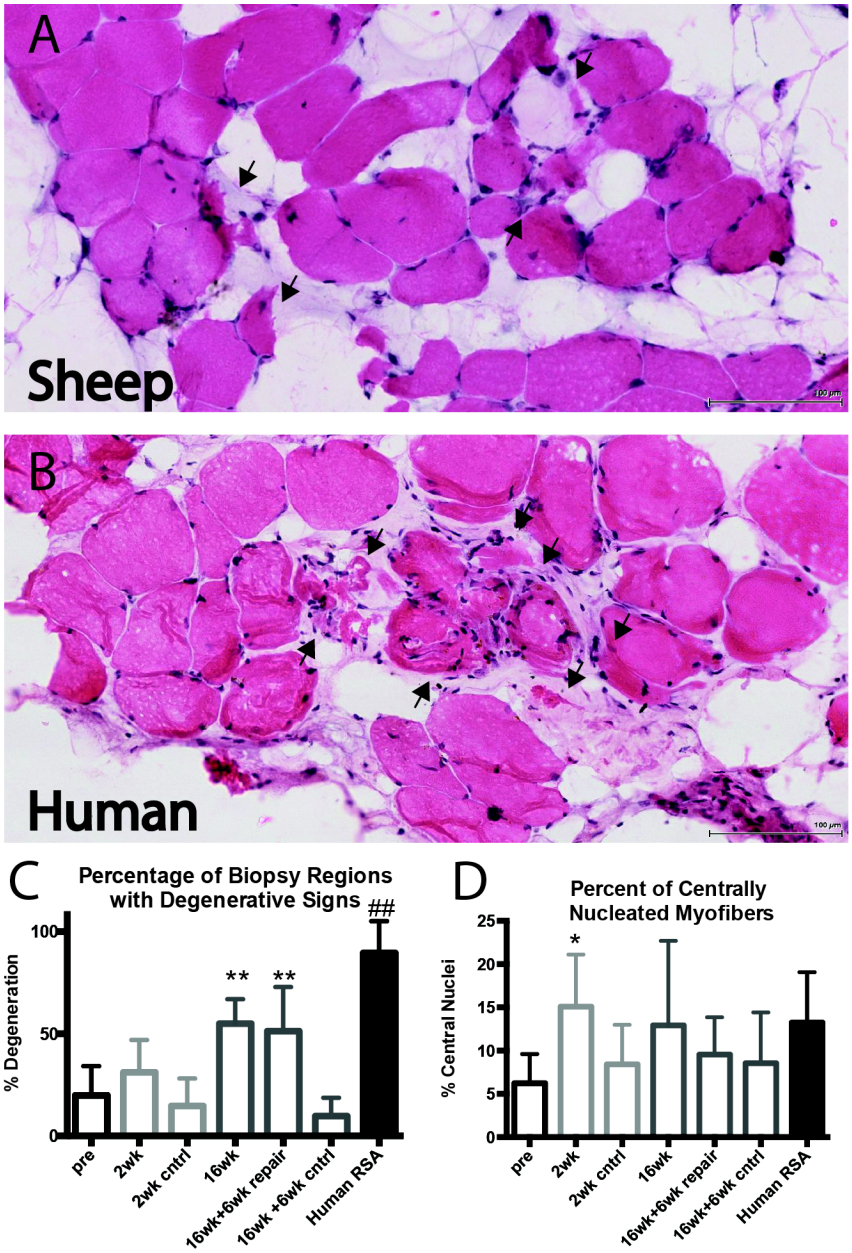

Figure 7.3 Example H&E from sheep (A) and human (B) biopsies demonstrating muscle degeneration (arrowheads). (C) Percentage of muscle biopsy regions containing signs of muscle degeneration. Degeneration was significantly elevated at 16 weeks and 6 weeks post-repair compared to all other time points (**, $p \leq 0.005$). Incidence of degeneration was significantly increased in human RSA biopsies compared to all sheep time points (##, $p \leq 0.005$). (D) Percentage of centrally-nucleated muscle fibers. Centralized nuclei were significantly elevated at 2 weeks compared to pre (*, $p = 0.045$), but were not significantly different across any other time point. There was no significant difference in centralized nuclei between sheep and human biopsies at any time point.

Accumulation and Localization of Fat

Whole-muscle fat accumulation was measured with the density (HU) of the muscle tissue in CT and as percentage of fat in MRI Dixon sequence, which showed a continuous increase of fatty infiltration from a mean of 63±7 HU (Goutallier 0) and 12±4% at tendon release to 54±4 HU (Goutallier 0) and 17±4% after 6 weeks, 26±11 HU (Goutallier 2) and 50±9% after 16 weeks, and continued further to 11±13 HU (Goutallier 4) and 60±8% 6 weeks after successful repair[7] (Fig. 1B).

At the tissue level, the incidence of fat both around and between fascicles was relatively high at baseline, with inter-fascicular fat in 25.1±12.1% and intra-fascicular fat in 13.8±5.0% of biopsy regions (Fig. 4). No change in the prevalence of fat occurred after two weeks of unloading. Similar to whole-muscle fatty infiltration, after sixteen weeks of unloading the incidence of inter-fascicular fat nearly doubled to 49.7±17.7% of biopsy regions ($p=0.053$), while intra-fascicular fat more than tripled to 42.5±23.0% ($p=0.0034$). After six weeks of repair, inter-fascicular fat continued to trend upward to 71.8±15.9% ($p=0.189$ compared to 16 weeks), though interestingly, the number of regions containing intra-fascicular fat remained stable at 43.6±21.6% (Fig. 4). At these chronic time points, there was no significant difference in the incidence of either inter- or intra-fascicular fat in sheep compared to humans.

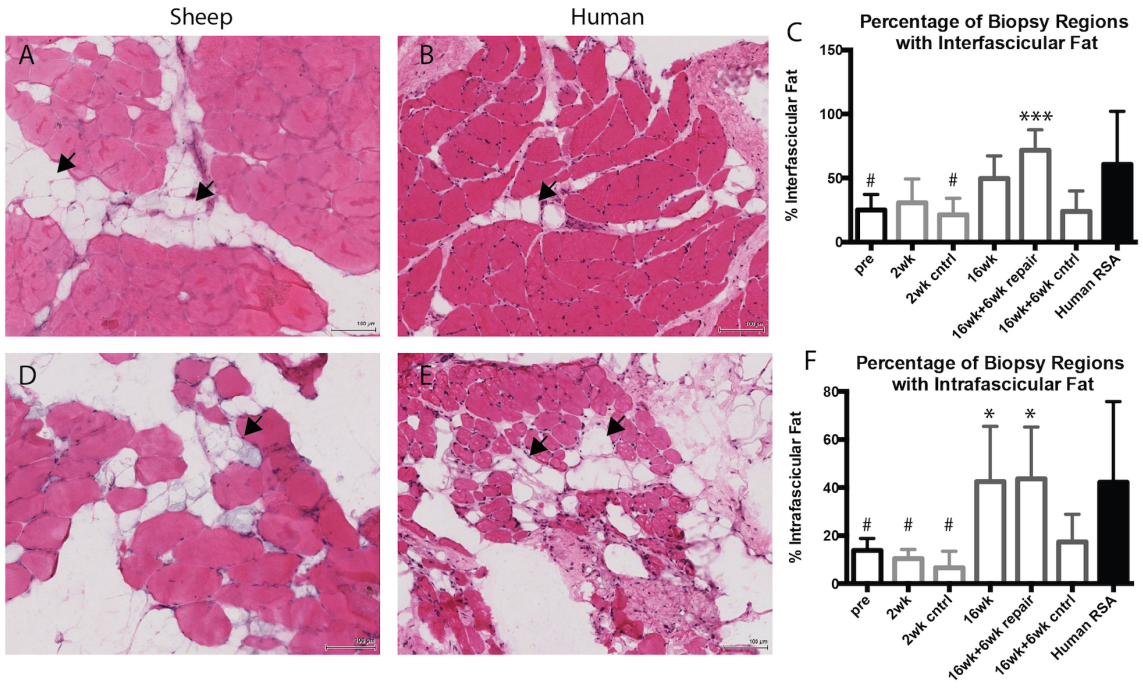

Figure 7.4 Example H&E of interfascicular (A,B) and intrafascicular (D,E) fat in sheep and human biopsies (arrowheads). (C) Interfascicular fat trended upward in the sheep at 16 weeks post-injury ($p=0.053$), with a significant increase compared to pre-injury and two weeks post-injury after six weeks of repair (***, $p\leq0.0007$). The incidence of interfascicular fat in injured sheep muscle was not significantly different from human biopsies at any time points. (F) Intrafascicular fat was significantly elevated after 16 weeks of unloading (*, $p\leq0.034$) compared to 2 weeks and all control time points, with no significant change after 6 weeks of repair. Incidence of intrafascicular fat was greater in human biopsies compared to 2 week and control time points in sheep (#, $p\leq0.05$), but was not significantly different compared with later sheep time points.

Importantly, the incidence of degeneration adjacent to intra-fascicular fat was significantly increased from just 5.5±4.7% of sheep biopsy regions at baseline to 28.8±9.2% after sixteen weeks of unloading ($p=0.0026$) (Fig. 5). No significant decrease in this metric was observed after six weeks of repair, though a subset of samples (3/6) did trend toward a decrease in the co-localization of degenerating fibers with intra-fascicular fat. Here again the sheep model compared favorably with the human condition, with no significant difference in this degenerative metric found between chronically torn human and sheep muscle.

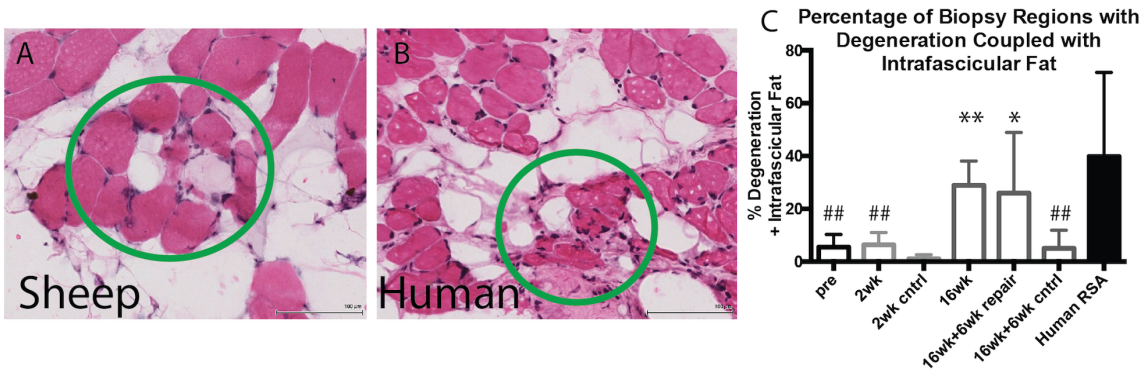

Figure 7.5 Degenerating muscle fibers directly adjacent to intrafascicular fat in sheep (A) and human (B) muscle biopsies (green circles). (C) Incidence of this phenomenon was significantly elevated after 16 weeks of unloading in the sheep, with no change after 6 weeks of repair, compared to 2 weeks of unloading and all control time points (*, $p \leq 0.005$ and $p \leq 0.02$, respectively). Human biopsies contained significantly higher incidence of this metric compared to 2 week and all sheep control time points (##, $p \leq 0.005$), with no significant difference between human and sheep biopsies at later 16 week and 16 weeks/6 weeks repair time points.

Gene Expression Changes after Chronic Unloading

A total of 601 (531 up, 70 down) and 1673 (1434 up, 239 down) genes were differentially regulated in sheep RC compared to pre-operation baseline after 16 weeks of unloading and 6 weeks of repair, respectively. At both time points, GO terms related to increased cellular stress, regulated cell death, fat differentiation, and fibroblast proliferation, as well as regulation of innervation, cell migration, and sarcomere organization, were enriched in the set of up-regulated genes (Table 1). No significant enrichment was found at either time point among down-regulated genes (Supplemental Data). At 16 weeks of tear there was additional enrichment of regulators of muscle stem cell function, and of inhibitors of cell growth, muscle tissue development, and innervation. After 6 weeks of repair, additional ontologies related to muscle stem cell proliferation and differentiation, muscle hypertrophy/development, response to load/activity, inhibition of programmed cell death, re-innervation, and inflammation were significantly enriched.

Table 7.1 Gene ontologies enriched after tear and repair of sheep RC. Positive (+) and negative (-) regulators of each process are indicated separately where appropriate.

	0/ -/ +	16 Weeks Tear	16 + 6 Weeks Repair
Cellular Stress	0	GO:0071470, GO:2000379, GO:0080134, GO:0033554	GO:0070301, GO:0034614, GO:0097237, GO:0042542, GO:0034599, GO:0000302, GO:0006979, GO:0001666, GO:0009636, GO:0036293, GO:0080135, GO:0033554, GO:0006950, GO:0080134
Regulated Cell Death	0	GO:0042981, GO:0043067, GO:0010941	GO:0006915, GO:0042981, GO:0043067, GO:0010941, GO:0012501, GO:0008219
	-		GO:2001237, GO:0043069, GO:0060548
	+	GO:0043068, GO:0010942, GO:0043065	GO:0008630, GO:0043065, GO:0010942, GO:0043068
Cell Migration	0	GO:0050920, GO:0030334, GO:2000145, GO:0040012, GO:0048870, GO:0040011, GO:0016477	GO:0030334, GO:2000145, GO:0040012
	-	GO:0030336, GO:2000146, GO:0040013	GO:2000146, GO:0030336, GO:0040013
	+	GO:2000147, GO:0030335, GO:0040017	GO:0030335, GO:2000147, GO:0040017
Muscle Stem Cell Proliferation	0		GO:0014842, GO:0014857
Muscle Stem Cell Differentiation	0	GO:2001014, GO:0051153, GO:0051147	GO:2001014, GO:0051147, GO:0051153, GO:0051146, GO:0042692
	-	GO:2001015	
	+		GO:0014902, GO:0051155, GO:0051149
Hypertrophy / Muscle Development	0	GO:0060537, GO:0014706, GO:0040008, GO:0061061	GO:0061387, GO:1901861, GO:0055001, GO:0048634, GO:0055002, GO:0060537, GO:0014706, GO:0061061, GO:0007517
	-	GO:0045843, GO:0048635, GO:1901862, GO:0045926	
	+		GO:0014896, GO:0016202, GO:0045927
Response to Load/Activation	0		GO:0006942, GO:0014823, GO:0090257, GO:0009612
Sarcomere Organization	0	GO:0060297, GO:0030036	GO:0031032, GO:0030239, GO:0030036
Innervation	0	GO:0051963, GO:0007416, GO:0050803, GO:0050807, GO:0021915, GO:0043523, GO:0010975, GO:1901214, GO:0051960, GO:0045664, GO:0050767, GO:0048699, GO:0022008, GO:0007399, GO:0030182	GO:0030516, GO:1901214, GO:0045664, GO:0050767, GO:0010975, GO:0051960, GO:0048667, GO:0030182, GO:0048699, GO:0022008
	-	GO:0051965, GO:0010977, GO:0050768, GO:0051961	GO:0050768
	+	GO:0010976, GO:0051962, GO:0045666, GO:0050769	GO:0045773, GO:0050772, GO:0010976, GO:0050769, GO:0045666, GO:0051962
Inflammation	0	GO:0002573, GO:0045619, GO:1902105	GO:0032663, GO:0032479, GO:0045637, GO:0070663, GO:0043122, GO:0048534
	-		
	+		GO:0070665, GO:0071222, GO:0050671, GO:0071219, GO:0032496
Fibroblast Proliferation	0	GO:0048145	GO:0048145
	-		
	+	GO:0048146	GO:0048146
Fat Differentiation/ Adipogenesis	0	GO:0045598	GO:0045598, GO:0008610, GO:0006629
	-		
	+	GO:0045600	

Within the subset of genes for which human data was available, we found similar trends after both 16 weeks of tear and 6 weeks of repair, as pro-myogenic and pro-adipogenic expression was increased while anti-myogenic, inflammatory and fibrotic gene expression was largely unchanged (Fig.

6). These trends differed from human RC biopsies primarily in the anti-myogenic and fibrotic ontologies, as anti-myogenic genes tended to be increased and fibrotic genes decreased in human muscles.

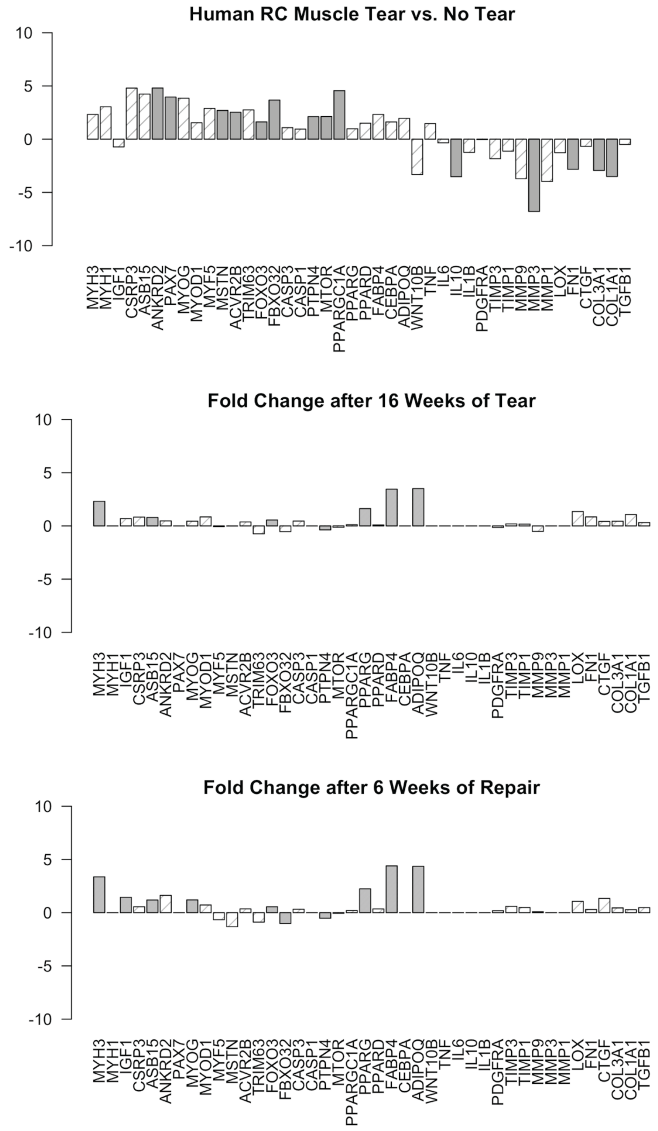

Figure 7.6 Fold change in the subset of genes for which human data was available. Genes with significant differences from reference samples are indicated by shaded bars in (A) human patients with RC tear and confirmed muscle presence in biopsy vs. patients without RC tear, (B) 16 week post-tear sheep biopsy vs. pre-operated control, and (C) 6 week post-repair sheep biopsy vs. pre-operated control.

Discussion

Chronic rotator cuff tears remain a clinical and scientific challenge, particularly in the most advanced states of disease. Further complicating the development of effective treatments for RC disease

is the lack of a clinically validated animal model that would allow for more controlled study of the processes that govern the most advanced and intractable stages of the disease. While many animal models emulate the muscle atrophy of human RC disease[10, 23, 27, 28], there is little evidence in these models of the muscle fiber damage or degeneration that appear to characterize advanced human RC disease. The sheep model of RC disease was evaluated for muscle degeneration due to the robust muscle loss and fat accumulation known to occur in this established model.

The most obvious radiological indication of chronic RC tendon tear in humans is fatty infiltration[22], which is proportionally associated with musculotendinous retraction[31], and is thought to be the result of shortening muscle fibers and increasing pennation[24, 44]. In the clinic, the progression of tear size[37], muscle atrophy[47], and fat accumulation[9, 20] are typically scored on semi-quantitative scales[26, 37], using either MRI or CT. These scores are then used to infer chronicity and reparability of the lesion. In scientific settings, fully quantitative measurement methods have meanwhile become available and are used especially for evaluation of volumetric changes of the muscle and intramuscular fat content (i.e. MRI – DIXON). In contrast to the possibility of longitudinal evaluation (including pre- and post-injury evaluation) in basic (animal) research settings, such quantitative data are rarely available in humans. Despite some shortcomings[45], the available data suggest that the sheep model is comparable to man in terms of fat accumulation[35], but may not reproduce the degree of muscle loss observed in the clinic due to stabilization of tendon retraction as seen intra-operatively and on CT scans. While the addition of neurectomy of the suprascapular nerve to the sheep model resulted in enhanced atrophy, this combined injury model resulted in distinctly different structural, histological, biomolecular, and radiographic degeneration pattern compared to isolated tendon release[12], which limits its use as a pre-clinical model.

Interestingly, muscle loss at the organ level did not result in radial atrophy at the muscle fiber level. Fiber CSA's were increased after 2 weeks of retraction, possibly due to isovolumetric effects of fiber shortening, and returned to baseline CSA after 16 weeks. This suggests serial sarcomere deletion (i.e. longitudinal atrophy) between two and sixteen weeks[8]. Despite this, atrophy-related gene expression was not enriched for at 16 weeks. Based on fiber size alone, the force producing capacity of these fibers

would be preserved, albeit with a diminished working range[17, 46]. However, this idea should be confirmed experimentally with singe fiber active mechanics, as genes related to sarcomere organization were enriched in both tear and repair here, and studies in humans have suggested diminished specific force in fibers from torn human RC on the basis of sarcomere disorganization[30]. Importantly, this baseline fiber CSA is similar to fiber areas found in advanced human RC disease, where signs of atrophy at the muscle fiber level (i.e. small muscle fibers) are not prevalent[18].

The prevalence of muscle damage and degeneration at the fiber level in the uninjured sheep muscles both prior to tear and in the non-operated contralateral muscles was somewhat surprising, though difficult to contextualize without the appropriate human control data. Despite potentially high baseline levels of degeneration (discussed below), a significant increase in the proportion of biopsy regions containing degenerative markers was observed after sixteen weeks of injury without any apparent reduction after six weeks of repair. Consistent with histological findings, genes associated with growth inhibition, cellular stress, and apoptotic processes were all enriched 16 weeks after tear, with the latter two remaining enriched after 6 weeks of repair. It is unclear why the sheep does not display peak degeneration at the same level as human biopsies, though differences in chronicity and the relative fraction of muscle in each biopsy (which is greater in sheep) may contribute to the higher levels observed in humans.

Similar to degenerative signs, centrally nucleated muscle fibers indicative of regeneration were approximately double the 3% generally considered to be clinically pathological[5] at baseline. Unlike degeneration, centralized nuclei did not increase after 16 weeks of tear or after 6 weeks of repair despite an acute increase at 2 weeks. This is reflected in the gene expression data as well, where enrichment for cell migration, muscle stem cell differentiation, mitotic arrest was found. However, after 6 weeks of repair genes related to muscle stem cell proliferation and differentiation, myofibril assembly, and hypertrophy were all enriched, suggesting a regenerative response at the expression level that does not translate to tissue-level changes in either degeneration-regeneration or atrophy-hypertrophy. While it is possible that 6 weeks is too brief an interval after repair to see the effects of these expression trends,

previous studies suggest that repair does not significantly restore muscle volume[11, 12]. As such, future studies should investigate the causes of this blunted muscle recovery observed in the face of pro-myogenic signaling, as this may provide insight into the lack of muscle regeneration following tendon repair in humans.

While the sheep matches the gross fat accumulation found in humans, it is equally important from a clinical modeling perspective that the cellular pattern of fat accumulation is clinically relevant, as the mechanisms of fat accumulation, including the cellular sources and spatial patterns by which fat replaces muscle, remain largely unknown. One prevailing theory of fat infiltration is that it is a space-filling mechanism in which the voids created between muscle fascicles during muscle retraction are occupied by adipocytes, which then serve as a mechanical buffer for normal muscle action[32]. In that paradigm, the fat primarily occupies the space between fascicles, while fascicular structures remain intact. In advanced human disease, this theory may account for the fat observed between fascicles, but does not explain the high prevalence of intra-fascicular fat, in which muscle fibers appear to be replaced by fat without any apparent disruption to the fascicular organization. Here, we show that the sheep model recapitulates this pattern of intra-fascicular fat accumulation, including intra-fascicular fat adjacent to degenerative fibers similar to findings in human muscle[18]. This latter finding opens the possibility of using the sheep model to study the specific cellular and molecular mechanisms driving both muscle degeneration and the subsequent fibrosis and fatty replacement that appears to signify a state of terminal degeneration in human RC muscle. Indeed, after 16 weeks of tear and 6 weeks of repair there was enrichment of fibroblast proliferation and fat differentiation and metabolic genes. The sheep model may also be useful in elucidating the mechanisms of lipid droplet accumulation[30] and brown-to-beige fat conversion[33] previously described in humans, as well as in validating the many interesting findings from small animal models, including the possible role of fibro/adipogenic progenitors in the process of fat infiltration[3].

One possible explanation for the increased degeneration/regeneration at baseline that must be recognized is the presence of what appears to be sarcocystic parasites found in a small number of muscle fibers[4] (accompanied by enrichment of genes associated with xenobiotic responses (GO:0009410,

GO:0071214, GO:0071216)). Though muscle fibers containing parasites were not considered damaged or degenerated for the purposes of this study, the parasites may nonetheless cause an infected muscle fiber to appear damaged or become more susceptible to damage throughout the fiber, leading to a high baseline rate of degeneration.

Despite the possibility of this additional degenerative pressure on the muscle, these data provide strong evidence that the sheep model does develop a degenerative phenotype similar to that found in large and chronic human RC tears, where muscle regeneration is outpaced by muscle degeneration. Even more importantly from a modeling perspective is the fact that like human RC muscle, mechanical repair fails to reverse muscle degeneration or stimulate muscle regeneration in the sheep. However, despite the control of injury time course afforded by the sheep model compared to human, there remains the challenge of studying the disperse processes of muscle degeneration and fat accumulation, wherein only a small fraction of fibers are actively degenerating in a given section at a given point in time. This aspect of muscle degeneration must be taken into account when utilizing traditional genomic and proteomic approaches, where strategies for amplifying the signal from the cells of interest are likely necessary to effectively characterize the biological drivers degenerative processes.

Conclusion

The goal of this work was to validate a sheep model of RC disease by comparing rates of muscle atrophy, degeneration-regeneration, and specific patterns of fat accumulation (including their associated gene expression patterns) found in advanced human RC disease with those found in mechanically unloaded sheep RC muscle. Like the human RC, chronically unloaded sheep RC muscle demonstrates significant muscle loss and fat accumulation. Importantly, as in advanced human RC disease the sheep does not display significant muscle fiber atrophy and contains significant evidence of muscle fiber degeneration at both the tissue and gene expression level. This suggests that, like human RC muscle, the primary mode of muscle loss in the sheep model is accumulated muscle fiber damage and death without a concurrent increase in muscle fiber regeneration. Furthermore, the specific pattern and degree of fat

accumulation, including the presence of intra-fascicular fat adjacent to degenerating muscle fibers, is also comparable to human RC muscle. Together, these findings support the use of the sheep model to investigate important outstanding questions in the field of RC disease research, including studies of the cell types and molecular mechanisms that lead to muscle degeneration, impaired regeneration, and the accumulation and replacement of contractile muscle fibers with adipose tissue.

Acknowledgements

This chapter, in part is currently being prepared for submission for publication of the material. Michael C. Gibbons, Severin Ruoss, Kathleen M. Fisch, Brigitte von Rechenberg, Martin Flück, Christian Gerber, Samuel R. Ward. The dissertation/thesis author was the primary investigator of this material.

References

1. Gladstone JN, Bishop JY, Lo IK, Flatow EL. 2007. Fatty infiltration and atrophy of the rotator cuff do not improve after rotator cuff repair and correlate with poor functional outcome. The American journal of sports medicine 35:719-728.

2. Liu X, Laron D, Natsuhara K, Manzano G, Kim HT, Feeley BT. 2012. A mouse model of massive rotator cuff tears. The Journal of Bone & Joint Surgery 94:e41.

3. Liu X, Manzano G, Kim HT, Feeley BT. 2011. A rat model of massive rotator cuff tears. Journal of orthopaedic research 29:588-595.

4. Kim HM, Galatz LM, Lim C, Havlioglu N, Thomopoulos S. 2012. The effect of tear size and nerve injury on rotator cuff muscle fatty degeneration in a rodent animal model. Journal of shoulder and elbow surgery 21:847-858.

5. Gerber C, Meyer D, Schneeberger A, Hoppeler H, Von Rechenberg B. 2004. Effect of tendon release and delayed repair on the structure of the muscles of the rotator cuff: an experimental study in sheep. The Journal of Bone & Joint Surgery 86:1973-1982.

6. Farshad M, Meyer DC, Nuss KM, Gerber C. 2012. A modified rabbit model for rotator cuff tendon tears: functional, histological and radiological characteristics of the supraspinatus muscle. Shoulder & Elbow 4:90-94.

7. Oh JH, Chung SW, Kim SH, Chung JY, Kim JY. 2014. 2013 Neer Award: Effect of the adipose-derived stem cell for the improvement of fatty degeneration and rotator cuff healing in rabbit model. Journal of Shoulder and Elbow Surgery 23:445-455.

8. Rubino LJ, Stills Jr HF, Sprott DC, Crosby LA. 2007. Fatty infiltration of the torn rotator cuff worsens over time in a rabbit model. Arthroscopy: The Journal of Arthroscopic & Related Surgery 23:717-722.

9. Zumstein MA, Jost B, Hempel J, Hodler J, Gerber C. 2008. The clinical and structural long-term results of open repair of massive tears of the rotator cuff. J Bone Joint Surg Am 90:2423-2431.

10. Barton ER, Gimbel JA, Williams GR, Soslowsky LJ. 2005. Rat supraspinatus muscle atrophy after tendon detachment. Journal of orthopaedic research 23:259-265.

11. Soslowsky LJ, Carpenter JE, DeBano CM, Banerji I, Moalli MR. 1996. Development and use of an animal model for investigations on rotator cuff disease. Journal of shoulder and elbow surgery 5:383-392.

12. Safran O, Derwin KA, Powell K, Iannotti JP. 2005. Changes in rotator cuff muscle volume, fat content, and passive mechanics after chronic detachment in a canine model. J Bone Joint Surg Am 87:2662-2670.

13. Gerber C, Meyer DC, Von Rechenberg B, Hoppeler H, Frigg R, Farshad M. 2012. Rotator Cuff Muscles Lose Responsiveness to Anabolic Steroids After Tendon Tear and Musculotendinous Retraction An Experimental Study in Sheep. The American journal of sports medicine 40:2454-2461.

14. Luan T, Liu X, Easley JT, Ravishankar B, Puttlitz C, Feeley BT. 2015. Muscle atrophy and fatty infiltration after an acute rotator cuff repair in a sheep model. Muscles, ligaments and tendons journal 5:106.

15. Beeler S, Ek ET, Gerber C. 2013. A comparative analysis of fatty infiltration and muscle atrophy in patients with chronic rotator cuff tears and suprascapular neuropathy. Journal of Shoulder and Elbow Surgery 22:1537-1546.

16. Gerber C, Meyer DC, Flück M, Valdivieso P, von Rechenberg B, Benn MC, Wieser K. 2016. Muscle Degeneration Associated With Rotator Cuff Tendon Release and/or Denervation in Sheep. The American Journal of Sports Medicine:0363546516677254.

17. Lebaschi A, Deng XH, Zong J, Cong GT, Carballo CB, Album ZM, Camp C, Rodeo SA. 2016. Animal models for rotator cuff repair. Annals of the New York Academy of Sciences.

18. Gerber C, Schneeberger AG, Perren SM, Nyffeler RW. 1999. Experimental Rotator Cuff Repair. A Preliminary Study*. The Journal of Bone & Joint Surgery 81:1281-1290.

19. Steinbacher P, Tauber M, Kogler S, Stoiber W, Resch H, Sänger A. 2010. Effects of rotator cuff ruptures on the cellular and intracellular composition of the human supraspinatus muscle. Tissue and Cell 42:37-41.

20. Goutallier D, Postel J-M, Bernageau J, Lavau L, Voisin M-C. 1994. Fatty muscle degeneration in cuff ruptures: pre-and postoperative evaluation by CT scan. Clinical orthopaedics and related research 304:78-83.

21. Gerber C, Meyer DC, Frey E, von Rechenberg B, Hoppeler H, Frigg R, Jost B, Zumstein MA. 2009. Neer Award 2007: Reversion of structural muscle changes caused by chronic rotator cuff tears using continuous musculotendinous traction. An experimental study in sheep. Journal of Shoulder and Elbow Surgery 18:163-171.

22. Flück M, Ruoss S, Möhl CB, Valdivieso P, Benn MC, von Rechenberg B, Laczko E, Hu J, Wieser K, Meyer DC. 2016. Genomic and lipidomic actions of nandrolone on detached rotator cuff muscle in sheep. The Journal of Steroid Biochemistry and Molecular Biology.

23. Gibbons MC, Singh A, Anakwenze O, Cheng T, Pomerantz M, Schenk S, Engler AJ, Ward SR. 2017. Histological Evidence of Muscle Degeneration in Advanced Human Rotator Cuff Disease. The Journal of Bone & Joint Surgery 99:190-199.

24. Goutallier D, Postel J-M, Gleyze P, Leguilloux P, Van Driessche S. 2003. Influence of cuff muscle fatty degeneration on anatomic and functional outcomes after simple suture of full-thickness tears. Journal of Shoulder and Elbow Surgery 12:550-554.

25. Mendias CL, Roche SM, Harning JA, Davis ME, Lynch EB, Enselman ERS, Jacobson JA, Claflin DR, Calve S, Bedi A. 2015. Reduced muscle fiber force production and disrupted myofibril architecture in patients with chronic rotator cuff tears. Journal of Shoulder and Elbow Surgery 24:111-119.

26. Meyer GA, Gibbons MC, Sato E, Lane JG, Ward SR, Engler AJ. 2015. Epimuscular Fat in the Human Rotator Cuff Is a Novel Beige Depot. Stem cells translational medicine:sctm. 2014-0287.

27. Gibbons MC, Fisch KM, Pichika R, Cheng T, Engler AJ, Schenk S, Lane JG, Singh A, Ward SR. 2018. Heterogeneous muscle gene expression patterns in patients with massive rotator cuff tears. PloS one 13:e0190439.

28. Ruoss S, Möhl CB, Benn MC, von Rechenberg B, Wieser K, Meyer DC, Gerber C, Flück M. Costamere protein expression and tissue composition of rotator cuff muscle after tendon release in sheep. Journal of Orthopaedic Research:n/a-n/a.

29. Minamoto VB, Hulst JB, Lim M, Peace WJ, Bremner SN, Ward SR, Lieber RL. 2007. Increased efficacy and decreased systemic-effects of botulinum toxin A injection after active or passive muscle manipulation. Developmental Medicine & Child Neurology 49:907-914.

30. Dubowitz V, Sewry CA, Oldfors A. 2013. Muscle Biopsy: A Practical Approach, Expert Consult; Online and Print, 4: Muscle Biopsy: A Practical Approach: Elsevier Health Sciences;

31. Ritchie ME, Phipson B, Wu D, Hu Y, Law CW, Shi W, Smyth GK. 2015. limma powers differential expression analyses for RNA-sequencing and microarray studies. Nucleic acids research:gkv007.

32. Goutallier D, Postel JM, Bernageau J, Lavau L, Voisin MC. 1994. Fatty muscle degeneration in cuff ruptures. Pre- and postoperative evaluation by CT scan. Clin Orthop Relat Res:78-83.

33. Meyer DC, Farshad M, Amacker NA, Gerber C, Wieser K. 2012. Quantitative analysis of muscle and tendon retraction in chronic rotator cuff tears. The American journal of sports medicine 40:606-610.

34. Kim SY, Sachdeva R, Li Z, Lee D, Rosser BW. 2015. Change in the pathologic supraspinatus: a three-dimensional model of fiber bundle architecture within anterior and posterior regions. BioMed research international 2015.

35. Thompson SM, Reilly P, Emery RJ, Bull AM. 2011. An anatomical description of the pennation angles and central tendon angle of the supraspinatus both in its normal configuration and with full thickness tears. Journal of shoulder and elbow surgery 20:899-903.

36. Patte D. 1990. Classification of rotator cuff lesions. Clinical orthopaedics and related research 254:81-86.

37. Zanetti M, Gerber C, Hodler J. 1998. Quantitative assessment of the muscles of the rotator cuff with magnetic resonance imaging. Investigative radiology 33:163-170.

38. Fuchs B, Weishaupt D, Zanetti M, Hodler J, Gerber C. 1999. Fatty degeneration of the muscles of the rotator cuff: assessment by computed tomography versus magnetic resonance imaging. Journal of Shoulder and Elbow Surgery 8:599-605.

39. Lippe J, Spang JT, Leger RR, Arciero RA, Mazzocca AD, Shea KP. 2012. Inter-rater agreement of the Goutallier, Patte, and Warner classification scores using preoperative magnetic resonance imaging in patients with rotator cuff tears. Arthroscopy: The Journal of Arthroscopic & Related Surgery 28:154-159.

40. Vidt ME, Santago AC, Tuohy CJ, Poehling GG, Freehill MT, Kraft RA, Marsh AP, Hegedus EJ, Miller ME, Saul KR. 2016. Assessments of fatty infiltration and muscle atrophy from a single magnetic resonance image slice are not predictive of 3-dimensional measurements. Arthroscopy: The Journal of Arthroscopic & Related Surgery 32:128-139.

41. Nozaki T, Tasaki A, Horiuchi S, Ochi J, Starkey J, Hara T, Saida Y, Yoshioka H. 2016. Predicting Retear after Repair of Full-Thickness Rotator Cuff Tear: Two-Point Dixon MR Imaging Quantification of Fatty Muscle Degeneration—Initial Experience with 1-year Follow-up. Radiology 280:500-509.

42. Friden J, Ponten E, Lieber RL. 2000. Effect of muscle tension during tendon transfer on sarcomerogenesis in a rabbit model. The Journal of hand surgery 25:138-143.

43. Ward SR, Hentzen ER, Smallwood LH, Eastlack RK, Burns KA, Fithian DC, Friden J, Lieber RL. 2006. Rotator cuff muscle architecture: implications for glenohumeral stability. Clinical orthopaedics and related research 448:157-163.

44. Gibbons MC, Sato EJ, Bachasson D, Cheng T, Azimi H, Schenk S, Engler AJ, Singh A, Ward SR. 2016. Muscle architectural changes after massive human rotator cuff tear. Journal of Orthopaedic Research.

45. Gerber C, Meyer DC, Flück M, Benn MC, von Rechenberg B, Wieser K. 2015. Anabolic steroids reduce muscle degeneration associated with rotator cuff tendon release in sheep. The American journal of sports medicine 43:2393-2400.

46. Meyer DC, Hoppeler H, von Rechenberg B, Gerber C. 2004. A pathomechanical concept explains muscle loss and fatty muscular changes following surgical tendon release. Journal of orthopaedic research 22:1004-1007.

47. Davies MR, Liu X, Lee L, Laron D, Ning AY, Kim HT, Feeley BT. 2016. TGF-β Small Molecule Inhibitor SB431542 Reduces Rotator Cuff Muscle Fibrosis and Fatty Infiltration By Promoting Fibro/Adipogenic Progenitor Apoptosis. PloS one 11:e0155486.

48. Dubey J, Speer C, Callis G, Blixt J. 1982. Development of the sheep–canid cycle of Sarcocystis tenella. Canadian Journal of Zoology 60:2464-2477.

Chapter 8. Transcriptional Profile of Supraspinatus Muscle in a Rabbit Model of Rotator Cuff Tear over Time – Implications for Degenerative Mechanisms and Therapeutic Approaches

Abstract

Understanding the transcriptional profile that defines the response of rotator cuff muscles to acute and chronic tear is fundamental to developing therapeutic strategies to muscle loss and restore function in patients with rotator cuff disease. Here, we employed next-generation sequencing and gene set enrichment analysis to characterize changes in the transcriptional profile of supraspinatus muscles in a clinically relevant rabbit model of rotator cuff tear over time. Gene set enrichment in down-regulated genes showed a persistent diminution of anabolic and mitochondrial/metabolic gene expression across acute and chronic time points, while ubiquitin-proteasome related genes were down-regulated only at the most chronic 16 week time point. Inflammatory genes were up-regulated across the time course, though the inflammatory signature early did not include the chronic or phagocytic processes that were up-regulated at later time points. Along the same lines, processes related to cell damage, and membrane damage in particular, were enriched for at the 16 week time point relative to both contralateral sham and the 4 week time point, suggesting a progressive onset of muscle fiber degeneration consistent with the histological results previously reported in these muscles. Given these findings, it is clear that understanding the molecular disease state of a given patient is critical to selecting the correct therapeutic course for that patient, as some interventions (i.e. exercise) may in fact accelerate muscle damage in the most chronic stages of disease where muscle degeneration, and not atrophy, appears to drive progressive functional losses.

Introduction

Rotator cuff tear (RCT) affects one in five people in the general population, with age, obesity, and metabolic disease all increasing risk[1]. While the primary injury occurs in the tendon, detrimental muscular changes and accumulation of fat within the scapular fossae are closely associated with surgical

and functional outcomes after tendon repair[2]. Recent evidence suggests that in chronic human tears, muscle cell death via accumulated damage of muscle fiber membranes and disorganization of myofibrils is a primary cause of irreversible muscle loss and functional deficits, as these clinical features are poorly explained by atrophic muscle loss alone[3]. However, studying the time course and molecular mechanisms of muscle degeneration in human biopsies is difficult; tear initiation and progression in humans takes place over months or years[4] and the demographics and comorbidities of the patient population are highly variable. Thus, an animal model is required that develops the same degenerative phenotype in response to tendon tear as is found clinically.

Several studies have developed and utilized variations of massive RCT in the rabbit[5-7]. At the whole muscle level, these models demonstrated fat accumulation and diminished muscle volume consistent with massive human tears[5-7]. Based on this clinical similarity, the rabbit was also a prime candidate as a model for cell-level degenerative features, though these had not previously been explored explicitly. In parallel with the current study, we demonstrated that the rabbit exhibits both atrophic and degenerative muscle loss similar to that found clinically. Specifically, we found that the posterolateral aspect (i.e. posterior distal region) of the supraspinatus demonstrated the most severe degenerative phenotype following tenotomy.

Therefore, the goal of this study was to use transcriptome-level analysis of the posterior distal region of tenotomized supraspinatus muscles to define the biological processes that underlie the pathological changes that occur over time in response to rotator cuff tear. In so doing, we expected to define the molecular pathways that govern early- and late-stage RC disease, and in particular the biological processes that govern muscle degeneration in chronic tears. If a distinct transcriptional signature can be defined for atrophic versus degenerative stages of disease, or for the transition from primarily atrophic to primarily degenerative muscle loss, such data could be applied to patients in the future to provide better stratification and tailored treatment plans based on individual biological stages of disease.

Methods

Twenty-four New Zealand White rabbits were randomly assigned to 2, 4, 8, or 16 week time points. Under approval of the appropriate institutional animal care and use committee, each animal underwent tenotomy of the supraspinatus tendon using an anterolateral, deltoid splitting approach. After blunt dissection of the surrounding soft tissue to allow for muscle retraction, a penrose drain was sutured to the tendon using 2/0 silk to prevent scar formation and reloading of the muscle. Animals were sacrificed at the prescribed time points via intravenous pentobarbital injection. A section of muscle from the postero-lateral region (~70mg) was then placed in All-Protect (Qiagen) for 24 hours at room temperature, after which it was stored at -80^{o}C prior to RNA isolation.

Tissue was homogenized in Buffer RLT (Qiagen RNeasy Fibrous Tissue Mini Kit) for 10 minutes using a 5mm bead shaken at 30 strokes/second on a TissueLyser II bead beater. RNA isolation was then completed using the RNeasy Fibrous Tissue Mini Kit in combination with a QIAcube robot according to the manufacturer's instructions. RNA concentration was determined using a QIAxpert spectrophotometer, and RNA was stored at -80^{o}C prior to library preparation.

RNA sequencing libraries were generated from 1 ug of total RNA using Illumina's TruSeq Stranded mRNA Sample Prep Kit following manufacturer's instructions, modifying the shear time to 5 minutes. RNA libraries were multiplexed and sequenced with 75 basepair (bp) single reads (SR75) to a depth of approximately 20 million reads per sample on an Illumina HiSeq4000. Quality control of the raw fastq files was performed using the software tool FastQC (Babraham Institute, Bioinformatics Group), and sequencing reads were aligned to the rabbit genome (Ensembl OryCun2.0) using the STAR v2.5.1a aligner[8].

Read quantification was performed with RSEM3 v1.3.0 and Ensembl annotation (Oryctolagus_cuniculus.OryCun2.0.91.gtf). Lowly expressed genes were filtered out (cpm > 1 in at least one sample) and trimmed mean of M-values (TMM)[9] normalization was applied. The R BioConductor packages edgeR[10] and limma[11] were used to implement the limma-voom method[12] for differential

expression analysis. The experimental design was modeled upon time point and treatment (~0 + time_treatment), which included an intra-animal correlation coefficient. Significance was defined by using an adjusted p-value cut-off of 0.05 after multiple testing correction using a moderated t-statistic in limma.

Gene ontology enrichment analysis for biological processes was performed on significantly up- and down-regulated (adjusted $p < 0.05$, log2(fold-change) > 0.5) gene sets for each comparison of interest (Table 1) using PANTHER[13-15]. Due to poor existing annotations of the rabbit genome, human analogs were used for ontology analysis. Enrichment was tested against all human genes in the PANTHER database using Fisher's Exact test with False Discovery Rate multiple test correction (FDR < 0.05).

Results

A total of 12,886 genes were expressed at significant levels in this study. Using overall counts of differentially expressed genes as a measure of total transcriptional activity, we found that 60% of differentially expressed genes at 2 weeks were down-regulated, indicative of a general trend toward transcriptional repression at this time point. In contrast, later time points did not show any strong trends in this metric, suggesting that global transcriptional repression is a transient response to tenotomy. Evaluating the same metric between sham-normalized time points, which provides insight into how the transcriptional programs change from time point to time point, highlighted a large alteration in expression profile from 4 to 16 weeks. The differentially expressed genes between these time points are likely involved in the transition from acute/sub-chronic disease mechanisms to chronic and irreversible mechanisms of muscle loss, as detailed below.

At two weeks, ontologies associated with acute inflammation, cellular stress and survival, inhibition of muscle growth, positive regulation of muscle stem cell differentiation, and activation of platelet-derived growth factor (PDGF) responsive cells (i.e. pericytes and smooth muscle cells) were enriched for among up-regulated genes, while the majority of enrichment in down-regulated genes was

found in metabolic genes, particularly those involved in ATP production, oxidative phosphorylation, transcription, and protein synthesis.

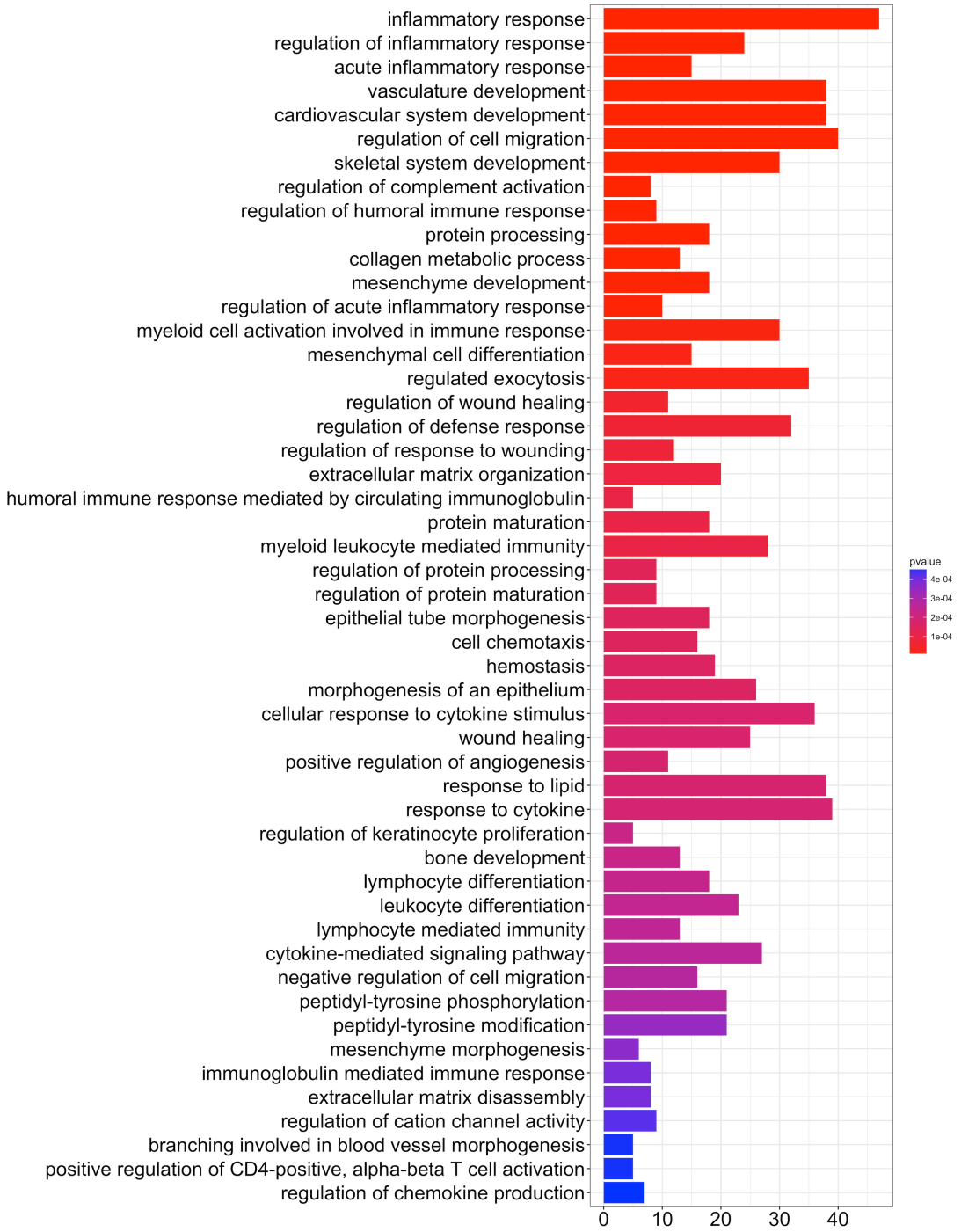

Figure 8.1 Top 50 biological processes up-regulated after 2 weeks of tenotomy, ranked by p-value. For specificity, the top four GO levels were dropped.

Figure 8.2 Top 50 down-regulated biological processes after 2 weeks of tenotomy, ranked by p-value. For specificity, the top four GO levels were dropped.

Four weeks after tenotomy, enrichment analysis indicated increased lipid and cholesterol storage and metabolism, and inhibition of muscle hypertrophy/contractile machinery synthesis, with only limited

enrichment for inflammatory processes (TNF-related signaling). At 8 weeks, when the number of differentially expressed genes was lowest, there was significant enrichment for genes involved in the negative regulation of programmed cell death (including apoptosis), TNFα production, and metabolic processes. At both 4 and 8 weeks, the number of genes with each annotation was small (<15).

Week 16 demonstrated the greatest deviations of tenotomized muscles from sham. Genes associated with transcription and energy generation, particularly those involved in mitochondrial respiration, were significantly enriched among down-regulated genes, as were genes involved in ubiquitin-proteasome protein catabolism, macroautophagy, and muscle cell development and differentiation.

Figure 8.3 Top 50 down-regulated biological processes after 16 weeks of tenotomy, ranked by p-value. For specificity, the top four GO levels were dropped.

Several ontologies with implications for chronic disease mechanisms were enriched among up-regulated genes at 16 weeks. Chronic inflammation, leukocyte regulation (migration, maturation, and

apoptosis), lymphocyte activation (proliferation and differentiation), and response to stress (osmotic and reactive oxygen species) were all enriched, indicative of a stressful, chronic inflammatory milieu not found at earlier time points. Similarly, genes associated with membrane-damaging elements of the complement system (i.e. the membrane-attack complex) were increased at 16 weeks. Membrane damage is further indicated by three findings: enrichment for production of membrane phospholipid (i.e. sphyngolipid) synthesis, enrichment for proteoglycan catabolic processes, and diminished intracellular calcium sequestration and increased calcium import, as intracellular calcium is a critical mediator of membrane repair[16] (though it should also be noted that increased cytosolic calcium also controls calpain-mediated proteolysis and cell death[17; 18]). Consistent with the transcriptional and histological signature of muscle membrane damage and cell death was enrichment for phagocytosis- and lysosome-related genes at this time point. However, both pro- and anti-apoptotic genes were enriched at 16 weeks, which together with increased NF-kB signaling[19] and the processes described above suggests competition between pathways of cell survival[20], apoptosis[17; 21; 22], and necrosis[23; 24]. Furthermore, genes related to cytoskeletal organization (with the most enrichment in inhibitors of reorganization) were up-regulated, suggesting impaired or sub-optimal cytoskeletal remodeling (and thereby impaired function[25]) within remaining muscle fibers. Finally, ontologies associated with accumulation of fat and fibrosis (i.e. fibroblast proliferation, extracellular matrix remodeling, and lipid storage) were enriched at 16 weeks, commensurate with the chronic expansion of these non-muscle tissues found histologically.

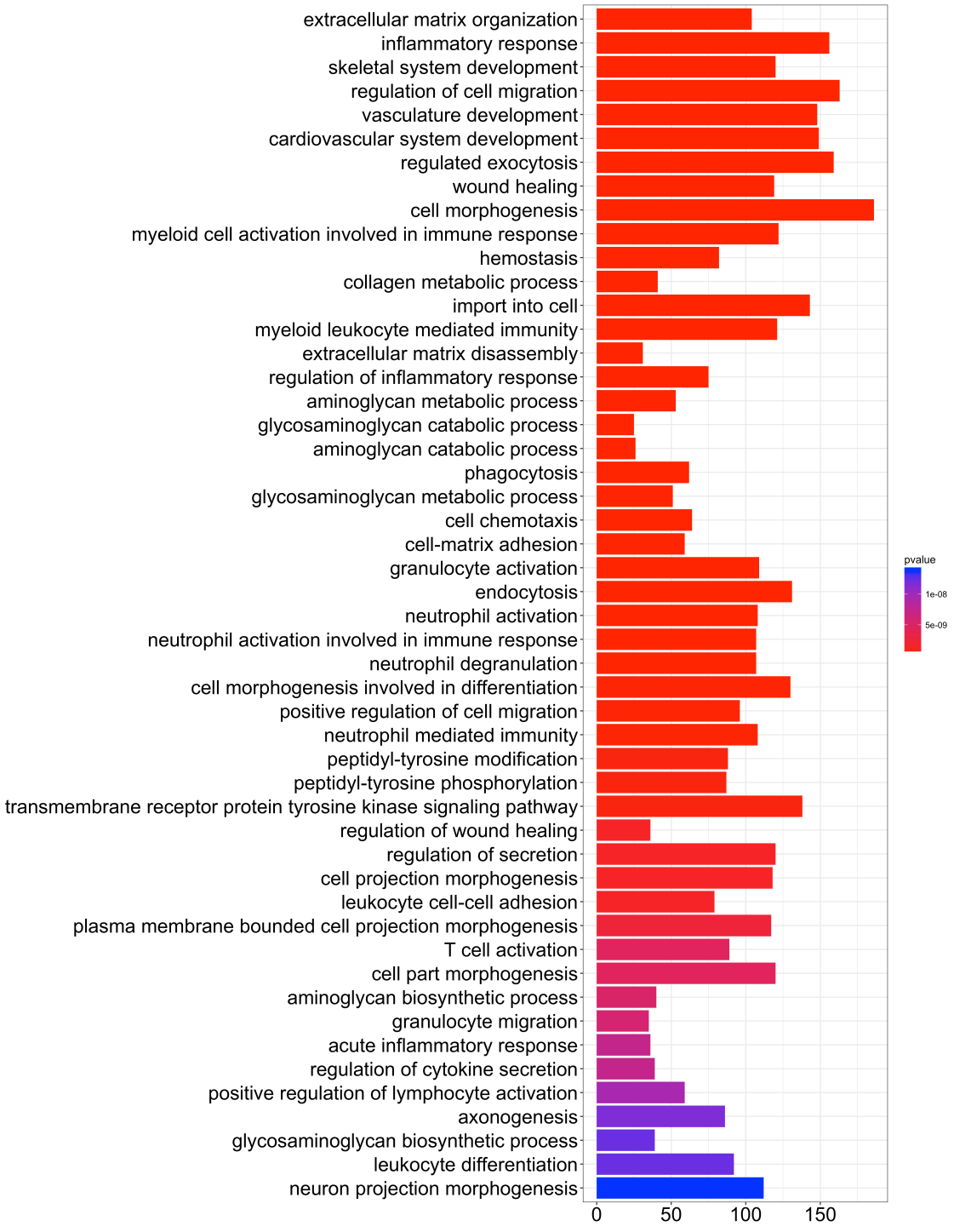

Figure 8.4 Top 50 up-regulated biological processes after 16 weeks of tenotomy, ranked by p-value. For specificity, the top four GO levels were dropped.

To provide insight into the processes that change over time, sham-normalized expression values were compared between time points (Table 1). No genes were differentially expressed between adjacent time points, suggesting that changes in expression occur gradually. While a small number of genes were differentially expressed between 2 and 16 weeks, there was no enrichment for any individual ontology. Between 4 and 16 weeks however, several ontologies were enriched within differentially regulated genes. Enrichment among up-regulated genes showed that the increased inflammation, stress signaling (though not stressors directly), calcium transport, and altered/impaired cytoskeletal organization found at 16 weeks are amplified not only relative to sham, but also relative to the sub-chronic 4-week time point as well. Similarly, enrichment analysis suggested the decrease in ubiquitin-proteasome protein catabolism and diminished protein synthesis observed at 16 weeks relative to sham was progressive, as these ontologies decreased relative to the sub-chronic 4 week time point as well.

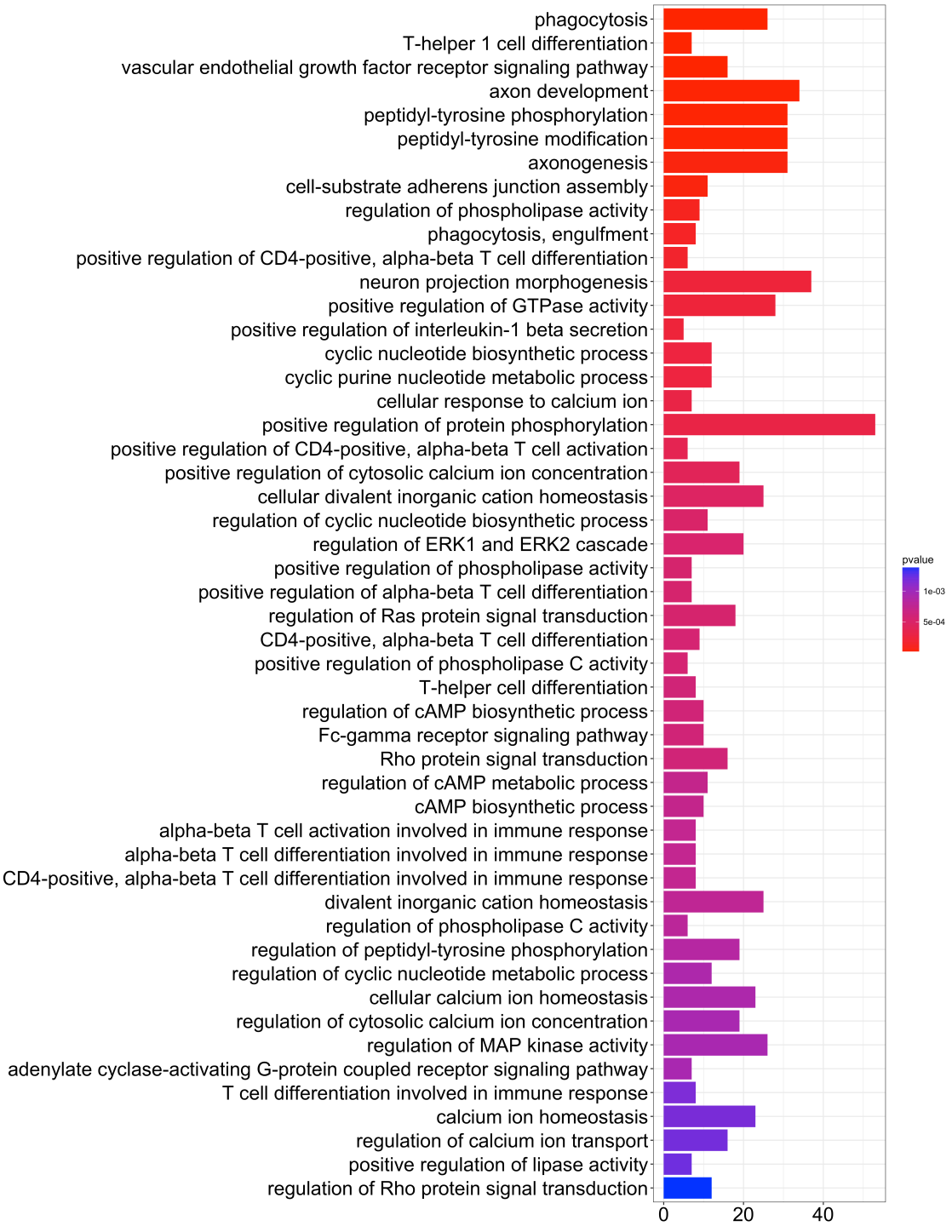

Figure 8.5 Top 50 enriched biological processes among genes up-regulated at 16 weeks relative to 4 weeks after tenotomy, with sham normalization at each time point. Processes ranked by p-value.

Discussion

Muscle fiber atrophy and degeneration each contribute to diminished muscle volume in chronic RC tears[3; 26]. However, the time course over which each of these mechanisms act, and the transcriptional profiles that define the distinct stages of disease, are not well-defined. Here, we employed a validated rabbit model of RCT that displays a phenotype of muscle atrophy and degeneration similar to human disease in order to describe the transcriptional changes associated with the acute and chronic phases of tenotomy-induced muscle loss, summarized in Figure 6.

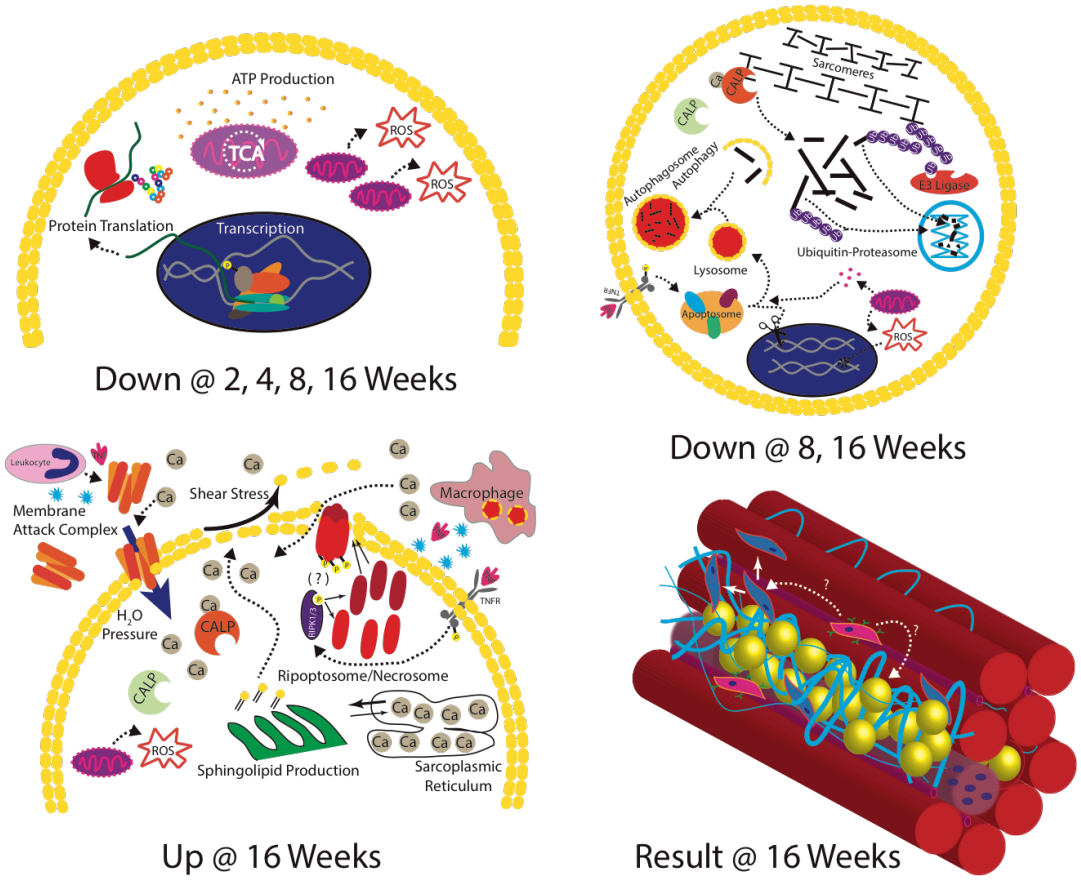

Figure 8.6 Summary of differentially regulated pathways in acute and chronic rabbit RCT. Genes involved in energy generation and protein synthesis (top left) were down-regulated across all time points, while genes involved in protein catabolism were down-regulated in chronic tear (top right). Instead of classical atrophy, the transcriptional profile indicated increased cell stress and membrane damage (bottom left) at chronic time points, supporting the hypothesis that cell-extrinsic degenerative mechanisms drive muscle fiber loss and the associated fatty and fibrotic processes that define chronic tear (bottom right).

At the early 2-week time point, the expression signature indicated a pro-inflammatory, anti-anabolic response. Enrichment for increased inflammatory gene expression (especially acute inflammation and wound response ontologies) was consistent with the induction of injury, while the significant enrichment among down-regulated genes for ontologies related to synthesis of RNA and ATP suggested deficiencies in protein and energy generation, respectively. Despite significant atrophy at the muscle fiber level, no enrichment for proteolytic genes[27] (i.e. ubiquitin-proteasome or autophagosome) was found in the up-regulated gene set, though this does not rule out the participation of these pathways before 2 weeks. Finally, the enrichment for positive regulators of muscle stem cell differentiation[28] was consistent with the small increase in centralized nuclei at 2 weeks, suggesting that at least in the acute phase the muscle generates a regenerative response to injury.

The number of differentially-regulated genes at four and eight weeks was lower than either 2 or 16 weeks, which may be interpreted as a coordinated regression toward muscle homeostasis following resolution of the initial injury/unloading response that precedes the development of chronic disease features. However, the enrichment of genes associated with growth arrest and cell survival at these intermediate times suggests that pressure toward muscle cell death was still present, particularly at the 8-week time point where few other ontologies were enriched. It should also be noted that one animal from the 8-week group was dropped due to sequencing data quality issues, which likely contributed to the reduction in statistically significant differences detected.

After sixteen weeks of tenotomy the transcriptional profile departs strikingly from sham. The increase in chronic inflammation and cellular stress combined with the increase in genes related to membrane damage and repair (i.e. sphingolipid production[29], calcium transport/release[16; 17; 30; 31]) and basement membrane degradation (i.e. proteoglycan catabolism and synthesis[32; 33]) indicate an environment conducive to muscle fiber death and satellite cell inhibition, as both abnormal inflammation and loss of basal lamina integrity are known inhibitors of normal satellite cell function[34-37]. Despite the accumulated damage that is apparent histologically and at the transcriptional level, there does not appear to be any enrichment for either an anabolic or regenerative response. Instead, genes related to energy and protein

synthesis generally, and cytoskeletal organization and contractile apparatus (i.e. sarcomere structure and function) specifically, are *down*-regulated at 16 weeks.

While the down-regulation of proteolytic pathway transcripts may be interpreted as an inhibition of atrophy, the apparent environment of cellular and oxidative stress would more likely necessitate an increase, not a decrease, in these cell-autonomous mechanisms of protein hygiene[38-40]. This is particularly relevant given the indicated increase in intracellular calcium, which likely leads to increased calpain-mediated proteolysis[41; 42] (a known mediator of muscle degradation in rotator cuff muscles[43]), where insufficient catabolism of damaged or cleaved proteins through the ubiquitin-proteasome and autophagosome could lead to protein aggregates that in turn could impair contractile function and ultimately accelerate the onset of cell death[44]. Thus, it appears that decreased skeletal muscle synthesis and exogenous protein damage and degradation, rather than increased protein degradation via classical atrophy mechanisms (which appear to be inhibited at this time point), is responsible for progressive loss of muscle volume in this system.

This data does appear to rule out cell-intrinsic, atrophic mechanisms of muscle loss in chronic tear. However, the remaining evidence does not clearly indicate a single degenerative mechanism, likely because degeneration is a combination of several parallel injurious processes. Based on terms enriched for here, the loss of muscle membrane and basal lamina integrity may be the result of increased complement-mediated membrane attack[24], degranulation product-induced or oxidative damage, ripoptosome or necrosome-mediated pore formation[23] (though the rabbit does not currently have annotations for several constituents of the necroptosome as they exist in humans and smaller rodents), or simple overload in tension or shear caused by mechanical mismatches with the matrix or disorganization of the contractile apparatus that leads to mechanical disruption of the sarcolemma[45]. Increased expression of both innate and adaptive immune cell-related genes and pro-inflammatory cytokines in chronic tear suggests that these degenerative mechanisms are at least partially driven by increased inflammation, but whether the initiation of muscle fiber damage is caused by inflammatory cells or inflammatory cells are recruited after some inflammation-independent muscle cell damage or death remains unknown.

The implications of these findings for therapeutic strategies are potentially wide-ranging, particularly as they relate to repair and rehabilitation strategies. In otherwise healthy muscle, high-intensity and eccentric exercise (and lower intensity, concentric exercise to a lesser degree[46]) is known to stimulate mitochondrial biogenesis and contractile protein synthesis[47-53], which may improve the apparent deficits in energy and force generation capacity in torn RC muscles. However, these exercise's effects on inflammation and short-term structural integrity of muscle may be detrimental in chronically torn RC. Though the long-term affects of exercise are considered anti-inflammatory and anabolic in muscle and non-muscle tissues[54; 55], the immediate effect of exercise in muscle is a pro-inflammatory response that increases monocyte/macrophage activation combined with disruption of native muscle architecture (Z-disc streaming, myofilament disorganization, sarcolemmal disruption)[46-48; 56]. At the same time, clinical data suggests that mechanical loading/reloading either from pre-op rehabilitation[57] or surgical tendon repair[58] is effective in only a subset of patients, and even then success is based primarily on pain relief and maintenance of muscle quality rather than reversal of pathologic muscle changes. The data presented here may offer an explanation for failure of rehabilitation – in early- and mid-stage disease, muscle damage (degeneration) may be limited and muscle loss may be driven primarily by metabolic deficits and reductions in contractile protein synthesis, while in late-stage disease muscle fiber damage, likely caused or exacerbated by chronic inflammatory processes, may serve as the primary cause of muscle loss. Under this hypothesis, we would expect muscle in the former group to be competent to withstand the acute physical and biochemical stress of exercise, while these same effects may further damage muscle in the latter group, which already has an impaired ability to reorganize and regenerate in the face of injury.

There are several limitations inherent to the analytical strategy employed here. While whole-transcriptome analyses are powerful for describing general trends, generating data to support mechanistic hypothesis, and identifying or ruling out broad pathways, such analyses alone cannot definitively characterize specific degenerative mechanisms. In this case, there is the further limitation of the gene- and ontology-level annotations available for the rabbit genome; between rabbit genes that do not map to human genes and genes without annotations generally, 30.7% (3957/12886) of all genes expressed in this

study were not adequately annotated for inclusion in downstream analysis. The dropout rate was similar for each list of significantly differentially expressed genes. These limitations are in addition to the limitations of gene set enrichment generally, which include inconsistent annotations and insensitivity to expression magnitudes, among other shortcomings.

Here, our analysis is further complicated by the relatively small number of muscle fibers that are actively degenerating at the time of muscle harvest. As such, whole-muscle transcriptomics may not be sensitive enough to detect the full molecular signature of active degeneration, as the pool of RNA from degenerating fibers is small relative to RNA from non-degenerating fibers. Similarly, changes in cell composition may affect the transcriptional profile[59] – for example, fat and fibrosis were increased histologically at 16 weeks, as was the expression of genes related to adipocyte differentiation, lipid storage, and ECM deposition. The extent to which expression changes were dependent on changes in the cell pool composition versus changes in per-cell transcription cannot be answered using a whole-muscle homogenate approach, but should be explored in future studies using techniques that allow profiling of individual cells and cell populations.

Conclusion

Chronic and irreversible muscle loss following RCT is a key determinant of patient outcomes. However, exploration of the transcriptional signature of muscle degeneration has been limited by inadequate models and complications inherent to expression profiling of patient biopsies. Using a validated rabbit model of RCT, we show that metabolic and anabolic deficiencies underlie both acute and chronic disease processes, while expression indicative of unresolved inflammation, membrane and cytoplasmic disruption, and fat and fibrotic processes define the chronic, degenerative response to tenotomy. Based on these data, the conventional approaches to exercise and muscle reloading in patients with the largest, most chronic tears should be carefully considered, as exercise may exacerbate the negative processes apparent in chronic disease. Thus, future work should focus on two goals: one, appropriately characterizing the disease state of patients prior to reloading protocols and determining the

patients for whom mechanical reloading (including repair) will be most beneficial, and two, developing therapeutic approaches (potentially including alternative exercise protocols) that will maximize hypertrophic and regenerative processes while minimizing the potentially detrimental effects of reloading as they relate to increased muscle damage and inflammation.

Acknowledgements

RNA sequencing was conducted at the IGM Genomics Center, University of California, San Diego, La Jolla, CA. Data analysis was carried out in part by the Center for Computational Biology & Bioinformatics, Department of Medicine, University of California, San Diego, La Jolla, CA, USA. This projected was funded in part by an Orthopedic Research Education Foundation Resident Research Project Grant (MVV) and by the National Institutes of Health (UL1TR001442 of CTSA).

This chapter, in part, is currently being prepared for submission for publication of the material. Michael C. Gibbons, Mario Vargas-Vila, Kathleen M. Fisch, Anshu Singh, Samuel R. Ward. The dissertation/thesis author was a primary investigator of this material.

References

1. Yamamoto A, Takagishi K, Osawa T, Yanagawa T, Nakajima D, Shitara H, Kobayashi T. 2010. Prevalence and risk factors of a rotator cuff tear in the general population. Journal of Shoulder and Elbow Surgery 19:116-120.

2. Gladstone JN, Bishop JY, Lo IK, Flatow EL. 2007. Fatty infiltration and atrophy of the rotator cuff do not improve after rotator cuff repair and correlate with poor functional outcome. The American journal of sports medicine 35:719-728.

3. Gibbons MC, Singh A, Anakwenze O, Cheng T, Pomerantz M, Schenk S, Engler AJ, Ward SR. 2017. Histological Evidence of Muscle Degeneration in Advanced Human Rotator Cuff Disease. The Journal of Bone & Joint Surgery 99:190-199.

4. Hebert-Davies J, Teefey SA, Steger-May K, Chamberlain AM, Middleton W, Robinson K, Yamaguchi K, Keener JD. 2017. Progression of Fatty Muscle Degeneration in Atraumatic Rotator Cuff Tears. JBJS 99:832-839.

5. Fabis J, Kordek P, Bogucki A, Synder M, Kolczynska H. 1998. Function of the rabbit supraspinatus muscle after detachment of its tendon from the greater tubercle: Observations up to 6 months. Acta orthopaedica Scandinavica 69:570-574.

6. Farshad M, Meyer DC, Nuss KM, Gerber C. 2012. A modified rabbit model for rotator cuff tendon tears: functional, histological and radiological characteristics of the supraspinatus muscle. Shoulder & Elbow 4:90-94.

7. Rubino LJ, Stills Jr HF, Sprott DC, Crosby LA. 2007. Fatty infiltration of the torn rotator cuff worsens over time in a rabbit model. Arthroscopy: The Journal of Arthroscopic & Related Surgery 23:717-722.

8. Dobin A, Davis CA, Schlesinger F, Drenkow J, Zaleski C, Jha S, Batut P, Chaisson M, Gingeras TR. 2013. STAR: ultrafast universal RNA-seq aligner. Bioinformatics 29:15-21.

9. Robinson MD, Oshlack A. 2010. A scaling normalization method for differential expression analysis of RNA-seq data. Genome biology 11:1.

10. Robinson MD, McCarthy DJ, Smyth GK. 2010. edgeR: a Bioconductor package for differential expression analysis of digital gene expression data. Bioinformatics 26:139-140.

11. Ritchie ME, Phipson B, Wu D, Hu Y, Law CW, Shi W, Smyth GK. 2015. limma powers differential expression analyses for RNA-sequencing and microarray studies. Nucleic acids research:gkv007.

12. Law CW, Chen Y, Shi W, Smyth GK. 2014. voom: Precision weights unlock linear model analysis tools for RNA-seq read counts. Genome biology 15:R29.

13. Ashburner M, Ball CA, Blake JA, Botstein D, Butler H, Cherry JM, Davis AP, Dolinski K, Dwight SS, Eppig JT. 2000. Gene Ontology: tool for the unification of biology. Nature genetics 25:25.

14. Consortium GO. 2016. Expansion of the Gene Ontology knowledgebase and resources. Nucleic acids research 45:D331-D338.

15. Mi H, Huang X, Muruganujan A, Tang H, Mills C, Kang D, Thomas PD. 2016. PANTHER version 11: expanded annotation data from Gene Ontology and Reactome pathways, and data analysis tool enhancements. Nucleic acids research 45:D183-D189.

16. Cheng X, Zhang X, Yu L, Xu H. 2015. Calcium signaling in membrane repair. Seminars in cell & developmental biology: Elsevier; pp. 24-31.

17. Orrenius S, Zhivotovsky B, Nicotera P. 2003. Regulation of cell death: the calcium–apoptosis link. Nature reviews Molecular cell biology 4:552-565.

18. Squier MK, Miller AC, Malkinson AM, Cohen JJ. 1994. Calpain activation in apoptosis. Journal of cellular physiology 159:229-237.

19. Piva R, Belardo G, Santoro MG. 2006. NF-κB: a stress-regulated switch for cell survival. Antioxidants & redox signaling 8:478-486.

20. Beg AA, Baltimore D. 1996. An essential role for NF-κB in preventing TNF-α-induced cell death. Science 274:782-784.

21. Elmore S. 2007. Apoptosis: a review of programmed cell death. Toxicologic pathology 35:495-516.

22. Kerr JF, Wyllie AH, Currie AR. 1972. Apoptosis: a basic biological phenomenon with wideranging implications in tissue kinetics. British journal of cancer 26:239.

23. Berghe TV, Linkermann A, Jouan-Lanhouet S, Walczak H, Vandenabeele P. 2014. Regulated necrosis: the expanding network of non-apoptotic cell death pathways. Nature reviews Molecular cell biology 15:135.

24. Engel AG, Biesecker G. 1982. Complement activation in muscle fiber necrosis: demonstration of the membrane attack complex of complement in necrotic fibers. Annals of neurology 12:289-296.

25. Mendias CL, Roche SM, Harning JA, Davis ME, Lynch EB, Enselman ERS, Jacobson JA, Claflin DR, Calve S, Bedi A. 2015. Reduced muscle fiber force production and disrupted myofibril architecture in patients with chronic rotator cuff tears. Journal of Shoulder and Elbow Surgery 24:111-119.

26. Steinbacher P, Tauber M, Kogler S, Stoiber W, Resch H, Sänger A. 2010. Effects of rotator cuff ruptures on the cellular and intracellular composition of the human supraspinatus muscle. Tissue and Cell 42:37-41.

27. Bonaldo P, Sandri M. 2013. Cellular and molecular mechanisms of muscle atrophy. Disease models & mechanisms 6:25-39.

28. Yin H, Price F, Rudnicki MA. 2013. Satellite cells and the muscle stem cell niche. Physiological reviews 93:23-67.

29. Lokar M, Kabaso D, Resnik N, Sepčić K, Kralj-Iglič V, Veranič P, Zorec R, Iglič A. 2012. The role of cholesterol-sphingomyelin membrane nanodomains in the stability of intercellular membrane nanotubes. International journal of nanomedicine 7:1891.

30. Alderton JM, Steinhardt RA. 2000. Calcium influx through calcium leak channels is responsible for the elevated levels of calcium-dependent proteolysis in dystrophic myotubes. Journal of Biological Chemistry 275:9452-9460.

31. Turner PR, Westwood T, Regen CM, Steinhardt RA. 1988. Increased protein degradation results from elevated free calcium levels found in muscle from mdx mice. Nature 335:735-738.

32. Heydemann A, McNally EM. 2007. Consequences of disrupting the dystrophin-sarcoglycan complex in cardiac and skeletal myopathy. Trends in cardiovascular medicine 17:55-59.

33. Iozzo RV. 2005. Basement membrane proteoglycans: from cellar to ceiling. Nature reviews Molecular cell biology 6:646.

34. Bentzinger CF, Wang YX, Dumont NA, Rudnicki MA. 2013. Cellular dynamics in the muscle satellite cell niche. EMBO reports 14:1062-1072.

35. Boldrin L, Neal A, Zammit PS, Muntoni F, Morgan JE. 2012. Donor Satellite Cell Engraftment Is SignificantlyAugmented When the Host Niche Is Preserved and Endogenous Satellite Cells Are Incapacitated. Stem Cells 30:1971-1984.

36. Boonen KJ, Rosaria-Chak KY, Baaijens FP, van der Schaft DW, Post MJ. 2009. Essential environmental cues from the satellite cell niche: optimizing proliferation and differentiation. American Journal of Physiology-Cell Physiology 296:C1338-C1345.

37. Dhawan J, Rando TA. 2005. Stem cells in postnatal myogenesis: molecular mechanisms of satellite cell quiescence, activation and replenishment. Trends in cell biology 15:666-673.

38. Ding W-X, Ni H-M, Gao W, Yoshimori T, Stolz DB, Ron D, Yin X-M. 2007. Linking of autophagy to ubiquitin-proteasome system is important for the regulation of endoplasmic reticulum stress and cell viability. The American journal of pathology 171:513-524.

39. Shang F, Taylor A. 2011. Ubiquitin–proteasome pathway and cellular responses to oxidative stress. Free Radical Biology and Medicine 51:5-16.

40. Glickman MH, Ciechanover A. 2002. The ubiquitin-proteasome proteolytic pathway: destruction for the sake of construction. Physiological reviews 82:373-428.

41. Bartoli M, Richard I. 2005. Calpains in muscle wasting. The international journal of biochemistry & cell biology 37:2115-2133.

42. Huang J, Forsberg NE. 1998. Role of calpain in skeletal-muscle protein degradation. Proceedings of the national academy of sciences 95:12100-12105.

43. Ruoss S, Möhl CB, Benn MC, von Rechenberg B, Wieser K, Meyer DC, Gerber C, Flück M. Costamere protein expression and tissue composition of rotator cuff muscle after tendon release in sheep. Journal of Orthopaedic Research:n/a-n/a.

44. Maisonneuve E, Ezraty B, Dukan S. 2008. Protein aggregates: an aging factor involved in cell death. Journal of bacteriology 190:6070-6075.

45. Gibbons MC, Singh A, Engler AJ, Ward SR. 2017. The Role of Mechanobiology in Progression of Rotator Cuff Muscle Atrophy and Degeneration. Journal of Orthopaedic Research.

46. Willoughby DS, VanEnk C, Taylor L. 2003. EFFECTS OF CONCENTRIC AND ECCENTRIC CONTRACTIONS ON EXERCISEINDUCED MUSCLE INJURY, INFLAMMATION, AND SERUM IL-6. Journal of Exercise Physiology online 6.

47. Buford TW, MacNeil RG, Clough LG, Dirain M, Sandesara B, Pahor M, Manini TM, Leeuwenburgh C. 2014. Active muscle regeneration following eccentric contraction-induced injury is similar between healthy young and older adults. Journal of Applied Physiology 116:1481-1490.

48. Friden J, Lieber R. 2001. Eccentric exercise-induced injuries to contractile and cytoskeletal muscle fibre components. Acta Physiologica Scandinavica 171:321-326.

49. Darr KC, Schultz E. 1987. Exercise-induced satellite cell activation in growing and mature skeletal muscle. Journal of Applied Physiology 63:1816-1821.

50. Jones SW, Hill RJ, Krasney PA, O'CONNER B, Peirce N, Greenhaff PL. 2004. Disuse atrophy and exercise rehabilitation in humans profoundly affects the expression of genes associated with the regulation of skeletal muscle mass. The FASEB journal 18:1025-1027.

51. Raue U, Slivka D, Jemiolo B, Hollon C, Trappe S. 2006. Myogenic gene expression at rest and after a bout of resistance exercise in young (18–30 yr) and old (80–89 yr) women. Journal of Applied Physiology 101:53-59.

52. Schoenfeld BJ. 2012. Does exercise-induced muscle damage play a role in skeletal muscle hypertrophy? The Journal of Strength & Conditioning Research 26:1441-1453.

53. Safdar A, Little JP, Stokl AJ, Hettinga BP, Akhtar M, Tarnopolsky MA. 2011. Exercise increases mitochondrial PGC-1α content and promotes nuclear-mitochondrial cross-talk to coordinate mitochondrial biogenesis. Journal of Biological Chemistry 286:10605-10617.

54. Gielen S, Adams V, Möbius-Winkler S, Linke A, Erbs S, Yu J, Kempf W, Schubert A, Schuler G, Hambrecht R. 2003. Anti-inflammatory effects of exercise training in the skeletal muscle of patients with chronic heart failure. Journal of the American College of Cardiology 42:861-868.

55. Petersen AMW, Pedersen BK. 2005. The anti-inflammatory effect of exercise. Journal of applied physiology 98:1154-1162.

56. Sorichter S, Puschendorf B, Mair J. 1998. Skeletal muscle injury induced by eccentric muscle action: muscle proteins as markers of muscle fiber injury. Exercise immunology review 5:5-21.

57. Millett PJ, Wilcox III RB, O'holleran JD, Warner JJ. 2006. Rehabilitation of the rotator cuff: an evaluation-based approach. JAAOS-Journal of the American Academy of Orthopaedic Surgeons 14:599-609.

58. Gerber C, Fuchs B, Hodler J. 2000. The Results of Repair of Massive Tears of the Rotator Cuff*†. The Journal of Bone & Joint Surgery 82:505-505.

59. Gibbons MC, Fisch KM, Pichika R, Cheng T, Engler AJ, Schenk S, Lane JG, Singh A, Ward SR. 2018. Heterogeneous muscle gene expression patterns in patients with massive rotator cuff tears. PloS one 13:e0190439.

Chapter 9. Cellular Constituents and Potential Mechanisms of Muscle Degeneration in Chronic Human Musculoskeletal Conditions

Abstract

Many chronic musculoskeletal conditions are associated with 'fatty infiltration' of the local stabilizing muscles. While atrophy has long been implicated as the mechanism of muscle loss in these conditions, more recent evidence has emerged demonstrating a degenerative phenotype of muscle loss consisting of disrupted muscle fiber membranes, infiltration of cells into muscle fibers, and possible replacement of muscle fibers by adipose tissue. Here, we use human lumbar spine pathology as a model system to provide a more comprehensive analysis of the morphological features of this mode of muscle loss, including an analysis of the cell populations found in actively degenerating versus histologically normal muscle regions within single biopsy sections. Using longitudinal sections, we show that degeneration of muscle fibers is localized within a fiber (i.e. focal), and is characterized by discontinuous or ragged membrane disruption, cellular infiltration, and apparently vacant space containing limited numbers of nuclei and hyper-contractile cell debris. Macrophages, leukocytes, and PDGFRβ-positive progenitor cells were all larger in both proportion and total number in degenerating regions, while only modestly larger myogenic cell numbers (but not proportion) were found. By better understanding the time course of degeneration in single fibers, including dynamic changes in cell populations and investigation into the molecular mechanisms of cell death in regions of active degeneration, we will be able to develop therapies that more effectively target muscle loss in patients with chronic musculoskeletal disease.

Introduction

Impaired muscle function is a hallmark of many musculoskeletal conditions that decrease quality of life for millions of patients annually. There are myriad causes of diminished muscle force production, ranging from simple loss of contractile protein volume, to sarcomere disorganization, to disruption in E-C coupling. In the first scenario, loss of functional contractile tissue can occur by either atrophy or

degeneration (i.e. muscle cell death). Therefore, these two terms are often used interchangeably in the clinical literature. This is problematic because disparate and often competing biological mechanisms govern atrophy and degeneration respectively. In turn, treatment modalities should be tailored to the underlying pathological mechanism, as failure to do so may lead to ineffective and possibly even detrimental effects of intervention.

Atrophy, which can be caused by mechanical or electrochemical unloading, or unmet metabolic demand, is a well-defined, muscle-intrinsic process mediated by the activation of the ubiquitin-proteasome and autophagic pathways that actuate protein catabolism[1-3]. On the single fiber level, atrophic fibers have smaller cytoplasmic volumes, but intact cellular machinery. By reloading the muscle it is possible to activate anabolic pathways and inhibit catabolic pathways, leading to muscle fiber hypertrophy, restoration of contractile tissue volume, and resulting in increased force production and improved function[4].

In contrast, muscle degeneration is a broader term encompassing a wide array of muscle-extrinsic physical and biochemical insults that lead to muscle fiber damage which left unchecked eventually leads to necrosis[5-7]. Classic examples are found in Duchenne muscular dystrophy and inflammatory myopathies, where muscle fiber membranes are disrupted by a specific protein deficiency and altered mechanical loading[6; 8], or T-cell mediated autoimmune attack[9], respectively. Although the term "degeneration" has been used to describe muscle loss in chronic musculoskeletal conditions (i.e. lumbar spine pathology, rotator cuff disease), historically only atrophic muscle loss had been described at the muscle fiber level. More recently, active muscle degeneration has been described in these chronic conditions, despite the lack of a clear primary etiology[10; 11]. In a range of degenerative models, fibers display characteristics such as membrane disruption, myophagocytosis, cellular infiltration, fiber splitting, and cytoplasmic disruptions (core, moth-eaten, and targetoid fibers)[12; 13]. Similar to atrophy, acute muscle degeneration does not necessarily lead to pathology, as cell death is typically followed by clearance of muscle fiber debris[14] and satellite cell-driven regeneration signified by a centralized myonucleus[15; 16].

However, when regeneration is impaired or insufficient to replace degenerated fibers, or when the

rate of degeneration outpaces regeneration, contractile tissue volume is reduced over time[16; 17]. Importantly, reloading of chronically degenerating muscle fibers with activity or exercise can result in further fiber damage and loss of function, instead of the expected hypertrophic response allowing for recovery from atrophy[18; 19]. Further confounding the effort to distinguish between muscle atrophy and degeneration is the observation that adipose tissue accumulation seems occurs regardless of the mechanism of muscle loss, though recent evidence suggests that the location of fat accumulation relative to the fascicular structure may be related to the mechanism of muscle loss[11; 20]. This relationship is so prevalent that the degree of fat accumulation in areas no longer occupied by muscle, commonly referred to as "fatty infiltration", is the most commonly used clinical indicator of muscle health and recovery prognosis[21-23]. Despite its clinical utility, little is known about the biological mechanisms that govern the replacement of muscle by fat.

In order to better understand the degenerative process outside the context of specific genetic or immunogenic conditions with specific causes of muscle degeneration (i.e. muscular dystrophy, autoimmunity, or myotoxin), we focused on a clinical condition in which reduced muscle volume contributes to poor functional outcomes and decreased quality of life: chronic lumbar spine pathology. Up to 85% of individuals experience LBP within their lifetime [24-26], and LBP is highly correlated with pathological changes of the bony and soft tissue structures that make up the spine[27; 28]. The lumbar spine muscles demonstrate decreased muscle cross-sectional area (CSA) and evidence of fatty infiltration with age and as disease severity progresses[21; 29-32], which correlates with poor clinical outcomes[23; 27; 33; 34]. More recent evidence suggests that this population demonstrates a histotype of muscle degeneration [11] similar to that found in rotator cuff tear[20], a condition which shares many other clinical and pathological features with lumbar spine pathology [23; 35]. In both systems this newly characterized mode of degenerative muscle loss diverges from previous reports that suggest atrophy is the key mode of contractile tissue loss in chronic orthopedic disease, though the cellular and molecular mediators of this form of muscle degeneration, and the number of conditions that display this degenerative phenotype, remain unknown.

The distinction between atrophy and degeneration is clinically relevant because optimal treatment

will depend on the mechanism of muscle loss and subsequent fat accumulation. For example, in an atrophic system, treatments aimed at blocking atrophy and/or promoting hypertrophy, such as resistance exercise, will likely improve outcomes. By contrast, in a degenerating system, this same approach may not address the underlying pathology of muscle cell death[36], and could even contribute to further injury. This idea is clinically supported by the lack of muscles' responsiveness to repair and rehabilitation in many patients with chronic musculoskeletal conditions[35-41].

Here, we aimed to provide deeper insight into the cellular processes found in chronic muscle degeneration by: 1) providing a detailed description of the degenerative phenotype (i.e. focal vs. global, membrane vs. cytoplasm vs. extracellular space, etc.) in both axial and longitudinal sections that may suggest potential mechanistic targets, and 2) identifying and quantifying the cells associated with these degenerating regions. With these data, we also expected to uncover new insights into the molecular mechanisms of muscle fiber death and degeneration.

Methods

Intraoperative biopsies of the lumbar multifidus muscle were collected under appropriate Institutional Review Board approvals in patients undergoing posterior approach spinal decompression (discectomy, laminectomy, or laminoforaminotomy) or fusion surgical procedures for chronic degenerative lumbar spine pathology (N=34). Muscle samples were pinned at in vivo length and flash frozen in liquid nitrogen cooled isopentane and stored at -80^{o}C. Prior to sectioning, samples were embedded in optimal cutting temperature media, and histological sections were generated on a Leica cryostat at -20^{o}C.

Axial and longitudinal biopsy sections were stained with Hematoxylin and Eosin (H&E) and evaluated to describe the morphology and spatial pattern of degeneration within single fibers as well as the orientation of degenerating fibers relative to non-muscle tissues and cells. To quantify specific cell types and structures within and around degenerating fibers, a serial immunohistochemistry/ hematoxylin and eosin (IHC/H&E) protocol was developed to allow identification of normal and degenerating regions

via H&E and cell type quantification via IHC labeling, as detailed below.

Prior to immunofluorescent staining, sections were blocked with 1% bovine serum albumin. Inflammatory cell markers of macrophages (CD68, Leica NCL-CD68-KP1), leukocytes (CD45, Biolegend HI30), and T-cells (CD3, Biolegend SK7) were used to label inflammatory cells within and surrounding degenerating muscle fibers, which were counterstained with anti-laminin to visualize disrupted muscle fiber membranes and DAPI (Vector Labs H-1200) to visualize nuclei. A similar strategy was used to quantify the localization of quiescent (Pax7), activated (MyoD), and committed (Myogenin) satellite cells as well as multi-potent resident progenitors including pericytes and fibro/adipogenic-progenitor (PDGFRβ).

Immediately after IHC imaging, each slide was H&E stained. A single rater then used the H&E images to identify degenerating regions of interest (ROIs) (defined by cellular infiltration of muscle fibers, membrane disruption, and/or cytoplasmic disruption (i.e. core or targetoid fibers [11; 13; 20])) as well as regions within the same section that were considered histologically normal, if present. Then, using an overlay of the IHC image, a separate rater quantified the total number of cells and the number of cells positive for the given IHC marker in each ROI.

Results

In axial histological sections of human multifidus muscle from the spine, we noted a pattern of muscle degeneration characterized by distinct hypercellular regions within muscle fibers in which sarcolemmal integrity was compromised and sarcoplasmic volume was reduced (Figure 1). In the longitudinal plane, degeneration appears to start at the muscle fiber membrane, where increased nuclear numbers and heterogeneous eosin staining combined with a jagged muscle fiber border represent the most common manifestation of the degenerative phenotype (Figure 2A,B). From this active region, the fibers demonstrated divergent phenotypes; in one direction, the fiber appeared normal, but in the other, the space occupied by the fiber was primarily vacant, with smaller regions of ragged or hyper-contracted cellular material consistent with muscle fiber necrosis, similar to the 'ghost fibers' described by Webster

et. al [42] (Figure 2C).

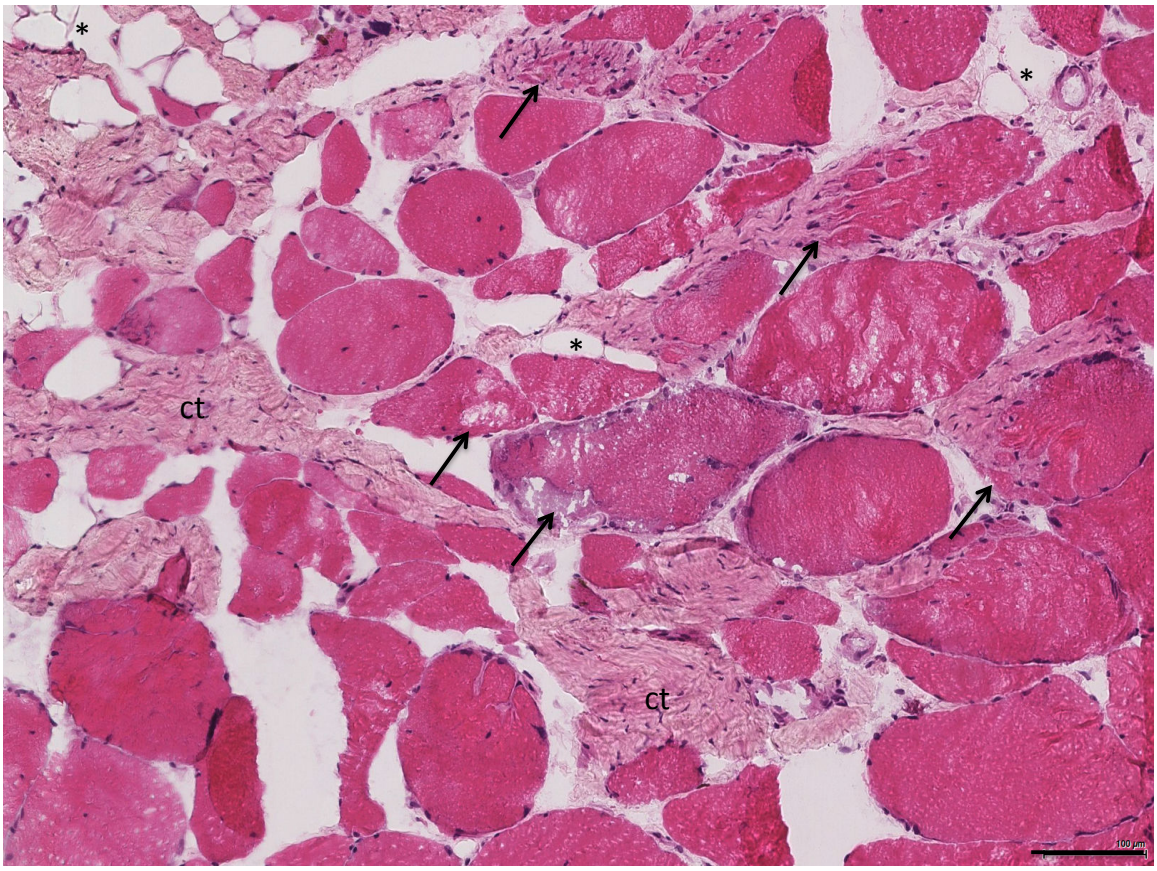

Figure 9.1 Axial Hematoxyline & Eosin (H&E) stains from the multifidus muscle in the spine in individuals with lumbar spine pathology. Black arrows indicate muscle fibers that demonstrate signs of degeneration; i.e. cellular infiltration, membrane disruptions, and cytoplasmic disruptions. Large proportions of connective tissue (ct) and clusters of adipocytes (*) can be observed throughout the tissue. Black scale bars are 100um.

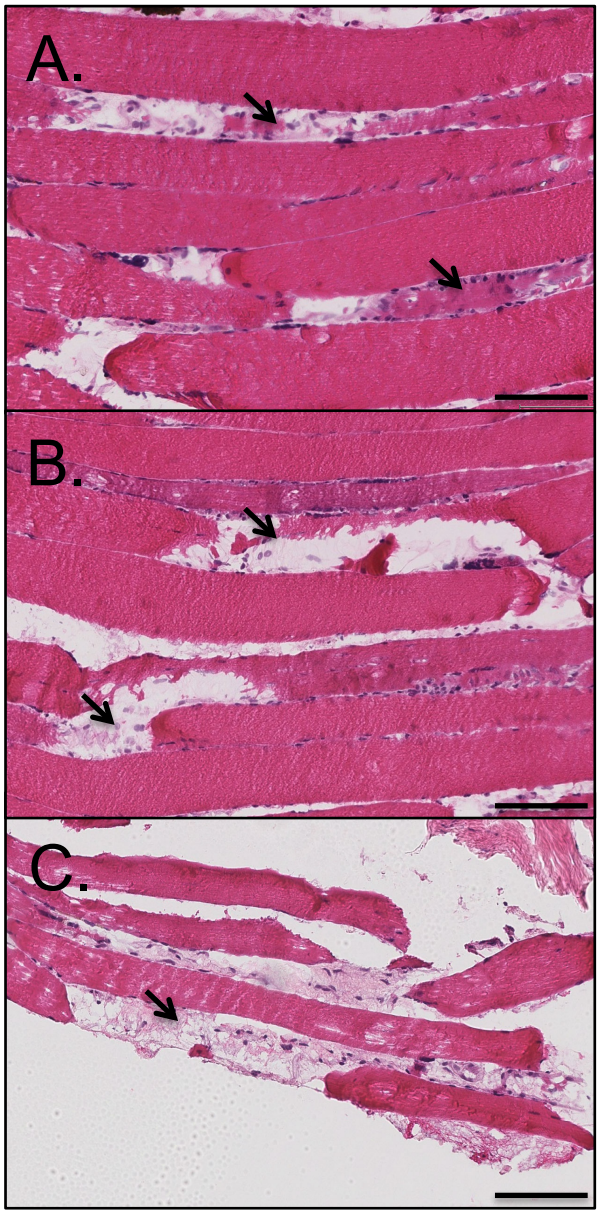

Figure 9.2 Representative H&E stained sections demonstrating varying severities of muscle degeneration in the longitudinal plane of the multifidus muscle in the spine. Areas of degeneration are signified by regions of hypercellularity and adjacent empty space where the remaining portion of the muscle fiber would normally be (arrows). Images are magnified at 20x. Black line is 100um.

As expected, there were significantly more nuclei in degenerating versus histologically normal regions (3.2:1 ratio) (Figure 3A). Myogenic cells, indicated by Pax7 (quiescent SCs) (Figure 4A), MyoD (activated SCs)(Figure 4B), and Myogenin (committed SCs) (Figure 4C), together made up less than 5%

of the cells in degenerating regions on average, with a similar percentage found in histologically normal regions. Due to the differences in total nuclei, this represents a modest expansion in total number of muscle progenitors in degenerating regions.

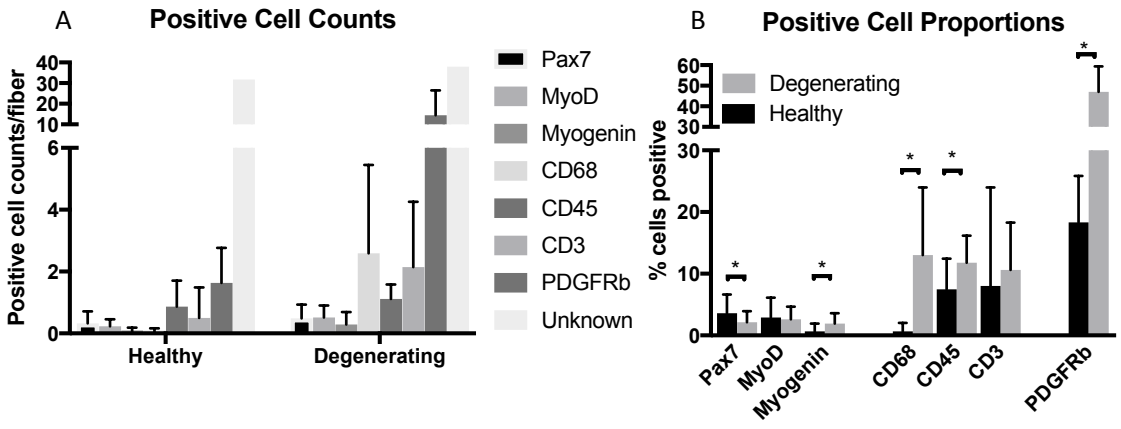

Figure 9.3 (A) The average total number of cells positive for each marker within a given degenerating region. (B) The average percentage of cells positive for each marker within a given degenerating region.

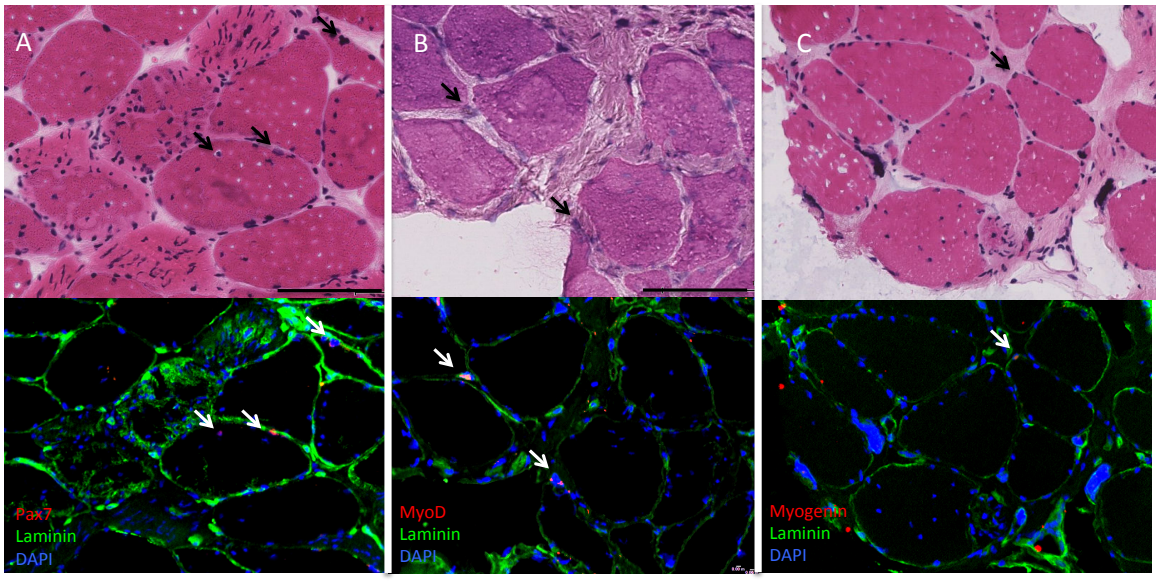

Figure 9.4 Representative images of nuclei positive for markers of quiescent (Pax7+, A), activated (MyoD+, B), and committed (Myogenin+, C) muscle progenitor cells.

Inflammatory cells comprised less than 10% of cells in healthy regions on average, with less than

1% of cells positive for CD68 (macrophages) (Figure 5A) and 8% of cells positive for CD45 (pan-leukocyte) (Figure 5B) and CD3 (pan T-cell) Figure 5C). In contrast, nearly 25% of cells were positive for inflammatory markers in degenerative regions. Macrophages made up 12% of the cells in degenerating regions, and while a similar percentage of T-cells (8%) was found, a slightly larger percentage (12%) of cells stained positive for CD45. Again, differences in total nuclei within degenerating regions imply that despite similar percentages, the total number of each inflammatory cell population is increased with degeneration.

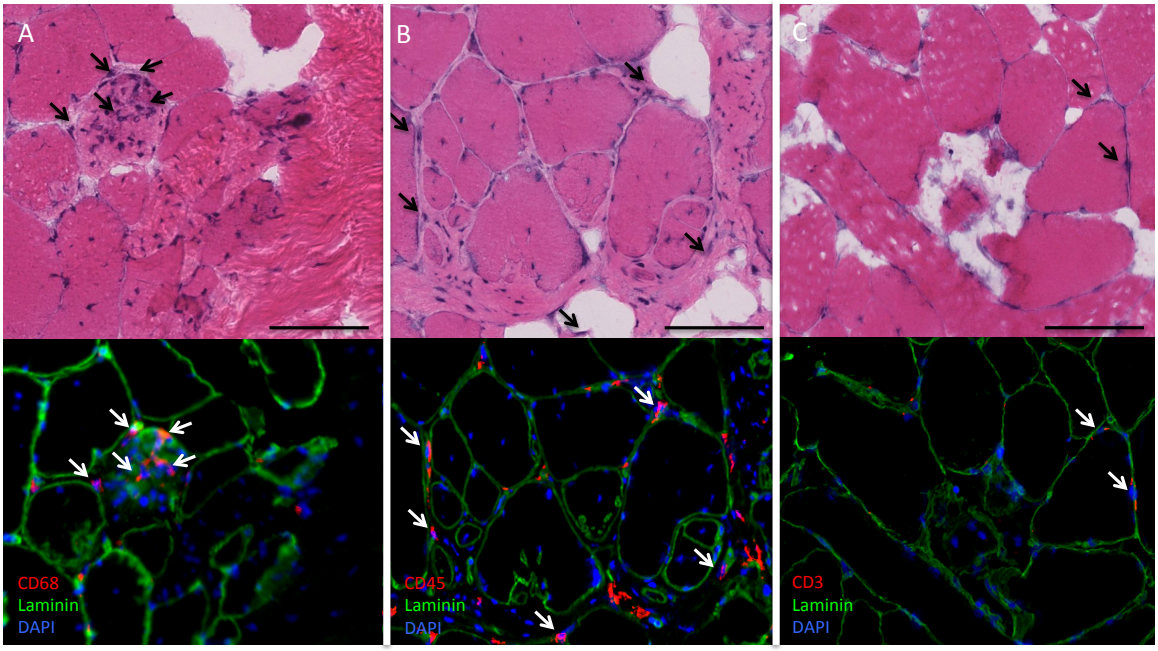

Figure 9.5 Representative images of inflammatory cells positive for macrophage (CD68, A), pan-white blood cell (CD45, B), and pan-T cell (CD3, C) markers.

In healthy regions, 18% of nuclei were positive for the multi-potent stem cell marker PDGFRβ. In the setting of histologically normal fibers, these cells had few projections, and were generally found at the intersection of multiple fibers. In contrast, PDGFRβ-positive projections were found surrounding and in some cases even penetrating into degenerating fibers, with many apparently normal fibers adjacent to degenerating regions similarly surrounded by such projections (Figure 6). As a result, 47% of nuclei in degenerative regions were associated with PDGFRβ-positivity, representing a significant increase in both

the fraction and total number of these progenitors in degenerating regions.

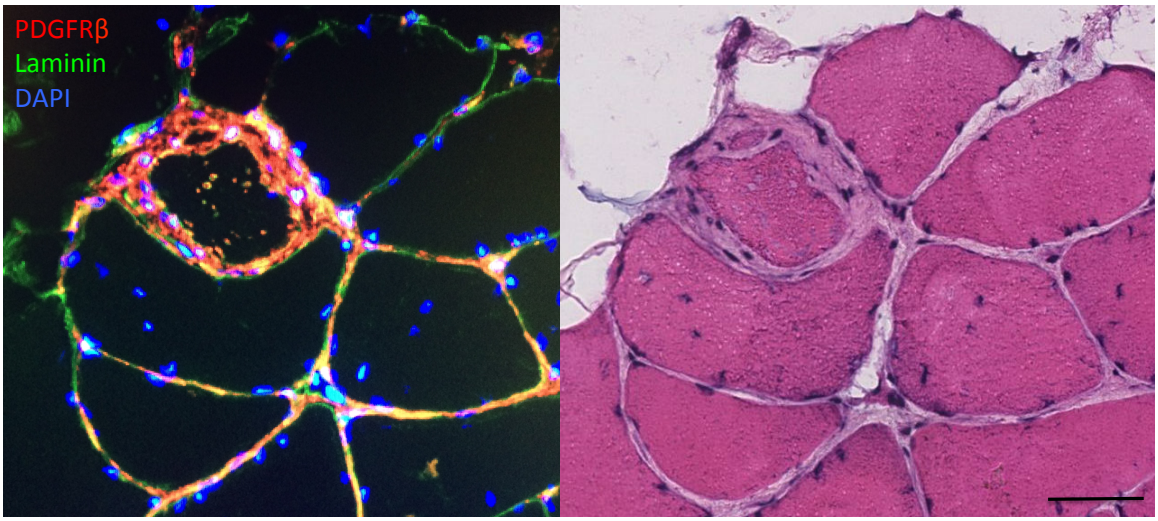

Figure 9.6 Representative image of a degenerating fiber surrounded by PDGFRβ+ cells (50μm scale bar).

Although it was not possible to stain each individual section for all cell types simultaneously, 69% of the cells in healthy regions were not accounted for with myogenic, inflammatory, or multi-potent progenitor cell markers whereas 25% of these cells were unaccounted for in the degenerating regions. Proportions of cell types in healthy and degenerated fibers are illustrated in Figure 3B.

Discussion

The key findings in this paper are that degenerating regions of muscle in individuals with chronic lumbar spine pathology are hypernuclear, and contain large proportions of fibro-adipogenic-progenitor cells, followed by a slightly larger proportion of inflammatory cells, but unchanged levels of myogenic cells relative to normal regions of muscle. These data are the first to quantify distributions of cell populations within both healthy and degenerating regions of muscle in patients with a chronic musculoskeletal condition. Here, we provide new insights into the potential mechanisms and cellular constituents of these processes through detailed analysis of the degenerative phenotype, including quantification of the cell populations present in degenerating and histologically normal muscle regions.

Diminished contractile tissue volume can result from either decreasing cell size (atrophy) or gross cell death (referred to generally as degeneration), and is correlated to diminished function and poor

prognosis in many chronic orthopedic conditions[27; 28; 35]. The biological mechanisms that govern atrophy and the spectrum of degenerative/cell death modalities each have distinct morphological and molecular signatures, which in turn have unique implications for optimal clinical treatment strategies. Progressive atrophy, which by definition preserves muscle fiber membrane integrity and total fiber number while decreasing fiber size[43], was long considered the primary mechanism of muscle loss in these conditions. However, more recent work has shown a limited role for atrophy, and described a degenerative mechanism of muscle loss in multiple orthopedic maladies, including lumbar spine pathology[11; 20]. Here, more complete analyses of the morphology and cellular composition of degenerating regions provides potential insight into the role of apoptotic versus necrotic muscle fiber death in patients with lumbar spine pathology.

Whereas apoptotic cells tend to maintain plasma membrane integrity while decreasing in size (often to the point of hyper-contractility)[44; 45], necrotic cells are characterized by cell membrane (as well as intracellular membrane) disruption or permeabilization[46; 47], exposure of cytoplasmic elements (i.e. DAMPs) to the extracellular space [48], and ultimately cytolytic rupture due to osmotic pressure imbalance [49]. Indeed, apoptosis-related signaling has been implicated in some models of atrophy, though in these contexts apoptotic signaling is thought to serve as a homeostatic process to maintain myonuclear domain (i.e. nuclear "trimming") and does not lead to muscle fiber death[50; 51]. Moreover, some studies suggest that muscle is resistant to classical apoptotic cell death, at least in the context of myositis[52]. In these biopsies, the morphology of degenerating regions is clearly consistent with necrotic cell death, as fiber membranes and cytoplasm are disrupted and non-myogenic cells appear to penetrate into degenerating fibers. Because apoptotic and necrotic cell death processes (which themselves have several sub-modalities) can have potentially profound differences in their secondary effects on inflammatory signaling [48; 49; 53] and activation of resident stem cells, identifying necrosis as the primary mode of muscle fiber death is clinically significant, while future studies will be needed to identify the specific molecular mechanisms that drive muscle cell death in these conditions.

Consistent with the finding that necrosis is the predominant form of cell death in degenerating

regions was the increased inflammatory cell presence in degenerating compared to normal regions[54; 55], though it should be noted that inflammation also plays a role in apoptotic cell death[56]. Importantly, though macrophage accumulation and activation is expected regardless of the mechanism of cell death due to the role of phagocytosis in removing cellular debris after cell death[57; 58], the magnitude and composition of the pro-inflammatory response generally varies depending on the cell death signaling cascade[44; 49; 59-61]. Here, macrophage presence in degenerating regions was consistent with degenerative or necrotic cell death found in inflammatory myopathies[62], rhabdomyolysis[63], and toxin-induced muscle necrosis[64]. Moreover, the increase in leukocyte number, and T-cells in particular, is consistent with a necrotic phenotype, as apoptosis is not typically associated with an adaptive immune response while both programmed and organic necrosis are known to increase T-cell migration and activation[65].

Despite the increased overall cell number in degenerating regions compared to normal regions, a proportional increase in myogenic progenitors was not observed. In otherwise healthy muscle, fiber death is followed by mobilization and expansion of satellite cells and other progenitor cells (most notably pericytes and fibro/adipogenic progenitors) that together mediate muscle regeneration[5; 15; 16; 66-70]. Here, the fraction of SCs relative to total nuclei was not different between normal and degenerating regions, and was consistent with previously reported SC fractions in healthy muscle[71]. This is may provide insight into the irreversibility of muscle degeneration in lumbar spine pathology and similar orthopedic conditions – regardless of the mechanism of cell death, limited activation of myogenic cells in the face of degeneration will likely lead to incomplete regeneration in the short term and net loss of functional muscle volume over time.

The large proportion of PDGFRβ-positive cells in degenerating regions suggests that this cell type may be a key player contributing to the tissue compositional changes observed with degeneration. While the precise cell population demarcated by PDGFRβ positivity is still debated[72-74], in healthy muscle these cells are reported to have a supportive role of myogenesis via phagocytosis of debris from degenerating fibers[69], secretion of pro-myogenic extracellular matrix and growth factors[67; 74-76], and to a lesser extent, direct fusion with regenerating fibers[77]. However, when the coordination of inflammatory

cues is disrupted, as appears to be the case in lumbar spine pathology and other chronic orthopedic conditions, these cells may take on fibroblastic or adipogenic phenotypes[74; 75]. Indeed, this cell population has been implicated in the terminal fatty and fibrotic composition of muscles in many diseases[19; 73; 74; 78]. Here, PDGFRβ-positive cells appear to penetrate into fibers with otherwise normal-appearing cytosol and intact membranes distal to the point of disruption, which suggests a more active role for these cells in the initiation and propagation of fiber degeneration.

The observation that there are a large number of cells that were not accounted for in the included stains is likely reflective of the resident myonuclei within a fiber. However, while the relative proportion and number of these unstained cells is consistent with myonuclear counts in the healthy muscle regions, the higher total number of unidentified cells in the degenerated regions suggests that there may be additional cell types that are not myonuclei that serve some additional function not accounted for here. One possibility is a muscle-specific cell with a function analogous to that of an osteoclast's role in bone resorption (i.e. a "myoclast"), that initiates cellular infiltration and breakdown of the muscle fiber. However the discrepancy in myonuclear number and some other possible cell type requires further investigation.

A primarily limitation of this analysis is our inability to resolve the time course of degeneration – while the fibers included in our definition of 'active degeneration' are clearly damaged, there is likely a spectrum from 'early' to 'late' degneration included in these regions. This also means that regions in the earliest and most terminal degenerative states are omitted from our analysis. Understanding how cell populations surrounding degenerative fibers change from initiation to terminal degeneration is a key next step to defining the degenerative mechanism in these conditions. Similarly, future studies should focus on identifying specific markers and regulators of necrotic cell death in order to definitively identify the molecular mechanisms of cell death present in these patient populations.

Beyond our limited ability to define the time course of degeneration across degenerating regions in a single biopsy section, we are also limited by the heterogeneity across patients in terms of comorbidities as well as chronicity and severity of disease. Similarly, although we were able to make

comparisons within a single section between degenerating and histologically normal regions, in this context the normal reference is derived from a muscle that on the whole-muscle level is not clinically normal or healthy. As such, the inability to obtain muscle biopsies from healthy control subjects may underestimate the true magnitude of difference between cell populations in healthy versus degenerating tissue.

Conclusions

Muscle volume loss and fatty infiltration are common features in chronic degenerative musculoskeletal conditions such as lumbar spine pathology. However, the mechanisms underlying the loss of functional contractile tissue in these conditions are more complex than simple atrophy. Here, we demonstrate that muscle degeneration, characterized by punctate regions of muscle fiber necrosis displaying both hyper- and hypo-cellular regions in the same fiber, is a common feature of spine muscle pathology. Innate and adaptive immune cells and multi-potent resident progenitors are more prevalent than myogenic satellite cells in degenerative regions, which support the hypothesis that limited regeneration combined with necrotic mechanisms of cell death, which are mediated in large part by inflammatory signals and immune cell-derived products, are responsible for progressive muscle loss in patients with chronic orthopedic disease. By improving our understanding of the degenerative mechanisms that drive this particular form of muscle loss, we will facilitate the improvement of strategies aimed at preventing degeneration and stimulating regeneration of muscle tissue in these patients.

Acknowledgements

Funding for this work was provided by NIH 1TL1TR001443 awarded to BS and HD088437, and HD073180 awarded to SRW.

This chapter, in part, is currently being prepared for submission for publication of the material. Bahar Shahidi, Michael C. Gibbons, Mary Esparza, Vinko Zlomislic, R Todd Allen, Anshu Singh, Christian Gerber, Steve R. Garfin, Samuel R. Ward. The dissertation/thesis author was a primary investigator of this material.

References

1. Bonaldo P, Sandri M. 2013. Cellular and molecular mechanisms of muscle atrophy. Dis Model Mech 6:25-39.

2. Glass DJ. 2005. Skeletal muscle hypertrophy and atrophy signaling pathways. Int J Biochem Cell Biol 37:1974-1984.

3. Evans WJ. 2010. Skeletal muscle loss: cachexia, sarcopenia, and inactivity. The American journal of clinical nutrition 91:1123S-1127S.

4. Reitsma W. 1969. Skeletal muscle hypertrophy after heavy exercise in rats with surgically reduced muscle function. Am J Phys Med 48:237-258.

5. Tidball JG. 2005. Inflammatory processes in muscle injury and repair. Am J Physiol Regul Integr Comp Physiol 288:R345-353.

6. Wallace GQ, McNally EM. 2009. Mechanisms of muscle degeneration, regeneration, and repair in the muscular dystrophies. Annual review of physiology 71:37-57.

7. Sorichter S, Puschendorf B, Mair J. 1998. Skeletal muscle injury induced by eccentric muscle action: muscle proteins as markers of muscle fiber injury. Exercise immunology review 5:5-21.

8. Heydemann A, McNally EM. 2007. Consequences of disrupting the dystrophin-sarcoglycan complex in cardiac and skeletal myopathy. Trends in cardiovascular medicine 17:55-59.

9. Zong M, Lundberg IE. 2011. Pathogenesis, classification and treatment of inflammatory myopathies. Nature Reviews Rheumatology 7:297-306.

10. Gibbons MC, Singh A, Anakwenze O, Cheng T, Pomerantz M, Schenk S, Engler AJ, Ward SR. 2017. Histological Evidence of Muscle Degeneration in Advanced Human Rotator Cuff Disease. J Bone Joint Surg Am 99:190-199.

11. Shahidi B, Hubbard JC, Gibbons MC, Ruoss S, Zlomislic V, Allen RT, Garfin SR, Ward SR. 2017. Lumbar multifidus muscle degenerates in individuals with chronic degenerative lumbar spine pathology. Journal of Orthopaedic Research.

12. Preedy V, Peters T. 2002. Skeletal muscle: pathology, diagnosis and management of disease: Cambridge University Press;

13. Dubowitz V, Sewry CA, Oldfors A. 2013. Muscle Biopsy: A Practical Approach, Expert Consult; Online and Print, 4: Muscle Biopsy: A Practical Approach: Elsevier Health Sciences;

14. Tidball JG. 2011. Mechanisms of muscle injury, repair, and regeneration. Compr Physiol 1:2029-2062.

15. Lepper C, Partridge TA, Fan C-M. 2011. An absolute requirement for Pax7-positive satellite cells in acute injury-induced skeletal muscle regeneration. Development 138:3639-3646.

16. Ciciliot S, Schiaffino S. 2010. Regeneration of mammalian skeletal muscle: basic mechanisms and clinical implications. Current pharmaceutical design 16:906-914.

17. Langen RC, Schols AM, Kelders MC, van der Velden JL, Wouters EF, Janssen-Heininger YM. 2006. Muscle wasting and impaired muscle regeneration in a murine model of chronic pulmonary inflammation. American journal of respiratory cell and molecular biology 35:689-696.

18. Mendias CL, Roche SM, Harning JA, Davis ME, Lynch EB, Sibilsky Enselman ER, Jacobson JA, Claflin DR, Calve S, Bedi A. 2015. Reduced muscle fiber force production and disrupted myofibril architecture in patients with chronic rotator cuff tears. J Shoulder Elbow Surg 24:111-119.

19. Gibbons MC, Singh A, Engler AJ, Ward SR. 2017. The Role of Mechanobiology in Progression of Rotator Cuff Muscle Atrophy and Degeneration. Journal of Orthopaedic Research.

20. Gibbons MC, Singh A, Anakwenze O, Cheng T, Pomerantz M, Schenk S, Engler AJ, Ward SR. 2017. Histological Evidence of Muscle Degeneration in Advanced Human Rotator Cuff Disease. The Journal of Bone & Joint Surgery 99:190-199.

21. Kjaer P, Bendix T, Sorensen JS, Korsholm L, Leboeuf-Yde C. 2007. Are MRI-defined fat infiltrations in the multifidus muscles associated with low back pain? BMC Med 5:2.

22. Wren TA, Bluml S, Tseng-Ong L, Gilsanz V. 2008. Three-point technique of fat quantification of muscle tissue as a marker of disease progression in Duchenne muscular dystrophy: preliminary study. American Journal of Roentgenology 190:W8-W12.

23. Goutallier D, Postel J-M, Gleyze P, Leguilloux P, Van Driessche S. 2003. Influence of cuff muscle fatty degeneration on anatomic and functional outcomes after simple suture of full-thickness tears. Journal of Shoulder and Elbow Surgery 12:550-554.

24. Andersson GB. 1999. Epidemiological features of chronic low-back pain. Lancet 354:581-585.

25. Manchikanti L, Singh V, Datta S, Cohen SP, Hirsch JA, Physicians ASoIP. 2009. Comprehensive review of epidemiology, scope, and impact of spinal pain. Pain Physician 12:E35-70.

26. Collaborators UBoD. 2013. The state of US health, 1990-2010: burden of diseases, injuries, and risk factors. JAMA 310:591-608.

27. Chen YY, Pao JL, Liaw CK, Hsu WL, Yang RS. 2014. Image changes of paraspinal muscles and clinical correlations in patients with unilateral lumbar spinal stenosis. Eur Spine J 23:999-1006.

28. Suri P, Fry AL, Gellhorn AC. 2015. Do Muscle Characteristics on Lumbar Spine Magnetic Resonance Imaging or Computed Tomography Predict Future Low Back Pain, Physical Function, or Performance? A Systematic Review. PM R.

29. Alaranta H, Tallroth K, Soukka A, Heliövaara M. 1993. Fat content of lumbar extensor muscles and low back disability: a radiographic and clinical comparison. J Spinal Disord 6:137-140.

30. Shahidi B, Parra CL, Berry DB, Hubbard JC, Gombatto S, Zlomislic V, Allen RT, Hughes-Austin J, Garfin S, Ward SR. 2016. Contribution of Lumbar Spine Pathology and age to Paraspinal Muscle Size and fatty Infiltration. Spine (Phila Pa 1976).

31. Goubert D, Oosterwijck JV, Meeus M, Danneels L. 2016. Structural Changes of Lumbar Muscles in Non-specific Low Back Pain: A Systematic Review. Pain Physician 19:E985-E1000.

32. Goutallier D, Postel J-M, Bernageau J, Lavau L, Voisin M-C. 1994. Fatty muscle degeneration in cuff ruptures: pre-and postoperative evaluation by CT scan. Clinical orthopaedics and related research 304:78-83.

33. Airaksinen O, Herno A, Kaukanen E, Saari T, Sihvonen T, Suomalainen O. 1996. Density of lumbar muscles 4 years after decompressive spinal surgery. Eur Spine J 5:193-197.

34. Sihvonen T, Herno A, Paljärvi L, Airaksinen O, Partanen J, Tapaninaho A. 1993. Local denervation atrophy of paraspinal muscles in postoperative failed back syndrome. Spine (Phila Pa 1976) 18:575-581.

35. Gladstone JN, Bishop JY, Lo IK, Flatow EL. 2007. Fatty infiltration and atrophy of the rotator cuff do not improve after rotator cuff repair and correlate with poor functional outcome. The American journal of sports medicine 35:719-728.

36. Käser L, Mannion AF, Rhyner A, Weber E, Dvorak J, Müntener M. 2001. Active therapy for chronic low back pain: part 2. Effects on paraspinal muscle cross-sectional area, fiber type size, and distribution. Spine (Phila Pa 1976) 26:909-919.

37. Danneels LA, Vanderstraeten GG, Cambier DC, Witvrouw EE, Bourgois J, Dankaerts W, De Cuyper HJ. 2001. Effects of three different training modalities on the cross sectional area of the lumbar multifidus muscle in patients with chronic low back pain. Br J Sports Med 35:186-191.

38. Hebert JJ, Fritz JM, Thackeray A, Koppenhaver SL, Teyhen D. 2015. Early multimodal rehabilitation following lumbar disc surgery: a randomised clinical trial comparing the effects of two exercise programmes on clinical outcome and lumbar multifidus muscle function. Br J Sports Med 49:100-106.

39. Shahtahmassebi B, Hebert JJ, Stomski NJ, Hecimovich M, Fairchild TJ. 2014. The effect of exercise training on lower trunk muscle morphology. Sports Med 44:1439-1458.

40. Gerber C, Fuchs B, Hodler J. 2000. The Results of Repair of Massive Tears of the Rotator Cuff*†. The Journal of Bone & Joint Surgery 82:505-505.

41. Schoenfeld BJ. 2012. Does exercise-induced muscle damage play a role in skeletal muscle hypertrophy? The Journal of Strength & Conditioning Research 26:1441-1453.

42. Webster MT, Manor U, Lippincott-Schwartz J, Fan C-M. 2016. Intravital imaging reveals ghost fibers as architectural units guiding myogenic progenitors during regeneration. Cell Stem Cell 18:243-252.

43. Bonaldo P, Sandri M. 2013. Cellular and molecular mechanisms of muscle atrophy. Disease models & mechanisms 6:25-39.

44. Kerr JF, Wyllie AH, Currie AR. 1972. Apoptosis: a basic biological phenomenon with wideranging implications in tissue kinetics. British journal of cancer 26:239.

45. Danial NN, Korsmeyer SJ. 2004. Cell death: critical control points. Cell 116:205-219.

46. Cherin P, Herson S, Crevon M, Hauw J, Cervera P, Galanaud P, Emilie D. 1996. Mechanisms of lysis by activated cytotoxic cells expressing perforin and granzyme-B genes and the protein TIA-1 in muscle biopsies of myositis. The Journal of rheumatology 23:1135-1142.

47. Engel AG, Biesecker G. 1982. Complement activation in muscle fiber necrosis: demonstration of the membrane attack complex of complement in necrotic fibers. Annals of neurology 12:289-296.

48. Pisetsky DS. 2011. Cell death in the pathogenesis of immune-mediated diseases: the role of HMGB1 and DAMP-PAMP complexes. Swiss medical weekly 141:w13256.

49. Berghe TV, Linkermann A, Jouan-Lanhouet S, Walczak H, Vandenabeele P. 2014. Regulated necrosis: the expanding network of non-apoptotic cell death pathways. Nature reviews Molecular cell biology 15:135.

50. Allen DL, Roy RR, Edgerton VR. 1999. Myonuclear domains in muscle adaptation and disease. Muscle & nerve 22:1350-1360.

51. Dupont-Versteegden EE. 2006. Apoptosis in skeletal muscle and its relevance to atrophy. World journal of gastroenterology: WJG 12:7463.

52. Nagaraju K, Casciola-Rosen L, Rosen A, Thompson C, Loeffler L, Parker T, Danning C, Rochon PJ, Gillespie J, Plotz P. 2000. The inhibition of apoptosis in myositis and in normal muscle cells. The Journal of Immunology 164:5459-5465.

53. Tews D. 2002. Apoptosis and muscle fibre loss in neuromuscular disorders. Neuromuscular Disorders 12:613-622.

54. GROUNDS MD, Torrisi J. 2004. Anti-TNFα (Remicade®) therapy protects dystrophic skeletal muscle from necrosis. The FASEB Journal 18:676-682.

55. Dalakas MC. 1991. Polymyositis, dermatomyositis, and inclusion-body myositis. New England Journal of Medicine 325:1487-1498.

56. Nakazawa H, Chang K, Shinozaki S, Yasukawa T, Ishimaru K, Yasuhara S, Yu Y-M, Martyn JJ, Tompkins RG, Shimokado K. 2017. iNOS as a driver of inflammation and apoptosis in mouse skeletal muscle after burn injury: possible involvement of Sirt1 S-nitrosylation-mediated acetylation of p65 NF-κB and p53. PloS one 12:e0170391.

57. Arnold L, Henry A, Poron F, Baba-Amer Y, Van Rooijen N, Plonquet A, Gherardi RK, Chazaud B. 2007. Inflammatory monocytes recruited after skeletal muscle injury switch into antiinflammatory macrophages to support myogenesis. The Journal of experimental medicine 204:1057-1069.

58. Arnold L, Perrin H, De Chanville CB, Saclier M, Hermand P, Poupel L, Guyon E, Licata F, Carpentier W, Vilar J. 2015. CX3CR1 deficiency promotes muscle repair and regeneration by enhancing macrophage ApoE production. Nature communications 6:8972.

59. Elmore S. 2007. Apoptosis: a review of programmed cell death. Toxicologic pathology 35:495-516.

60. Trapani JA. 1995. Target cell apoptosis induced by cytotoxic T cells and natural killer cells involves synergy between the pore-forming protein, perforin, and the serine protease, granzyme B. Internal Medicine Journal 25:793-799.

61. Choi JJ, Reich CF, Pisetsky DS. 2005. The role of macrophages in the in vitro generation of extracellular DNA from apoptotic and necrotic cells. Immunology 115:55-62.

62. Dorph C, Englund P, Nennesmo I, Lundberg IE. 2006. Signs of inflammation in both symptomatic and asymptomatic muscles from patients with polymyositis and dermatomyositis. Annals of the rheumatic diseases 65:1565-1571.

63. Hikida RS, Staron RS, Hagerman FC, Sherman WM, Costill DL. 1983. Muscle fiber necrosis associated with human marathon runners. Journal of the neurological sciences 59:185-203.

64. Harris J, Cullen M. 1990. Muscle necrosis caused by snake venoms and toxins. Electron microscopy reviews 3:183-211.

65. Sciorati C, Rigamonti E, Manfredi A, Rovere-Querini P. 2016. Cell death, clearance and immunity in the skeletal muscle. Cell death and differentiation 23:927.

66. Charge SB, Rudnicki MA. 2004. Cellular and molecular regulation of muscle regeneration. Physiological reviews 84:209-238.

67. Fiore D, Judson RN, Low M, Lee S, Zhang E, Hopkins C, Xu P, Lenzi A, Rossi FM, Lemos DR. 2016. Pharmacological blockage of fibro/adipogenic progenitor expansion and suppression of regenerative fibrogenesis is associated with impaired skeletal muscle regeneration. Stem cell research 17:161-169.

68. Goetsch SC, Hawke TJ, Gallardo TD, Richardson JA, Garry DJ. 2003. Transcriptional profiling and regulation of the extracellular matrix during muscle regeneration. Physiological genomics 14:261-271.

69. Heredia JE, Mukundan L, Chen FM, Mueller AA, Deo RC, Locksley RM, Rando TA, Chawla A. 2013. Type 2 innate signals stimulate fibro/adipogenic progenitors to facilitate muscle regeneration. Cell 153:376-388.

70. Vracko R, Benditt EP. 1972. Basal lamina: the scaffold for orderly cell replacement observations on regeneration of injured skeletal muscle fibers and capillaries. The Journal of cell biology 55:406-419.

71. Cooper R, Tajbakhsh S, Mouly V, Cossu G, Buckingham M, Butler-Browne G. 1999. In vivo satellite cell activation via Myf5 and MyoD in regenerating mouse skeletal muscle. Journal of cell science 112:2895-2901.

72. Joe AW, Yi L, Natarajan A, Le Grand F, So L, Wang J, Rudnicki MA, Rossi FM. 2010. Muscle injury activates resident fibro/adipogenic progenitors that facilitate myogenesis. Nature cell biology 12:153-163.

73. Uezumi A, Fukada S-i, Yamamoto N, Takeda Si, Tsuchida K. 2010. Mesenchymal progenitors distinct from satellite cells contribute to ectopic fat cell formation in skeletal muscle. Nature cell biology 12:143-152.

74. Birbrair A, Zhang T, Wang Z-M, Messi ML, Enikolopov GN, Mintz A, Delbono O. 2013. Role of pericytes in skeletal muscle regeneration and fat accumulation. Stem cells and development 22:2298-2314.

75. Birbrair A, Zhang T, Wang Z-M, Messi ML, Mintz A, Delbono O. 2014. Pericytes: multitasking cells in the regeneration of injured, diseased, and aged skeletal muscle. Frontiers in aging neuroscience 6:245.

76. Kostallari E, Baba-Amer Y, Alonso-Martin S, Ngoh P, Relaix F, Lafuste P, Gherardi RK. 2015. Pericytes in the myovascular niche promote post-natal myofiber growth and satellite cell quiescence. Development 142:1242-1253.

77. Dellavalle A, Maroli G, Covarello D, Azzoni E, Innocenzi A, Perani L, Antonini S, Sambasivan R, Brunelli S, Tajbakhsh S. 2011. Pericytes resident in postnatal skeletal muscle differentiate into muscle fibres and generate satellite cells. Nature communications 2:499.

78. Lin S-L, Kisseleva T, Brenner DA, Duffield JS. 2008. Pericytes and perivascular fibroblasts are the primary source of collagen-producing cells in obstructive fibrosis of the kidney. The American journal of pathology 173:1617-1627.

Chapter 10. Conclusion

Rotator cuff tears remain one of the most clinically challenging orthopedic ailments, with limited long-term functional recovery and high incidence of repair failure. While much work has rightly focused on the quality and repair of the tendon itself, here I focused on the rotator cuff muscles, as muscle quality is a strong predictor of clinical outcomes and rehabilitation and repair alone do not reverse the muscle loss and fat accumulation that result from chronic tear. Without functional muscle, even anatomically intact repairs will suffer from functional deficits, and thus the overarching goal of this dissertation was to determine the physiological and biological causes of muscle loss in chronic disease, with the ultimate goal of informing the development of more effective treatment strategies for patients with chronic rotator cuff tears.

In the early chapters of this dissertation, I focused on characterization of human rotator cuff muscles in the context of chronic, massive tears. In chapter 2, I discovered that in contrast to full-thickness tears, which display expected sarcomere subtraction and maintenance of sarcomere length in response to muscle retraction and fiber shortening, sarcomeres in muscles from massive RC tears are significantly shorter. This suggests a failure of normal remodeling behavior, and implies that anatomical repair of massive tears moves the muscle off of the length-tension curve, to the detriment of muscle function.

In chapters 3 and 4, my goal was to define the mechanism of muscle loss in biopsies from patients with the most severe RC disease states. Despite the interchangeable use of terms such as ‘fatty atrophy’, ‘fatty degeneration’, and ‘fatty infiltration’ used throughout the literature, the biology underlying atrophy and degeneration are fundamentally different. Using biopsies from patients with the most advanced stages of RC disease, I discovered a novel degenerative mode of muscle loss involving disruption of muscle fiber membrane and cytoplasm, infiltration of cells into muscle fibers (i.e. myophagocytosis), and intra-fascicular accumulation of fat suggestive of terminal degeneration of muscle fibers. Gene expression analysis of these same biopsies demonstrated a strong compositional effect on the measured expression profile, a finding which should inform the interpretation of past gene expression

studies and the design of future expression studies. Furthermore, within the muscle-containing subset, distinct high- and low-expression groups emerged that imply the existence of distinct biological stages of disease.

Chapters 5, 6, and 7 focus on the characterization and development of animal models of RC tear. Chapter 5 demonstrates the failure of the mouse model to recapitulate the phenotype of advance human RC disease even with the addition of a non-physiologic nerve injury. In contrast, Chapter 6 and Chapter 7 demonstrate that both rabbit and sheep developed a degenerative phenotype similar to that found in human, and thus may be used for exploring biological mechanisms of disease as well as evaluating new therapeutic approaches to treating muscle degeneration in the context of rotator cuff tear.

The final component of Chapter 7, and all of Chapter 8, explored gene expression patterns in the sheep and rabbit models. In the rabbit, I demonstrated an acute response to tenotomy consisting of reduced expression of metabolic and anabolic programs and increased inflammation at 2 weeks, elements of which persisted through 8 weeks where survival signaling was most prominent. By 16 weeks of tenotomy in both the rabbit and sheep, I found an expression profile indicative of cell membrane damage, reduced energy and protein synthesis, and increased chronic inflammation, cell death, and phagocytosis, as well as increased cell survival signaling. Interestingly, expression related to ubiquitin-proteasome mediated protein degradation was reduced at 16 weeks, suggesting that classical atrophy is not involved in muscle volume loss in chronic RC disease. While future mechanistic studies are needed, these data offer strong support for my overall hypothesis that, rather than atrophy, a combination of muscle fiber damage and deficient or inhibited anabolic, metabolic, and regenerative capacity are responsible for the irreversible muscle loss in chronic RC tears.

Finally, in Chapter 9 I leveraged access to muscle biopsies from patients with lumbar spine pathology, a second source of human muscle that contains a similar degenerative phenotype to that found in RC tear, to determine the cellular composition of actively degenerating regions of muscle fibers. I found that muscle stem cells and T-cell fractions are similar between histologically normal and actively degenerating muscle fibers. The limited number of muscle stem cells surrounding degenerative regions is

consistent with the lack of regenerative activity described in previous Chapters, and while the regulatory role of T cells in the degenerative process remains to be elucidated these cells do not appear to directly actuate degeneration. In contrast, the fractions of macrophages and PDGFRβ+ progenitors suggests potential roles for each of these cell types in degenerative processes. Macrophages appear almost exclusively around degenerating fibers, though whether this is a function of a canonical response to released intracellular components and clearance of necrotic cell debris or a pathological assault of an otherwise healthy muscle fiber remains unknown. PDGFRβ+ progenitors, participants in muscle regeneration in otherwise healthy muscle but capable of differentiating into either adipocytes or fibroblasts in pathological conditions, more than double surrounding degenerating fibers – combined with the lack of muscle stem cell presence and the long-term accumulation of adipocytes and fibrous tissue within muscle fascicles in Chapter 3, maladaptive fate choice in this cell population remains the most likely source of intra-fascicular adipocytes in chronic RC tear.

The implications of these data combined with current muscle biology and physiology and muscle stem cell literature on the current RC tear disease mechanism and treatment paradigms are wide-ranging. In particular, the findings of Chapters 2, 3, 4, 8, and 9 suggest that massive tears with high levels of degeneration may be resistant to or even harmed by standard exercise and repair strategies, as these interventions are known to cause muscle damage in the short term. It is possible that, in the face of reduced anabolic and metabolic capacity, damaged muscle fiber membranes and abnormal sarcomere organization, and apparent deficits in muscle stem cell-driven regeneration, the muscle fiber damage caused by high intensity exercise and or high-strain repair may in fact accelerate the already increased rate of muscle cell death. By better understanding the biological state of a given patient's muscle, it may be possible to better fractionate patients into those that will respond to physical therapy and those that will not – and in the future, to select or develop personalized rehabilitation and repair strategies that will provide the desired regenerative and hypertrophic stimuli without the risk of further damaging muscles already prone to irreversible muscle fiber death.

In conclusion, this dissertation provided new insights into the muscle architecture, tissue- and cell-level composition, and gene expression patterns that define chronic, massive rotator cuff tears. In human muscle, I discovered deficiencies in sarcomere remodeling and a new mode of muscle loss in advanced human RC disease, along with evidence that macrophages and non-myogenic muscle resident progenitors are the primary cells surrounding actively degenerating fibers. After validating rabbit and sheep models of chronic, massive RC tear (and demonstrating significant deficiencies in the mouse model), I used transcriptome-wide gene expression profiling to generate evidence supporting the existence of cell damage and degeneration, as well as impaired anabolic, metabolic, and regenerative capacity that together may explain why muscle fibers are lost, and why this loss of fibers is irreversible in chronic rotator cuff disease. Moving forward, this body of work should be used as the foundation for new therapeutic approaches to address both atrophic and degenerative muscle loss in RC tears, including more personalized rehabilitation plans that take in to account the biological state of the muscle, mechanistic studies to confirm the cellular and molecular initiators and controllers of this newly discovered form of muscle degeneration, and development of regenerative therapeutic agents that can be used alone or in combination with rehabilitation and tendon repair to restore RC muscle function in these patients.